AD_____

Award Number: DAMD17-02-1-0602

TITLE: p38 Mitogen-activated Protein Kinase in Metastasis Associated with Transforming Growth Factor Beta

PRINCIPAL INVESTIGATOR: Andrei Bakin, Ph.D.

CONTRACTING ORGANIZATION: Health Research, Incorporated
                                             Buffalo, NY 14263

REPORT DATE: June 2006

TYPE OF REPORT: Final

PREPARED FOR: U.S. Army Medical Research and Materiel Command
                         Fort Detrick, Maryland 21702-5012

DISTRIBUTION STATEMENT: Approved for Public Release;
                                        Distribution Unlimited

The views, opinions and/or findings contained in this report are those of the author(s) and should not be construed as an official Department of the Army position, policy or decision unless so designated by other documentation.

REPORT DOCUMENTATION PAGE

Form Approved
OMB No. 0704-0188

Public reporting burden for this collection of information is estimated to average 1 hour per response, including the time for reviewing instructions, searching existing data sources, gathering and maintaining the data needed, and completing and reviewing this collection of information. Send comments regarding this burden estimate or any other aspect of this collection of information, including suggestions for reducing this burden to Department of Defense, Washington Headquarters Services, Directorate for Information Operations and Reports (0704-0188), 1215 Jefferson Davis Highway, Suite 1204, Arlington, VA 22202-4302. Respondents should be aware that notwithstanding any other provision of law, no person shall be subject to any penalty for failing to comply with a collection of information if it does not display a currently valid OMB control number. **PLEASE DO NOT RETURN YOUR FORM TO THE ABOVE ADDRESS.**

1. REPORT DATE	2. REPORT TYPE	3. DATES COVERED
01-06-2006	Final	15 May 2002 – 14 May 2006

4. TITLE AND SUBTITLE

p38 Mitogen-activated Protein Kinase in Metastasis Associated with Transforming Growth Factor Beta

5a. CONTRACT NUMBER

5b. GRANT NUMBER
DAMD17-02-1-0602

5c. PROGRAM ELEMENT NUMBER

6. AUTHOR(S)

Andrei Bakin, Ph.D.

5d. PROJECT NUMBER

5e. TASK NUMBER

5f. WORK UNIT NUMBER

7. PERFORMING ORGANIZATION NAME(S) AND ADDRESS(ES)

Health Research, Incorporated
Buffalo, NY 14263

8. PERFORMING ORGANIZATION REPORT NUMBER

9. SPONSORING / MONITORING AGENCY NAME(S) AND ADDRESS(ES)
U.S. Army Medical Research and Materiel Command
Fort Detrick, Maryland 21702-5012

10. SPONSOR/MONITOR'S ACRONYM(S)

11. SPONSOR/MONITOR'S REPORT NUMBER(S)

12. DISTRIBUTION / AVAILABILITY STATEMENT
Approved for Public Release; Distribution Unlimited

13. SUPPLEMENTARY NOTES
Original contains colored plates: ALL DTIC reproductions will be in black and white.

14. ABSTRACT Malignant breast cancers express high levels of transforming growth factor beta1 (TGF-β1). TGF-β1 is a potent tumor suppressor, but, paradoxically, it has been implicated in metastasis by stimulating epithelial to mesenchymal transition (EMT), cell migration, invasion, and changes in tumor microenvironment. The goal is to develop therapies that selectively suppress oncogenic function of TGF-β1. The premise to this study was our original observation that inhibition of p38 mitogen-activated protein kinase (p38MAPK) selectively blocked TGFβ-induced EMT and cell migration but not growth-inhibitory function of TGF-β1. This suggested that the p38MAPK pathway is critical for oncogenic function of TGF-β1. The purpose of this proposal was to define in vitro and in vivo the role of the p38MAPK pathway in oncogenic function of TGF-β1 in metastasis. We provide evidence that autocrine TGF-β1-MAPK signaling in breast cancer cells contributes to tumor cell migration, invasion, and, importantly, to tumor angiogenesis. The mechanisms involve at least two distinct pathways mediated by MMP9/gelatinase-B and p38MAPK. p38MAPK is required for cell motility and tumor angiogenesis but it is dispensable for regulation of MMP9. MEK-ERK and TAK1 contribute to MMP9 expression. Thus, MEK-ERK, TAK1, and p38MAPK represent potential targets for anticancer/metastastic therapy associated with oncogenic TGF-β1.

15. SUBJECT TERMS
Breast Cancer

16. SECURITY CLASSIFICATION OF:			17. LIMITATION OF ABSTRACT	18. NUMBER OF PAGES	19a. NAME OF RESPONSIBLE PERSON USAMRMC
a. REPORT	**b. ABSTRACT**	**c. THIS PAGE**			**19b. TELEPHONE NUMBER** *(include area code)*
U	U	U	UU	103	

Standard Form 298 (Rev. 8-98)
Prescribed by ANSI Std. Z39.18

Table of Contents

Introduction

Metastatic mammary tumor cells express high levels of transforming growth factor beta1 (TGF-b1). Although TGF-b1 is a potent tumor suppressor, it can promote formation of highly metastatic tumors by stimulating an epithelial to mesenchymal transition (EMT), migration, invasion, and changes in tumor microenvironment. The molecular mechanisms of EMT, cell migration and invasion induced by TGF-b1 are not well understood. Given the dual function of TGF-b1, it is important to develop therapies that suppress oncogenic function of TGF-b and enhance tumor suppressor function. Our preliminary studies showed that pharmacological inhibitors of the p38 mitogen activated protein kinase (p38MAPK) pathway inhibited TGFb-induced cell migration but did not affect ability of TGF-b1 to inhibit cell growth. We hypothesized that that the p38MAPK pathway plays a critical role in oncogenic function of TGF-b1 and may represent a potential target for selective therapeutic intervention. The purpose of this proposal was (1) to examine *in vitro* the role of the p38 MAPK pathway in EMT, tumor cell motility and invasiveness, and (2) to evaluate the role of p38 MAPK in tumor growth and metastasis *in vivo*.

Body

To investigate the role of the p38 MAPK pathway in TGF-b-mediated metastasis we used breast cancer cell line MDA-MB-231, which express TGF-b1 receptors and exhibits TGF-b1 responses including cell migration and invasion. Additional cell lines were used to investigate the role of p38MAPK in EMT (NMuMG mouse mammary epithelial cells, SiHa cervical carcinoma cells, A549 lung carcinoma cells), and cell migration/invasion (4T1 and EMT6 mouse mammary carcinoma cells).

Task 1. To examine *in vitro* the role of the p38MAPK pathway in tumor cell motility and invasiveness.
   a. Examine the effect of p38MAPK inhibitors on motility, invasiveness and growth of tumor cells.
   b. Engineer retroviruses expressing dominant negative (DN) and constitutively active mutants. These retroviruses will encode Enhanced Green Fluorescent Protein (EGFP) for subsequent selection by flow cytometry.
   c. Generate cell lines by retroviral infection of tumor cells. Characterize cell lines regarding the level of expression of dominant negative proteins and their effect on p38MAPK activity.
   d. Examine the spreading, motility and invasiveness of engineered tumor cells.

Task 2. To evaluate the effect of p38MAPK inhibitors on tumor growth and metastasis *in vivo*.
   a. Examine the effect of p38MAPK inhibitors on metastasis formation and tumor growth in mice.
   b. Evaluate the role of p38MAPK in metastasis using genetically engineered mammary tumor cell lines. We will use mouse and human mammary tumor cell lines expressing dominant negative mutants obtained and characterized in Task 1.

Table 1. Constructs for Task1.

Construct	Mutation	Tag
ALK5-K232R	DN ALK5/TbRI, ATP-binding deficient	HA at C-terminus
ALK5-T204D	CA ALK5/TbRI, activation loop	HA at C-terminus
TbRII-K277R	DN-TbRII, ATP-binding deficient receptor	HA at C-terminus
TAK1-K63W	Inactive (DN) TAK1	No tag
MKK3AL and MKK6AL	Inactive MKK3 and MKK6	HA, N-terminus
p38AGF	Inactive p38MAPK, Ala/Phe of ThrGlyTyr	Flag, N-terminus

The experimental design is presented in Figure 1. The TGF-b1-p38MAPK pathway was modulated by introduction of dominant-negative (DN) and constitutively active (CA) mutants of TGF-b1 type I (ALK5) and type II receptor and kinases in the p38MAPK cascade: TGF-b-activated kinase 1 (TAK1), Mitogen-activated protein kinase kinase 3 and 6 (MKK3, MKK6), and p38MAPK (see Table 1 and Figure 1). Cells were infected with retroviruses and GFP-positive cells were selected by flow cytometry. Selection was repeated twice and produced more than 98% pure population of GFP-positive cells (see Figure1).

Fig. 1. (A) Kinase mutants of TGF-β type I receptor (TβRI/Alk5), and dominant-negative mutants of TAK1, MKK6, and p38 MAPK (see panel B) were subcloned in the pBMN-IRES-EGFP bi-cistronic retroviral vector. Amphitropic retroviruses were generated using Phoenix cells. EGFP-positive cells were selected after two repeats of FACS.

TGF-b-p38MAPK signaling contributes to EMT and cell migration

Initial studies with p38MAPK kinase inhibitors (SB203580, SB202190, PD169316) showed that blockade of p38MAPK signaling inhibits TGF-b-induced epithelial to mesenchymal transdifferentiation (EMT) [1] and cell migration [1, 2]. Our study has provided evidence that TGF-b1 activates p38MAPK pathway in epithelial and fibroblastic cell lines [1]. The dynamics is similar to Smad2/3 phosphorylation and can be blocked by dominant-negative (DN) TGF-b type II or I receptors [1]. Inhibition of the p38MAPK pathway reduces TGFb-mediated expression of fibronectin without inhibition of Smad2/3 phosphorylation (Figure 2).

Fig. 2. Effect of p38MAPK inhibitor SB202190 on expression of fibronectin (A) and phosphorylation of Smad2/3 (B) in cells treated with 2 ng/ml TGF-β1.

Expression of kinase-inactive TbRII-K277R or ALK5-K232R (DN-TbRI) blocked EMT and activation of p38MAPK, whereas expression of constitutively active ALK5-T204D resulted in EMT and phosphorylation of MKK3/6 and p38MAPK [1]. Expression of kinase-inactive MKK3 or MKK6 inhibited EMT and the reorganization of the actin cytoskeleton (formation of stress fibers) [1]. Furthermore, we found that dominant negative Rac1N17 blocked TGFb-induced activation of the p38MAPK pathway and EMT, suggesting that Rac1 mediates activation of the p38MAPK pathway in mammary epithelial cells. Thus, these studies implicated the Rac1-MKK3/6-p38MAPK pathway in TGFb-mediated EMT and cell migration.

Fig. 3. Effect of kinase-mutants on phosphorylation of Smad2/3 (A) and expression of fibronectin in MDA-MB-231 cells treated with 2 ng/ml TGF-β1, and 20 uM of H-7 or 10 uM SB202190.

In a separate study, we have shown that kinase-active ALK5-204D can rescue dominant-negative effects of TbRII-K277R on cell migration [2]. This effect was associated with MAPK and phosphatidyl-inositol-3 kinase (PI3K) signaling, as application of kinase inhibitors blocked ALK5-204D-mediated cell migration [2]. ALK5-204D increased a basal phosphorylation of Smad2/3 and expression of fibronectin, an extracellular matrix protein, which is involved in tumor metastasis. Kinase-inactive ALK5-K232R and TbRII-K277R or treatment 5

with p38MAPK inhibitors blocked TGFb-induced expression of fibronectin, an extracellular matrix protein, which is involved in tumor metastasis (see Figure 3), suggesting a critical role for this pathway in the tumor promoting activity of TGF-b1. We found that p38MAPK inhibitors do not affect the antiproliferative activity of TGF-b1.

Thus, these studies further indicated that the TGF-b-p38MAPK pathway contributes to pro-metastatic properties of carcinoma cells including breast cancer.

TGF-b-p38MAPK signaling regulates the actin cytoskeleton

The actin cytoskeleton is critically involved in cell motility, invasion, proliferation and cell survival. Our initial study has shown that formation of actin stress fibers in response to TGF-b1 is blocked by p38MAPK inhibitors and DN-MKK3/6 [1]. Subsequently, we found that formation of actin stress fibers requires *de novo* protein synthesis [3]. The analysis of gene expression showed that TGF-b1 up-regulates expression of high-molecular-weight tropomyosins and this is reduced by application of p38MAPK inhibitors [3]. Tropomyosins are actin-binding proteins that stabilize actin filaments and are required for cytokinesis, migration and invasion [4]. However, formation of stable actin filaments like stress fibers has been associated with reduced cell motility [5]. We found that high levels of tropomyosins increase formation of stress fibers and reduce cell motility [3]. However, in MDA-MB-231 cells the ability of TGF-b1 to induce stress fibers is negatively regulated by MEK-ERK signaling [3]. Blockade of MEK-ERK signaling using MEK inhibitor U0126 increases tropomyosin levels and results in stress fibers in response to TGF-b1 in MDA-MB-231 cells [3]. We further show that Smad3/4 signaling also contributes to transcription of Tpm1 and Tpm2 genes [3]. Transfection of small interfering RNA to Smad4 or tropomyosins blocks TGF-b1-mediated stress fiber formation [3].
These studies have shown that p38MAPK and Smad3/4 mediate induction of tropomyosins and regulation of cell motility by TGF-b1. The levels of tropomyosins correlate with TGF-b1 induction of stress fibers and control of cell motility [3].
To address the role of tropomyosins in TGF-b1 control of cell motility we investigated tropomyosin expression, stress fiber response, and cell motility in several epithelial cell lines. We have discovered that in metastatic breast and colon cell lines TPM1 gene is silent and this is associated with hypermethylation of the promoter [6]. Demethylation of DNA using 5-aza-deoxycytidine (5-aza-dC) restored ability of TGF-b1 to induce stress fibers without changes in Smad activation and MEK-ERK signaling [6]. We have identified a CpG island in the TPM1 promoter and have shown that it is highly methylated in metastatic cell lines [6]. Re-expression of TPM1 gene product in MDA-MB-231 cells using Tet-Off system reduced cell motility and increased stress fibers. In a separate study (submitted for publication), we have shown that TPM1 controls cell invasion by regulating focal adhesions and activity of matrix metalloproteinases (MMP9). Together, these studies show that p38MAPK and Smad signaling are critically involved in the multi-level control of cell motility, adhesion, and invasion.

TGF-b-p38MAPK signaling is important for tumor cell invasion and metastasis

To study the contribution of TGFb-p38MAPK signaling in invasion, we have used metastatic breast cancer MDA-MB-231 cell line. These cells were genetically modified to express kinase mutants of the TGF-b type I receptor (TbRI), Alk5 (see Figure1 and Table 1). The manuscript describing these studies has been submitted for publication. Matrigel invasion assays showed that autocrine TGF-b1 signaling enhances invasiveness of cells. DN-ALK5 reduced basal and TGF-b1-induced invasion of transwells coated with Matrigel (Figure 4). Active ALK5-T204D increased cell invasiveness. This was associated with up-regulation of proMMP9/gelatinase B, but not in gelatinase A (Figure 4C, D).
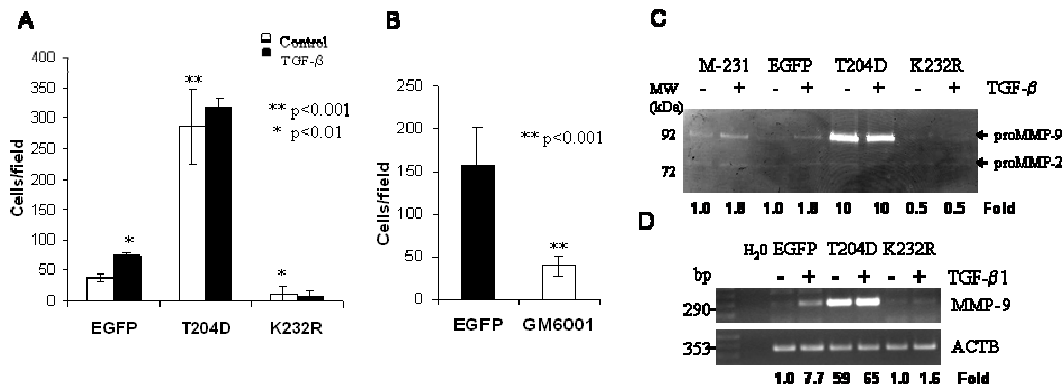
Fig. 4. Invasion of MDA-MB-231 cells. (A) DN-ALK5 blocks whereas CA-ALK5 promotes invasion of Matrigel transwells. Triplicate experiment, repeated at least two times. Five fields are counted. (B) MMP inhibitor GM6001 blocks cell invasion. (C) Gelatin zymography assay shows that TGF-b1 up-regulates MMP9, but not MMP2. This is blocked by DN-ALK5. (D) RT-PCR shows that TGF-b1 regulates MMP9 mRNA level.

p38MAPK has been implicated in regulation of matrix proteases contributing to the invasive phenotype of carcinoma cells [7, 8]. Studies with using pharmacological MAPK inhibitors showed involvement of MEK-ERK and p38MAPK but not JNK in regulation of MMP9 (Figure 5). However, p38MAPK inhibitors (SB203580 and SB202190) reduced MMP9 levels only when they also affected
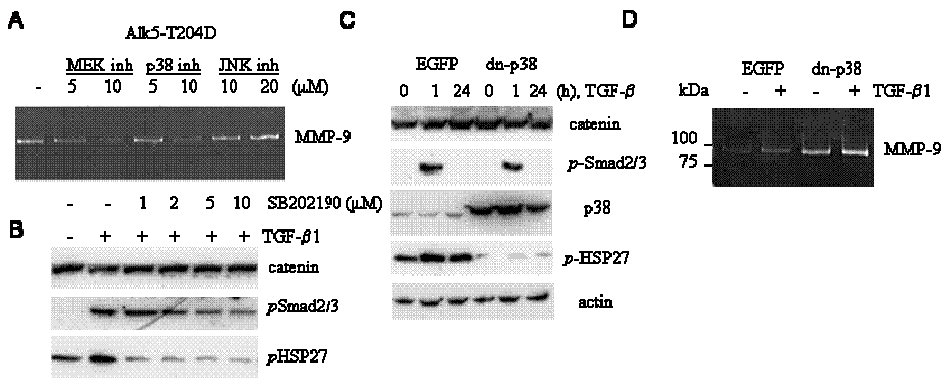
Fig. 5. (A) Gelatin zymography of 48h-conditioned media of MDA-MB-231-ALK5-T204D cells treated with kinase inhibitors U0126, SB202190, SP600125 (JNK). (B) Immunoblot of phospho-Smad2/3, phospho-HSP27, and alpha-catenin (control) in MDA-MB-231 cells treated with SB202190. (C) Immunoblot of in cells expressing DN-p38alpha. (D) zymography of 48h-conditioned media from MDA-MB-231-DN-p38 cells.

activity of receptor-mediated phosphorylation of Smad2/3 (Figure 5A, B). In cells expressing DN-p38alpha (p38AGF), production of MMP9 was not reduced, although phosphorylation of HSP27 was effectively blocked (Figure 5C, D). These results were confirmed using siRNA to p38alpha (data not shown). However, cells expressing DN-p38 were impaired in cell motility and invasion. Together, these studies show that p38MAPK is a critical factor in cell motility, and, therefore, cell invasion although it is not involved in regulation of MMP9 by TGF-b1.

TGF-b signaling in metastasis

The role of TGF-b signaling in metastasis was investigated using genetically modified MDA-MB-231 cells in tail-vein and orthotopic xenograft models in SCID mice. Briefly, tumor cells (1×10^6) re-suspended in 0.1 ml of sterile Hank's solution were injected using a 28-G needle into tail vein of 8 week-old female SCID mice. Mice were sacrificed 4 weeks thereafter, and lungs were stained with 15% Indian black ink via trachea. Macrometastic lesions on lung surfaces were counted from all four lung leaves. These studies showed a 4-fold increase in lung surface metastases in Alk5-T204D-injected mice (Figure 6).

Tumor take, growth, and formation of metastases to lungs, bone, liver, and lymph nodes by the control and
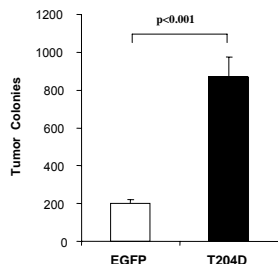
Fig.6. MDA-MB-231 cells expressing active TβRI-T204D receptor and control EGFP cells were injected in tail vein of SCID mice (1×10^6/mice, 8mice/group). Four weeks later mice were euthanized and lungs were stained with 15% black Indian ink. Lung surface macro-metastases were counted. $P<0.001$ compared to control using ANOVA test.

genetically modified MDA-MB-231 cells were examined in a spontaneous metastasis model [9] by placing tumor cells in mammary fat pad of female SCID mice (Fig. 6). Briefly, exponentially growing breast cancer cells (1×10^6) in 0.1 ml Hank's buffered salt solution (HBSS) were inoculated into the surgically exposed mammary fat pad (m.f.p.) of 7-8 weeks old female SCID mice. The growth of primary tumors was monitored weekly by measuring tumor diameters with calipers. Primary tumors were removed at 1cm of diameter (typically, 30-35 days after inoculation) and frozen in liquid N_2 or formalin-fixed. After 4-5 weeks, the mice were sacrificed and lungs, bones, livers, and
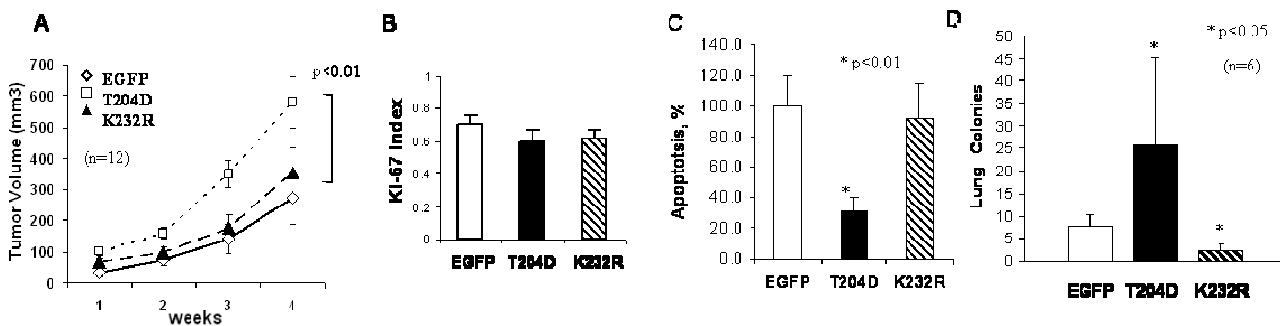
Fig. 7. Orthotopic xenograft model of MDA-MB-231 cells in SCID mice. (A) Control EGFP and ALK5 mutant-expressing cells were placed into mammary gland fat pad of 8-week old female SCID mice (1×10^6/mice, 12 mice/group). Tumor size was measured with calipers. (B) Proliferation index was determined as ratio of Ki67-positive cells relative to total cell numbers counted at 20X magnification. 5 fields per slide, at least 300 cells per field. (C) Apoptotic index in tumors was determined by TUNEL staining at 400X magnification. (D) Lung surface metastases, 6 mice/group. P values were calculated using ANOVA test.

lymph nodes were collected and histological analysis for metastases was performed at the RPCI pathology core facility. Mammary tumors were also evaluated by light microscopy and immunohistochemistry (IHC). Twelve female SCID mice per group were used. ALK5-T204D xenografts showed reduced latency time for appearance of palpable tumors and enhanced growth of primary tumors without an effect on Ki67 proliferation index (Figure 7). TUNEL staining of apoptotic cells within the tumor showed reduced level of apoptosis in active ALK-T204D tumors (Figure 7C). The analysis of lung surface metastasis using Indian ink staining showed a reduction in a number of metastasis of DN-ALK5 and increased metastases in active ALK5 tumors. These findings indicate that autocrine TGF-b1 signaling enhances metastasis.

MMP9 in TGFb-mediated metastasis and tumor angiogenesis

TGF-b1 treatment as well as constitutively active ALK5-T204D up-regulated MMP9 mRNA levels (Figure 8A). To address the role of MMP9 in TGF-b-mediated metastasis, EGFP and ALK5-T204D expressing MDA-MB-231 cells were infected with retrovirus encoding siRNA to MMP9. RT-PCR analysis showed suppression of MMP9 without off-target effect on MMP2 and PAI-1 (Figure 8A). Accordingly, siRNA-MMP9 reduced invasion of Martrigel-coated transwells but did not affect cell migration on plastic (Figure 8B, C). These findings show that MMP9 is required for 3-D migration through etracellular matrix (ECM) but not migration on plastic.
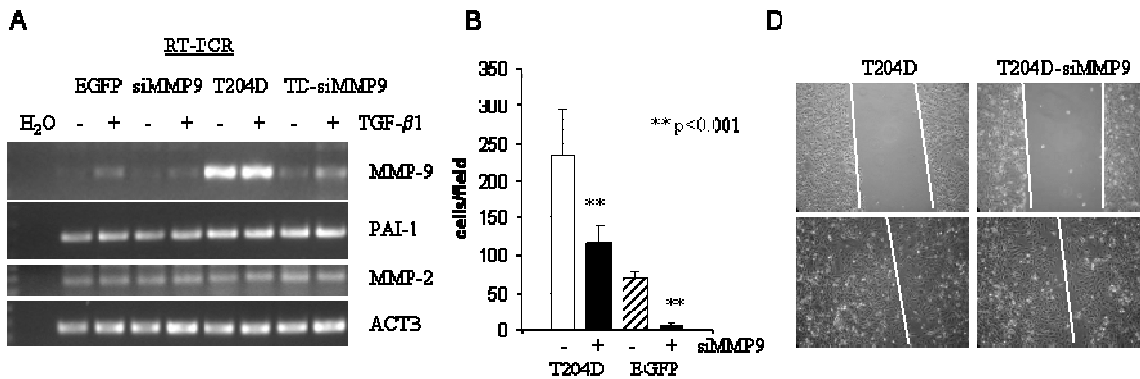
Fig. 8. Suppression of MMP9 using siRNA. (A) RT-PCR analysis of MMP9, MMP2, and PAI-1 in MDA-MB-231 cells expressing EGFP, EGFP plus siMMP9, ALK5-T204D, and ALK5-T204D plus siMMP9. (B) Invasion of Matrigel-coated transwells. Incubation time was 24 h, 1x10^5 cells loaded on membrane. Experiments were done in triplicate and cells were counted from five fields for each membrane. (C) Wound closure in monolayers of MDA-MB-231 expressing ALK5-T204D, and ALK5-T204D plus siMMP9.

siRNA to MMP9 (siMMP9) reduced lung metastases of ALK5-T204D cells in both tail-vein (experimental metastasis) and orthotopic (spontaneous metastasis) models in SCID mice (Fig. 9).
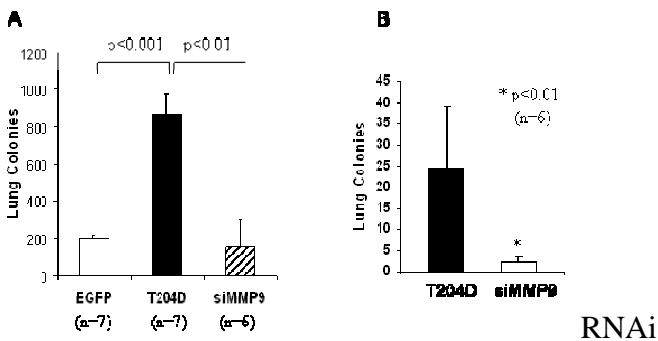
Fig. 9. (A) Lung surface metastasis of MDA-MB-231 cells injected into the tail-vein of SCID mice. Cells express EGFP (control), EGFP and ALK5-T204D (T204D), and EGFP, ALK5-T204D plus siMMP9 (siMMP9). (B) Lung surface metastasis of MDA-MB-231 cells (T204D and siMMP9) placed orthotopically in mammary gland fat pads of SCID mice.

RNAi to MMP9 (shMMP9) also significantly reduced xenograft growth (Fig. 10), although cell growth in culture and Ki67 index were not affected (data not shown). The analysis of tumor tissues after CD31 staining for endothelial cells showed a significant decrease of microvessel density in siMMP9 xenografts (Fig. 10). The microvessel density was also reduced in ALK5-K232R xenografts (Figure 10). Microvessel density affects tumor oxygenation. We hypothesized that the extensive vasculature found in T204D tumors may enhance tumor oxygenation. To test this possibility the oxygenation of tumors was compared using hypoxyprobe assay [10]. The analysis showed the presence of extensive areas of hypoxia within the EGFP tumors compared to the T204D tumors (Figure 10C), confirming the results of CD31 and TUNEL staining.
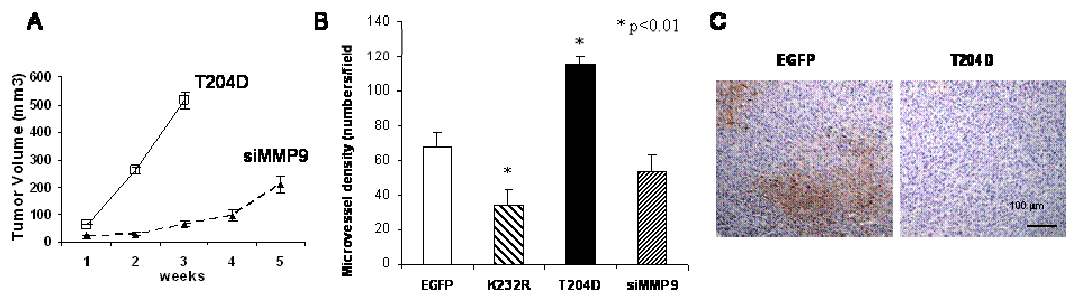
Fig. 10. (A) The volume of MDA-MB-231 xenografts (T204D and T204D-siMMP9). **(B)** Tumor microvessel density (CD31 staining) was determined at 400X magnification in 8 fields/section. The results are presented as mean number of microvessels per field (0.2mm3). **(C)** Pimonidazole staining (hypoxyprobe, brown staining) shows a reduced level of hypoxia in ALK5-T204D compared to EGFP tumors. Bar, 100µm.

Together these findings show that the TGF-b1 pathway plays an important role in regulation of tumor neovasculature and MMP-9 is a critical component of this program.

p38MAPK in TGFb-mediated metastasis and tumor angiogenesis

To address the role of p38MAPK in metastasis, MDA-MB-231 cells expressing dominant negative mutant p38alpha (p38AGF) and cells expressing DN-TAK1 (TAK1-K63W) were used in spontaneous and experimental metastasis studies (Fig. 15). Flag-tagged p38AGF and TAK1-K63W were expressed using retroviral vector pBMN-IRES-EGFP, which also allows expression of EGFP from Internal Ribosome Entry Site (IRES), see Fig. 1. Expression of DN-p38 decreased phosphorylation of downstream target HSP27 but did not affect phosphorylation of Smad2/3 (Fig. 5C) and did not block up-regulation of MMP9 (Fig. 5D). These data indicate that p38MAPK does not affect activation of Smads and that p38 is not required for regulation of MMP9.

Expression of DN-mutants delayed appearance of palpable tumors and xenograft growth when cells were placed orthotopically in mammary gland fat pads of SCID mice (Fig. 11 A-B). In experimental metastasis
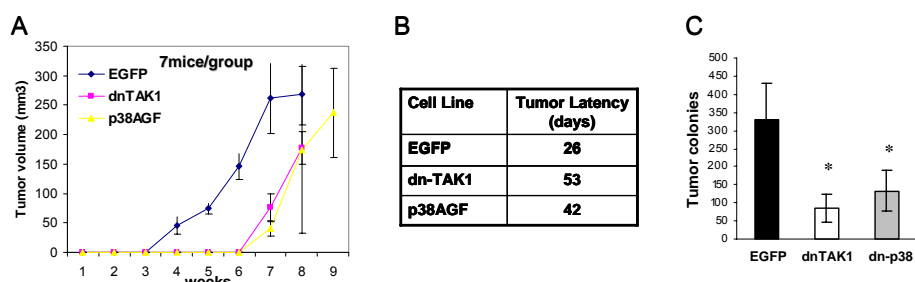
Fig. 11. (A) The growth of tumor cell xenografts expressing EGFP control, DN-TAK1, and DN-p38. **(B)** Tumor latency represents the time of appearance of palpable tumors. **(C)** Experimental metastasis model. MDA-MB-231 cells were injected in tail-vein of SCID mice (1x10^6/mice, 8mice/group). Four weeks later mice were euthanized and lungs were stained with 15% black Indian ink. Lung surface macro-metastases were counted. P<0.001 compared to control using ANOVA test.

model, DN-TAK1 and DN-p38 cells injected via tail vein formed significant fewer lung surface metastases than control EGFP cells (Fig. 11C). These studies provide evidence that p38MAPK contributes to TGF-b-mediated metastasis although the mechanism is likely to be independent of MMP9.

To address the reason for reduction in tumor growth, we analyzed microvascular density in tumor sections after CD31 staining. The analysis showed a decrease in the level of microvascular density in
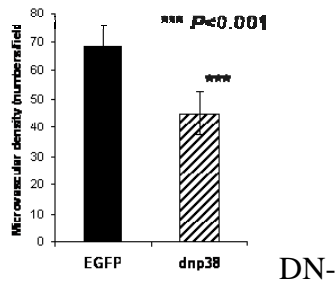
Fig. 12. (A) Microvessel density in xenografts of MDA-MB-231 control (EGFP) and DN-p38MAPK cells. The analysis of CD31 staining was done at 400X magnification in 8 fields/section. The results are presented as mean number of microvessels per field (0.2mm3).

DN-p38MAPK compared to control EGFP xenografts (Figure 12). Whether this is associated with regulation of VEGF expression or other factors is subject of further investigation. One approach is to compare expression profiles of control, K232R, siMMP9, and DN-p38MAPK tumors. Total RNAs from all these samples are collected and will be analyzed by Affymetrix microarrays.

Together these studies suggest that autocrine TGF-b1 signaling in tumor cells contributes to tumor angiogenesis. The mechanism involves at least two distinct pathways controlled by MMP9 and p38MAPK. Importantly, TGF-b1 up-regulation of MMP9 does not require p38MAPK.

Description of Experimental Procedures

Transcription Assay. The transcriptional assays will be performed as described in [3] using the following luciferase reporters: 3TP-Lux [11] containing a fragment of PAI-1 promoter was a gift of J. Massague, Memorial Sloan-Kettering Cancer Institute, New York, NY; pGL2-MMP-9-Lux containing a 670bp fragment of the human MMP-9 promoter was obtained from J. Bromberg, Memorial Sloan-Kettering Cancer Institute, New York, NY. Firefly luciferase (Luc) and *Renilla reniformis* luciferase (Rl) activities in cell lysates are measured using the Dual Luciferase Reporter Assay System (Promega) and presented as Relative Luciferase Units. All assays are done in triplicate wells and each experiment is repeated at least twice.

RT-PCR analysis. RNA extraction is performed using Versagene RNA kit (Centra, Minneapolis, MN). Transcripts are amplified using 50 ng/µL of total RNA and one-step RT-PCR system from Invitrogen. Primer sequences: β-actin (ACTB), Acc#NM_007393, forward: GCTGGTCGTCGACAACGGCTC, reverse: CAAACATGATCTGGGTCATCTTTTC; MMP-9, Acc#NM_004994, forward: TTCATCTTCCAAGGCCAATC, reverse CAGAAGCCCCACTTCTTGTC.

Wound closure assay. The assay is performed as described previously [1]. MDA-MB-231 cells are seeded in 12-well plates and pre-incubated for 24h in serum-free IMEM (Invitrogen) prior to wounding with plastic tip across the cell monolayer. The wound closure is estimated as the ratio of the remaining wounded area relative to the initial area. Experiments are repeated 3 times.

Proliferation assay. Cell proliferation is measured in MTS assays according to manufacturer's protocol (Promega).

Matrigel invasion assay. Cells are mildly trypsinized and washed twice in IMEM with 0.1% BSA. Cells $(1x10^5)$ are seeded in the upper chamber coated with Matrigel (Calbiochem). After 20h of incubation, the non-migrating cells in the upper chamber are scraped away and cells present on the lower surface of the insert are stained with Diff-Quik Stain (Biochemical Sciences Inc., Swedesboro, NJ). Cells are counted from 5 random fields in three wells.

Gelatin zymography. Conditioned media of cells incubated in serum-free IMEM for 48h is removed and centrifuged. SDS-PAGE gels are co-polymerized with gelatin at a final concentration of 1 mg/ml. After electrophoresis, the gels are renatured in 2.5% Triton X-100 and incubated at 37^oC for 24h in 5 mM $CaCl_2$ and 50mM Tris-HCl buffer, pH 7.5, containing 0.05% NaN_3. The gels are stained with 0.5% Coomassie Blue R-250 and destained in 10% methanol and 5% acetic acid in water. Gelatinolytic activities are detected as transparent bands on the blue background. The band densities are evaluated using NIH-Image software.

Animal studies using an orthotopic xenograft model. Female SCID/CB17 mice, 8 weeks of age, are obtained from a colony of SCID/CB17 mice that is bred and maintained at the Department of Laboratory Animal Resources (DLAR) facility at the RPCI. All animals are kept three to five mice per cage in microisolator units and provided with water and food *ad libitum* according to a protocol approved by the Institute Animal Care and Use Committee at RPCI. The facility has been certified by the American Association for Accreditation of Laboratory Animal Care and in accordance with current regulation and standards of the U.S. Department of

Agriculture and the U.S. Department of Health and Human Services. Exponentially growing breast cancer cells (1×10^6) in 0.1 ml Hank's buffered salt solution are inoculated into the surgically exposed mammary fat pad (m.f.p.) of 7- to 8-week-old female SCID mice. The growth of primary tumors is monitored by measuring tumor diameters with electronic calipers every 3-4 days continuously from the third week after injection. Volumes are calculated using the formula (length)x(width)^2 /2. Primary tumors are removed at 1 cm diameter, ~30-35 days after appearance of palpable tumors. After 4-5 weeks, the mice are sacrificed, lungs, spleens, livers are collected for histological analysis at the RPCI Pathology Core Facility.

Immunohistochemistry. Tumor specimens are fixed immediately in 10% (v/v) formalin and then embedded in paraffin. For CD31 staining, harvested tumors are fixed in Zink fixative (BD Biosciences). Before immunostaining, conventional H&E-stained sections are prepared for general histopathologic evaluation. For Ki-67 staining, formalin-fixed tissue sections are incubated for 1h at room temperature with the rabbit polyclonal primary antibodies to human Ki-67. Biotinylated secondary goat anti-rabbit antibodies are applied for 30 mins followed by 30 min incubation with the ABC reagent (Vector Labs). Ki-67 labeling index is calculated as the percentage of positive tumor nuclei divided by the total number of tumor cells examined. At least 1,000 tumor cells per specimen are examined in five random fields using light microscopy at 400X magnification. For CD31 staining harvested tumors are fixed in Zink fixative for overnight and then processed for paraffin sections. The rat antimouse primary antibody to CD31 (BD Biosciences) is applied for 1h at room temperature followed by 30 min incubations with biotinylated secondary antirat antibody (BD Biosciences) and the streptavidin complex (Zymed). The analysis of microvessel density was performed as described in [12]. Tumor sections were scanned at 100X magnification for the areas containing the highest number of discrete CD31-positive microvessels ("microvessel hot spots"). Necrotic and immediately adjacent areas where microvessels are sparse were excluded from counting. CD31-positive vessels were counted at 400X magnification in 8 fields of each tumor section. The results were presented as mean number of microvessels/field (0.2mm^3) ± St Dev.

Apoptosis assay. TUNEL staining is used for *in situ* detection of apoptotic cells in paraffin sections of tumor tissues using the ApopTag in situ detection kit (ApopTag Plus Peroxidase In Situ Apoptosis Detection Kit, Chemicon, cat # S7101) following the manufacturer's recommendations. Cells are examined in five random fields using light microscopy at 400-fold magnification.

Statistical Analysis. Data are compared using the Student's t test. Differences are considered significant when $P < 0.05$.

Key Research Accomplishments

- p38MAPK signaling contributes to TGF-b-mediated epithelial-mesenchymal transition (EMT) and cell migration but not to cell-cycle arrest in response to TGF-b1. We show that p38MAPK mediates actin cytoskeleton remodeling in response to TGF-b1 by contributing to expression (fibronectin, tropomyosin) and signaling (phosphorylation of HSP27) programs.
- TGF-b-p38MAPK signaling is important for tumor cell invasion and metastasis. Expression of constitutively active T204D mutant of TGF-b type I receptor (TbRI/ALK5) increases lung macro-metastases in spontaneous and experimental metastasis models in part by enhancing migration and invasion of tumor cells via the p38 MAPK pathway. Dominant negative ALK5-K232R and DN-p38MAPK reduce cell migration, invasion, and formation of metastasis.
- TGF-b1 stimulates invasiveness of breast cancer cells in part by up-regulating MMP9 levels. Suppression of MMP9 by small interfering RNA (siRNA) reduces tumor cell invasiveness. p38 MAPK is not required for up-regulation of MMP9, although it is important for invasive migration.
- TGF-b signaling in tumor cells regulates tumor angiogenesis and MMP9 is important factor in this program. Stable expression of small interfering RNA to MMP9 reduces tumor growth, tumor angiogenesis, and formation of metastases by MDA-MB-231 cells in SCID mice.
- p38MAPK contributes to TGF-b-mediated metastasis although the mechanism is likely to be independent of MMP9. Dominant negative TAK1 and p38 MAPK reduce growth of breast carcinoma xenografts in SCID

12

mice. In experimental metastasis model in SCID mice, MDA-MB-231 cells expressing DN-TAK1 or DN-p38 formed significantly reduced amount of lung surface metastases compared to control cells. DN-p38 does not block up-regulation of MMP9, although it effectively inhibits phosphorylation of HSP27.

- p38MAPK contributes to TGF-b-mediated tumor angiogenesis. DN-p38MAPK reduces tumor growth and tumor microvascular density. The mechanism is likely to be independent of MMP9.
- These studies provide evidence that autocrine TGF-b1 signaling in tumor cells contributes to breast cancer progression by regulating tumor angiogenesis. The mechanism involves at least two distinct pathways mediated by MMP9 and p38MAPK. Thus, these studies highlight new venues for future research on the mechanism of TGF-b1 function in cancer progression as well as provide directions for development of drugs specifically affecting pro-oncogenic function of TGF-b1.

Reportable Outcomes

Manuscripts:
1. **Bakin** A., Rinehart, C., Tomlinson A. K., Arteaga C. L., p38 mitogen-activated protein kinase is required for TGFβ-mediated fibroblastic transdifferentiation and cell migration. *J Cell Sci*. 2002 Aug 1;**115**(Pt 15):3193-206.
2. Dumont N., **Bakin** A.V., and Arteaga CL. Autocrine TGF-β signaling mediates smad-independent motility in human cancer cells. *J Biol Chem* 2003 Jan 31;278(5):3275-85.
3. **Bakin** AV, Safina A, Rinehart C, Daroqui C, Darbary H, Helfman D. A critical role of tropomyosins in TGF-(beta) regulation of the actin cytoskeleton and cell motility in epithelial cells. Mol Bio Cell, 15:4682-4694, 2004.
4. **Bakin** AV, Stourman V, Sekhar RK, Rinehart C, Yan X, Meredith MJ, Arteaga CL, Freeman ML. Smad3-ATF3 signaling mediates TGF-β suppression of genes encoding phase ii detoxifying proteins. Free Radical Biology and Medicine 38:375-387, 2005.
5. Varga A.E., Quan L., Stourman NV, Safina A, Li X., Sossey-Alaoui K., **Bakin** AV. Silencing of the tropomyosin 1 gene by DNA methylation alters tumor suppressor function of TGF beta. *Oncogene*, 2005, **24** (32), 5043-5052.
6. Rossi MR, Ionov Y, **Bakin** AV, Cowell JK. Truncating mutations in the ACVR2 gene attenuates activin signaling in prostate cancer cells. *Cancer Genetics and Cytogenetics*, 2005, 123-129.
7. Sossey-Alaoui K, Ranalli TA, Li X, **Bakin** A, Cowell JK. WAVE3 promotes cell motility and invasion through the regulation of MMP-1, MMP-3 and MMP-9- expression. *Exp Cell Res*., 308:135-145, 2005.
8. Safina A., Vendette E., **Bakin** A.V. ALK5 promotes tumor angiogenesis by up-regulating matrix metalloproteinase-9 in tumor cells (submitted)
9. Zheng Q, Safina A, Bakin AV, Tumor suppressor function of tropomyosin in the TGF-β pathway. (submitted)
10. Safina A., Rinehart, C., Arteaga, C. L., **Bakin**, A.V. p38 MAPK, Sp1 and Smads contribute to TGFβ-induced expression of fibronectin. (in preparation)

Abstracts:
1. Bakin, A.V., Rinehart, C. TGFβ regulates expression of target genes and p38 MAPK signaling to induce changes in the actin cytoskeleton. AACR, 2003, Abstract #102164.
2. Bakin, A.V., Rinehart, C., Arteaga, C. L. p38Mapk, Sp1 and Smads contribute to TGFβ-induced expression of fibronectin. AACR Special Conference on the role of the TGFbeta superfamily in the pathogenesis of cancer and other diseases, January 15-19, 2003 La Jolla, CA
3. Bakin, A.V., Daroqui C., Safina A. TGF−β and ERK differentially regulate genes involved in the formation of stable actin filaments. Advances in Breast Cancer Research: Genetics, Biology, and Clinical Implications. October 8-12, 2003, Huntington Beach, CA.
4. Bakin, A.V., Daroqui C., Safina A. TGF−β and ERK signaling differentially regulate genes involved in actin stress fiber formation. Annual AACR meeting, 2004, Abstract # 130.

5. Bakin, A.V., Safina A., Daroqui C., Lei Q., Varga A., Helfman D., TGF-β regulation of epithelial cell motility via tropomyosin-mediated actin stress fibers. The 10th International Congress of the Metastasis Research Society "Progress Against Tumor Progresssion". September 17-20th, 2004. Genoa, Italy. Abstract #2 (Short talk).
6. Bakin AV, Varga A., Safina A., Zheng Q., The role of tropomyosin in metastatic switch in TGF-beta function during cancer progression. Annual AACR meeting, April 16-20th, 2005, Anaheim, CA. Abstract # 228.
7. Safina A., Vendette E., Varga A., Bakin AV, TGFb-p38MAPK signaling contributes to tumor invasion and pulmonary metastases by increasing MMP9 activity and cell motility. Annual AACR meeting, April 16-20th, 2005, Anaheim, CA. Abstract # 4347 (Minisymposium, Tumor Biology 30).
8. Bakin, AV, Zheng, Q, Varga, A V. A critical role of tropomyosin in TGF-beta-mediated control of cell invasion and metastasis. 97th Annual Meeting • April 1 - 5, 2006 Washington, DC. Abstract#2763.
9. Safina, A, Vandette, E, and Bakin AV. TGF-β-MAPK signaling enhances metastases by stimulating tumor cell invasion and changes in tumor microenvironment. 97th Annual Meeting • April 1 - 5, 2006 Washington, DC. Abstract#3524.
10. Varga, AE, Safina, AF, VanDette, EK, Bakin, AV. Rivalry between TGF-β1 and oncogenic Ras in actin cytoskeletal dynamics and cell migration. AACR Special Conference "TGF-beta in Cancer and Other Diseases". February 8-12, 2006, the Hyatt Regency, La Jolla, CA.
11. ERK and p38MAPK signaling are required for TGF-β-mediated tumor cell invasion and metastasis Bakin AV, Safina, AF, Vandette, EK. AACR Special Conference "TGF-beta in Cancer and Other Diseases". February 8-12, 2006, the Hyatt Regency, La Jolla, CA.
12. Eaton, M, Zheng, Q, Stourman, NV, Freeman, M, Bakin AV. ATF3 plays a critical role in TGF-beta-mediated regulation of glutathione levels in epithelial cells. AACR Special Conference "TGF-beta in Cancer and Other Diseases". February 8-12, 2006, the Hyatt Regency, La Jolla, CA.

The following materials have been generated:
1. Retroviral vectors based on pBMN-IRES-EGFP, which encode: TGF-β type I receptor wild type, Alk5-WT, and kinase-inactive Alk5-232R, kinase-active Alk5-204D; dominant-negative (DN) mutants for p38α, p38AGF; MKK3, MKK3AL; MKK6, MKK6AL; Rac1, RacN17; TGFbeta-activated kinase (TAK1), dominant-negative mutant TAK1-K63W; dominant-negative mutant PAK1-N205 (DN-PAK1).
2. MDA-MB-231 cell lines expressing wild type and mutants of ALK5 and TGF-β type II receptor; Rac1-N17; p38AGF; MKK6AL; DN-PAK1.
3. MDA-MB-231 expressing small interfering RNA to MMP9.
4. MDA-MB-231 Tet-Off cell lines. In these cells, expression of a gene of interest is controlled by a tetracycline-regulated promoter.

Conclusions

These studies provide evidence that autocrine TGF-b1 signaling in tumor cells contributes to breast cancer progression by regulating tumor cell migration and invasion, and by altering tumor microenvironment. We show that TGF-b1 signaling regulate tumor angiogenesis. The mechanisms involve at least two distinct pathways mediated by MMP9 and p38MAPK. We show that ERK and TAK1 are involved in regulation of MMP9. Although p38MAPK is not involved in MMP9 expression, it is required for expression of several genes involved in regulation of cell motility (tropomyosin) and tumor microenvironment (fibronectin). Thus, the TAK1-MKK6-p38 MAPK signaling cascade may represent a potential target for anticancer/metastastic therapy and the activity of this cascade may also serve as a marker of metastasis, and could be used for prognosis of breast cancer progression. These studies highlight new venues for future research on the mechanism of TGF-b1 function in cancer progression as well as provide directions for development of drugs specifically affecting pro-oncogenic function of TGF-b1.

References

1. Bakin, A.V., et al., *p38 mitogen-activated protein kinase is required for TGF{beta}-mediated fibroblastic transdifferentiation and cell migration.* J Cell Sci, 2002. **115**(15): p. 3193-3206.
2. Dumont, N., A.V. Bakin, and C.L. Arteaga, *Autocrine Transforming Growth Factor-beta Signaling Mediates Smad-independent Motility in Human Cancer Cells.* J. Biol. Chem., 2003. **278**(5): p. 3275-3285.
3. Bakin, A.V., et al., *A Critical Role of Tropomyosins in TGF-{beta} Regulation of the Actin Cytoskeleton and Cell Motility in Epithelial Cells.* Mol. Biol. Cell, 2004. **15**(10): p. 4682-4694.
4. Perry, S.V., *Vertebrate tropomyosin: distribution, properties and function.* J Muscle Res Cell Motil, 2001. **22**(1): p. 5-49.
5. Pawlak, G. and D.M. Helfman, *Cytoskeletal changes in cell transformation and tumorigenesis.* Curr Opin Genet Dev, 2001. **11**(1): p. 41-7.
6. Varga, A.E., et al., *Silencing of the Tropomyosin-1 gene by DNA methylation alters tumor suppressor function of TGF-[beta].* Oncogene, 2005. **24**(32): p. 5043-5052.
7. Johansson, N., et al., *Expression of collagenase-3 (MMP-13) and collagenase-1 (MMP-1) by transformed keratinocytes is dependent on the activity of p38 mitogen-activated protein kinase.* J Cell Sci, 2000. **113**(Pt 2): p. 227-35.
8. Huang, S., et al., *Urokinase plasminogen activator/urokinase-specific surface receptor expression and matrix invasion by breast cancer cells requires constitutive p38alpha mitogen-activated protein kinase activity.* J Biol Chem, 2000. **275**(16): p. 12266-72.
9. Price, J.E., et al., *Tumorigenicity and metastasis of human breast carcinoma cell lines in nude mice.* Cancer Res, 1990. **50**(3): p. 717-21.
10. Bhattacharya, A., et al., *Lack of Microvessels in Well-Differentiated Regions of Human Head and Neck Squamous Cell Carcinoma A253 Associated with Functional Magnetic Resonance Imaging Detectable Hypoxia, Limited Drug Delivery, and Resistance to Irinotecan Therapy .* Clin Cancer Res, 2004. **10**(23): p. 8005-8017.
11. Attisano, L., et al., *Identification of human activin and TGF beta type I receptors that form heteromeric kinase complexes with type II receptors.* Cell, 1993. **75**(4): p. 671-80.
12. Weidner, N., et al., *Tumor angiogenesis and metastasis--correlation in invasive breast carcinoma.* N Engl J Med, 1991. **324**(1): p. 1-8.

Appendices

Biographical Sketch
Reprints of seven papers which have been published.

BIOGRAPHICAL SKETCH

Provide the following information for the key personnel and other significant contributors in the order listed on Form Page 2.

NAME	POSITION TITLE
Andrei V. Bakin	Assistant Professor

EDUCATION/TRAINING *(Begin with baccalaureate or other initial professional education, such as*

INSTITUTION AND LOCATION	DEGREE *(if applicable)*	YEAR(s)	FIELD OF STUDY
Moscow State University, Moscow, Russia	M.S.	1984	Chemistry/ Biochemistry
Moscow State University, Moscow, Russia	Ph.D.	1990	Molecular Biology

A. POSITIONS AND HONORS

1990-1991	Research Fellow, A. N. Belozersky Institute of Physico-Chemical Biology, Moscow State University, Moscow USSR
1990-1991	Visiting Scientist, Department of Chemistry, University of Texas, Austin, TX
1991-1995	Postdoctoral Fellow, Roche Institute of Molecular Biology, Nutley, NJ
1995-1999	Postdoctoral Fellow, Department of Developmental Neurobiology, St. Jude Children's Research Hospital, Memphis, TN
1999-2003	Research Assistant Professor, Dept. of Medicine, Vanderbilt University, Nashville, TN
2003-present	Assistant Professor, Dept. of Cancer Genetics, Roswell Park Cancer Institute, Buffalo, NY
2005-present	Scientific Reviewer, DOD Breast Cancer Program, Pathology
2005-present	Scientific Reviewer, NIH/NCI Fellowships

B. PUBLICATIONS (Selected from 30 peer reviewed articles)

Bakin AV, Borisova OF, Shatsky IN, Bogdanov AA. Spatial organization of template polynucleotides on the ribosome determined by fluorescent methods. J Mol Biol 221:441-453, 1991.

Shatsky IN, Bakin AV, Bogdanov AA, Vasiliev VD. How does the mRNA pass through the ribosome? Biochimie 73:937-945, 1991.

Ofengand J, Bakin A, Nurse K. The functional role of conserved sequences of 16S ribosomal RNA in protein synthesis. In The Translational Apparatus (ed. K.H. Nierhaus AR, Subramanian VA, Erdmann F, Franceschi, Wittman-Liebold B), Plenum Press, NY, 1993.

Bakin A, Ofengand J. Four newly located pseudouridylate residues in Escherichia coli 23S ribosomal RNA are all at the peptidyl transferase center: analysis by the application of a new sequencing technique. Biochemistry 32:9754-9762, 1993.

Bakin A, Lane B, Ofengand J. Clustering of pseudoridines at the peptidyl transferase center of yeast ribosomes. Biochemistry, 33:13475-13483, 1994.

Bakin A, Ofengand J. Mapping to nucleotide resolution of pseudouridine residues in large subunit ribosomal RNAs from representative eukaryotes, prokaryotes, archaebacteria, mitochondria and chloroplasts. J Mol Biol 266:246-268, 1997.

Bakin A, Ofengand J. Mapping pseudouridine residues in RNA to nucleotide resolution. In Methods in Molecular Biology: Protein Synthesis: Methods and Protocols (ed. R Martin), Humana Press, Totowa, NJ, 297-309, 1997.

Bakin A, Curran T. Cell transformation by the fos oncogene is mediated by DNA 5-methylcytosine transferase. Science 283:387-390, 1999.

Bakin AV, Tomlinson AK, Bhowmick NA, Moses HL, Arteaga CL. Phosphatidylinositol 3-kinase function is required for TGFbeta -mediated epithelial to mesenchymal transition and cell migration. J Biol Chem 275:36803-36810, 2000.

Bhowmick NA, Ghiassi M, Bakin A, Aakre M, Lundquist CA, Engel ME, Arteaga CL, Moses HL. TGFb mediates epithelial to mesenchymal transdifferentiation through a RhoA-dependent mechanism. Mol Biol Cell 12:27-36, 2001.

Shin I, Bakin AV, Rodeck U, Brunet A, Arteaga CL. TGFbeta enhances epithelial cell survival via Akt-dependent regulation of FKHRL1. Mol Biol Cell 12:3328-3339, 2001.

Bakin AV, Rinehart C, Tomlinson AK, Arteaga CL. p38 mitogen-activated protein kinase is required for TGF -mediated fibroblastic transdifferentiation and cell migration. J Cell Sci 115:3193-206, 2002.

Shin I, Yakes FM, Rojo F, Shin NY, Bakin AV, Baselga J, Arteaga CL. PKB/Akt mediates cell-cycle progression by phosphorylation of p27^{Kip1} at threonine 157 and modulation of its cellular localization. Nat Med 8:1145-1152, 2002.

Dumont N, Bakin AV, Arteaga CL. Autocrine TGFbeta signaling mediates smad-independent motility in human cancer cells. J Biol Chem 278:3275-3285, 2003.

Bakin AV, Safina A, Rinehart C, Daroqui C, Darbary H, Helfman D. A critical role of tropomyosins in TGF-(beta) regulation of the actin cytoskeleton and cell motility in epithelial cells. Mol Bio Cell, 15:4682-4694, 2004.

Bakin AV, Stourman V, Sekhar RK, Rinehart C, Yan X, Meredith MJ, Arteaga CL, Freeman ML. Smad3-ATF3 signaling mediates TGF-β suppression of genes encoding phase ii detoxifying proteins. Free Radical Biology and Medicine 38:375-387, 2005.

Varga AE, Stourman NV, Zheng Q, Safina A, Quan L, Li X, Sossey-Alaoui K, Bakin AV. Silencing of Tropomyosin-1 gene by DNA methylation alters tumor suppressor function of TGF-β. Oncogene 1-10, 2005.

Sossey-Alaoui K, Ranalli TA, Li X, Bakin A, Cowell JK. WAVE3 promotes cell motility and invasion through the regulation of MMP-1, MMP-3 and MMP-9- expression. Exp Cell Res 308:135-145, 2005.

Rossi MR, Ionov Y, Bakin AV, Cowell JK. Truncating mutations in the ACVR2 gene attenuates activin signaling in prostate cancer cells. Cancer Geneti Cytogenet, 163:123-129,2005.

Original Contribution

Smad3–ATF3 signaling mediates TGF-β suppression of genes encoding Phase II detoxifying proteins

Andrei V. Bakin[a],*, Nina V. Stourman[a], Konjeti R. Sekhar[b], Cammie Rinehart[c], Xuexian Yan[b], Michael J. Meredith[d], Carlos L. Arteaga[c], Michael L. Freeman[b],*

[a]Department of Cancer Genetics, Roswell Park Cancer Institute, Buffalo, NY 14263, USA
[b]Radiation Oncology, Vanderbilt-Ingram Cancer Center, Vanderbilt University, Nashville, TN 37232, USA
[c]Division of Medical Oncology, Vanderbilt-Ingram Cancer Center, Vanderbilt University, Nashville, TN 37232, USA
[d]Department of Oral Molecular Biology, Oregon Health and Science University, Portland, OR 97201, USA

Abstract

This study provides evidence that in mammary epithelial cells the pluripotent cytokine TGF-β1 repressed expression of multiple genes involved in Phase II detoxification. GCLC, the gene that encodes the catalytic subunit of the enzyme glutamate cysteine ligase, the rate-limiting enzyme in the biosynthesis of glutathione, was used as a molecular surrogate for investigating the mechanisms by which TGF-β suppressed Phase II gene expression. TGF-β was found to suppress luciferase reporter activity mediated by the human GCLC proximal promoter, as well as reporter activity mediated by the GCLC antioxidant response element, ARE4. TGF-β downregulated expression of endogenous GCLC mRNA and GCLC protein. TGF-β suppression of the Phase II genes correlated with a decrease in cellular glutathione and an increase in cellular reactive oxygen species. Ectopic expression of constitutively active Smad3E was sufficient to inhibit both reporters in the absence of TGF-β, whereas dominant negative Smad3A blocked TGF-β suppression. Smad3E suppressed Nrf2-mediated activation of the GCLC reporter. We demonstrate that TGF-β increased ATF3 protein levels, as did transient overexpression of Smad3E. Ectopic expression of ATF3 was sufficient to suppress the GCLC reporter activity, as well as endogenous GCLC expression. These results demonstrate that Smad3–ATF3 signaling mediates TGF-β repression of ARE-dependent Phase II gene expression and potentially provide critical insight into mechanisms underlying TGF-β1 function in carcinogenesis, tissue repair, and fibrosis.
© 2004 Elsevier Inc. All rights reserved.

Keywords: TGF-β; Smad; Nrf2; Glutathione; ATF3; Free radicals

The superfamily of Phase II detoxification proteins is defined by the ability to conjugate organic donor molecules (e.g., glutathione, UDP-glucuronic acid, or acetyl coenzyme A) to xenobiotics [1]. Conjugation of xenobiotics usually results in their detoxification and/or subsequent efflux, decreasing the mutagenic/carcinogenic intracellular burden [1]. It should be recognized, however, that in some cases, conjugation can generate activated carcinogens [2]. Proteins such as NAD(P)H:quinone oxidoreductase (DT-diaphorase),

glutathione S-transferases (GST), UDP-glucuronosyltransferases, Mn superoxide dismutase (SOD), catalase, thioredoxin, and glutamate cysteine ligase (GCL) are representative members of the Phase II family. Many of these proteins are essential for the detoxification of reactive oxygen species, another function defining Phase II metabolism.

Phase II gene expression is regulated, in part, by a common *cis*-acting regulatory element. This element, identified in mouse and rat models [3,4], is termed an antioxidant response element (ARE). Point mutation analysis allowed identification of a core sequence within the ARE (5′-TGACnnnGC-3′) that is essential for basal, as well as inducible expression [5]. Work by Venugopal and Jaiswal [6] and Itoh et al. [7] has demonstrated that the transcription

factor NF-E2-related factor 2 (Nrf2), a Cap'n' Collar basic leucine zipper transcription factor, positively regulates ARE-mediated gene expression.

Basal and inducible Phase II gene expression has been ascertained in Nrf2 null and wild-type mice. Disruption of Nrf2 expression resulted in a loss of constitutive glutathione *S*-transferase Alpha1, Alpha2, Mu1, Mu2, Mu3, Mu4, and Mu6 expression in hepatic tissues [8]. Inducible expression of GST Alpha1, Mu1, Mu3, Pi1, and Pi2; NAD(P)H:quinone oxidoreductase; glutamate cysteine ligase modifier subunit (GCLM); Mn SOD; and heme oxygenase 1 was also attenuated in Nrf2 null hepatic tissues [8–11]. In the intestine, induction of many Phase II genes by either synthetic cancer chemopreventive agents or phytochemicals was blunted in the Nrf2 null animals [11]. Similarly, constitutive and inducible expression of the GCL catalytic subunit (GCLC) and GCLM was diminished in Nrf2 null tissues [8,12]. GCLC and GLCM encode the catalytic and modifier subunits of glutamate cysteine ligase, the rate-limiting enzyme for the synthesis of glutathione. These experiments highlight the importance of Nrf2 for the regulation of ARE-mediated basal and inducible Phase II gene expression.

Loss of Nrf2-mediated Phase II gene expression results in increasing tissue-specific susceptibility to carcinogens [9], as well as attenuated antioxidant activity in tissues [13], thereby increasing susceptibility to injury and toxins (e.g., [14,15]). Thus, diminished Nrf2-mediated Phase II gene expression has the potential to produce profound effects on tissue responses to stress (such as oxidative stress).

The cytokines of the transforming growth factor β (TGF-β) family participate in the regulation of cell growth, differentiation, and apoptosis, as well as carcinogenesis [16,17]. TGF-β binds to the transmembrane serine–threonine kinase type II and type I receptor complex and triggers phosphorylation of receptor-associated Smad2 and Smad3 proteins (R-Smads), which upon phosphorylation heterodimerize with Smad4 and translocate into the nucleus where they regulate transcription of target genes [18]. In the nucleus R-Smads can interact with several transcription factors including AP-1 family members and RUNX2/Cbfa1 [9]. Smads can interact with transcriptional coactivators p300/CBP and transcriptional corepressors such as TGIF, Ski, and HDAC [19]. Thus, Smads can mediate TGF-β intracellular signaling by either activating or repressing expression of target genes.

Recent work has provided rigorous support for TGF-β-mediated generation of reactive oxygen species (ROS) as intermediates in some aspects of the TGF-β signaling cascade [20,21]. Experimental evidence suggests that Phase II gene expression is a novel target for TGF-β repression. TGF-β has been shown to suppress extracellular, CuZn, and Mn superoxide dismutase; catalase; glutathione peroxidase; glutathione *S*-transferases; and GCLC mRNA expression, as well as enzyme activity in a number of cell types [22–28]. Suppression of Phase II gene expression was accompanied

Table 1
Genes downregulated in response to TGF-β in NMuMG cells at 24 h

Gene	Accession No.	Fold repressed	Nrf2[a] regulated	Verified[b]	*p* value[c]
GCLC	BG076460	3.5	Yes	Northern	<0.05
GST Pi2	BG76872	4.9	Yes	Northern	<0.05
GST Mu1	BG086970	5.3	Yes	SQ RT-PCR	<0.05
GST Alpha4	BG073190	5.2	Yes		
Catalase	BG076235	2.8	Yes	SQ RT-PCR	<0.05
UDP–glucuronosyltransferase 1	BG076072	6.0	Yes	SQ RT-PCR	<0.05
Selenoprotein P	BG088394	2.7	Yes	SQ RT-PCR	<0.05
Ferroxidase	BG068359	4.8	Yes		
UDP–glucose dehydrogenase	BG068439	4.8	Yes		
Isocitrate dehydrogenase 2 (NADP$^+$)	BG081213	4.3	Yes		
Superoxide dismutase 1	BG074045	1.8	Yes		
Ubiquitin 2	AU045483	3.3	Yes		
Cytochrome b_5	BG065259	2.7	ND		
Fatty acid CoA ligase	BG069344	5.9	ND		
Phosphoserine aminotransferase	BG084015	4.0	Yes		
3-Oxoacyl CoA thiolase mitochondrial	BG085346	3.6	Yes		
Lysosomal α-glucosidase	BG085155	5.0	Yes		
Spi 1-4	AAH21850	12	Yes	SQ RT-PCR	<0.05
Gro1 cl1 chemokine ligand 1	BG080268	2.0	Yes		
Lgals4, lectin	BG065730	3.3	ND		
Id1	BG076619	2.9	ND		
Id2	BG084290	9.8	Yes	SQ RT-PCR	<0.05
Cyclin D2	BG085335	3.0	ND		

[a] Yes, gene regulated by Nrf2 as reported in [8–12].
[b] Verified, Northern blotting or semiquantitative (SQ) RT-PCR was used to confirm microarray results.
[c] *p* value relative to control, untreated cells, as determined by ANOVA.

by elevation of ROS generation [24,26,29]. To date, however, the intracellular signaling pathways responsible for this suppression have not been well understood.

In this study we show that TGF-β signaling can lead to repression of ARE-mediated gene expression. Using GCLC as a molecular surrogate, we found that TGF-β-mediated suppression requires participation of Smad3 and Smad 4 transcription factors, as well as de novo protein synthesis. Importantly, we found that activating transcription factor 3 (ATF) is involved in Smad-dependent repression in response to TGF-β. Thus, these studies suggest that Smads and ATF3 are required for suppression of ARE-mediated Phase II gene expression by TGF-β1. Further elucidation of this pathway is important, in part because it helps to lay a foundation for understanding ROS metabolism in cells exposed to TGF-β.

Material and methods

Cell culture and reagents

NMuMG cell lines were purchased from the American Type Culture Collection (Manassas, VA, USA) and were maintained in Dulbecco's modified Eagle's medium supplemented with 10% fetal calf serum (FCS). Before experimentation, the serum concentration was lowered to 5%. The SW480.7 clone 15.13 [30] was a gift from Dr. Joan Massagué (Memorial Sloan–Kettering Cancer Center, New York, NY, USA) and was maintained in Dulbecco's modified Eagle's medium supplemented with 10% FCS, 0.3 mg/ml zeocin, and 0.7 mg/ml G418. Dermal mouse fibroblasts from wild-type and Smad3 null mice were provided by Drs. Anita Roberts and Kathleen Flanders (NIH). TGF-β1 was obtained from R&D Systems (Minneapolis, MN, USA). The following antibodies were used: Smad4 (Transduction Laboratories, San Diego, CA, USA); actin, α-catenin, Flag M2 (Sigma); GCLC (Lab Vision); and ATF3 (Santa Cruz).

RNA isolation and cDNA microarray analysis

RNA from mouse nontumor mammary epithelial NMuMG cells treated with 2 ng/ml TGF-β1 for 4, 8, and 24 h was extracted as described previously [31]. The National Institute of Aging's (NIA) 15,000 cDNA microarray was printed by the Vanderbilt Microarray Shared Resource. The mouse 15,000 NIA microarray contains 15,247 genes of known and unknown function. Total RNA from each sample (35 μg) was labeled and hybridized with the microarray. Detailed descriptions of the gene array list, microarray hardware, labeling, hybridization, and processing procedures are available from http://array.mc.vanderbilt.edu/Pages/Protocols/Protocols.htm. The array slides were scanned with an Axon 4000 scanner (Axon Instruments, Foster City, CA, USA) at a resolution of 10 μm. The reference RNA from untreated NMuMG cells was labeled

by using cyanine 3–dUTP, and the RNA samples from TGF-β1-treated cells were labeled with cyanine 5–dUTP. This experiment was performed in triplicate. Data were analyzed using GenePix4.0 software. Three independent replicates of TGF-β treatment, RNA isolation and labeling, and microarray hybridization including self–self control were performed.

Data filtering and normalization

Image analysis and the calculation of average foreground signal adjusted for local channel-specific background were performed with GENEPIX software. Spots with signal intensities in both channels less than 100 were excluded. If at least one channel had intensity above 100, the intensity under 100 was set at 100. The average number of clones filtered from analysis was 110 for the NIA 15K array. Each array was separately globally normalized to make the median value of $\log_2$ ratio equal to 0.

Northern blot analysis

The GCLC and GST Pi2 cDNAs spotted on the microarrays (GenBank Accession Nos. BG076460 and BG076872) were generated by PCR, verified by DNA sequencing matched through BLAST analysis (www.ncbi.
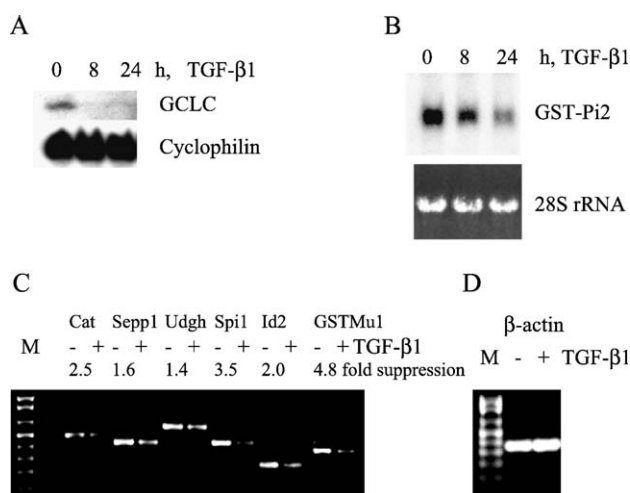

Fig. 1. TGF-suppressed expression of genes encoding Phase II detoxification enzymes. (A, B) Northern blot analyses of GCLC (A) and GST Pi2 (B) mRNA from mouse NMuMG cells treated with 2 ng/ml TGF-β1 for 24 h. Cyclophilin probe and ethidium bromide staining of 28S RNA were used as controls. (C, D) Semiquantitative reverse transcription PCR analysis of mRNA levels in total RNA samples isolated from NMuMG cells treated with 2 ng/ml TGF-β1 for 24 h. Lanes: Cat, catalase; Sepp1, selenoprotein P1; Udgh, UDP-glucuronosyltransferase 1; Spi1, serine protease inhibitor 1-4; Id2; GST Mu1; and β-actin (control). PCR samples were fractionated on separate agarose gels and stained with ethidium bromide. The PCR data shown were obtained in a single large experiment that was repeated three times. Fluorescence images were quantitated using image analysis software. The fold suppression represents the relative intensity of a band compare to untreated sample, corrected for changes in β-actin expression.

nlm.nih/BLAST/) to the GenBank database, and used as probes for Northern blot analysis. Total RNA samples (20 μg/lane) obtained from NMuMG cells treated with 2 ng/ml TGF-β1 for 4, 8, and 24 h were subjected to Northern blot analysis. The GCLC and GST Pi2 cDNA probes were labeled by random priming with [α-^{32}P]dCTP, followed by hybridization in ULTRAhyb buffer (Ambion, Inc.). Washed filters were exposed to a phosphor screen and the quantitative analysis was performed using the Molecular Imager FX Pro System (Bio-Rad). Ethidium bromide staining or cyclophilin expression was used to control for RNA loading.

Immunoblot and immunoprecipitation analysis

Protein extracts (40 μg/lane) from NMuMG cells were analyzed as described in [32] using antibodies to actin, α-catenin (Sigma), lamin, ATF3 (Santa Cruz), and GCLC (Lab Vision). The detection was performed using an enhanced chemiluminescence kit (Amersham Biosciences).

For immunoprecipitation, cells were washed twice in ice-cold PBS and solubilized at 4°C in PBS containing 0.01% Triton X-100, 0.5% Na deoxycholate, and 0.1% SDS plus 1 mM AEBSF. Solubilized protein was cleared with protein A/G and immunoprecipitated using antibody to ATF3 followed by addition of protein A/G (Oncogene). The washed pellet was solubilized in 5 × SDS sample buffer.

Plasmids and other constructs

The Nrf2 expression vector was a gift from Dr. Y.W. Kan. The vectors expressing Smad3E and Smad3A were a
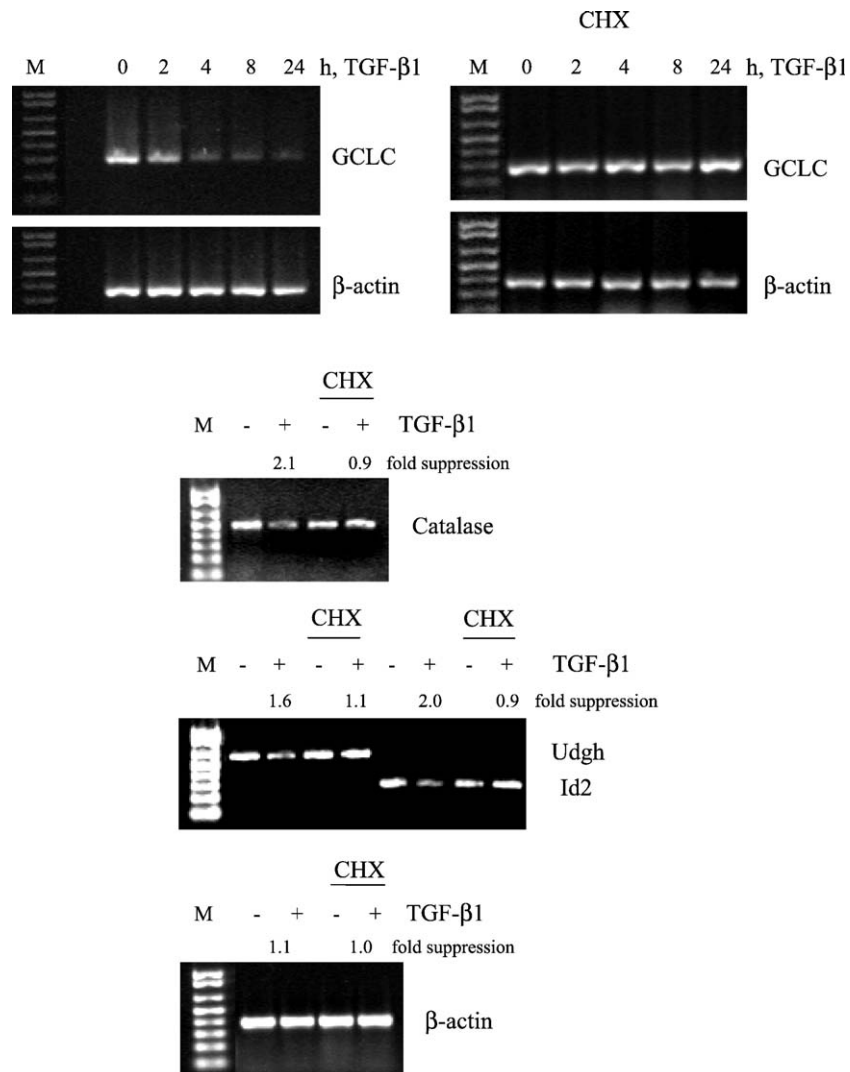
Fig. 2. TGF-β suppression of Phase II gene expression requires de novo protein synthesis. SQ RT-PCR was used to quantitate expression of GCLC, catalase, UDP–glucuronosyltransferase 1 (Udgh), Id2, and β-actin in total RNA samples obtained from NMuMG cells treated with 2 ng/ml TGF-β1 in the absence or presence of 10 μg/ml cycloheximide (CHX) for 24 h. PCR samples obtained from a single large experiment were fractionated on separate agarose gels and stained with ethidium bromide. Fluorescence images were quantitated by image analysis software and corrected for changes in β-actin expression. The fold suppression represents the relative intensity of a band compared to untreated sample.

gift from Dr. J. Massagué. The ATF3 expression vector was a gift from Dr. T. Hai.

Transcriptional assays

Cells were seeded in 24-well plates and transfected with one of the following plasmids at a concentration of 0.1 μg/ml pGL3/GCLC-Lux, 0.1 μg/ml pGL3/ARE4-Lux, or 0.002 μg/ml pCMV-Renilla (Promega, Madison, WI, USA) using FuGENE6 reagent (Roche Molecular Biochemicals) according to the manufacturer's protocol. Firefly luciferase (Lux) and *Renilla reniformis* luciferase (Rl-Lux) activities in cell lysates were determined using the Dual Luciferase Reporter Assay System (Promega) according to the manufacturer's protocol in a Monolight 2010 luminometer (Analytical Luminescence Laboratory, San Diego, CA, USA). Luciferase activity was normalized to Rl-Lux activity to account for transfection efficiency and presented as relative luciferase units. All assays were done in triplicate wells.

Measurement of ROS and glutathione (GSH)

GSH concentrations were measured as described previously in [33]. Cells were lysed in ice-cold 10% perchloric acid and subjected to high-performance liquid chromatography (HPLC). ROS production was measured in NMuMG cells after exposure to 5 ng/ml TGF-β1 for 48 h using the oxidative-sensitive dye C-400 (Molecular Probes) as described in [34].

Semiquantitative RT-PCR analysis

Amplification of transcripts was performed using 125 ng of total RNA and the one-step RT-PCR system from Invitrogen according to the manufacturer's protocol. Primer sequences are available upon request. The optimal number of PCR cycles was determined for each primer set to ensure that product formation was linear with the number of cycles used. Amplification of β-actin was used as an internal control. PCR samples were separated on agarose gel and stained with ethidium bromide, and fluorescent images were quantitated using Bio-Rad image analysis software. The fold of suppression represents the relative intensity of a band compared to untreated sample, corrected for β-actin expression. RT-PCR was repeated at least three times. PCR product sizes were compared to a 1-kb Plus DNA ladder from Invitrogen that yielded ladder bands of 100, 200, 300, 400, 500, 650, 850, 1000, 1650, 2000, and 12,000 kb.

Statistical analysis

Experiments were repeated three or more times and data were compared using Student's *t* test or ANOVA. Statistical significance was accepted at $p < 0.05$.

Results

Exposure to TGF-β suppresses expression of multiple genes encoding Phase II detoxification proteins

NMuMG cells, a nontumor mammary epithelial cell line, were treated with 2 ng/ml TGF-β for 24 h. Total RNA was isolated and a cDNA microarray analysis performed. mRNA levels of 27 genes were suppressed at least 2.5-fold by the TGF-β treatment compared to untreated control cells. Nearly 80% of the downregulated genes encode Phase II detoxification enzymes including GST Pi2, GST Alpha4, GST Mu1, catalase, and GCLC (see Table 1). Of note, the GCLC and GST Pi2 genes were represented by two EST clones with similar levels of downregulation. Northern blot analysis confirmed downregulation of GCLC and GST Pi2 mRNA levels by TGF-β treatment at 8 and 24 h (Figs. 1A and 1B). The suppression of several selected genes was confirmed by an alternative method: semiquantitative RT-PCR [35] (Fig. 1C). These results demonstrate that TGF-β can downregulate expression of multiple genes involved in Phase II metabolism.

TGF-β suppression of Phase II detoxification genes requires novel protein synthesis

To test whether TGF-β repression was a direct effect, cells were exposed to TGF-β and the protein synthesis inhibitor cycloheximide. Cotreatment with 10 μg/ml cycloheximide blocked TGF-β-mediated repression of GCLC, catalase, Udgh, and Id2 gene expression (Fig. 2 and Table 2). TGF-β repression of GCLC mRNA was observed within 2 h of TGF-β treatment. Recent studies have also reported inhibition of GCLC mRNA by TGF-β in hepatocytes, which was not affected by actinomycin D treatment but blocked by cycloheximide [28]. Thus, these results suggest that TGF-β repression of

Table 2
TGF-β-mediated suppression of gene expression[a]

Gene	–CHX	+CHX
GCLC	Not detected[b]	1.0
Catalase	2.3	1.0
Selenoprotein P	1.6	
UDP–glucuronosyltransferase 1	1.5	1.0
Spi 1-4	3.5	
GST Mu1	4.8	
GST Pi2	5.0	

Cells were cotreated with 0 or 10 μg/ml cycloheximide (CHX) and TGF-β1.

[a] Cells were treated with 0 or 2 ng/ml TGF-β1 for 24 h. Data summarized from Figs. 1 and 2. The fold suppression represents relative gene expression in cells treated with TGF-β1 compared to untreated sample, corrected for changes in β-actin expression.

[b] GCLC expression was not detected after 24 h of exposure to 2 ng/ml TGF-β1.

Phase II detoxification genes involves de novo protein synthesis.

TGF-β suppresses glutathione synthesis and increases ROS production in NMuMG cells

The GCLC gene encodes the catalytic subunit of the enzyme glutamate cysteine ligase, the rate-limiting enzyme in the biosynthesis of glutathione. Immunoblot analysis indicated that TGF-β decreased expression of the 73-kDa GCLC polypeptide detected in NMuMG cells (Fig. 3A). Under these conditions we did not observe accumulation of the 60-kDa GCLC fragment that has been reported for TGF-β-treated hepatocytes [28]. Evaluation of GSH concentrations indicated a 30% reduction in NMuMG cells after 16 h of TGF-β treatment (Fig. 3B; $p < 0.05$, Student's t test). We next used the oxidation-sensitive dye C-400 to determine intracellular ROS concentrations in NMuMG cells. Treatment with 5 ng/ml TGF-β for 48 h induced a twofold increase in dye oxidation, measured as an increase in fluorescence (Fig. 3C). Analysis at earlier time points did not reveal significant increases, consistent with the work of [27]. These results demonstrate a correlation between TGF-β repression of GCLC mRNA and loss of GCLC protein and GSH concentrations. The increase in ROS observed is consistent with loss of intracellular GSH, catalase, and superoxide dismutase (see Table 1).
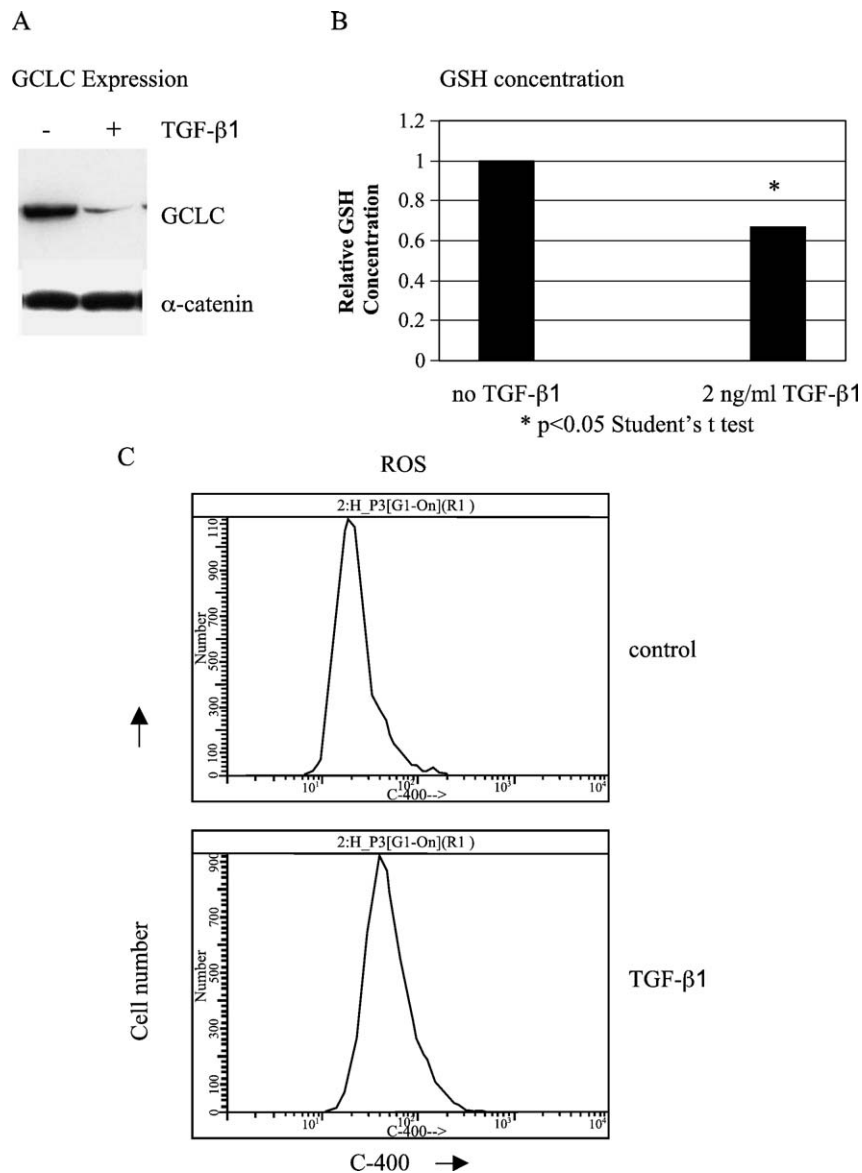
Fig. 3. TGF-β treatment reduced GCLC expression and glutathione levels and increased ROS production in NMuMG cells. (A) Immunoblot analyses of GCLC in NMuMG cells exposed to 2 ng/ml TGF-β1 for 24 h. (B) Detection of GSH in NMuMG cells. Cells were exposed to 2 ng/ml TGF-β for 24 h, washed, lysed with ice-cold 10% perchloric acid, and analyzed by HPLC. (C) Reactive oxygen species (ROS) were measured in NMuMG cells after exposure to 5 ng/ml TGF-β for 48 h. Cells were labeled with the oxidative-sensitive dye C-400.

Smad signaling represses ARE-dependent GCLC expression

The ability of Smad signaling to mediate TGF-β repression of GCLC transcription was investigated using a luciferase reporter construct derived from the human GCLC proximal promoter and consisting of a 3924-bp fragment (−3678 to + 246) [37]. The GCLC proximal promoter region contains a functional ARE (ARE4) [36]. Point mutations within the ARE4 GCLC sequence abrogate gene expression [36,37], a consequence of loss of Nrf2 binding activity [37]. Thus, expression of this reporter is strictly dependent upon Nrf2–ARE interactions [36–38].

In NMuMG cells transiently transfected with the GCLC-Lux reporter, treatment with TGF-β for 16 h reduced GCLC-Lux activity by 40% (Fig. 4A; $p < 0.05$, ANOVA). These results are quantitatively similar to those obtained by [27]. We have extended those results and now show that TGF-β suppressed activity from an ARE-Lux reporter by 50% compared to untreated cells (Fig. 4B; $p < 0.05$, ANOVA). ARE4-Lux reporter activity is directed by the sequence 5′-CCCCGTGACTCAGCGCTTTGT-3′. Suppression of the ARE4-Lux reporter was of a magnitude similar to that observed for GCLC-Lux repression. These data identify the antioxidant response element as a target for TGF-β repression.

TGF-β-mediated suppression of GCLC and ARE4 reporters was not a consequence of loss of Nrf2 protein,
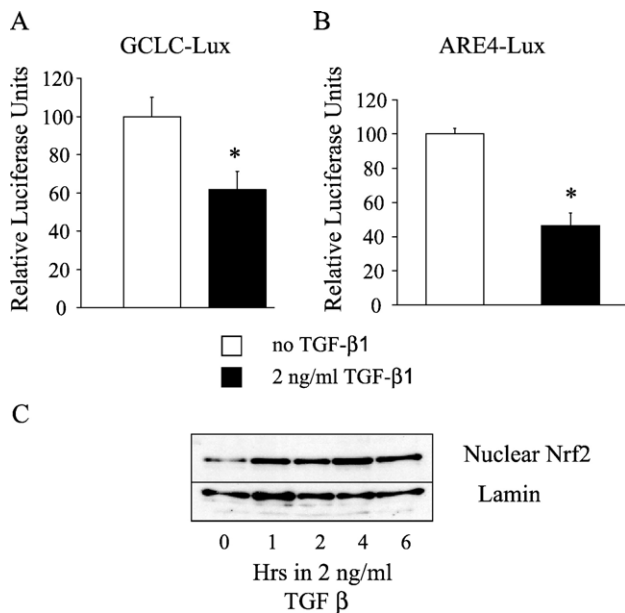
Fig. 4. TGF-β suppressed luciferase reporter activity derived from either 4 kb of the human GCLC proximal promoter [37] or ARE4 [36,38]. NMuMG cells were transiently cotransfected with (A) a GCLC-Lux reporter and pCMVRenilla as a control or (B) an ARE4-Lux reporter and pCMVRenilla as a control. The cells were treated with 2 ng/ml TGF-β1 for 16 h. Each data point represents the mean ± SD of three wells. *$p < 0.05$ compared to non-TGF-β-treated control, ANOVA. (C) Immunoblot of nuclear Nrf2 after exposure of NMuMG cells to TGF-β for the indicated times.
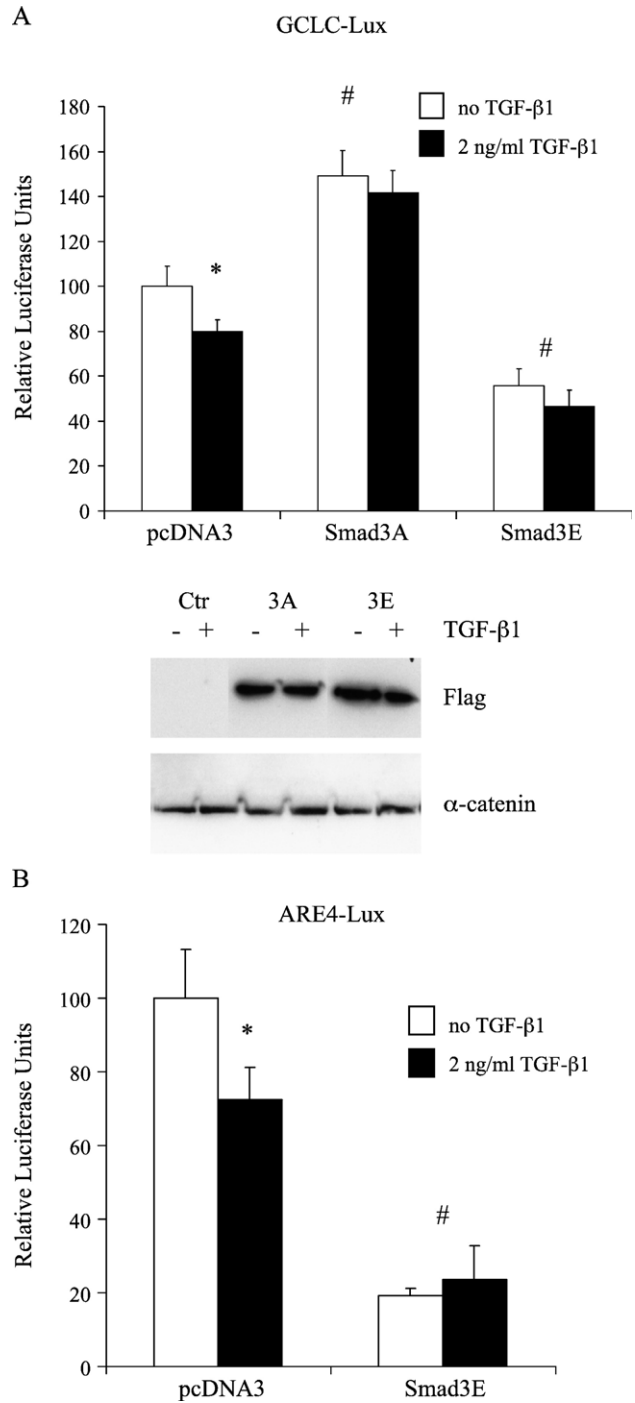
Fig. 5. Regulation of the GCLC-Lux and the ARE4-Lux reporters by Smad3 mutants. (A) Luciferase reporter activity in NMuMG cells cotransfected with the GCLC-Lux reporter and pCMVRenilla along with expression vectors encoding dominant negative Smad3A or constitutively active Smad3E or empty vector control. The immunoblot illustrates expression of FLAG-tagged Smad3A and FLAG-tagged Smad3E expression in NMuMG cells transfected with FLAG-tagged Smad3 mutants or a control empty vector. (B) Luciferase reporter activity in NMuMG cells cotransfected with the ARE4-Lux reporter and pCMVRenilla along with an expression vector encoding constitutively active Smad3E or empty vector control. After transfection, cells were exposed to 2 ng/ml TGF-β for 24 h. Each data point represents the mean ± SD of three wells. *$p < 0.05$, ANOVA, compared to non-TGF-β-treated control; #$p < 0.05$, ANOVA, compared to cells transfected with control vector pcDNA3.

A

B
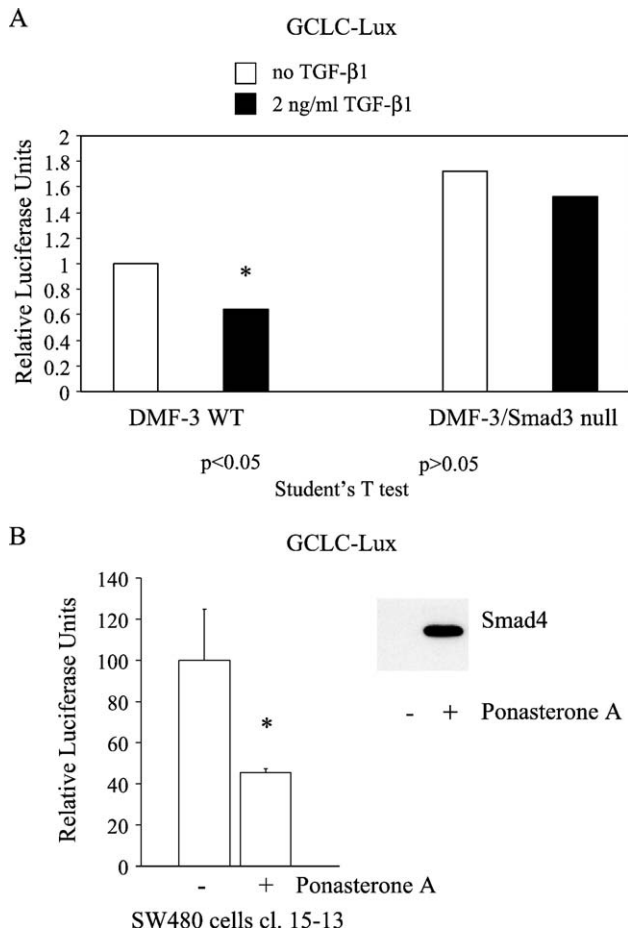
Fig. 6. Regulation of the GCLC reporter in Smad3- and Smad4-deficient cells. (A) GCLC-luciferase activity in mouse dermal fibroblasts derived from wild-type or Smad3 null animals transiently transfected with the GCLC-Lux reporter and either Smad3 expression vector or empty vector. After transfection, cells were exposed to 2 ng/ml TGF-β for 24 h. (B) SW480.7 cells were transiently transfected with the GCLC-Lux reporter. Cells were either left untreated or treated with 3 μM ponasterone for 48 h to induce Smad4 expression. Smad4 expression was determined by immunoblot analysis in cells used for the luciferase assay. Each data point represents the mean ± SD of three wells. *$p < 0.05$ compared to non-TGF-β-treated control.

as demonstrated by the immunoblot of nuclear Nrf2 levels (Fig. 4C).

To examine whether Smad3 mediated ARE suppression, NMuMG cells were transfected with Smad3 mutants in which three serines in the carboxy-terminal motif SSXS were substituted with glutamic acid to mimic phosphorylation (Smad3E) or with alanine residues blocking phosphorylation (Smad3A) [39]. Smad3E and Smad3A function as constitutively active or dominant negative factors in TGF-β transcriptional responses [39]. Smad3 was chosen for investigation as it has been implicated in suppressive activities (e.g., [40]).

TGF-β treatment was found to suppress both the GCLC-Lux and the ARE4-Lux reporters in cells transfected with the pcDNA3 control vector (Fig. 5). The degree of GCLC-Lux suppression observed was similar to that observed by

[27]. Ectopic expression of Smad3A abrogated TGF-β-mediated repression of the GCLC-Lux reporter. Indeed, reporter activity was statistically higher than control (Fig. 5A; $p < 0.05$, ANOVA). These results suggest that loss of Smad signaling enhanced reporter activity. Conversely, transfection of a constitutively active Smad3E protein inhibited both GCLC-Lux activity and ARE4-Lux activity compared to control ($p < 0.05$, ANOVA). Furthermore, addition of TGF-β did not affect the degree of repression observed ($p > 0.05$, ANOVA). These results are consistent with the hypothesis that TGF-β-mediated repression utilizes Smad3 signaling.

To complement ectopic expression studies, we examined the activity of the GCLC reporter in Smad3-deficient mouse dermal fibroblasts and in SW480 colon cancer cells that exhibit regulated expression of Smad4 [30]. Dermal fibroblasts derived from Smad3-deficient mice showed a 1.6-fold higher level of luciferase activity compared to wild-type cells (Fig. 6A, open histograms, $p < 0.05$ ANOVA), consistent with results obtained from ectopic expression of Smad3A (Fig. 5A). Whereas TGF-β was able to suppress GCLC-Lux activity in wild-type cells ($p < 0.05$, Student's t test), repression was lost in the mutant cells ($p > 0.05$, Student's t test) (Fig. 6A). Reexpression of Smad4 in SW480 cells by treatment with 3 μM ponasterone A for 48 h decreased luciferase activity by 60% (Fig. 6B, $p < 0.05$, ANOVA). These results indicate that both Smad3 and Smad4 contribute to the regulation of the GCLC promoter by TGF-β.

Smad3E represses Nrf2-regulated GCLC reporter activity

We next examined effects of Nrf2 on the GCLC-Lux reporter activity in NMuMG cells. Transfection of Nrf2 increased GCLC-Lux reporter activity (Fig. 7; $p < 0.05$, ANOVA). To examine whether Smad3 affected Nrf2-
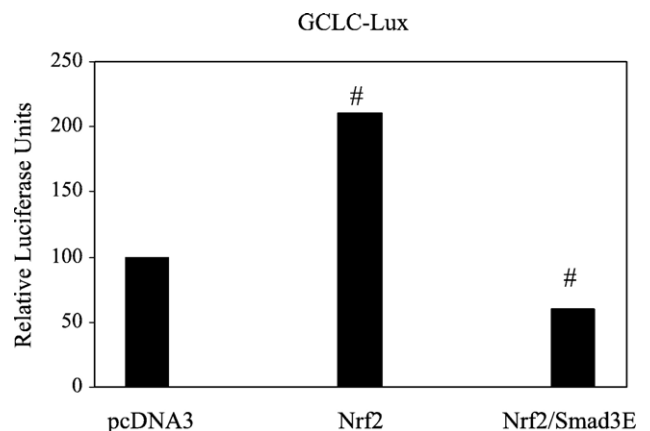

Fig. 7. Smad3 downregulates Nrf2-dependent activation of the GCLC promoter. Luciferase activity in NMuMG cells transiently cotransfected with the GCLC-Lux reporter vector and expression vectors for pcDNA3 (control), Nrf2, and/or Smad3E is shown. Each data point represents the mean ± SD of three wells. #$p < 0.05$ compared to control vector (pcDNA3), ANOVA.

mediated regulation of the GCLC promoter we used the Smad3E mutant that accumulates in the nucleus in the absence of ligand. Cotransfection of Smad3E with Nrf2 reduced luciferase activity of GCLC-Lux reporter (Fig. 7). The observation that Smad3E was able to suppress Nrf2 activation of the GCLC-Lux reporter suggests that repression may occur via a nonstoichiometric mechanism.

ATF3 signaling downregulates ARE4-mediated activity

Our results suggest that TGF-β suppression of GCLC expression involves synthesis of a mediator(s). Recent studies have shown that TGF-β can increase the expression of the transcription factor ATF3 [41,42], which can function as a transcriptional repressor [43]. Consequently, ATF3 expression was examined. Immunoblotting demonstrated

(1) increased ATF3 expression in TGF-β-treated NMuMG cells and (2) increased ATF3 expression in cells ectopically expressing Smad3E (Fig. 8A). Immunofluorescence analysis of cells treated with TGF-β confirmed the increase in ATF3 expression (Fig. 8B). TGF-β-mediated elevation of ATF3 was rapid, occurring within 2 h of treatment (Fig. 8C; a 1.8-fold increase compared to untreated cells), the same time frame as for suppression of GCLC mRNA (Fig. 2). Cycloheximide was found to block TGF-β1-mediated elevation of ATF3 expression (Fig. 8C; a 1.0-fold increase compared to untreated cells). The fold increase in ATF3 expression was determined by quantitating the immunoblot bands using image analysis software and correcting for changes in β-actin expression. These experiments illustrate enhanced ATF3 expression that was mediated by TGF-β or constitutively active Smad3E and that required de novo protein synthesis.
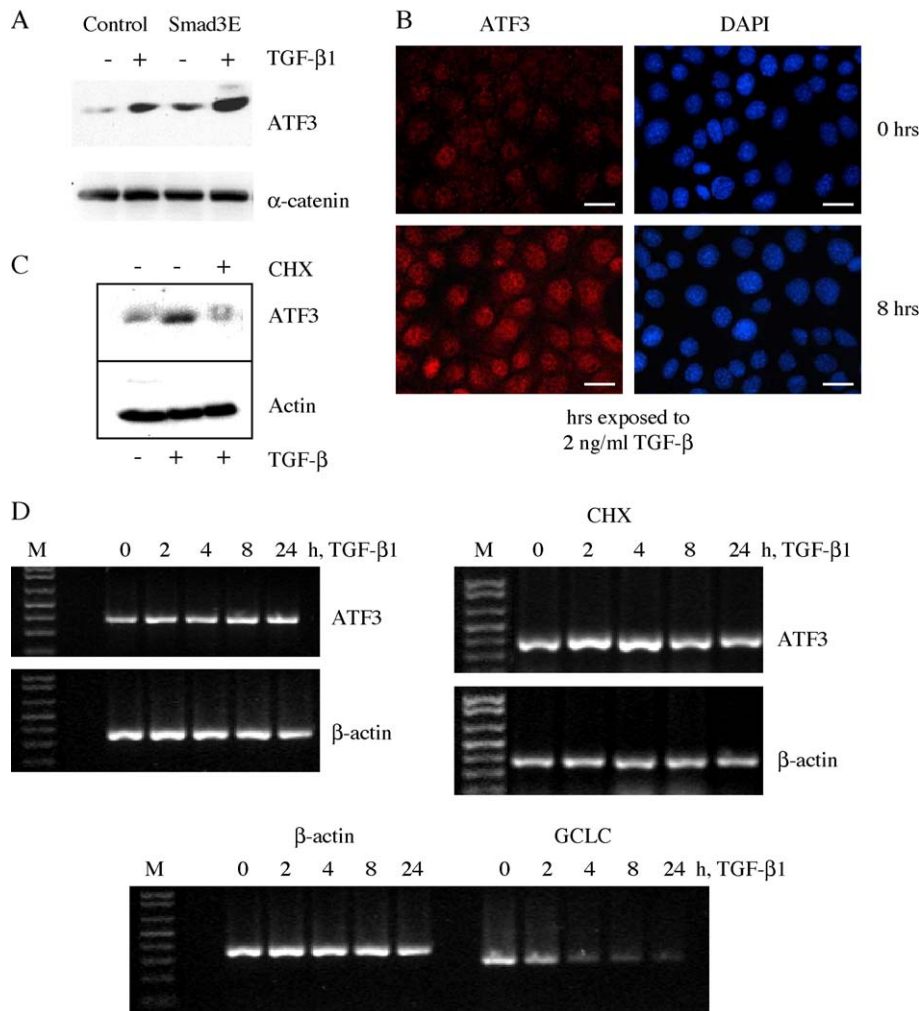
Fig. 8. ATF3 expression is increased in cells treated with TGF-β and/or transfected with Smad3E. (A) Immunoblot showing ATF3 expression in NMuMG cells transfected with Smad3E expression vector or a control empty vector. α-Catenin is a control for loading. Cells were treated with 2 ng/ml TGF-β for 16 h. (B) Immunofluorescent staining for ATF3 in NMuMG cells exposed to TGF-β for 0 or 8 h. (C) Immunoblot illustrating that cycloheximide blocks TGF-β1-mediated expression of ATF3. Cells were exposed to 2 ng/ml TGF-β1 for 2 h. As indicated, cells were exposed to 10 μg/ml cycloheximide for 1 h before and during a 2-h TGF-β treatment. (D) Detection of ATF3 and GCLC by SQ-RT-PCR in total RNA samples from NMuMG cells treated with 2 ng/ml TGF-β1 (±cycloheximide) for 24 h. β-Actin is a control.

ATF3 mRNA levels were not increased by TGF-β treatment, as measured by semiquantitative RT-PCR ($p > 0.05$, ANOVA; Fig. 8C). These results were not a consequence of technical limitations, as GCLC mRNA was shown to be downregulated in the same experiment (Fig. 8D), suggesting that TGF-β regulated ATF3 expression at the posttranscriptional level.

We next examined the relationship between ATF3 and GCLC expression. ATF3 was found to rapidly associate with Nrf2 in response to TGF-β treatment, as measured by immunoprecipitation of ATF3 and immunoblotting of Nrf2 (Fig. 9A). Ectopic expression of ATF3 was found to suppress the ARE4 luciferase reporter (Fig. 9A; $p < 0.05$, ANOVA) and endogenous GCLC expression (Fig. 9B). Thus, ATF3 was shown to exhibit a repressive function.

Discussion

This study investigated TGF-β-regulated gene expression in normal mouse mammary epithelial NMuMG cells. We report that nearly 80% of TGF-β-suppressed genes identified in the microarray analysis encode Phase II detoxifying proteins, including GCLC, GST Pi2, GST Alpha4, GST Mu1, and catalase. Downregulation of these genes correlated with reduction in intracellular glutathione levels and an increase in ROS. These results are consistent with the work of others who have shown that TGF-β repressed the expression of CuZn, extracellular, and Mn superoxide dismutase; catalase; glutathione peroxidase; glutathione *S*-transferase; selenoprotein P; glutathione reductase; glutaredoxin; and GCLC. Suppression of these genes was accompanied by loss of intracellular glutathione and increases in intracellular ROS [22–28,42]. Taken all together, these reports suggest that Phase II gene expression may represent a novel target for TGF-β repression. Therefore, this investigation was undertaken in order to elucidate the signaling pathway(s) responsible for the suppression.

The gene GCLC was used as a molecular surrogate for studying TGF-β-mediated repression of Phase II genes. The proximal promoter region in GCLC contains a functional ARE [36]. Functionality of the ARE was demonstrated by point mutation, by GMSAs, and by examining GCLC expression in mice containing an Nrf2 null mutation [12,36,38]. Nrf2 has been shown to positively regulate ARE-mediated gene expression [6,7]. Our studies with a GCLC luciferase reporter showed that TGF-β suppressed reporter activity. Expression of Smad3 and Smad4 was required for the suppression of the GCLC promoter. Constitutively active Smad3E was shown to suppress reporter activity, whereas dominant negative Smad3A blocked TGF-β suppression of the GCLC reporter. Complementary experiments with Smad3 null dermal mouse fibroblasts and SW480 colon cancer cells with inducible expression of Smad4 provided confirmational support.
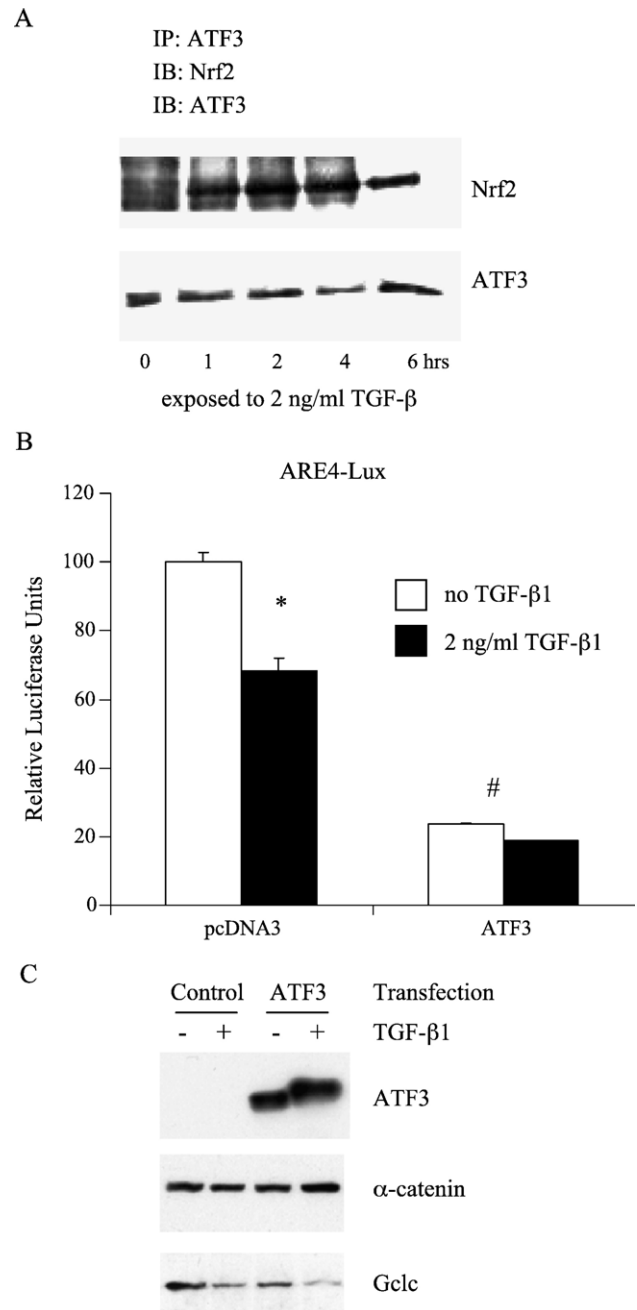
Fig. 9. ATF3 mediates TGF-β suppression of GCLC expression. (A) ATF3 rapidly associates with Nrf2 in response to TGF-β1. NMuMG cells were exposed to 2 ng/ml TGF-β1 for the indicated times; cells were solubilized and immunoprecipitated with antibody to ATF3. This was followed by immunoblotting with antibody to Nrf2. The blot was stripped and reprobed with antibody to ATF3. (B) Effects of ATF3 transfection on luciferase activity of the ARE4-Lux reporter in NMuMG cells. pcDNA3 is a control. Cells were treated with 2 ng/ml TGF-β for 16 h. Each data point represents the mean ± SD of three wells. *$p < 0.05$ compared to non-TGF-β treated control, ANOVA; #$p < 0.05$ compared to control vector, ANOVA. (C) Immunoblot analysis of ATF3 and GCLC expression in NMuMG cells transfected with ATF3 expression vector or a control empty vector. α-Catenin is a loading control. Cells were treated with 2 ng/ml TGF-β1 for 16 h.

In the proximal promoter region for GCLC, Nrf2 binds an ARE known as ARE4 [36]. We found that TGF-β suppressed ARE4-dependent reporter expression. Ectopic expression of constitutively active Smad3E repressed ARE-dependent reporter activity even in the absence of TGF-β. Finally, Smad3E repressed Nrf2-mediated activation of a GCLC reporter, an activity that is strictly dependent upon Nrf2 [36,37]. These results suggest that Phase II gene suppression by TGF-β is a consequence of ARE repression. These novel observations complement the work of Jardine et al. [27], who found that c-Jun/Fra-1 dimer binding to a distal region on the GCLC promoter contributes to TGF-β suppression of GCLC in A549 cells.

The downregulation of Phase II genes by TGF-β required a de novo protein synthesis and was not affected by inhibition of p38MAPK (data not shown), suggesting involvement of Smad-dependent expression of a mediator(s). A requirement for de novo protein synthesis for TGF-β-mediated downregulation of GCLC has been also shown in hepatocytes [28,29]. These observations, coupled with the knowledge that the ARE4 sequence does not contain a Smad binding site and that antibodies to Smad3 failed to displace ARE4 DNA binding activity in gel-mobility assays (data not shown), suggest that Smads may act indirectly, which is consistent with a requirement for de novo protein synthesis.

Our results suggest that ATF3 is an important component in the suppression of GCLC transcription in response to TGF-β. Treatment of cells with TGF-β or ectopic expression of constitutively active Smad3E increased ATF3 protein. TGF-β-mediated elevation of ATF3 required de novo protein synthesis and was observed 2 h after addition of TGF-β. ATF3 was found to rapidly associate with Nrf2 in response to TGF-β. We found that ectopic expression of ATF3 effectively suppressed an ARE4 reporter and expression of endogenous GCLC in NMuMG cells. However, the experiments presented do not rule out the possibility that Smad3 has a more direct role in the suppression of ARE-mediated gene expression, beyond that of elevating ATF3 expression. Nor can we exclude the participation of other TGF-β-mediated pathways in activation of ATF3 expression.

Stress-inducible transcription repressor ATF3 is a member of the activating transcription factor/cAMP-responsive element binding protein family of transcription factors [43]. Although it has been reported that TGF-β upregulates ATF3 transcription in a Smad-dependent manner [41], we did not find regulation of ATF3 mRNA in NMuMG cells. Consistent with our results, it has been recently shown that TGF-β does not upregulate ATF3 mRNA in FaO hepatoma cells [27]. ATF3 expression is regulated at multiple levels, including transcriptional autorepression [44] and protein stability [45].

ATF3-mediated repression can be the result of ATF3 binding to a cAMP-responsive element (CRE; TGACGTCA [41]). Because AREs contain an imperfect CRE, TGACTCA,

GMSAs were undertaken to determine if ATF3 was binding to ARE4. NMuMG cells were exposed to TGF-β for up to 6 h before isolation of nuclei for GMSA (unpublished results). The data indicate that DNA binding activity was not diminished by exposure to TGF-β, consistent with the work of [27]. Addition of ATF3 antibodies to the GMSA did not affect DNA binding activity (data not shown). Although the mechanism by which ATF3 suppresses ARE-dependent gene expression remains to be determined, this investigation has demonstrated that TGF-β signaling can repress ARE-mediated gene expression via a mechanism involving Smad–ATF3 signaling.

Our results, coupled with the work of others [22–28], indicate that TGF-β can markedly suppress expression of key enzymes involved in the biosynthesis and regeneration of glutathione and in scavenging ROS (e.g., catalase and SOD). Suppression leads to a reduction of intracellular glutathione levels and an increase in intracellular ROS. Consistent with our results, it has been shown that TGF-β-mediated generation of ROS in hepatocytes is a delayed process involving changes in gene expression [29]. Downregulation of catalase, GCLC, and glutathione peroxidase and of glutathione levels has been implicated in generation of ROS in pancreatic β cells, hepatocytes, and alveolar epithelial cells [23,26,46]. TGF-β can also stimulate the release of hydrogen peroxide by osteoblasts [47], lung fibroblasts, and endothelial cells [14,48,49,53]. Collectively, our results suggest that TGF-β suppression of ARE-regulated Phase II detoxification mediated by Smad–ATF3 signaling may result in an increase in intracellular ROS. Elevated ROS concentrations have the potential to impact certain aspects of TGF-β signaling cascades and carcinogenesis, as well as liver, renal, and pulmonary fibrogenesis [20,21,50–52]. Thus, this study provides critical insights into the mechanism of TGF-β suppression of ARE-regulated Phase II detoxification that may underlie TGF-β1-mediated generation of ROS during tissue pathogenesis.

References

[1] McCarver, D. G.; Hines, R. N. The ontogeny of human drug-metabolizing enzymes: phase II conjugation enzymes and regulatory mechanisms. *J. Pharmacol. Exp. Ther.* **300:**361–366; 2002.

[2] Guengerich, F. P. Metabolism of chemical carcinogens. *Carcinogenesis* **21:**345–351; 2000.

[3] Friling, R. S.; Bensimon, A.; Tichauer, Y.; Daniel, V. Xenobiotic-inducible expression of murine glutathione S-transferase Ya subunit gene is controlled by an electrophile-responsive element. *Proc. Natl. Acad. Sci. USA* **87:**6258–6262; 1990.

[4] Favreau, L. V.; Pickett, C. B. Transcriptional regulation of the rat NAD(P)H:quinone reductase gene: identification of regulatory elements controlling basal level expression and inducible expression by planar aromatic compounds and phenolic antioxidants. *J. Biol. Chem.* **266:**4556–4561; 1991.

[5] Nguyen, T.; Sherratt, P. J.; Pickett, C. B. Regulatory mechanisms controlling gene expression mediated by the antioxidant response element. *Annu. Rev. Pharmacol. Toxicol.* **43:**233–260; 2003.

[6] Venugopal, R.; Jaiswal, A. K. Nrf1 and Nrf2 positively and c-Fos and Fra1 negatively regulate the human antioxidant response element-mediated expression of NAD(P)H:quinone oxidoreductase1 gene. *Proc. Natl. Acad. Sci. USA* **93:**14960–14965; 1996.

[7] Itoh, K.; Chiba, T.; Takahashi, S.; Ishii, T.; Igarashi, K.; Katoh, Y.; Oyake, T.; Hayashi, N.; Satoh, K.; Hatayama, I.; Yamamoto, M.; Nabeshima, Y. An Nrf2/small Maf heterodimer mediates the induction of phase II detoxifying enzyme genes through antioxidant response elements. *Biochem. Biophys. Res. Commun.* **236:**313–322; 1997.

[8] Chanas, S. A.; Jiang, Q.; McMahon, M.; McWalter, G. K.; McLellan, L. I.; Elcombe, C. R.; Henderson, C. J.; Wolf, C. R.; Moffat, G. J.; Itoh, K.; Yamamoto, M.; Hayes, J. D. Loss of the Nrf2 transcription factor causes a marked reduction in constitutive and inducible expression of the glutathione S-transferase Gsta1, Gsta2, Gstm1, Gstm2, Gstm3 and Gstm4 genes in the livers of male and female mice. *Biochem. J.* **365:**405–416; 2002.

[9] Ramos-Gomez, M.; Kwak, M. K.; Dolan, P. M.; Itoh, K.; Yamamoto, M.; Talalay, P.; Kensler, T. W. Sensitivity to carcinogenesis is increased and chemoprotective efficacy of enzyme inducers is lost in nrf2 transcription factor-deficient mice. *Proc. Natl. Acad. Sci. USA* **98:**3410–3415; 2001.

[10] Kwak, M. K.; Itoh, K.; Yamamoto, M.; Sutter, T. R.; Kensler, T. W. Role of transcription factor Nrf2 in the induction of hepatic phase 2 and antioxidative enzymes in vivo by the cancer chemoprotective agent, 3H-1,2-dimethiole-3-thione. *Mol. Med.* **7:**135–145; 2001.

[11] McMahon, M.; Itoh, K.; Yamamoto, M.; Chanas, S. A.; Henderson, C. J.; McLellan, L. I.; Wolf, C. R.; Cavin, C.; Hayes, J. D. The Cap'n'Collar basic leucine zipper transcription factor Nrf2 (NF-E2 p45-related factor 2) controls both constitutive and inducible expression of intestinal detoxification and glutathione biosynthetic enzymes. *Cancer Res.* **61:**3299–3307; 2001.

[12] Chan, J. Y.; Kwong, M. Impaired expression of glutathione synthetic enzyme genes in mice with targeted deletion of the Nrf2 basic-leucine zipper protein. *Biochim. Biophys. Acta* **1517:**19–26; 2000.

[13] Hirayama, A.; Yoh, K.; Nagase, S.; Ueda, A.; Itoh, K.; Morito, N.; Hirayama, K.; Takahashi, S.; Yamamoto, M.; Koyama, A. EPR imaging of reducing activity in Nrf2 transcriptional factor-deficient mice. *Free Radic. Biol. Med.* **34:**1236–1242; 2003.

[14] Chan, K.; Kan, Y. W. Nrf2 is essential for protection against acute pulmonary injury in mice. *Proc. Natl. Acad. Sci. USA* **96:**12731–12736; 1999.

[15] Enomoto, A.; Itoh, K.; Nagayoshi, E.; Haruta, J.; Kimura, T.; O'Connor, T.; Harada, T.; Yamamoto, M. High sensitivity of Nrf2 knockout mice to acetaminophen hepatotoxicity associated with decreased expression of ARE-regulated drug metabolizing enzymes and antioxidant genes. *Toxicol. Sci.* **59:**169–177; 2001.

[16] Massague, J. TGF-beta signal transduction. *Annu. Rev. Biochem.* **67:**753–791; 1998.

[17] Roberts, A. B.; Wakefield, L. M. The two faces of transforming growth factor beta in carcinogenesis. *Proc. Natl. Acad. Sci. USA* **100:**8621–8623; 2003.

[18] Massague, J.; Blain, S. W.; Lo, R. S. TGFbeta signaling in growth control, cancer, and heritable disorders. *Cell* **103:**295–309; 2000.

[19] Itoh, S.; Thorikay, M.; Kowanetz, M.; Moustakas, A.; Itoh, F.; Heldin, C. H.; Ten Dijke, P. Elucidation of Smad requirement in transforming growth factor-beta type I receptor-induced responses. *J. Biol. Chem.* **278:**3751–3761; 2003.

[20] Herrera, B.; Murillo, M. M.; Alvarez-Barrientos, A.; Beltran, J.; Fernandez, M.; Fabregat, I. Source of early reactive oxygen species in the apoptosis induced by transforming growth factor-beta in fetal rat hepatocytes. *Free Radic. Biol. Med.* **36:**16–26; 2004.

[21] Liu, R. M.; Liu, Y.; Forman, H. J.; Olman, M.; Tarpey, M. M. Glutathione regulates transforming growth factor-beta-stimulated collagen production in fibroblasts. *Am. J. Physiol. Lung Cell Mol. Physiol.* **286:**L121–L128; 2004.

[22] Marklund, S. L. Regulation by cytokines of extracellular superoxide dismutase and other superoxide dismutase isoenzymes in fibroblasts. *J. Biol. Chem.* **267:**6696–6701; 1992.

[23] White, A. C.; Das, S. K.; Fanburg, B. L. Reduction of glutathione is associated with growth restriction and enlargement of bovine pulmonary artery endothelial cells produced by transforming growth factor-beta 1. *Am. J. Respir. Cell Mol. Biol.* **6:**364–368; 1992.

[24] Kayanoki, Y.; Fujii, J.; Suzuki, K.; Kawata, S.; Matsuzawa, Y.; Taniguchi, N. Suppression of antioxidative enzyme expression by transforming growth factor-beta 1 in rat hepatocytes. *J. Biol. Chem.* **269:**15488–15492; 1994.

[25] Arsalane, K.; Dubois, C. M.; Muanza, T.; Begin, R.; Boudreau, F.; Asselin, C.; Cantin, A. M. Transforming growth factor-beta1 is a potent inhibitor of glutathione synthesis in the lung epithelial cell line A549: transcriptional effect on the GSH rate-limiting enzyme gamma-glutamylcysteine synthetase. *Am. J. Respir. Cell Mol. Biol.* **17:**599–607; 1997.

[26] Islam, K. N.; Kayanoki, Y.; Kaneto, H.; Suzuki, K.; Asahi, M.; Fujii, J.; Taniguchi, N. TGF-beta1 triggers oxidative modifications and enhances apoptosis in HIT cells through accumulation of reactive oxygen species by suppression of catalase and glutathione peroxidase. *Free Radic. Biol. Med.* **22:**1007–1017; 1997.

[27] Jardine, H.; MacNee, W.; Donaldson, K.; Rahman, I. Molecular mechanism of transforming growth factor (TGF)-beta1-induced glutathione depletion in alveolar epithelial cells: involvement of AP-1/ARE and Fra-1. *J. Biol. Chem.* **277:**21158–21166; 2002.

[28] Franklin, C. C.; Rosenfeld-Franklin, M. E.; White, C.; Kavanagh, T. J.; Fausto, N. TGFbeta1-induced suppression of glutathione antioxidant defenses in hepatocytes: caspase-dependent post-translational and caspase-independent transcriptional regulatory mechanisms. *FASEB J.* **17:**1535–1537; 2003.

[29] Sanchez, A.; Alvarez, A. M.; Benito, M.; Fabregat, I. Cyclo-heximide prevents apoptosis, reactive oxygen species production, and glutathione depletion induced by transforming growth factor beta in fetal rat hepatocytes in primary culture. *Hepatology* **26:**935–943; 1997.

[30] Calonge, M. J.; Massague, J. Smad4/DPC4 silencing and hyperactive Ras jointly disrupt transforming growth factor-beta antiproliferative responses in colon cancer cells. *J. Biol. Chem.* **274:**33637–33643; 1999.

[31] Chomczynski, P.; Sacchi, N. Single-step method of RNA isolation by acid guanidinium thiocyanate–phenol–chloroform extraction. *Anal. Biochem.* **162:**156–159; 1987.

[32] Bakin, A. V.; Curran, T. Role of DNA 5-methylcytosine transferase in cell transformation by fos. *Science* **283:**387–390; 1999.

[33] Sekhar, K. R.; Meredith, M. J.; Kerr, L. D.; Soltaninassab, S. R.; Spitz, D. R.; Xu, Z. Q.; Freeman, M. L. Expression of glutathione and gamma-glutamylcysteine synthetase mRNA is Jun dependent. *Biochem. Biophys. Res. Commun.* **234:**588–593; 1997.

[34] Sekhar, K. R.; Yan, X. X.; Freeman, M. L. Nrf2 degradation by the ubiquitin proteasome pathway is inhibited by KIAA0132, the human homolog to INrf2. *Oncogene* **21:**6829–6834; 2002.

[35] Harris, M. N.; Ozpolat, B.; Abdi, F.; Gu, S.; Legler, A.; Muwuenyega, K. E.; Tirado-Gomez, M.; Lopez-Berestein, G.; Chen, X. Comparative proteomic analysis of all-trans-retinoic acid treatment reveals systematic post-transcriptional control mechanisms in acute promyelocytic leukemia. *Blood* **104:**1314–1323; 2004.

[36] Mulcahy, R. T.; Wartman, M. A.; Bailey, H. H.; Gipp, J. J. Constitutive and beta-naphthoflavone-induced expression of the human gamma-glutamylcysteine synthetase heavy subunit gene is

regulated by a distal antioxidant response element/TRE sequence. *J. Biol. Chem.* **272:**7445–7454; 1997.

[37] Sekhar, K. R.; Spitz, D. R.; Harris, S.; Nguyen, T. T.; Meredith, M. J.; Holt, J. T.; Guis, D.; Marnett, L. J.; Summar, M. L.; Freeman, M. L. Redox-sensitive interaction between KIAA0132 and Nrf2 mediates indomethacin-induced expression of gamma-glutamylcysteine synthetase. *Free Radic. Biol. Med.* **32:**650–662; 2002.

[38] Sekhar, K. R.; Soltaninassab, S. R.; Borrelli, M. J.; Xu, Z. Q.; Meredith, M. J.; Domann, F. E.; Freeman, M. L. Inhibition of the 26S proteasome induces expression of GLCLC, the catalytic subunit for gamma-glutamylcysteine synthetase. *Biochem. Biophys. Res. Commun.* **270:**311–317; 2000.

[39] Kretzschmar, M.; Doody, J.; Timokhina, I.; Massague, J. A mechanism of repression of TGFbeta/Smad signaling by oncogenic Ras. *Genes Dev.* **13:**804–816; 1999.

[40] Li, C.; Zhu, N. L.; Tan, R. C.; Ballard, P. L.; Derynck, R.; Minoo, P. Transforming growth factor-beta inhibits pulmonary surfactant protein B gene transcription through SMAD3 interactions with NKX2.1 and HNF-3 transcription factors. *J. Biol. Chem.* **277:**38399–38408; 2002.

[41] Kang, Y.; Chen, C. R.; Massague, J. A self-enabling TGFbeta response coupled to stress signaling: Smad engages stress response factor ATF3 for Id1 repression in epithelial cells. *Mol. Cell* **11:**915–926; 2003.

[42] Coyle, B.; Freathy, C.; Gant, T. W.; Roberts, R. A.; Cain, K. Characterization of the transforming growth factor-beta 1-induced apoptotic transcriptome in FaO hepatoma cells. *J. Biol. Chem.* **278:**5920–5928; 2003.

[43] Chen, B. P.; Liang, G.; Whelan, J.; Hai, T. ATF3 and ATF3 delta Zip: transcriptional repression versus activation by alternatively spliced isoforms. *J. Biol. Chem.* **269:**15819–15826; 1994.

[44] Wolfgang, C. D.; Liang, G.; Okamoto, Y.; Allen, A. E.; Hai, T. Transcriptional autorepression of the stress-inducible gene ATF3. *J. Biol. Chem.* **275:**16865–16870; 2000.

[45] Alam, J.; Killeen, E.; Gong, P.; Naquin, R.; Hu, B.; Stewart, D.; Ingelfinger, J. R.; Nath, K. A. Heme activates the heme oxygenase-1 gene in renal epithelial cells by stabilizing Nrf2. *Am. J. Physiol. Renal. Physiol.* **284:**F743–F752; 2003.

[46] Das, S. K.; White, A. C.; Fanburg, B. L. Modulation of transforming growth factor-beta 1 antiproliferative effects on endothelial cells by cysteine, cystine, and N-acetylcysteine. *J. Clin. Invest.* **90:**1649–1656; 1992.

[47] Shibanuma, M.; Kuroki, T.; Nose, K. Release of H_2O_2 and phosphorylation of 30 kilodalton proteins as early responses of cell cycle-dependent inhibition of DNA synthesis by transforming growth factor beta 1. *Cell Growth Differ.* **2:**583–591; 1991.

[48] Thannickal, V. J.; Hassoun, P. M.; White, A. C.; Fanburg, B. L. Enhanced rate of H_2O_2 release from bovine pulmonary artery endothelial cells induced by TGF-beta 1. *Am. J. Physiol.* **265:**L622–L626; 1993.

[49] Thannickal, V. J.; Fanburg, B. L. Activation of an H_2O_2-generating NADH oxidase in human lung fibroblasts by transforming growth factor beta 1. *J. Biol. Chem.* **270:**30334–30338; 1995.

[50] Poli, G. Pathogenesis of liver fibrosis: role of oxidative stress. *Mol. Aspects Med.* **21:**49–98; 2000.

[51] Yu, L.; Border, W. A.; Huang, Y.; Noble, N. A. TGF-beta isoforms in renal fibrogenesis. *Kidney Int.* **64:**844–856; 2003.

[52] Mastruzzo, C.; Crimi, N.; Vancheri, C. Role of oxidative stress in pulmonary fibrosis. *Monaldi Arch. Chest Dis.* **57:**173–176; 2002.

p38 mitogen-activated protein kinase is required for TGFβ-mediated fibroblastic transdifferentiation and cell migration

Andrei V. Bakin[1], Cammie Rinehart[1], Anne K. Tomlinson[1] and Carlos L. Arteaga[1,2,3,*]

[1]Departments of Medicine and [2]Cancer Biology, and [3]Vanderbilt-Ingram Cancer Center, Vanderbilt University School of Medicine, 777 Preston Research Building, Nashville, TN 37232, USA

*Author for correspondence (e-mail: carlos.arteaga@mcmail.vanderbilt.edu)

Summary

Transforming growth factor β (TGFβ) contributes to tumor progression by inducing an epithelial to mesenchymal transdifferentiation (EMT) and cell migration. We found that TGFβ-induced EMT was blocked by inhibiting activation of p38 mitogen-activated protein kinase (MAPK) with H-7, a protein kinase C inhibitor, and with SB202190, a direct inhibitor of p38MAPK. Inhibition of the p38MAPK pathway affected TGFβ-mediated phosphorylation of ATF2, but did not inhibit phosphorylation of Smad2. SB202190 impaired TGFβ-mediated changes in cell shape and reorganization of the actin cytoskeleton. Forced expression of dominant-negative (DN) MAPK kinase 3 (MKK3) inhibited TGFβ-mediated activation of p38MAPK and EMT. Expression of DN-p38α impaired TGFβ-induced EMT. Inhibition of p38MAPK blocked TGFβ-induced migration of non-tumor and tumor

mammary epithelial cells. TGFβ induced activation of the p38MAPK pathway within 15 minutes. Expression of TGFβ type II (TβRII) and type I (TβRI/Alk5) kinase-inactive receptors blocked EMT and activation of p38MAPK, whereas expression of constitutively active Alk5-T204D resulted in EMT and phosphorylation of MKK3/6 and p38MAPK. Finally, dominant-negative Rac1N17 blocked TGFβ-induced activation of the p38MAPK pathway and EMT, suggesting that Rac1 mediates activation of the p38MAPK pathway. These studies suggest that the p38MAPK pathway is required for TGFβ-mediated EMT and cell migration.

Key words: p38MAPK, TGFβ, Epithelial-mesenchymal transition, Cell migration, Rac1

Introduction

The transforming growth factor β (TGFβ) family of secreted factors regulates various biological processes, including cell proliferation, differentiation and apoptosis (Massague, 1998). TGFβs signal through cell-surface serine-threonine kinase type II and type I receptors. TGFβ binding to TGFβ type II (TβRII) receptor triggers its associaion with the TGFβ type I (TβRI) receptor (Massague, 1998). TβRII phosphorylates and activates TβRI, which, in turn, phosphorylates receptor-associated (RA) Smads (Smad2 and Smad3). RA-Smads bind Smad4 and translocate to the nucleus where they regulate transcription of target genes (Massague, 1998). In addition to Smads, TGFβ can activate Jun N-terminal kinase (JNK) (Atfi et al., 1997; Engel et al., 1999; Frey and Mulder, 1997), extracellular signal-regulated kinase (ERK) (Hartsough and Mulder, 1995), p38 mitogen-activated protein kinase (p38MAPK) (Hanafusa et al., 1999), and Akt (Bakin et al., 2000).

Smad-dependent signaling has been shown to be required for the antiproliferative activity of TGFβ, and components of this pathway are frequently mutated or silenced in several human cancers (de Caestecker et al., 2000). Tumors, however, frequently express high levels of TGFβ and inhibition of TGFβ signaling has been shown to reduce tumor invasiveness and metastasis (Akhurst and Balmain, 1999; Barrack, 1997; Cui et

al., 1996; Hojo et al., 1999). A number of studies provide evidence that TGFβ contributes to tumor cell invasion and metastasis by inducing mesenchymal transdifferentiation in epithelial cells (EMT) and stimulating cell migration (Akhurst and Balmain, 1999; Barrack, 1997; Oft et al., 1998). This TGFβ-mediated fibroblastic transdifferentiation is a complex process associated with alterations in epithelial cell junctions, changes in cell morphology, reorganization of the cell cytoskeleton, expression of fibroblastic markers (fibronectin, vimentin), and enhancement of cell migration (Bakin et al., 2000; Miettinen et al., 1994; Piek et al., 1999b).

The molecular mechanisms of TGFβ-mediated EMT and cell migration are not entirely understood. Studies with TGFβ receptors have shown that a truncated TGFβ/bone morphogenic protein (BMP) type I receptor, Alk2, blocks EMT in mouse NMuMG cells (Miettinen et al., 1994). Adenoviral expression of constitutively active human TβRI/Alk5 together with Smad2/3 can induce EMT in these cells (Piek et al., 1999b). Expression of a dominant-negative truncated form of TβRII decreases the formation of invasive spindle tumours (Portella et al., 1998). Adenoviral expression of Smad2/3 induced EMT only in the context of expression of constitutively active Alk5 (Piek et al., 1999b). Overexpression of Smad7, an inhibitor of Smad-dependent signaling, or dominant-negative Smad3 did not affect the transdifferentiation, arguing against

involvement of Smads in EMT (Bhowmick et al., 2001a). Inhibition of JNK with curcumin (Bakin et al., 2000) or by expression of dominant-negative JNK mutant (Bhowmick et al., 2001a) did not affect EMT. TGFβ did not activate the Ras-Raf-ERK1/2 cascade and MEK inhibitors (PD098059 and U0126) did not block EMT in NMuMG cells (Bakin et al., 2000; Piek et al., 1999b). We have recently shown that the phosphatidylinositide 3-kinase (PI3K)-Akt pathway contributes to EMT at the step of tight junction disruption (Bakin et al., 2000). The role of p38MAPK in TGFβ-mediated EMT has not been studied.

The p38MAPK pathway has been implicated in various biological responses to members of the TGFβ superfamily including TGFβ-stimulated migration of smooth muscle cells (Hedges et al., 1999), neuronal differentiation of PC12 cells induced by bone morphogenic protein 2 (BMP-2) (Iwasaki et al., 1999), growth/differentiation factor-5-induced chondrogenesis of ATDC-5 cells (Nakamura et al., 1999), and BMP-mediated cardiomyocyte differentiation (Monzen et al., 1999). Studies in Drosophila have shown that p38MAPKs are required for wing morphogenesis downstream of decapentaplegic (Dpp), a homologue of TGFβ (Adachi-Yamada et al., 1999). The p38MAPK pathway has also been implicated in TGFβ transcriptional responses (Hanafusa et al., 1999; Kucich et al., 2000; Sano et al., 1999).

The molecular mechanism(s) of TGFβ-induced activation of p38MAPK signaling are not defined. Mammalian p38MAPKs are activated by distinct upstream dual specificity MAPK kinases (MKK), MKK3 and MKK6 (Tibbles and Woodgett, 1999). TGFβ-activated kinase 1 (Tak1) phosphorylates MKK3/6 in TGFβ and BMP signaling (Shibuya et al., 1998; Yamaguchi et al., 1995). In addition, other MKK kinases including p21-activating kinase (PAK1) and mixed-lineage kinase (MLK) have been shown to phosphorylate MAPK kinases (MKK3/6) and induce p38MAPKs (Tibbles et al., 1996; Zhang et al., 1995). p38MAPK downstream targets include MAPK-activated protein kinase-2, mitogen- and stress-activated protein kinase-1 (MSK1), and transcription factors ATF2, CHOP, CREB and MEF2C (Tibbles and Woodgett, 1999). Recent studies have found that p38MAPKs are involved in the control of cell cytoskeleton and cell migration via phosphorylation of paxillin and heat shock protein 27 (HSP27) (Hedges et al., 1999).

In these studies we found that H-7, a protein kinase inhibitor, blocks TGFβ-induced EMT and activation of the p38MAPK pathway in NMuMG mouse mammary epithelial cells. The specific p38MAPK inhibitors, SB203580 and SB202190, impaired TGFβ-mediated changes in cell shape, the actin cytoskeleton, and cell migration. H-7 and the p38MAPK inhibitors blocked phosphorylation of ATF2, but did not inhibit TGFβ-mediated phosphorylation of Smad2. Expression of dominant-negative mutants (DN) of MKK3 or p38α inhibited TGFβ-mediated EMT. We also showed that TGFβ activates the MKK3/6-p38MAPK-ATF2 cascade within 15 minutes and expression of DN-MKK3 blocked TGFβ-mediated activation of p38MAPK and EMT. Kinase-inactive TGFβ type II and type I (Alk5) receptors blocked EMT and the activation of p38MAPK. Forced expression of kinase-active Alk5-T204D induced both EMT and phosphorylation of p38MAPK in NMuMG cells. Alk5-T204D-induced EMT was blocked by a p38MAPK inhibitor. Finally, we demonstrated that forced

expression of dominant-negative Rac1N17 blocked TGFβ-induced activation of the p38MAPK-ATF2 cascade and EMT.

Materials and Methods

Antibodies and other reagents

TGFβ1 and tumor necrosis factor α (TNFα) were obtained from R&D Systems. Antibodies to fibronectin, Rac1 and Smad2 were from Transduction Laboratories; antibodies to ZO-1 were from Chemicon; the monoclonal antibody to p38MAPK and rabbit polyclonal to haemaglutinin (HA) epitope were from Santa Cruz Biotechnology, Phalloidin-FITC, phalloidin-Texas Red, and Hoechst 3342 were from Molecular Probes. The β-tubulin-Cy3 antibody was from Sigma. Antibodies to phospho-Ser473 Akt, total Akt, phospho-MKK3/6, phospho-p38MAPK, and phospho-ATF2 were from New England BioLabs, and to C-terminal phospho-Smad2 from Upstate Biotechnology. LY294002, H-7, SB203580, and SB202190 were from Calbiochem. GDP and GTPγS were purchased from Sigma. The GST-ATF2 fusion protein was from New England Biolabs. TBS buffer contained 20 mM Tris-HCl, pH 7.6, 150 mM NaCl. TBST was TBS supplemented with 0.1% Tween 20 (v/v).

Cell culture

NMuMG mouse mammary epithelial cells, SiHa human cervical carcinoma cells, MDA-MB-231 human breast cancer cells and HEK293T human kidney cells were purchased from American Tissue Culture Collection (ATCC). Cells were cultured as recommended by ATCC. 4T1 tumor cells were provided by F. Miller (Karmanos Cancer Center, Detroit, MI) and cultured in 10% FBS-DMEM.

Plasmids and retroviral constructs

The retroviral vectors pGabe and pGabe-TβRII-K277R were provided by Martin Oft (UCSF, San Francisco, CA) and have been described previously (Oft et al., 1998). The TβRII-K277R construct contains an HA-tag at the N-terminus. Human wild-type Alk5, dominant-negative Alk5-K232R, and constitutively active Alk5-T204D constructs were provided by Masahiro Kawabata (The Cancer Institute, Tokyo, Japan). To generate pBMN-Alk5 constructs, the EcoRI/SalI fragments of Alk5 and Alk5-K232R including the C-terminal HA-tag were cloned in the retroviral pBMN-IRES-EGFP vector provided by Garry Nolan (Stanford University). The pBMN-Rac1N17 was engineered by cloning a BamHI-XhoI fragment encoding Rac1N17 from pCDNA3-Rac1N17 (a gift of Richard Cerione, Cornell University, Ithaca, NY) at the BamHI-SalI site of the retroviral pBMN-IRES-GFP vector. RhoAN19 and RhoAQ63L were previously described (Bakin et al., 2000). The pBMN-MKK3AL and pBMN-MKK6AL plasmids were generated by cloning SalI-NotI fragment of MKK6AL or XhoI-NotI fragment of MKK3AL from pCDNA3 vector into the retroviral pBMN-IRES-GFP vector. pCDNA3-MKK3AL and pCDNA3-MKK6AL plasmids were a gift of James Woodgett (The Ontario Cancer Institute, Toronto, Ontario). pBMN-p38AGF encoding a dominant-negative mutant of p38α and containing N-terminal Flag epithope was generated by cloning a HindIII-XbaI fragment of p38AGF from pcDNA3-p38AGF at the XhoI site of pBMN-IRES-GFP. pcDNA3-p38AGF was a gift of Roger Davies (University of Massachusetts, Worcester, MA). Plasmids phCMV-VSVG, encoding vesicular stomatitis virus glycoprotein (VSV-G), and pCMVgag-pol, containing the Moloney murine leukemia virus (MoMLV) gag and pol genes, were provided by Jane Burns (University of California at San Diego).

Retroviral infection of cells

Retroviruses were prepared by transfection of HEK293T cells with 15

µg DNA/100 mm dish of three plasmids encoding gag/pol, VSV-G, and the target construct, ratio 4:3:8. Supernatants from cells were collected for 3 days and combined, filtered through 0.4 µm filters, and stored in aliquots at –80°C. NMuMG cells were infected with supernatant containing retroviruses in the presence of 6 µg/ml Polybrene (Sigma) as described previously (Yee et al., 1994). Three days later, GFP-positive cells were selected by flow cytometry. Under these conditions more than 95% of selected cells expressed GFP at the time of experiments.

Immunoblot analysis

Cells were incubated in serum-free medium for 4 hours prior to treatment with TGFβ1. Cells were lysed in buffer containing 20 mM Tris, pH 7.4, 137 mM NaCl, 1% NP-40, 10% glycerol, 20 mM NaF, 1 mM Na orthovanadate, 1 mM PMSF, 2 µg/ml aprotinin, and 2 µg/ml leupeptin. Protein concentrations in cell lysates were determined by the Bradford method. Protein extracts (50 µg/lane) were separated by 12.5% SDS-PAGE and transferred to nitrocellulose membranes (100

mA, 2.5 hours). Membranes were blocked with 5% milk in TBST for 1 hour at room temperature (RT) and then incubated with primary antibodies in TBST plus 1% milk for 16 hours at 4°C, followed by incubation with secondary antibodies for 1 hour at RT. Membranes were washed three times in TBST and immunoreactive bands visualized by ECL (Pierce).

p38MAPK in vitro kinase assay

p38MAPK was precipitated from protein extracts (200 µg) with a p38MAPK monoclonal antibody (Santa Cruz Biotechnology) for 2 hours at 4°C. An in vitro kinase reaction was performed in a 40-µl volume by adding to the immune complexes 1 µg GST-ATF2 and 10 µCi [γ-^{32}P]ATP (specific activity 3000 Ci/mmol, New England Nuclear) for 20 minutes at 30°C in the presence of 10 µM PKA peptide inhibitor (Calbiochem). Reactions were terminated by the addition of Laemmli loading buffer and heating, followed by 15% SDS-PAGE and transfer to nitrocellulose (NC) membranes. Quantitative analysis of [γ-^{32}P]-labeled bands was performed using a
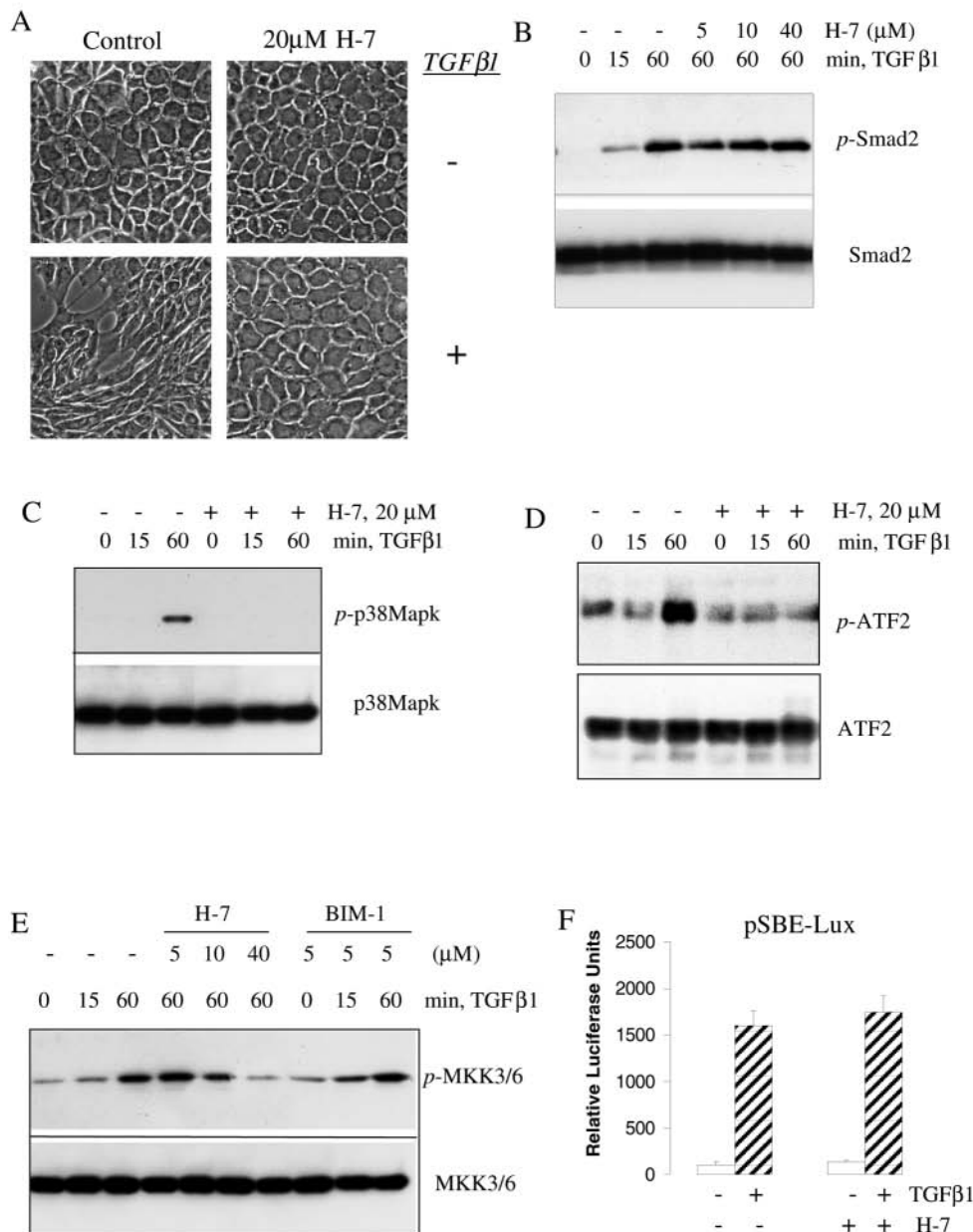
Fig. 1. Inhibition of TGFβ-mediated EMT and p38MAPK activation by H-7 kinase inhibitor. (A) NMuMG mammary epithelial cells were grown on glass coverslips for 24 hours and treated (bottom row) or not (top row) with 2 ng/ml TGFβ1 for 24 hours. Where indicated, cells were co-incubated with 20 µM H-7. Phase contrast images were taken at 200× magnification. (B-E) Immunoblot analysis of whole-cell extracts from NMuMG cells treated with 2 ng/ml TGFβ1 for the indicated times. Kinase inhibitors were added 60 minutes before TGFβ treatment. (B) Immunoblot detection of phospho-Smad2 and total Smad2. (C) Detection of phospho-p38MAPK total p38MAPK. (D) Inhibition of TGFβ-induced ATF2 phosphorylation by H-7. Immunoblots with antisera to phospho-ATF2 and total ATF2. (E) TGFβ-induced phosphorylation of MKK3/6 in cells co-treated with various concentrations of H-7 or 5 µM BIM-I, a PKC inhibitor. (F) Luciferase activity in NMuMG transfected with Smad-dependent reporter pSBE-Lux and pCMV-Rl vectors and treated with 1 ng/ml TGFβ1 for 16 hours in the absence or presence of 20 µM H-7. Each bar represents the mean±s.d. of three wells.

PhosphorImager (Molecular Dynamics). The same NC-membranes were probed with a monoclonal antibody to p38MAPK.

Immunofluorescence microscopy

NMuMG cells (10^5 cells/well) were grown in DMEM containing 5% FBS on glass coverslips (22×22 mm) for 24 hours before treatment with 2 ng/ml TGFβ1. Cells were fixed with 4% paraformaldehyde in phosphate-buffered saline (PBS) for 10 minutes at RT and then permeabilized with 0.05% Triton X-100 for 10 minutes. Cells were washed three times in PBS after each treatment. Cells were blocked with 3% milk in PBS for 30 minutes at RT, incubated for 60 minutes with primary antibodies diluted in 1% milk/PBS (1/300 for ZO-1, 1/500 for Smad2, 1/250 for fibronectin), and then with fluorescent secondary antibodies (1/500) for 45 minutes at RT. Microtubules were stained for 30 minutes at RT with β-tubulin-Cy3 diluted 1/250 in 1% milk/PBS. Actin was stained with phalloidin-FITC (4 units/ml) or phalloidin-Texas Red (2 units/ml). Cell nuclei were stained with 1 µg/ml Hoechst for 10 minutes at RT. Coverslips were mounted on 25×75 mm microslides (VWR Scientific) using AquaPolyMount (Polysciences). Fluorescent images were captured using a Princeton Instruments cooled CCD digital camera from a Zeiss Axiophot upright microscope.

Transcriptional assays

NMuMG cells ($3×10^4$) were seeded in 24-well plates and transfected with 0.16 µg/ml pSBE-Lux containing 12 repeats of Smad binding sequence (provided by J.-M. Gauthier, Laboratoire Glaxo Wellcome, Les Ulis Cedex, France) with 0.002 µg/ml pCMV-Rl (Promega, Madison, WI) using FuGENE6 reagent (Roche Molecular Biochemicals) according to the manufacturer's protocol. Cells were incubated for 8 hours in 0.5% FBS-DMEM prior to treatment with 1 ng/ml TGFβ1 for 16 hours. Firefly luciferase (Luc) and *Renilla reniformis* luciferase (RlLuc) activities in cell lysates were determined using the Dual Luciferase Reporter Assay System (Promega) according to the manufacturer's protocol in a Monolight 2010 luminometer (Analytical Luminescence Laboratory, San Diego, CA). Luc activity was normalized to RlLuc activity and presented as Relative Luciferase Units. All assays were done in triplicate wells and each experiment was repeated at least twice.

Affinity precipitation of Rac using GST-PBD

A fusion protein containing the GTPase-binding domain from human PAK1 (PBD) and glutathione S-transferase (GST) was expressed in *Escherichia coli* using pGEX-4T3-GST-PBD as described (Benard et al., 1999). pGEX-4T3-GST-PBD was kindly provided by Gary Bokoch (Scripps Research Institute). NMuMG cells ($2×10^7$/assay) were treated with 2 ng/ml TGFβ1 for 15 minutes followed by cell lysis in 20 mM Tris, pH

7.5, 150 mM NaCl, 5 mM $MgCl_2$, 1% NP-40, 5% glycerol, 20 mM NaF, 1 mM sodium orthovanadate, 1 mM PMSF, 2 µg/ml aprotinin, and 2 µg/ml leupeptin in the presence of 8 µg GT-PBD. Cell lysates were clarified by low speed centrifugation at 4°C. HEK293T cells transfected with Rac1N17 or Alk5 mutants were lysed in the same buffer. After clarification, cell lysates (350 µg/assay) were incubated with 8 µg GST-PBD. To prepare cytosolic Rac1 loaded with GDP or GTPγS, cell lysates (equivalent of $2×10^6$ cells) were incubated for 15 minutes at 30°C in the presence of 10 mM EDTA and 100 mM GTPγS or 1 mM GDP to facilitate nucleotide exchange (Benard et al., 1999). The loading reaction was terminated by addition of 60 mM $MgCl_2$. Affinity precipitation was performed using 15 µl of glutathione-Sepharose 4B beads (Pharmacia) for 1 hour at 4°C. The bead pellets were washed three times with 20 mM Tris, pH 7.5, 50 mM NaCl, 5 mM $MgCl_2$, 1 mM DTT, 1% NP-40 and 2 times in PBS. The bead pellet was finally suspended in 40 µl of Laemmli sample buffer. Proteins were separated on 15% SDS-PAGE, transferred to nitrocellulose membrane and immunoblotted with an antibody to Rac1 (Transduction Laboratories).

Migration assays

NMuMG or MDA-MB-231 cells ($1×10^5$/well) were plated in DMEM/0.5%FBS in the upper chamber of 5 µm pore (24-well) transwells (Costar, High Wycombe, UK) and incubated alone or with 2 ng/ml TGFβ1 in the absence or presence of SB202190. After 16
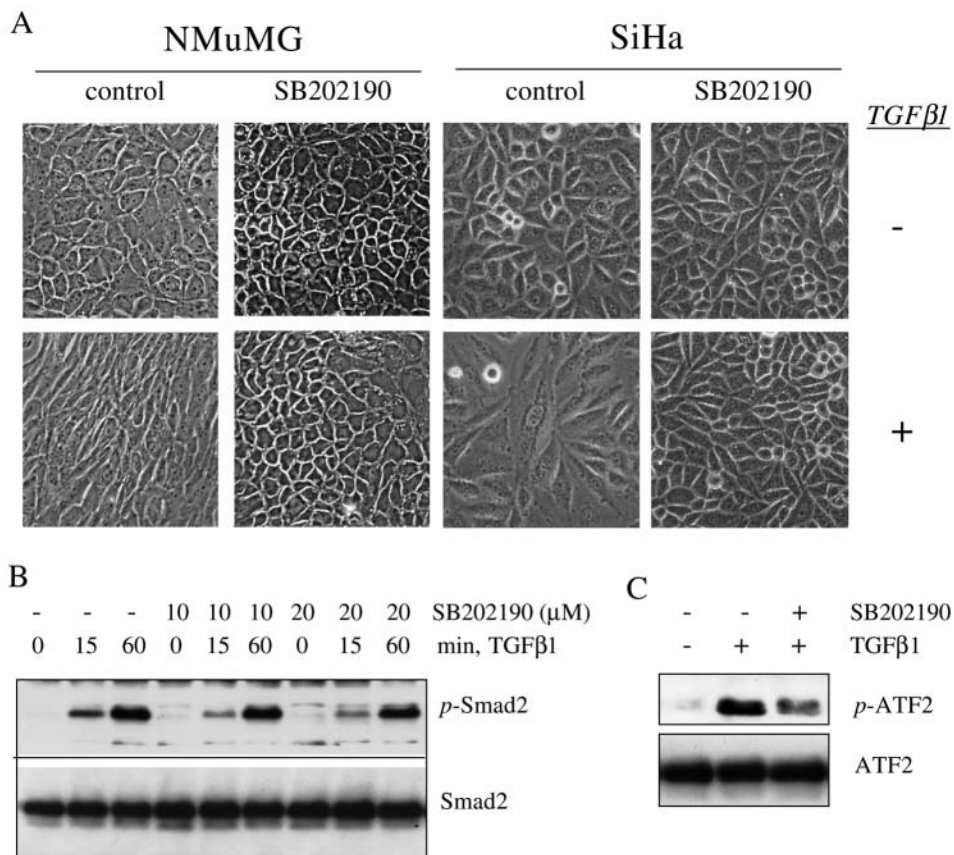

Fig. 2. Blockade of TGFβ-induced EMT by SB202190. (A) NMuMG cells grown on glass coverslips were treated (bottom row) or not (top row) with 2 ng/ml TGFβ1 for 24 hours in the absence or presence of 10 µM SB202190. Phase contrast images were taken at 200× magnification. (B) phospho-Smad2 and total Smad2 immunoblot analysis of whole-cell extracts from cells treated with 2 ng/ml TGFβ1 in the absence or presence of SB202190. (C) Immunoblots with antisera to phospho-ATF2 and total ATF2. SB202190 inhibits TGFβ-induced phosphorylation of ATF2.

hours, cells were fixed in 100% methanol and cells remaining at the top of the polycarbonate membrane were removed with cotton swabs. The cells that had migrated through pores to the lower surface were stained with Diff-quick stain (VWR Scientific). Membranes were mounted on 25×75 mm microslides. Four random images were recorded at 200× magnification and cells were counted. Experiments were performed in duplicate.

Wound closure assay

MDA-MB-231 and 4T1 cells (1-2×10⁵/well) were seeded in 12-well plates. Cells were incubated in serum-free medium for 32 hours prior to wounding. The wounds were made by scraping with plastic tip across the cell monolayer. Cells were treated with kinase inhibitors 60 minutes before wounding. The wounded cells were treated or untreated with 2 ng/ml TGFβ1. Phase contrast images were recorded at the time of wounding (0 hours) and 16 hours thereafter. The wound closure was estimated as the ratio of the remaining wound area relative to the initial wounded area. Experiments were repeated at least three times.

Results

H-7 inhibits TGFβ-mediated activation of p38MAPK and EMT

We investigated TGFβ-mediated EMT in NMuMG mouse mammary epithelial cells. These mammary epithelial cells have cuboidal cell shape and form tight and adherens junctions. Treatment with 2 ng/ml TGFβ for 24 hours induced changes in the cell morphology from cuboidal to an elongated spindle-like shape (Fig. 1A). Consistent with previous studies (Miettinen et al., 1994), TGFβ-mediated EMT was blocked in the presence of 20 μM H-7 (Fig. 1A). The inhibitors were added 60 minutes prior to addition of TGFβ and were present during a complete duration of the experiment. Although H-7 has been introduced as a protein kinase C (PKC) inhibitor, it can inhibit other kinases including PKA and PKG (Quick et al., 1992). Therefore, we investigated the effect of H-7 on the signaling pathways induced by TGFβ. We found that TGFβ1-induced phosphorylation of Smad2 was not affected by the presence of H-7 at the concentration that blocks EMT (Fig. 1C). Inhibition of JNK and ERK1/2 did not affect EMT (Bakin et al., 2000; Bhowmick et al., 2001a). Therefore, we tested whether H-7 affects TGFβ-mediated activation of the p38MAPK pathway using polyclonal antibodies to phosphorylated (active) MKK3/6 and p38MAPK. TGFβ-mediated phosphorylation of p38MAPK was blocked in the presence of 20 μM H-

7 (Fig. 1C). H-7 also inhibited TGFβ-induced phosphorylation of ATF2, a substrate of p38MAPK (Fig. 1D).

Next, we checked whether H-7 inhibits activation of MKK3/6. We found that TGFβ-induced phosphorylation of MKK3/6 was inhibited by H-7 in a dose-dependent manner (Fig. 1E), suggesting that H-7 inhibits a kinase upstream of MKK3/6. This kinase is downstream of TGFβ receptors as incubation with 5-40 μM H-7 did not block phosphorylation of Smad2 (Fig. 1B). Consistent with this result, H-7 did not block TGFβ-mediated activity of Smad-dependent luciferase reporter (Fig. 1F). Since H-7 can inhibit PKC, we examined activation of p38MAPK in the presence of another PKC
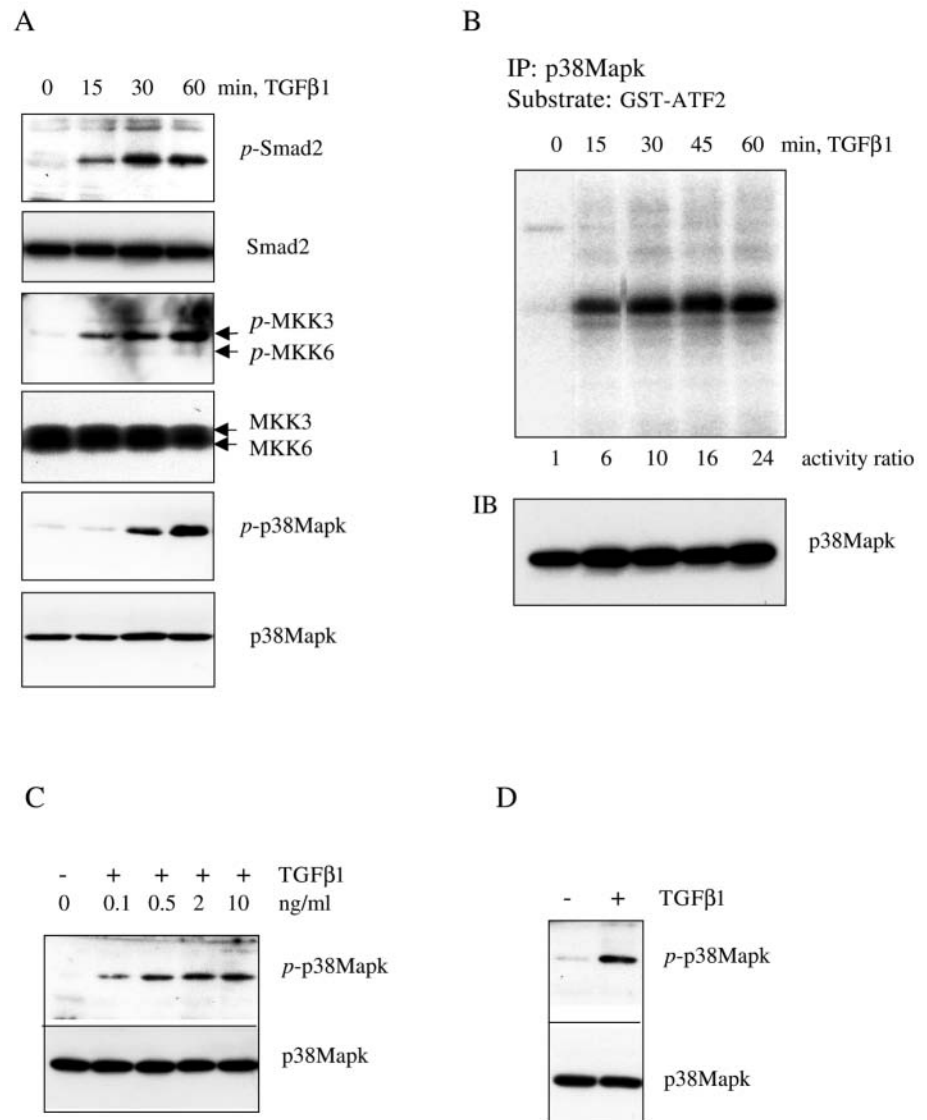
Fig. 3. Activation of the p38MAPK pathway in response to TGFβ. NMuMG cells were incubated in serum-free medium for 4 hours before addition of TGFβ1. (A) Immunoblot analyses with antibodies to phospho-Smad2, phospho-MKK3/6 and phospho-p38MAPK, and total Smad2, MKK3/6 and p38MAPK. (B) Detection of p38MAPK kinase activity in whole-cell extracts from NMuMG cells treated with 2 ng/ml TGFβ1 using GST-ATF2 as substrate. The products were separated by SDS-PAGE and transferred onto nitrocellulose-membrane. γ-^{32}P incorporation into ATF2 was quantitated using PhosphorImager. The membrane was probed with antibody to p38MAPK. (C) Immunoblot detection of TGFβ1 dose-dependent effect on p38MAPK phosphorylation at 60 minutes in NMuMG cells. (D) Induction of p38MAPK phosphorylation by 2 ng/ml TGFβ1 at 60 minutes in SiHa cells.

inhibitor, bisindolylmaleimide-I (BIM-I) (Davies et al., 2000). Treatment of cells with doses of BIM-I (1-5 µM) that block typical PKCs (Davies et al., 2000) did not affect phosphorylation of MKK3/6 in response to TGFβ (Fig. 1D). These results suggest that H-7 impairs TGFβ signaling by inhibiting activation of the p38MAPK pathway downstream of TGFβ receptors, and not through its effect on PKCs.

p38MAPK is involved in TGFβ-mediated EMT

To test whether p38MAPK is involved in EMT, we used specific inhibitors of p38MAPK, SB202190 and SB203580 that do not

affect JNK, MEK1/2 and ERK1/2 (Davies et al., 2000). Microscopic examination showed that cell elongation induced by TGFβ in NMuMG cells was blocked by co-treatment with 10 µM SB202190 (Fig. 2A). Similarly, the p38MAPK inhibitor blocked TGFβ-induced cell elongation in cervical cancer epithelial SiHa cells (Fig. 2A). Previous studies have shown that these p38MAPK inhibitors may affect the kinase activity of TGFβ receptors (Eyers et al., 1998). Therefore, we examined their effect on TGFβ-receptor-dependent phosphorylation of Smad2. Treatment of cells with TGFβ in the presence of SB202190 did not significantly affect the expression and TGFβ-induced phosphorylation of Smad2 (Fig. 2B), whereas it
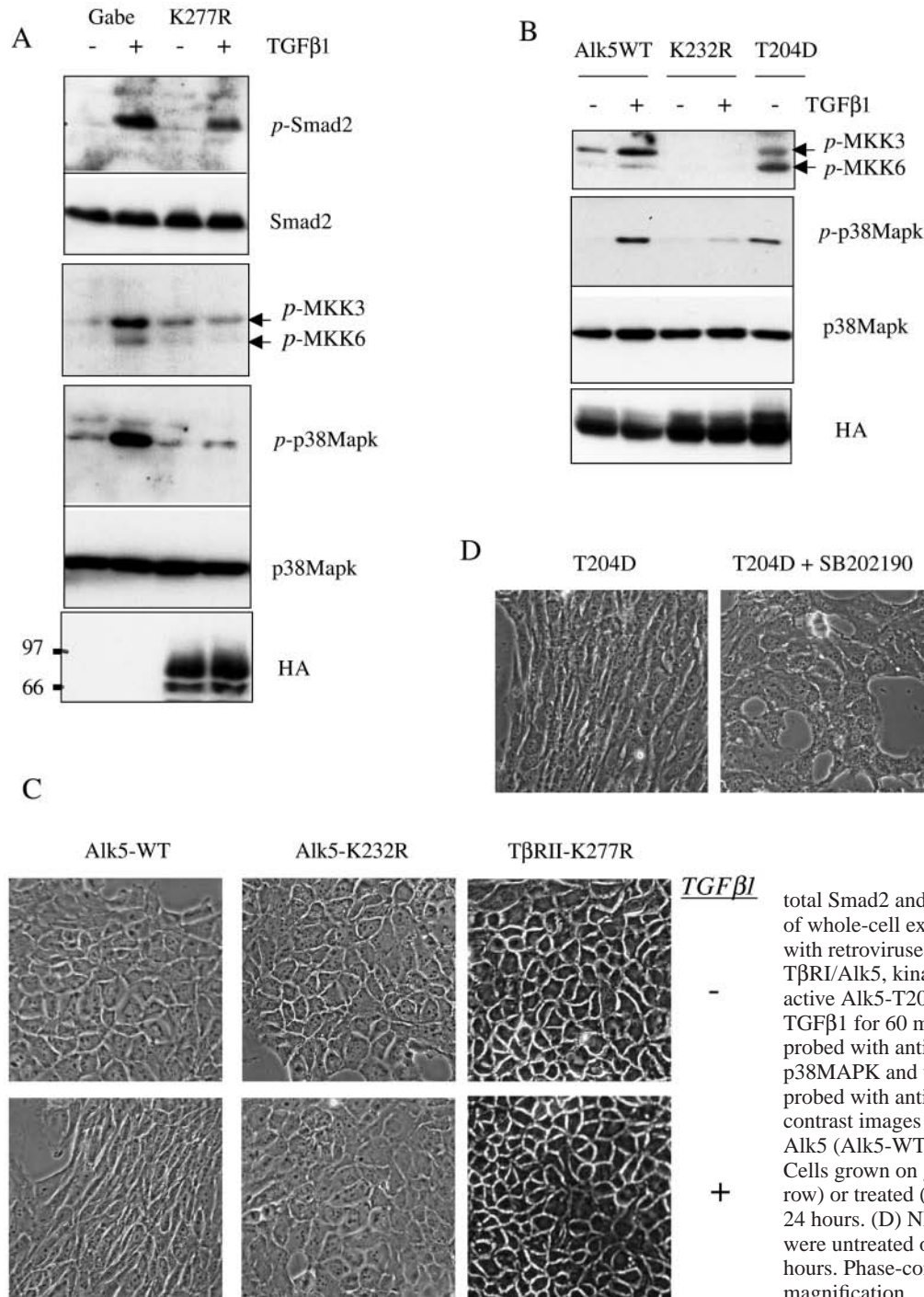
Fig. 4. Effect of kinase mutant TGFβ receptors on TGFβ-induced EMT and activation of the p38MAPK pathway.
(A) Immunoblot analyses of whole-cell extracts from NMuMG cells infected with retrovirus encoding TβRII-K277R or control virus (Gabe). Cells were treated with 2 ng/ml TGFβ1 for 60 minutes. Expression of HA-tagged TβRII-K277R was detected with antisera to the HA-epitope. Dominant-negative TβRII-K277R inhibits phosphorylation of Smad2, MKK3/6 and p38MAPK in response to TGFβ. Membranes were re-probed with antibodies to total Smad2 and p38MAPK. (B) Immunoblot analyses of whole-cell extracts from NMuMG cells infected with retroviruses encoding HA-tagged wild-type (WT) TβRI/Alk5, kinase-inactive Alk5-K232R, and kinase-active Alk5-T204D. Cells were treated with 2 ng/ml TGFβ1 for 60 minutes, and protein extracts were probed with antibodies to phospho-MKK3/6, phospho-p38MAPK and total p38MAPK. Membranes were re-probed with antisera to the HA-epitope. (C) Phase contrast images of NMuMG cells expressing wild-type Alk5 (Alk5-WT), Alk5-K232R, and TβRII-K277R. Cells grown on glass coverslips were untreated (top row) or treated (bottom row) with 2 ng/ml TGFβ1 for 24 hours. (D) NMuMG cells expressing Alk5-T204D were untreated or treated with 15 µM SB202190 for 24 hours. Phase-contrast images were recorded at 200× magnification.

reduced phosphorylation of ATF2 (Fig. 2C). Similar results were obtained with SB203580 (data not shown).

TGFβ activates the p38MAPK pathway in NMuMG and SiHa cells

We next examined activation of the p38MAPK pathway in response to TGFβ. Protein extracts were prepared from cells starved in serum-free medium for 4 hours and treated with TGFβ1. Phosphorylation of MKK3/6 was detected after 15 minutes of TGFβ treatment reaching a maximum at 60 minutes, whereas an increase in p38MAPK phosphorylation at Thr180/Tyr182 was observed at 30 minutes and reached a plateau at 60 minutes (Fig. 3A). To confirm the immunoblot data, we tested p38MAPK-specific activity using an in vitro kinase assay with GST-ATF2 fusion protein as substrate. Treatment with TGFβ increased γ-^{32}P incorporation into GST-ATF2 in a time-dependent fashion, sixfold at 15 minutes and reaching a maximal stimulation of 24-fold above control by 60 minutes (Fig. 3B). This increase in p38MAPK kinase activity at 15 minutes may reflect a higher sensitivity of the in vitro kinase assay compared with detection of phosphorylated p38MAPK by immunoblot. TGFβ-induced activation of p38MAPK was dose-dependent with 0.1 ng/ml being sufficient to induce phosphorylation of p38MAPK with a maximal effect observed between 0.5 and 2 ng/ml (Fig. 3C). Treatment of SiHa human cervical carcinoma cells with TGFβ1 for 60 minutes resulted in phosphorylation of p38MAPK (Fig. 3D), suggesting activation of p38MAPK signaling in response to TGFβ1 in these cells.

Kinase activities of TGFβ receptors are required for TGFβ-induced p38MAPK activation

To confirm the role of TGFβ receptors in activation of p38MAPK, we engineered cells expressing TβRII-K277R, a kinase-inactive mutant of TGFβ type II receptor (Wrana et al., 1994). NMuMG cells were infected with retrovirus encoding TβRII-K277R and enhanced green fluorescent protein (EGFP) or with control retrovirus encoding EGFP only (Gabe). Fluorescent cells were selected by flow cytometry and expression of the HA-tagged mutant receptor was confirmed by immunoblot analysis (Fig. 4A). TGFβ-mediated phosphorylation of Smad2, MKK3/6, and

p38MAPK was inhibited in TβRII-K277R cells compared with control Gabe cells (Fig. 4B). TβRII-K277R also blocked EMT (Fig. 4D) and cell migration (Fig. 8A), indicating that TβRII kinase activity is required for these TGFβ responses.

To determine whether the activation of p38MAPK was TGFβ-specific, we expressed wild-type TβRI/Alk5 (Alk5-WT), kinase-inactive Alk5-K232R, or kinase active Alk5-
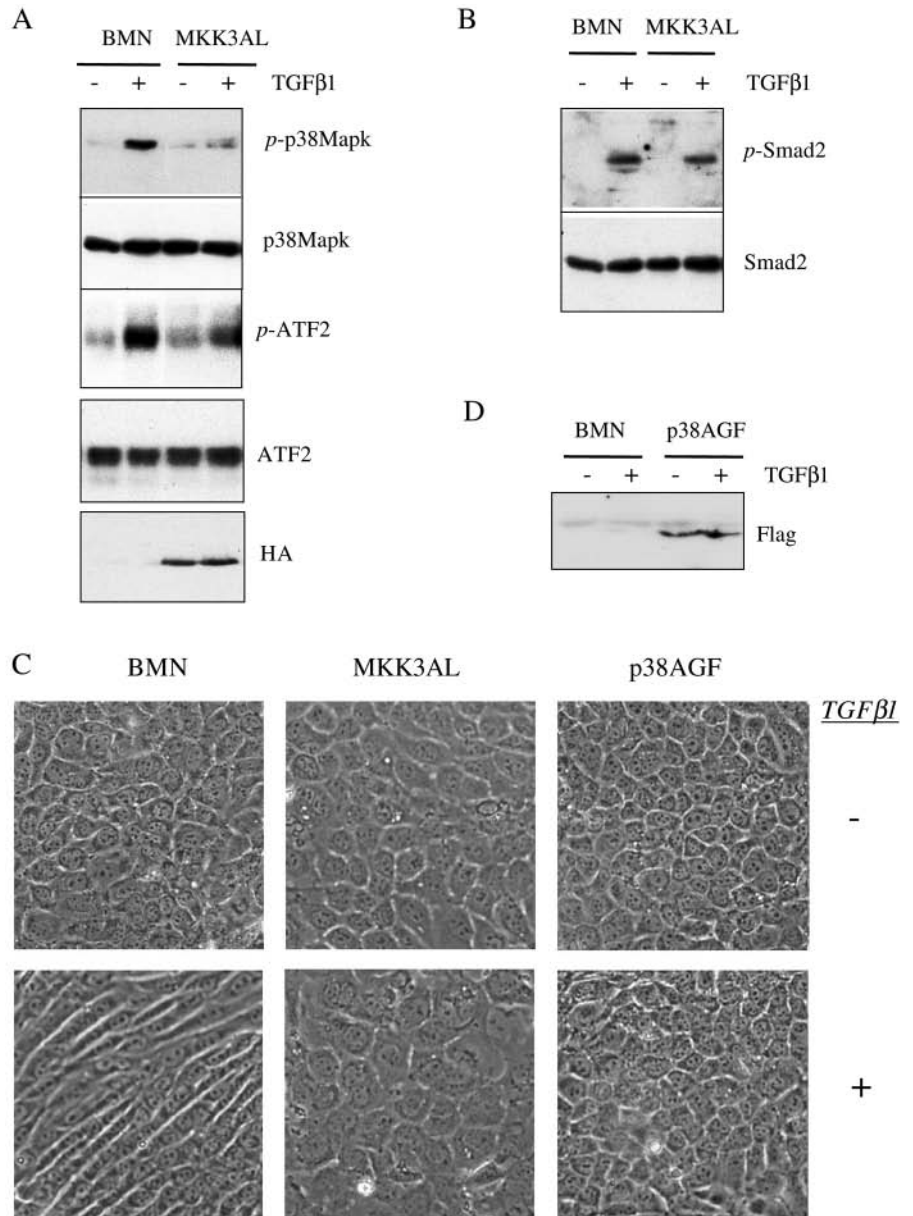
Fig. 5. Effect of dominant-negative MKK3AL and p38AGF on TGFβ-mediated EMT. (A) Immunoblot analysis of p38MAPK and ATF2 phosphorylation in NMuMG cells transfected with empty vector (BMN) or plasmid encoding HA-tagged MKK3AL. Thirty-six hours after transfection cells were treated with 2 ng/ml TGFβ1 for 60 minutes. Whole-cell extracts were probed with phospho-specific antisera, and re-probed with antisera to total protein. Expression of MKK3AL was detected with antisera to the HA-epitope. (B) Immunoblot detection of Smad2 phosphorylation in MKK3AL-expressing cells. (C) Phase-contrast images of NMuMG cells infected with control (BMN) retrovirus or retroviruses encoding dominant-negative MKK3 (MKK3AL) or p38α (p38AGF). Cells were untreated (top row) or treated with 2 ng/ml TGFβ1 for 24 hours. Images were recorded at 200× magnification. (D) Immunoblot detection of Flag-tagged p38AGF in NMuMG cells infected with p38AGF encoding retrovirus compared with control retrovirus (BMN).

T204D (Kawabata et al., 1995) in NMuMG cells. Alk5 mutants were expressed using a bi-cistronic retroviral vector encoding EGFP. GFP-positive cells were selected by flow cytometry and expression of mutants was confirmed by immunoblot analysis (Fig. 4B). Kinase-inactive Alk5-K232R significantly reduced TGFβ-induced phosphorylation of MKK3/6 and p38MAPK, whereas kinase active Alk5-T204D induced phosphorylation of MKK3/6 and p38MAPK in the absence of added ligand (Fig. 4B). Microscopic studies showed that TGFβ-induced EMT was impaired in cells expressing kinase-inactive Alk5-K232R. Cells expressing Alk5-T204D exhibited a fibroblastic morphology similar to Alk5-WT cells treated with TGFβ for 24 hours (Fig. 4C). Treatment of cells expressing Alk5-T204D with the p38MAPK inhibitor SB202190 reversed these morphological changes.

MKK3/6 kinases mediate activation of p38MAPK and EMT in response to TGFβ

Dual-specificity MKK3 and MKK6 kinases have been implicated in activation of p38MAPK (Raingeaud et al., 1996). Phosphorylation of both kinases is induced by TGFβ or by expression of active Alk5-T204D in NMuMG cells (Fig. 4B). Therefore, we tested the effect of dominant-negative MKK3AL (Huang et al., 1997; Zanke et al., 1996) on TGFβ-mediated activation of p38MAPK and EMT in NMuMG cells. Expression of HA-tagged MKK3AL reduced phosphorylation of endogenous p38MAPK and ATF2 (Fig. 5A), whereas expression and phosphorylation of Smad2 were not affected (Fig. 5B). Similar results were obtained with dominant-negative MKK6AL (data not shown). Next, we examined the effect of MKK3AL on EMT. TGFβ induced EMT in NMuMG cells infected with control retrovirus encoding EGFP only (BMN), whereas EMT was inhibited in MKK3AL-expressing cells (Fig. 5C). SB202190, a p38MAPK inhibitor, blocks activity of p38α and p38β but does not inhibit p38γ and p38δ (Davies et al., 2000). Since, SB202190 blocked EMT (Fig. 2A), we tested the effect of p38AGF, a dominant-negative mutant of p38α, on TGFβ-mediated EMT. TGFβ-induced morphological transformation in NMuMG infected with retroviruses encoding p38AGF was impaired compared with

cells infected with control BMN virus (Fig. 5C). These findings suggest that MKK3/6 kinases mediate TGFβ-induced activation of p38MAPK and EMT in NMuMG cells.

p38MAPK is involved in TGFβ-induced reorganization of the actin cytoskeleton

We characterized the effect of p38MAPK inhibitors on reorganization of the actin cytoskeleton in response to TGFβ. Microscopic examination of F-actin by staining with phalloidin-fluorescein showed a cortical arrangement of actin at the cell-cell junctions without significant stress fibers (Fig. 6A). Treatment with TGFβ1 for 24 hours induced formation of actin stress fibers arranged along the largest cell axis. SB202190 did not significantly change the actin organization in TGFβ-untreated cells, but impaired TGFβ-induced formation of actin stress fibers (Fig. 6A). Similar blockade of stress fiber formation was observed in cells pretreated with H-7 (data not shown). Examination of the actin cytoskeleton in MKK3AL cells showed that MKK3AL did not affect the cortical arrangement of actin in untreated cells, but inhibited TGFβ-induced actin stress fiber formation (Fig. 6B). These
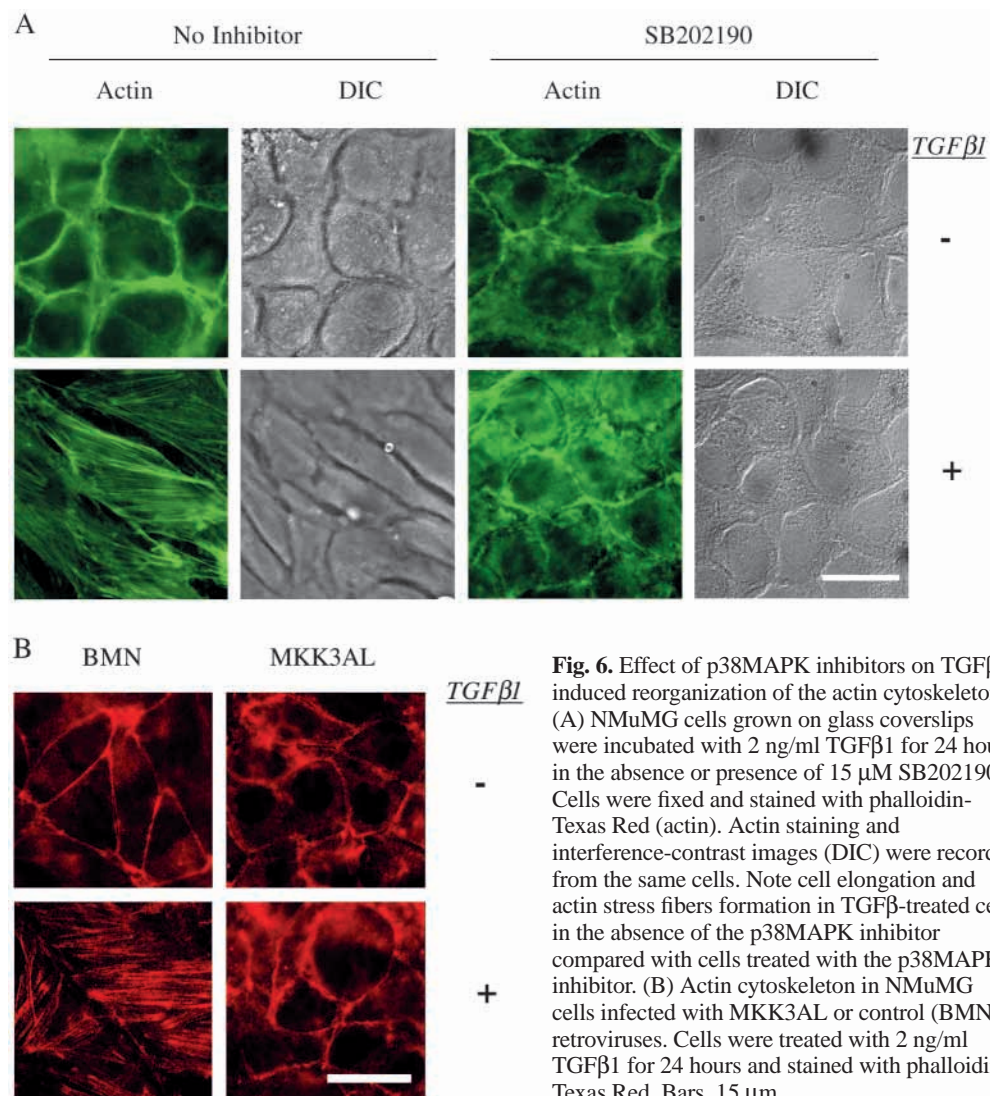
Fig. 6. Effect of p38MAPK inhibitors on TGFβ-induced reorganization of the actin cytoskeleton. (A) NMuMG cells grown on glass coverslips were incubated with 2 ng/ml TGFβ1 for 24 hours in the absence or presence of 15 μM SB202190. Cells were fixed and stained with phalloidin-Texas Red (actin). Actin staining and interference-contrast images (DIC) were recorded from the same cells. Note cell elongation and actin stress fibers formation in TGFβ-treated cells in the absence of the p38MAPK inhibitor compared with cells treated with the p38MAPK inhibitor. (B) Actin cytoskeleton in NMuMG cells infected with MKK3AL or control (BMN) retroviruses. Cells were treated with 2 ng/ml TGFβ1 for 24 hours and stained with phalloidin-Texas Red. Bars, 15 μm.

data suggest that p38MAPK contributes to the reorganization of the actin cytoskeleton induced by TGFβ during EMT.

Rac GTP-binding protein is involved in TGFβ-induced activation of p38MAPK and EMT

There is evidence that small GTP-binding proteins are involved in TGFβ signaling (Atfi et al., 1997; Bakin et al., 2000; Bhowmick et al., 2001a; Engel et al., 1999; Mucsi et al., 1996). Rac1 and CDC42 have been implicated in the activation of the MKK3/6-p38MAPK cascade in several systems (Coghlan et al., 2000; Tibbles et al., 1996; Uddin et al., 2000; Zhang et al., 1995). To test whether Rac1 or RhoA are involved in p38MAPK activation in response to TGFβ, we transfected dominant-negative RhoAN19 or Rac1N17 in NMuMG cells. Rac1N17 inhibited TGFβ1-induced phosphorylation of p38MAPK and its downstream substrate ATF2, whereas neither dominant-negative RhoAN19 nor constitutively active RhoAQ63L did not affect p38MAPK phosphorylation (Fig.

7A,B). These data suggest that Rac1 mediates p38MAPK activation in response to TGFβ.

To examine whether Rac1 activity is induced by TGFβ, we performed affinity precipitation assays using a fusion protein of the GTPase-binding domain (amino acids 67-152) from human PAK1 (PBD) and GST. The GST-PBD fusion protein has been shown to specifically bind active Rac1 loaded with GTP (Benard et al., 1999). Treatment of NMuMG cells for 15 minutes with TGFβ resulted in the increase in Rac1 binding to purified GST-PBD (Fig. 7C). GST-PBD effectively interacted with the active GTPγS-bound form of Rac1 but did not bind to the inactive GDP-bound form of Rac1 (Fig. 7C, left inset). To confirm that TGFβ receptors can mediate activation of Rac1, we expressed mutants of Alk5-TβRI in HEK293T cells. Kinase-inactive Alk5K232R reduced the level of active Rac1, whereas kinase-active Alk5T204D increased the amount of Rac1 bound to GST-PBD. Expression of dominant-negative Rac1N17 reduced the amount of Rac1 recovered from GST-PBD beads (Fig. 7D). Since active Rac1
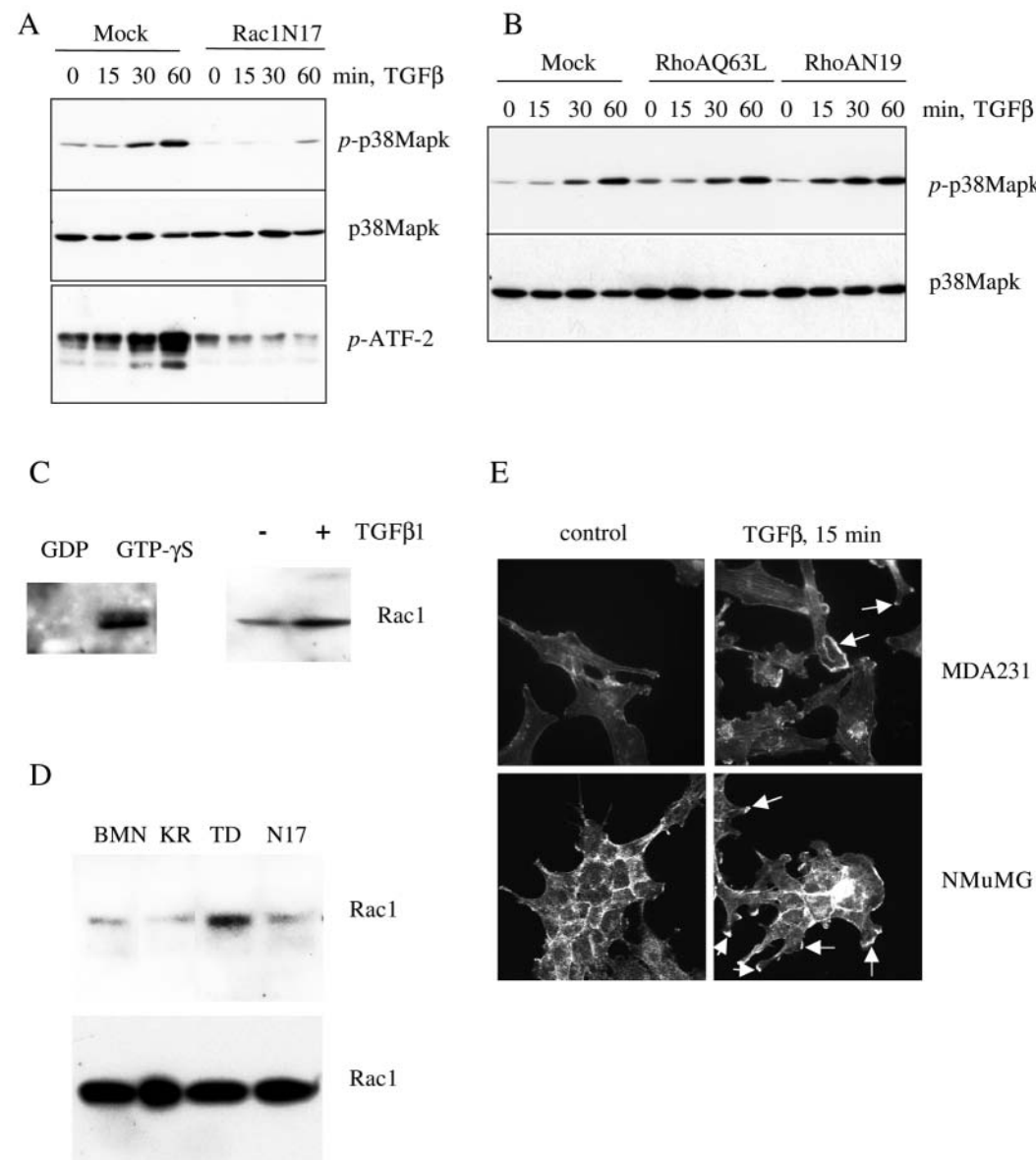
Fig. 7. Rac1 is involved in TGFβ-mediated activation of p38MAPK. (A) Immunoblot analysis of p38MAPK and ATF2 phosphorylation in cells expressing Rac1N17 and treated with 2 ng/ml TGFβ1. (B) p38MAPK phosphorylation in cells expressing RhoAN19 or RhoAQ63L. (C) NMuMG cells were treated with 2 ng/ml TGFβ1 for 15 minutes. Cell lysates were clarified and used for affinity precipitation with 8 μg of GST-PBD. Proteins bound to GST-PBD were separated on SDS-PAGE, transferred to nitrocellulose membrane and blotted with antibody to Rac1. The inset at the top-left shows the total signal detected using cell lysate pre-exchanged with either GTPγS or GDP as described in Materials and Methods. (D) 293T cells were transfected with control plasmid (BMN), kinase-inactive Alk5K232R, kinase-active Alk5T204D or dominant-negative Rac1N17. Cells were lysed 48 hours after transfection. Cell lysates were clarified and used for affinity precipitation with 8 μg of GST-PBD as described above. The bottom inset shows the Rac1 signal detected in total cell lysates. (E) Confocal images of F-actin in NMuMG cells treated with 2 ng/ml TGFβ1 for 15 minutes and stained with phalloidin-Texas Red. Arrows indicate the spots of actin polymerization at the cell edges.

mediates actin ruffling and lamellipodia formation (Hall, 1998), we examined F-actin in NMuMG and MDA-MB-231 cells treated with 2 ng/ml of TGFβ1 for 15 minutes. Confocal microscopy of cells stained with phalloidin-Texas Red showed that TGFβ induced actin ruffles, a phenotype associated with active Rac (Fig. 7E).

In order to examine the role of Rac1 in EMT, NMuMG cells were infected with a retrovirus encoding dominant-negative Rac1N17 and Green Fluorescent Protein (GFP). Immunoblot analysis showed at least twofold higher levels of Rac1 in cells infected with Rac1N17 retrovirus compared with cells infected with control BMN virus encoding GFP only (Fig. 8A). TGFβ induced phosphorylation of MKK3/6 and p38MAPK in cells infected with control retrovirus whereas, in Rac1N17 cells, this induction was significantly reduced (Fig. 8B). Rac1N17 did not significantly affect TGFβ-dependent phosphorylation of Smad2 (Fig. 8C). Microscopic examination showed that TGFβ1 induced cell elongation and the formation of actin stress fibers in control BMN cells, whereas these effects were impaired in cells expressing Rac1N17 (Fig. 8D). These findings suggest that Rac1 is involved in TGFβ-induced EMT and activation of p38MAPK.

p38MAPK inhibitors block TGFβ-mediated cell motility

TGFβ stimulates chemotaxis and migration of tumor and nontumor cells (Ashcroft et al., 1999; Postlethwaite et al., 1987). Recent studies implicated p38MAPK in TGFβ-induced chemotaxis of human neutrophils (Hannigan et al., 1998). We next tested the effect of p38MAPK inhibitors on TGFβ-mediated migration of NMuMG (nontumor) and MDA-MB-231 (tumor) cells. TGFβ stimulated approximately threefold the chemotactic migration of NMuMG cells through polycarbonate filters (Fig. 9A). Migration of NMuMG cells was significantly inhibited by SB202190, as were NMuMG cells infected with kinase-inactive TGFβ type II receptor (TβRII-K277R) compared with those infected with control Gabe retrovirus (Fig. 9A). TGFβ stimulated approximately sixfold migration of breast cancer MDA-MB-231 cells. This was also blocked by SB202190 (Fig. 9B).

To investigate further the role of p38MAPK in TGFβ-mediated cell migration, wounds were made in confluent cultures of MDA-MB-231 and 4T1 breast cancer cells. These cells are not growth inhibited by TGFβ1. Addition of TGFβ1 to serum-free medium accelerated the wound closure in both cell lines, whereas in the presence of the p38MAPK inhibitor

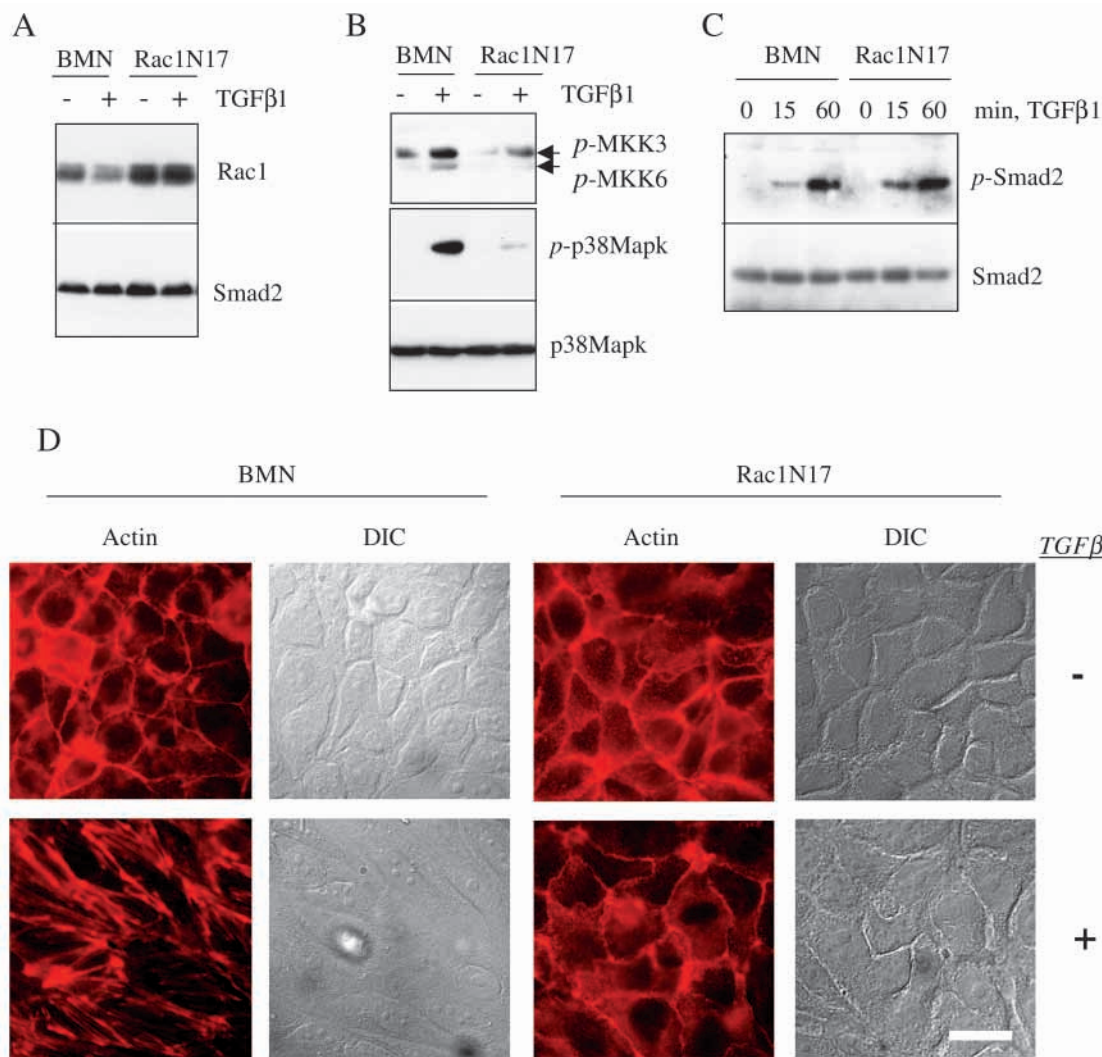Fig. 8. Dominant-negative Rac1N17 blocks TGFβ-mediated activation of p38MAPK and EMT. NMuMG cells were infected with retrovirus encoding Rac1N17 or control virus (BMN) and treated with 2 ng/ml TGFβ1. (A) Detection of Rac1N17 expression with antisera to Rac1. Cells infected with Rac1N17 show a higher level of Rac1 expression. (B) Immunoblot detection of MKK3/6 and p38MAPK phosphorylation in control (BMN) and Rac1N17 expressing cells. (C) Immunoblot with antisera to phospho-Smad2 and total Smad2. (D) Microscopic images from NMuMG cells infected with control retrovirus (BMN) or retrovirus encoding Rac1N17. Cells grown on glass coverslips were treated with 2 ng/ml TGFβ1 for 24 hours. Cells were stained with phalloidin-Texas Red (actin). Actin and interference-contrast images (DIC) were recorded from the same cells. Bar, 15 μm.
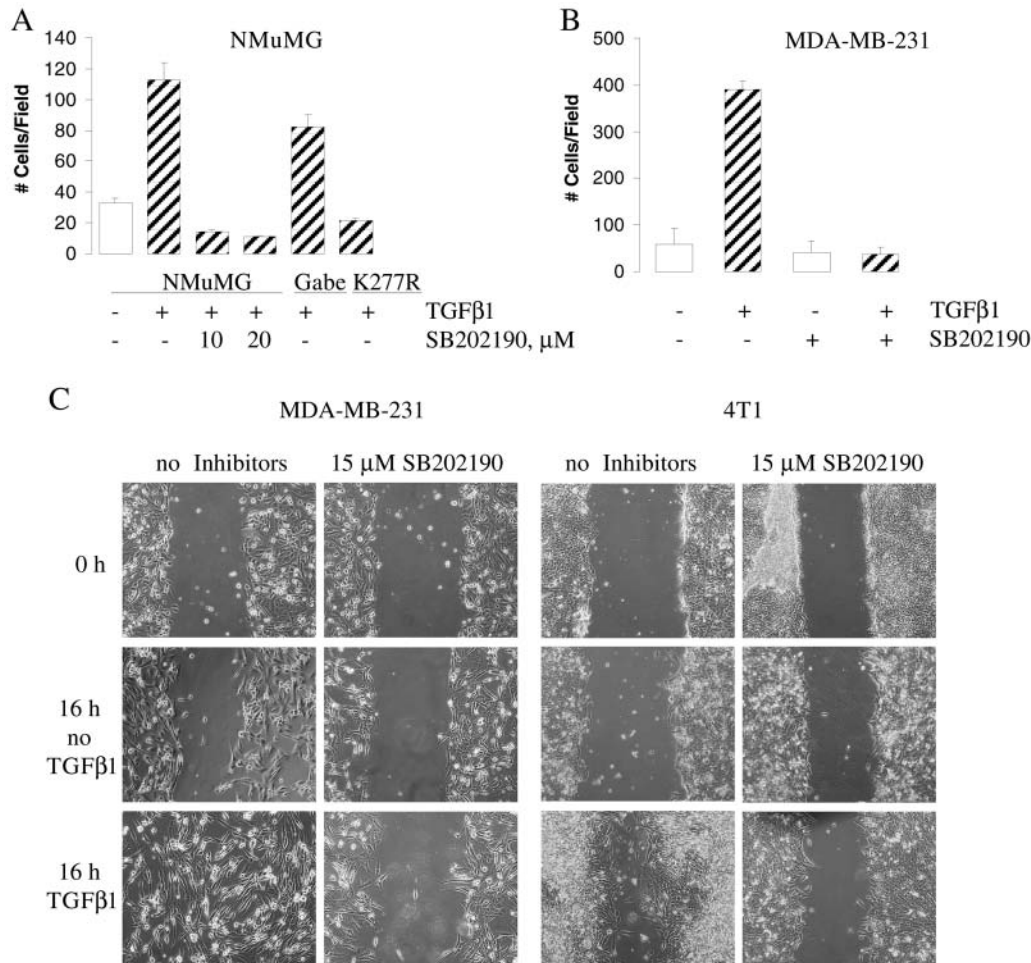
Fig. 9. Involvement of p38MAPK in TGFβ-mediated cell migration. (A,B) NMuMG or MDA-MB-231 cells (1×10^5/well) were seeded in the upper chamber of 5 μm pore transwells and 2 ng/ml TGFβ1 was added to the lower chamber. Cells were incubated for 16 hours in the absence or presence of SB202190, a p38MAPK inhibitor. Cells migrating through pores were stained and counted from four random fields. Experiments were performed in duplicates. Values are the mean ±s.d. of cells per field. Migration of NMuMG cells expressing kinase-inactive TβRII-K277R was compared with cells infected with control Gabe virus. (B) Blockade of MDA-MB-231 cell migration with 10 μM SB202190. (C) Wound closure in monolayers of MDA-MB-231 and 4T1 cells following 16 hours of treatment with 2 ng/ml TGFβ1 in the absence or presence of 10 μM SB202190. Phase contrast images were recorded at 100× magnification. Similar results were obtained three times.

the wounds stayed opened (Fig. 9D). These data suggest that p38MAPK is involved in TGFβ-induced cell migration.

Discussion

TGFβ can induce mesenchymal transdifferentiation in epithelial and endothelial cells (Boyer et al., 1999; Brown et al., 1999; Miettinen et al., 1994). Early studies have shown that protein kinase inhibitor H-7 blocks TGFβ-induced EMT but a particular signaling cascade affected by H-7 was not identified (Miettinen et al., 1994). We found that H-7 inhibited TGFβ-induced phosphorylation of MKK3/6 kinases, but did not affect phosphorylation of Smad2 and Smad-dependent transcriptional responses. These results suggest that H-7 affects a kinase that mediates signaling downstream of TGFβ receptors, but upstream of MKK3/6 kinases. This kinase is distinct from typical PKCs, since BIM-I, an inhibitor of typical PKCs, did not block TGFβ-induced EMT and phosphorylation of MKK3/6 and p38MAPK. The candidate kinases include atypical PKCs and kinase(s) implicated in activation of MKK3/6 such as PAK1 (Zhang et al., 1995), TAK1 (Yamaguchi et al., 1995), and MLK3 (Tibbles et al., 1996).

The H-7 studies suggested a critical role for the p38MAPK pathway in EMT. This hypothesis was further tested using the p38MAPK specific inhibitors, SB202190 and SB203580, which do not inhibit JNK, MEK1/2 and ERK1/2 kinases

(Davies et al., 2000). SB202190 and SB203580 blocked TGFβ-induced cell morphological changes in NMuMG mouse mammary epithelial cells and SiHa human cervical carcinoma cells. The p38MAPK inhibitors blocked TGFβ-induced phosphorylation of ATF2, a p38MAPK substrate, without effect on Smad2 phosphorylation, implying that under these experimental conditions the blockade of p38MAPK did not affect TGFβ receptor kinase activity.

To test whether activation of p38MAPK by TGFβ is a direct event, we investigated the kinetics of activating phosphorylation of MKK3/6 and p38MAPK. TGFβ induced phosphorylation of Smad2 and MKK3/6 kinases with similar kinetics (15 minutes). Phosphorylation of p38MAPK was delayed (30 minutes) suggesting that this event requires activation of MKK3/6. We further showed that dominant-negative mutants of MKK3 and MKK6 interfering with p38MAPK activation (Raingeaud et al., 1996) impaired TGFβ-induced phosphorylation of p38MAPK and ATF2, indicating that the MKK3/6-p38MAPK module mediates TGFβ signaling in NMuMG cells. The dose-dependent increase in p38MAPK activity was confirmed by in vitro kinase assay and by phosphorylation of ATF2.

To confirm the specificity of TGFβ signaling to p38MAPK we performed studies with TGFβ receptor mutants. Kinase-inactive type II receptor blocked EMT and phosphorylation of Smad2 as well as MKK3/6 and p38MAPK, indicating that

kinase function of TβRII is required for activation of p38MAPK and EMT. Kinase-inactive TβRI/Alk5-K232R also blocked TGFβ-induced activation of the p38MAPK pathway, whereas expression of kinase active Alk5-T204D resulted in phosphorylation of MKK3/6 and p38MAPK and EMT in the absence of added TGFβ1. Thus, kinase activities of both TGFβ receptors are required for TGFβ-induced activation of the p38MAPK pathway, and Alk5-T204D can signal to p38MAPK in the absence of added ligand. Alk5-T204D-induced EMT was inhibited by SB202190, a p38MAPK inhibitor, suggesting that p38MAPK mediates EMT induced by Alk5-T204D.

Activation of p38MAPK is mediated by Rac1/CDC42 GTP-binding proteins (Coghlan et al., 2000; Tibbles et al., 1996; Uddin et al., 2000; Zhang et al., 1995). Small GTP-binding proteins are also involved in TGFβ responses (Atfi et al., 1997; Bakin et al., 2000; Bhowmick et al., 2001a; Engel et al., 1999; Mucsi et al., 1996). We found that dominant-negative Rac1N17 impaired activation of the p38MAPK pathway in NMuMG cells, whereas RhoAN19 did not block this event. Expression of Rac1N17 did not affect phosphorylation of Smad2. These data suggest that Rac1 mediates TGFβ-induced p38MAPK activation independently of Smad activation. The mechanism of downstream signaling events is unclear. Previous studies showed that PAK1 mediates p38MAPK activation downstream of Rac1 and CDC42 (Zhang et al., 1995). Furthermore, TGFβ-activated kinase 1 (TAK1), has been implicated in p38MAPK activation in response to BMP and TGFβ in several cell systems (Yamaguchi et al., 1995).

Expression of dominant-negative Rac1N17 in NMuMG cells inhibited TGFβ1-induced changes in cell shape and the actin cytoskeleton suggesting involvement of Rac1 in TGFβ-induced EMT. This result is consistent with other reports. For example, both D-Rac and D-p38 have been reported to contribute to Dpp signaling during wing morphogenesis in *Drosophila* (Adachi-Yamada et al., 1999; Eaton et al., 1995). There is also evidence that Rac1 is required for EMT induced by hepatocyte growth factor (HGF) in MDCK cells (Ridley et al., 1995; Royal et al., 2000). Dominant-negative Rac/CDC42 mutants inhibit oncogenic Ras-induced cell transformation (Qiu et al., 1997; Qiu et al., 1995), and Ras has been shown to cooperate with TGFβ in the induction of EMT (Oft et al., 1996). In addition, Rho/Rac/CDC42 proteins are involved in morphogenesis by regulating the actin cytoskeleton (Hall, 1998). Therefore, Rac1 may contribute to TGFβ-induced EMT via its effects on the cell cytoskeleton and/or via activation of the p38MAPK pathway. In NMuMG cells, TGFβ1 induced actin ruffles and activation of Rac1 within 15 minutes (Fig. 7C,E). Expression of kinase-inactive Alk5K232R reduced, whereas constitutively active Alk5-T204D increased, Rac1 loading with GTP (Fig. 7D) and induced the formation of strong actin ruffles (data not shown). These results suggest that Rac activation and actin ruffling induced by TGFβ may precede the formation of actin stress fibers, which does not occur until 4 hours after addition of TGFβ1 (Bhowmick et al., 2001a).

Inhibitors of p38MAPK and dominant-negative MKK3AL impaired TGFβ-induced changes in cell morphology and reorganization of the actin cytoskeleton. Expression of the dominant-negative mutant of p38α also blocked TGFβ-mediated EMT. Together, these results suggest that the p38MAPK pathway contributes to TGFβ-induced alterations in the actin cytoskeleton and the cell shape during EMT.

Consistent with this hypothesis, p38MAPK has been shown to mediate regulation of the actin cytoskeleton in smooth muscle myocytes in response to TGFβ (Hedges et al., 1999), and in H_2O_2-induced rapid reorganization of the actin cytoskeleton in endothelial and mesenchymal cells (Huot et al., 1998). A recent study reported involvement of p38MAPK in TGFβ-mediated EMT (Bhowmick et al., 2001b). In this report, adenoviral transduction of dominant-negative p38β inhibited TGFβ-mediated EMT at the step of disruption of junctional complexes but did not alter actin reorganization. We found that p38MAPK inhibitors and dominant-negative MKK3AL affected actin stress fiber formation (Fig. 6). TGFβ and Alk5T204D activated both MKK3 and MKK6 in NMuMG cells (Figs 3, 4). This suggests that TGFβ may activate multiple p38MAPK isoforms in NMuMG cells as MKK3 preferentially activates p38α and p38γ, while MKK6 activates p38MAPKs α, β and γ (Enslen et al., 1998). Recent studies showed that p38α and p38β may have different functions (Wang et al., 1998) and different subcellular localization (Lee et al., 2000). p38MAPK inhibitors block activity of both p38α and p38β (Enslen et al., 1998) and MKK3AL impaired phosophorylation of p38MAPK in NMuMG cells as measured with an antibody that recognizes both α and β isoforms. Therefore, multiple p38MAPKs may be involved in TGFβ-induced EMT and mediate different aspects of EMT, potentially explaining the discrepancies with previous studies (Bhowmick et al., 2001b).

EMT is a complex process involving restructuring of the cell cytoskeleton, cell membrane and cell-cell junctions. Previous studies implicated several molecules in different aspects of EMT. Smad transcription factors have been shown to synergize with Alk5 in induction of EMT but no specific function has been associated with these factors (Piek et al., 1999a). PI3K/Akt may contribute to dissolution of tight junctions and to TGFβ transcriptional responses (Bakin et al., 2000). RhoA/Rock signaling has been implicated in the actin stress fiber formation (Bhowmick et al., 2001a). What aspect of EMT can be mediated by p38MAPK? p38MAPK can regulate the actin organization via HSP27 (Hedges et al., 1999; Huot et al., 1998). Therefore, p38MAPK may function in TGFβ-induced reorganization of the actin cytoskeleton in parallel or upstream of the RhoA/Rock pathway since dn-RhoA and Y27632, a Rock kinase inhibitor, did not affect activation of p38MAPK by TGFβ (data not shown). In addition, p38MAPK may contribute to the expression of TGFβ target genes that are casually involved in EMT because p38MAPK has been implicated in TGFβ-transcriptional responses by activating ATF2 and Sp1 (Park et al., 2000; Raingeaud et al., 1996; Sano et al., 1999).

Finally, we investigated the role of p38MAPK in TGFβ-induced migration of mouse and human mammary epithelial cells. The p38MAPK inhibitors blocked TGFβ-stimulated migration of NMuMG, MDA-MB-231 and 4T1 cells. These results are consistent with the proposed role of p38MAPK in TGFβ-mediated chemotaxis of human neutrophils (Hannigan et al., 1998) and smooth muscle cells (Hedges et al., 1999). Interestingly, Smad3-deficient keratinocytes and monocytes are impaired in the chemotactic response to TGFβ (Ashcroft et al., 1999), whereas p38MAPK inhibitors did not affect Smad2 phosphorylation (Fig. 2). These data suggest that the p38MAPK pathway may act in parallel or in cooperation with a Smad-dependent pathway in chemotactic responses to TGFβ.

The data presented suggest that p38MAPK signaling plays a critical role in TGFβ-induced EMT and cell migration. This pathway may be considered as a potential target of therapeutic interventions in neoplastic and inflammatory disorders associated with TGFβ-mediated EMT.

References

Adachi-Yamada, T., Nakamura, M., Irie, K., Tomoyasu, Y., Sano, Y., Mori, E., Goto, S., Ueno, N., Nishida, Y. and Matsumoto, K. (1999). p38 MAPK can be involved in TGF beta superfamily signal transduction in Drosophila wing morphogenesis. *Mol. Cell Biol.* **19**, 2322-2329.

Akhurst, R. J. and Balmain, A. (1999). Genetic events and the role of TGF beta in epithelial tumour progression. *J. Pathol.* **187**, 82-90.

Ashcroft, G. S., Yang, X., Glick, A. B., Weinstein, M., Letterio, J. L., Mizel, D. E., Anzano, M., Greenwell-Wild, T., Wahl, S. M., Deng, C. et al. (1999). Mice lacking Smad3 show accelerated wound healing and an impaired local inflammatory response. *Nat. Cell Biol.* **1**, 260-266.

Atfi, A., Djelloul, S., Chastre, E., Davis, R. and Gespach, C. (1997). Evidence for a role of Rho-like GTPases and stress-activated protein kinase/c-Jun N-terminal kinase (SAPK/JNK) in TGF beta-mediated signaling. *J. Biol. Chem.* **272**, 1429-1432.

Bakin, A. V., Tomlinson, A. K., Bhowmick, N. A., Moses, H. L. and Arteaga, C. L. (2000). Phosphatidylinositol 3-kinase function is required for TGFbeta-mediated epithelial to mesenchymal transition and cell migration. *J. Biol. Chem.* **275**, 36803-36810.

Barrack, E. R. (1997). TGF beta in prostate cancer: a growth inhibitor that can enhance tumorigenicity. *Prostate* **31**, 61-70.

Benard, V., Bohl, B. P. and Bokoch, G. M. (1999). Characterization of Rac and Cdc42 activation in chemoattractant-stimulated human neutrophils using a novel assay for active GTPases. *J. Biol. Chem.* **274**, 13198-13204.

Bhowmick, N. A., Ghiassi, M., Bakin, A., Aakre, M., Lundquist, C. A., Engel, M. E., Arteaga, C. L. and Moses, H. L. (2001a). TGFb mediates epithelial to mesenchymal transdifferentiation through a RhoA-dependent mechanism. *Mol. Biol. Cell* **12**, 27-36.

Bhowmick, N. A., Zent, R., Ghiassi, M., McDonnell, M. and Moses, H. L. (2001b). Integrin beta 1 signaling is necessary for transforming growth factor-beta activation of p38MAPK and epithelial plasticity. *J. Biol. Chem.* **276**, 46707-46713.

Boyer, A. S., Ayerinskas, I. I., Vincent, E. B., McKinney, L. A., Weeks, D. L. and Runyan, R. B. (1999). TGFbeta2 and TGFbeta3 have separate and sequential activities during epithelial-mesenchymal cell transformation in the embryonic heart. *Dev. Biol.* **208**, 530-545.

Brown, C. B., Boyer, A. S., Runyan, R. B. and Barnett, J. V. (1999). Requirement of type III TGF-beta receptor for endocardial cell transformation in the heart. *Science* **283**, 2080-2082.

Coghlan, M. P., Chou, M. M. and Carpenter, C. L. (2000). Atypical protein kinases C lambda and -zeta associate with the GTP-binding protein Cdc42 and mediate stress fiber loss. *Mol. Cell Biol.* **20**, 2880-2889.

Cui, W., Fowlis, D. J., Bryson, S., Duffie, E., Ireland, H., Balmain, A. and Akhurst, R. J. (1996). TGFbeta1 inhibits the formation of benign skin tumors, but enhances progression to invasive spindle carcinomas in transgenic mice. *Cell* **86**, 531-542.

Davies, S. P., Reddy, H., Caivano, M. and Cohen, P. (2000). Specificity and mechanism of action of some commonly used protein kinase inhibitors. *Biochem. J.* **351**, 95-105.

de Caestecker, M. P., Piek, E. and Roberts, A. B. (2000). Role of transforming growth factor-beta signaling in cancer. *J. Natl. Cancer Inst.* **92**, 1388-1402.

Eaton, S., Auvinen, P., Luo, L., Jan, Y. N. and Simons, K. (1995). CDC42 and Rac1 control different actin-dependent processes in the Drosophila wing disc epithelium. *J. Cell Biol.* **131**, 151-164.

Engel, M. E., McDonnell, M. A., Law, B. K. and Moses, H. L. (1999). Interdependent SMAD and JNK signaling in TGF-beta-mediated transcription. *J. Biol. Chem.* **274**, 37413-37420.

Enslen, H., Raingeaud, J. and Davis, R. J. (1998). Selective activation of p38 mitogen-activated protein (MAP) kinase isoforms by the MAP kinase kinases MKK3 and MKK6. *J. Biol. Chem.* **273**, 1741-1748.

Eyers, P. A., Craxton, M., Morrice, N., Cohen, P. and Goedert, M. (1998). Conversion of SB 203580-insensitive MAP kinase family members to drug-sensitive forms by a single amino-acid substitution. *Chem. Biol.* **5**, 321-328.

Frey, R. S. and Mulder, K. M. (1997). Involvement of ERK 2 and stress-activated protein kinase/JNK activation by TGF-beta in the negative growth control of breast cancer cells. *Cancer Res.* **57**, 628-633.

Hall, A. (1998). Rho GTPases and the actin cytoskeleton. *Science* **279**, 509-514.

Hanafusa, H., Ninomiya-Tsuji, J., Masuyama, N., Nishita, M., Fujisawa, J., Shibuya, H., Matsumoto, K. and Nishida, E. (1999). Involvement of the p38 MAPK pathway in TGFbeta-induced gene expression. *J. Biol. Chem.* **274**, 27161-27167.

Hannigan, M., Zhan, L., Ai, Y. and Huang, C. K. (1998). The role of p38 MAP kinase in TGF-beta1-induced signal transduction in human neutrophils. *Biochem. Biophys. Res. Commun.* **246**, 55-58.

Hartsough, M. T. and Mulder, K. M. (1995). Transforming growth factor beta activation of p44[IMAGE] in proliferating cultures of epithelial cells. *J. Biol. Chem.* **270**, 7117-7124.

Hedges, J. C., Dechert, M. A., Yamboliev, I. A., Martin, J. L., Hickey, E., Weber, L. A. and Gerthoffer, W. T. (1999). A role for p38(MAPK)/HSP27 pathway in smooth muscle cell migration. *J. Biol. Chem.* **274**, 24211-24219.

Hojo, M., Morimoto, T., Maluccio, M., Asano, T., Morimoto, K., Lagman, M., Shimbo, T. and Suthanthiran, M. (1999). Cyclosporine induces cancer progression by a cell-autonomous mechanism. *Nature* **397**, 530-534.

Huang, S., Jiang, Y., Li, Z., Nishida, E., Mathias, P., Lin, S., Ulevitch, R. J., Nemerow, G. R. and Han, J. (1997). Apoptosis signaling pathway in T cells is composed of ICE/Ced-3 family proteases and MAP kinase kinase 6b. *Immunity* **6**, 739-749.

Huot, J., Houle, F., Rousseau, S., Deschesnes, R. G., Shah, G. M. and Landry, J. (1998). SAPK2/p38-dependent F-actin reorganization regulates early membrane blebbing during stress-induced apoptosis. *J. Cell Biol.* **143**, 1361-1373.

Iwasaki, S., Iguchi, M., Watanabe, K., Hoshino, R., Tsujimoto, M. and Kohno, M. (1999). Specific activation of the p38 MAPK signaling pathway and induction of neurite outgrowth in PC12 cells by BMP-2. *J. Biol. Chem.* **274**, 26503-26510.

Kawabata, M., Imamura, T., Miyazono, K., Engel, M. E. and Moses, H. L. (1995). Interaction of the transforming growth factor-beta type I receptor with farnesyl-protein transferase-alpha. *J. Biol. Chem.* **270**, 29628-29631.

Kucich, U., Rosenbloom, J. C., Shen, G., Abrams, W. R., Hamilton, A. D., Sebti, S. M. and Rosenbloom, J. (2000). TGF-beta1 stimulation of fibronectin transcription in cultured human lung fibroblasts requires active geranylgeranyl transferase I, phosphatidylcholine-specific phospholipase C, protein kinase C-delta, and p38, but not erk1/erk2. *Arch. Biochem. Biophys.* **374**, 313-324.

Lee, S. H., Park, J., Che, Y., Han, P. L. and Lee, J. K. (2000). Constitutive activity and differential localization of p38alpha and p38beta MAPKs in adult mouse brain. *J. Neurosci. Res.* **60**, 623-631.

Massague, J. (1998). TGF-beta signal transduction. *Annu. Rev. Biochem.* **67**, 753-791.

Miettinen, P. J., Ebner, R., Lopez, A. R. and Derynck, R. (1994). TGF-beta induced transdifferentiation of mammary epithelial cells to mesenchymal cells: involvement of type I receptors. *J. Cell Biol.* **127**, 2021-2036.

Monzen, K., Shiojima, I., Hiroi, Y., Kudoh, S., Oka, T., Takimoto, E., Hayashi, D., Hosoda, T., Habara-Ohkubo, A., Nakaoka, T. et al. (1999). Bone morphogenetic proteins induce cardiomyocyte differentiation through the mitogen-activated protein kinase kinase kinase TAK1 and cardiac transcription factors Csx/Nkx-2.5 and GATA-4. *Mol. Cell. Biol.* **19**, 7096-7105.

Mucsi, I., Skorecki, K. L. and Goldberg, H. J. (1996). ERK and the small GTP-binding protein, Rac, contribute to the effects of TGF-beta1 on gene expression. *J. Biol. Chem.* **271**, 16567-16572.

Nakamura, K., Shirai, T., Morishita, S., Uchida, S., Saeki-Miura, K. and Makishima, F. (1999). p38 MAPK functionally contributes to chondrogenesis induced by growth/differentiation factor-5 in ATDC5 cells. *Exp. Cell Res.* **250**, 351-363.

Oft, M., Heider, K. H. and Beug, H. (1998). TGFbeta signaling is necessary for carcinoma cell invasiveness and metastasis. *Curr. Biol.* **8**, 1243-1252.

Oft, M., Peli, J., Rudaz, C., Schwarz, H., Beug, H. and Reichmann, E. (1996). TGF-beta1 and Ha-Ras collaborate in modulating the phenotypic plasticity and invasiveness of epithelial tumor cells. *Genes Dev.* **10**, 2462-2477.

Park, I. K., Lyu, M. A., Yeo, S. J., Han, T. H. and Kook, Y. H. (2000). Sp1 mediates constitutive and transforming growth factor beta-inducible expression of urokinase type plasminogen activator receptor gene in human monocyte-like U937 cells. *Biochim. Biophys. Acta* **1490**, 302-310.

Piek, E., Heldin, C. H. and ten Dijke, P. (1999a). Specificity, diversity, and regulation in TGF-beta superfamily signaling. *FASEB J.* **13**, 2105-2124.

Piek, E., Moustakas, A., Kurisaki, A., Heldin, C. H. and ten Dijke, P. (1999b). TGF-(beta) type I receptor/ALK-5 and Smad proteins mediate epithelial to mesenchymal transdifferentiation in NMuMG breast epithelial cells. *J. Cell Sci.* **112**, 4557-4568.

Portella, G., Cumming, S. A., Liddell, J., Cui, W., Ireland, H., Akhurst, R. J. and Balmain, A. (1998). Transforming growth factor beta is essential for spindle cell conversion of mouse skin carcinoma in vivo: implications for tumor invasion. *Cell Growth Differ.* **9**, 393-404.

Postlethwaite, A. E., Keski-Oja, J., Moses, H. L. and Kang, A. H. (1987). Stimulation of the chemotactic migration of human fibroblasts by transforming growth factor beta. *J. Exp. Med.* **165**, 251-256.

Qiu, R. G., Chen, J., Kirn, D., McCormick, F. and Symons, M. (1995). An essential role for Rac in Ras transformation. *Nature* **374**, 457-459.

Qiu, R. G., Abo, A., McCormick, F. and Symons, M. (1997). Cdc42 regulates anchorage-independent growth and is necessary for Ras transformation. *Mol. Cell. Biol.* **17**, 3449-3458.

Quick, J., Ware, J. A. and Driedger, P. E. (1992). The structure and biological activities of the widely used protein kinase inhibitor, H7, differ depending on the commercial source. *Biochem. Biophys. Res. Commun.* **187**, 657-663.

Raingeaud, J., Whitmarsh, A. J., Barrett, T., Derijard, B. and Davis, R. J. (1996). MKK3- and MKK6-regulated gene expression is mediated by the p38 mitogen-activated protein kinase signal transduction pathway. *Mol. Cell. Biol.* **16**, 1247-1255.

Ridley, A., Comoglio, P. and Hall, A. (1995). Regulation of scatter factor/hepatocyte growth factor responses by Ras, Rac, and Rho in MDCK cells. *Mol. Cell. Biol.* **15**, 1110-1122.

Royal, I., Lamarche-Vane, N., Lamorte, L., Kaibuchi, K. and Park, M. (2000). Activation of cdc42, rac, PAK, and rho-kinase in response to hepatocyte growth factor differentially regulates epithelial cell colony spreading and dissociation. *Mol. Biol. Cell* **11**, 1709-1725.

Sano, Y., Harada, J., Tashiro, S., Gotoh-Mandeville, R., Maekawa, T. and Ishii, S. (1999). ATF-2 is a common nuclear target of Smad and TAK1 pathways in TGF-beta signaling. *J. Biol. Chem.* **274**, 8949-8957.

Shibuya, H., Iwata, H., Masuyama, N., Gotoh, Y., Yamaguchi, K., Irie, K., Matsumoto, K., Nishida, E. and Ueno, N. (1998). Role of TAK1 and TAB1 in BMP signaling in early Xenopus development. *EMBO J.* **17**, 1019-1028.

Tibbles, L. A. and Woodgett, J. R. (1999). The stress-activated protein kinase pathways. *Cell. Mol. Life Sci.* **55**, 1230-1254.

Tibbles, L. A., Ing, Y. L., Kiefer, F., Chan, J., Iscove, N., Woodgett, J. R. and Lassam, N. J. (1996). MLK-3 activates the SAPK/JNK and p38/RK pathways via SEK1 and MKK3/6. *EMBO J.* **15**, 7026-7035.

Uddin, S., Lekmine, F., Sharma, N., Majchrzak, B., Mayer, I., Young, P. R., Bokoch, G. M., Fish, E. N. and Platanias, L. C. (2000). The Rac1/p38 mitogen-activated protein kinase pathway is required for interferon alpha-dependent transcriptional activation but not serine phosphorylation of Stat proteins. *J. Biol. Chem.* **275**, 27634-27640.

Wang, Y., Huang, S., Sah, V. P., Ross, J., Jr, Brown, J. H., Han, J. and Chien, K. R. (1998). Cardiac Muscle cell hypertrophy and apoptosis induced by distinct members of the p38 mitogen-activated protein kinase family. *J. Biol. Chem.* **273**, 2161-2168.

Wrana, J. L., Attisano, L., Wieser, R., Ventura, F. and Massague, J. (1994). Mechanism of activation of the TGF-beta receptor. *Nature* **370**, 341-347.

Yamaguchi, K., Shirakabe, K., Shibuya, H., Irie, K., Oishi, I., Ueno, N., Taniguchi, T., Nishida, E. and Matsumoto, K. (1995). Identification of a member of the MAPKKK family as a potential mediator of TGF-beta signal transduction. *Science* **270**, 2008-2011.

Yee, J. K., Miyanohara, A., LaPorte, P., Bouic, K., Burns, J. C. and Friedmann, T. (1994). A general method for the generation of high-titer, pantropic retroviral vectors: highly efficient infection of primary hepatocytes. *Proc. Natl. Acad. Sci. USA* **91**, 9564-9568.

Zanke, B. W., Rubie, E. A., Winnett, E., Chan, J., Randall, S., Parsons, M., Boudreau, K., McInnis, M., Yan, M., Templeton, D. J. et al. (1996). Mammalian mitogen-activated protein kinase pathways are regulated through formation of specific kinase-activator complexes. *J. Biol. Chem.* **271**, 29876-29881.

Zhang, S., Han, J., Sells, M. A., Chernoff, J., Knaus, U. G., Ulevitch, R. J. and Bokoch, G. M. (1995). Rho family GTPases regulate p38 MAPK through the downstream mediator Pak1. *J. Biol. Chem.* **270**, 23934-23936.

A Critical Role of Tropomyosins in TGF-β Regulation of the Actin Cytoskeleton and Cell Motility in Epithelial Cells

Andrei V. Bakin,*† Alfiya Safina,* Cammie Rinehart,‡ Cecilia Daroqui,§ Huferesh Darbary,* and David M. Helfman‖¶

*Department of Cancer Genetics, Roswell Park Cancer Institute, Buffalo, NY 14263; ‡Department of Medicine, Vanderbilt University, Nashville, TN 37232; §Research Area, Institute of Oncology "Angel H. Roffo," Buenos Aires, Argentina, C1417DTB; and ‖Cold Spring Harbor Laboratory, Cold Spring Harbor, NY 11724

We have investigated transforming growth factor beta (TGF-β)–mediated induction of actin stress fibers in normal and metastatic epithelial cells. We found that stress fiber formation requires de novo protein synthesis, p38Mapk and Smad signaling. We show that TGF-β via Smad and p38Mapk up-regulates expression of actin-binding proteins including high-molecular-weight tropomyosins, α-actinin and calponin h2. We demonstrate that, among these proteins, tropomyosins are both necessary and sufficient for TGF-β induction of stress fibers. Silencing of tropomyosins with short interfering RNAs (siRNAs) blocks stress fiber assembly, whereas ectopic expression of tropomyosins results in stress fibers. Ectopic-expression and siRNA experiments show that Smads mediate induction of tropomyosins and stress fibers. Interestingly, TGF-β induction of stress fibers was not accompanied by changes in the levels of cofilin phosphorylation. TGF-β induction of tropomyosins and stress fibers are significantly inhibited by Ras-ERK signaling in metastatic breast cancer cells. Inhibition of the Ras-ERK pathway restores TGF-β induction of tropomyosins and stress fibers and thereby reduces cell motility. These results suggest that induction of tropomyosins and stress fibers play an essential role in TGF-β control of cell motility, and the loss of this TGF-β response is a critical step in the acquisition of metastatic phenotype by tumor cells.

INTRODUCTION

There is solid evidence that the transforming growth factor beta (TGF-β) signaling pathway is a major cellular growth inhibitory and proapoptotic pathway in epithelial, endothelial, hematopoeitic, and other cell types (Roberts and Wakefield, 2003). However, clinical and experimental studies indicate that metastatic cancers of the breast and other tissues express elevated levels of TGF-β that appears to support the metastatic behavior of the tumor cells (Saito *et al.,* 2000; Derynck *et al.,* 2001). This apparent paradox has been associated with a progressive decline in the antitumorigenic function and a gain of protumorigenic activities of TGF-β, including induction of epithelial to mesenchymal transition (EMT) and tumor cell migration and invasion (Derynck *et al.,* 2001; Wakefield and Roberts, 2002). Oncogenic Ras, Src, and

Abbreviations used: TGF-β, transforming growth factor beta; Mapk, mitogene-activated protein kinase; TM, tropomyosin; siRNA, short-interfering RNA. NMuMG cells that were untreated or treated with 2 ng/ml TGF-β1 for 24 h in the absence or presence of 10 μM SB202190. The data represent an average of three independent experiments. Actn1, α-actinin1; Tpm3, tropomyosin3; Tpm4, tropomyosin4; Cnn2 (H2), calponin2 (H2).

ErbB2 as well as alterations in TGF-β signaling mediated by Smads, mitogen-activated protein kinases (Mapks), Rho kinases, and Akt/PKB are thought to contribute to the metastatic phenotype (Derynck and Zhang, 2003; Roberts and Wakefield, 2003).

The actin cytoskeleton plays a central role in the regulation of cellular processes linked to metastasis including cell proliferation, apoptosis, anchorage-independent cell growth, and cell migration and invasion (Pawlak and Helfman, 2001; Jaffe and Hall, 2002). TGF-β induces a rapid reorganization of the actin cytoskeleton, leading to membrane ruffling at the cell edges in both nontumorigenic and tumorigenic epithelial cells, whereas a prolonged incubation with TGF-β results in the formation of stress fibers (Bakin *et al.,* 2002; Edlund *et al.,* 2002). The immediate TGF-β–mediated changes in the actin cytoskeleton have been associated with activation of the Rho family of GTPases, Rac, CDC42, and RhoA (Bakin *et al.,* 2002; Edlund *et al.,* 2002), which control cell motility and invasive phenotypes by regulating organization of actin filaments (Jaffe and Hall, 2002). TGF-β regulates activity of these GTPases in various epithelial cell lines independently of Smad signaling (Bhowmick *et al.,* 2001; Bakin *et al.,* 2002; Edlund *et al.,* 2002). The interplay between Rho-like GTPases regulate both the protrusive and contractile forces required for cell migration, via a combination of actin polymerization, depolymerization, and the interaction of myosin-based motors with actin filaments (Etienne-Manneville and Hall, 2002). Although RhoA contributes to cell migration by inducing actomyosin contractility, RhoA can also inhibit cell movement by stimulating the assembly of stress fibers and focal adhesions associated with the cell substratum (Cox *et al.,* 2001). The TGF-β

induction of actin stress fibers has been shown to depend on Smad signaling (Piek *et al.,* 1999b), the RhoA-Rho kinase pathway (Bhowmick *et al.,* 2001), and p38Mapk signaling (Hannigan *et al.,* 1998; Bakin *et al.,* 2002; Edlund *et al.,* 2002). However, the cellular targets regulated by these pathways and their roles in TGF-β regulation of stress fibers and cell motility have not been defined.

Oncogenic transformation mediated by Ras and Src results in the disruption of actin stress fibers and focal adhesions, whereas restoration of actin stress fibers inhibits cell transformation and reduces metastasis (Pawlak and Helfman, 2001). The mechanisms mediating the disruption of stress fibers by the Ras-ERK pathway involve inhibition of the RhoA/ROCK pathway (Sahai *et al.,* 2001; Pawlak and Helfman, 2002a, 2002b; Vial *et al.,* 2003) and repression of actin-binding proteins involved in stabilization of actin filaments including tropomyosins and α-actinin (Pawlak and Helfman, 2001). Thus, the Ras-Erk pathway may modify TGF-β regulation of stress fibers and cell motility through one or both of these mechanisms.

In this study we demonstrate that expression of tropomyosins mediated by Smad and p38Mapk signaling is required for TGF-β regulation of stress fibers and cell motility. We show that the Ras-ERK pathway antagonizes TGF-β induction of stress fibers by suppressing expression of tropomyosins. TGF-β does not modulate cofilin phosphorylation, suggesting that the RhoA-ROCK-LIM kinase-cofilin pathway is not rate limiting. We provide evidence that tropomyosins are both necessary and sufficient for TGF-β induction of stress fibers. We show that expression of tropomyosins in metastatic cells results in stress fibers and reduces cell motility. These results suggest that loss of TGF-β–induced stress fibers is an essential characteristic of a prometastatic conversion of TGF-β function and that regulation of tropomyosin expression is an important component of this response.

MATERIALS AND METHODS

Antibodies, Plasmids, and Other Reagents

TGF-β1 was obtained from R&D Systems (Minneapolis, MN). The following antibodies were obtained from: to Smad2/3 (BD Transduction Laboratories, BD Biosciences, Lexington, KY); rabbit polyclonal to hemaglutinin (HA) epitope (Santa Cruz Biotechnology, Santa Cruz, CA); mouse monoclonal antibodies to tropomyosin (TM311), α-actinin, actin, and the Flag epitope (Sigma, St. Louis, MO); to phospho-Smad2, phospho-ERK1/2, phospho-p38Mapk, phospho-ATF2, phospho-HSP27, and HSP27 (Cell Signaling Technology, Beverly, MA). Phalloidin-Alexa Green and phalloidin-Texas Red were from Molecular Probes (Eugene, OR). Fluorescein-labeled anti-HA antibody was from Roche Applied Science (Indianapolis, IN). Plasmids encoding rat HA-tagged TM2 and TM3 isoforms were described previously (Gimona *et al.,* 1995). Inhibitors of p38Mapk (SB202190, SB203580, PD165319), MEK1/2 (PD098059, U0126), JNK (SP600125), Raf kinase, and protein synthesis (cycloheximide) were from Calbiochem (La-Jolla, CA). Phospho-cofilin antibody was provided by Dr. James Bamburg, Colorado State University (Fort Collins, CO).

Cell Culture

Mouse mammary epithelial NMuMG cells, human cervical carcinoma SiHa cells, human breast cancer MDA-MB-231 cells, human epidermoid carcinoma A431 cells, and human kidney HEK293T cells were purchased from American Tissue Culture Collection (ATCC, Manassas, VA). Cells were cultured as recommended by ATCC.

Adenoviral Infection of Cells

Adenoviruses encoding EGFP, Flag-tagged Smads, and the HA-tagged constitutively active TGF-β type I Alk5T204D receptor were produced using HEK-293T cells and stored in aliquots at −80°C. Cells grown on plastic dishes or glass coverslips were incubated for 3 h with supernatant containing adenoviruses at 5–10 MOI. Medium was replenished and cells were grown for additional 24 h before further treatments.

RNA Isolation and cDNA Microarray Analysis

RNA from mouse nontumor mammary epithelial NMuMG cells treated with 2 ng/ml TGF-β1 for 8 and 24 h was extracted as described in Bakin and Curran, (1999). Total RNA from each sample (35 μg) was labeled and hybridized with the NIA 15K Mouse array. Detailed descriptions of labeling and hybridization procedures are available from http://array.mc.vanderbilt.edu/Pages/Protocols/Protocols.htm. The array slides were scanned with an Axon 4000 scanner (Axon Instruments, Foster City, CA) at a resolution of 10 μm. The reference RNA from untreated NMuMG cells was labeled by using cyanine 3-dUTP (Cy3), and the RNA samples from TGFβ1-treated cells were labeled with cyanine 5-dUTP (Cy5). This experiment was performed in triplicate. Data were analyzed using GenePix4.0 software.

Immunoblot Analysis

Cells were incubated in medium containing 5% serum for 24 h before treatment with 2 ng/ml TGF-β1. Cells were lysed in buffer containing 20 mM Tris, pH 7.4, 137 mM NaCl, 1% NP-40, 10% glycerol, 20 mM NaF, 1 mM Na orthovanadate, 1 mM PMSF, 2 μg/ml aprotinin, and 2 μg/ml leupeptin. Immunoblot analyses of protein extracts were performed as described (Bakin *et al.,* 2002).

Northern Blot and Reverse Transcription-Polymerase Chain Reaction Analysis

A cDNA fragment of rat TM3 and a polymerase chain reaction (PCR)-generated fragment of α-actinin1 cDNA spotted on the microarrays (GenBank accession number BG077689) were used as probes for Northern blot analysis. Identity of α-actinin1 and calponin2 cDNAs were verified by DNA sequencing matched through BLAST analysis (www.ncbi.nlm.nih/BLAST/). Total RNA samples (15 μg/lane) obtained from NMuMG cells treated with 2 ng/ml TGF-β1 for 4, 8, and 24 h were subjected to Northern blot analysis as described previously (Bakin and Curran, 1999). Amplification of transcripts was performed using 50 ng/μL of total RNA and one-step reverse transcription (RT)-PCR system from Invitrogen (Carlsbad, CA) according to the manufacturing protocol. Primer sequences: β-actin, accession no. NM_007393, forward: GCTGGTCGTCGACAACGGCTC, reverse: CAAACATGATCT-GGGTCATCTTTTC; α-tropomyosin, accession no. NM_024427.2, forward: GCTGGTGTCACTGCAAAAGA, reverse: CCTGAGCCTCCAGTGACTTC; β-tropomyosin, accession no. NM_009416.2, forward: AAGGATGCCCAG-GAGAAACT, reverse: CTTCCTTCAGCTGCATCTCC; calponin2, accession no. NM_007725.1, forward: ACCCTGTGGACCTGTTTGAG, reverse: TG-GAAGAGTTGTCGCACTTG; PAI-1, accession no. M33960.1, forward: CCACCGACTTCGGAGTAAAA, reverse: GCGTGTCAGCTCGTCTACAG.

Immunofluorescence Microscopy

Cells (10^5cells/well) were grown in DMEM containing 5% fetal bovine serum (FBS) on glass coverslips (22×22 mm) for 24 h before treatment with 2 ng/ml TGF-β1. Cells were fixed with 4% paraformaldehyde and stained as described (Bakin *et al.,* 2002). Actin filaments (F-actin) were stained with phalloidin-Alexa Green or phalloidin-Texas Red, and tropomyosins were visualized using TM311 antibody. Fluorescent images were captured using Zeiss Axiophot upright microscope (Thornwood, NY) and Nikon TE2000-E inverted microscope (Garden City, NY). In some experiments cells were permeabilized with 0.05% Triton X-100 for 10 min followed by fixation and staining.

Wound Closure Assay

The assay was performed as described previously (Bakin *et al.,* 2002). MDA-MB-231 cells ($1–2 \times 10^5$/well) were seeded in 12-well plates and incubated in serum-free IMEM (Invitrogen) medium for 24 h before wounding with plastic tip across the cell monolayer. Kinase inhibitors were added 1 h before wounding. The cells were left untreated or treated with 2 ng/ml TGF-β1 for 16 h. The wound closure was estimated as the ratio of the remaining wounded area relative to the initial area. Experiments were repeated at least three times.

Transcriptional Assay

NMuMG cells (3×10^4) were seeded in 24-well plates and transfected with 0.16 μg/ml pSBE-Lux containing 12 repeats of Smad binding sequence (provided by J.-M. Gauthier, Laboratoire Glaxo Wellcome, Les Ulis Cedex, France) with 0.002 μg/ml pCMV-Rl (Promega, Madison, WI) using FuGENE6 reagent (Roche Molecular Biochemicals, Indianapolis, IN) according to the manufacturer's protocol. Cells were incubated for 8 h in 0.5% FBS-DMEM before treatment with 1 ng/ml TGF-β1 for 16 h. Firefly luciferase (Luc) and *Renilla reniformis* luciferase (Rl) activities in cell lysates were determined using the Dual Luciferase Reporter Assay System (Promega) according to the manufacturer's protocol in a Monolight 2010 luminometer (Analytical Luminescence Laboratory, San Diego, CA). Luc activity was normalized to Rl activity and presented as Relative Luciferase Units. All assays were done in triplicate wells and each experiment was repeated at least twice.
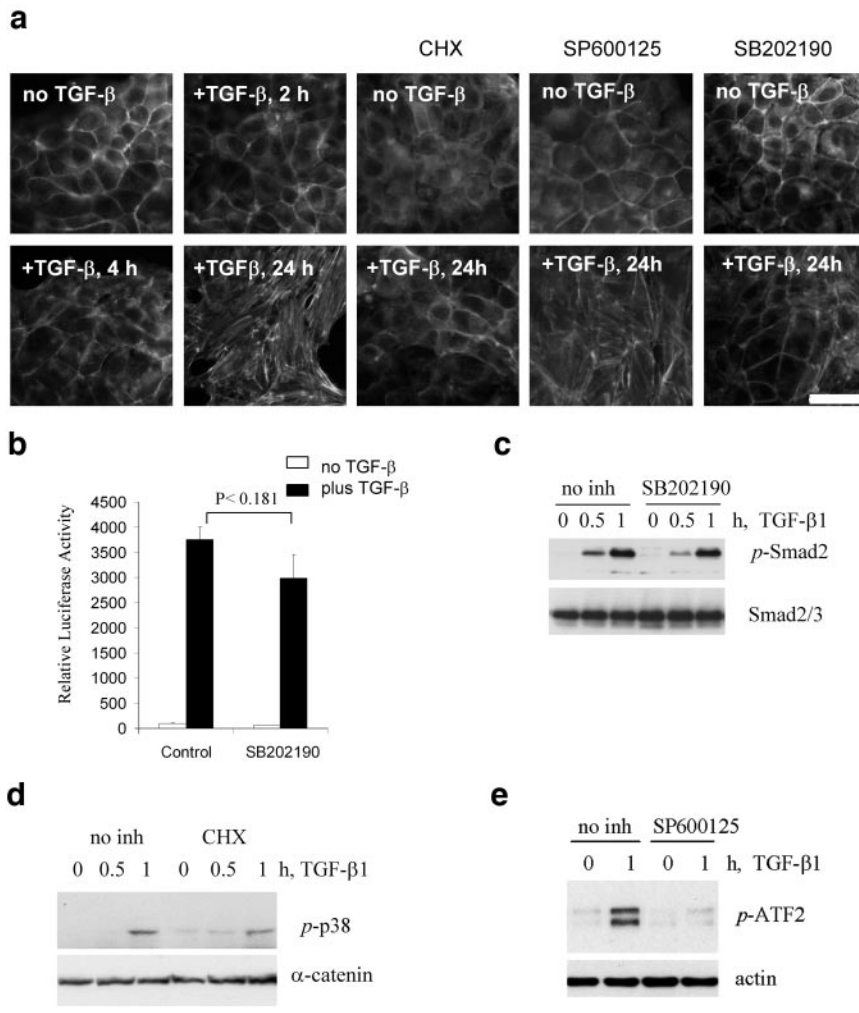
Figure 1. TGF-β1–induced actin stress fibers require p38Mapk and a novel protein synthesis. (a) Actin filaments staining with phalloidin-Alexa Green in cells treated with 2 ng/ml TGF-β1 in the absence or presence of inhibitors. Where it is indicated, cells were treated with 10 µg/ml cycloheximide (CHX) starting at 6 h after addition of TGF-β1. Kinase inhibitors (15 µM SP600125, a JNK inhibitor, and 10 µM SB202190, a p38Mapk inhibitor) were added 1 h before addition of TGFβ1. Scale bar, 15 µm. (b) Luciferase activity in NMuMG transfected with Smad-dependent reporter pSBE-Lux and pCMV-Rl vectors and treated with 1 ng/ml TGF-β1 for 16 h in the absence or presence of 15 µM SB202190. Each bar represents the mean ± SD of three wells. P value was determined by *t* test. The difference in luciferase activity in control and SB202190-treated cells is not statistically significant. (c) Immunoblot analysis of Smad2 phosphorylation in protein extracts (35 µg/well) from NMuMG cells treated with 2 ng/ml TGF-β1 in the absence or presence of 10 µM SB202190. (d) p38Mapk phosphorylation in response to TGF-β1 in protein extracts (35 µg/well) from SiHa cells cotreated with 10 µg/ml cycloheximide (CHX). (e) Inhibition of ATF2 phosphorylation by JNK inhibitors in protein extracts (35 µg/well) from NMuMG cells treated with 2 ng/ml TGF-β1.

Short Interference RNA Studies

RNA duplexes against human (cat. no. M-003902) and mouse (cat. no. M-004199) Smad4 were obtained from Dharmacon Research, Inc. (Lafayette, CO). RNA duplexes against tropomyosin (target sequence: AAGCAGCTGGAAGATGAGC) were designed using the siDESIGN program at the Dharmacon siDESIGN center. A scramble control RNA duplex labeled with rhodamine was obtained from Qiagen (Chatsworth, CA). Cells were transfected with RNA duplexes using Oligofectamine reagents (Invitrogen) following the manufacturers protocol. The cells were transferred onto glass coverslips or plastic dishes. Forty-eight hours posttransfection, the cells were treated with TGF-β1 for 24 h followed by immunoblot and immunofluorescence analysis.

RESULTS

TGF-β–induced Actin Stress Fiber Formation in Epithelial Cells Requires De Novo Protein Synthesis and p38Mapk

The mechanism of TGF-β–induced stress fiber (SF) formation was characterized in NMuMG mouse mammary epithelial cells. These cells exhibit a cuboidal cell morphology and a cortical organization of actin filaments in adhesion belts. Treatment of the cells with TGF-β1 for 24 h induced formation of actin microfilament bundles (Figure 1). Actin filaments in adhesion belts were not significantly affected in the first 4 h of TGF-β treatment compared with untreated cells (Figure 1a), and SFs were not observed until 8 h after TGF-β addition. SFs were well developed in cells incubated with TGF-β for 24 h. This TGF-β response was blocked by treatment of cells with the p38Mapk inhibitor, SB202190,

suggesting involvement of p38Mapk in TGF-β–regulated SFs. This inhibitor did not significantly affect phosphorylation of Smad2 and TGF-β–mediated activation of the Smad-dependent luciferase reporter activity (Figure 1, b and c). Similar results were also obtained with two other p38Mapk inhibitors (SB203580 and PD165319; our unpublished results). Treatment of cells with the JNK inhibitor, SP600125, did not block TGF-β–mediated SF formation (Figure 1a), although it effectively blocked phosphorylation of ATF2 (Figure 1e). Expression of kinase-inactive mutant of mitogen-activated protein kinase kinase 6 (MKK6) blocked phosphorylation of p38Mapk and SF formation (Bakin *et al.,* 2000, 2002). In previous studies we have shown that TGF-β does not activate the ERK pathway in NMuMG cells and inhibition of MEK1/2 does not block stress fiber formation. Similar results were obtained for human cervical carcinoma SiHa cells, in which TGF-β induces p38Mapk signaling and SFs (Bakin *et al.,* 2002). To investigate whether this process depends on de novo protein synthesis, cells were treated with cycloheximide, the protein synthesis inhibitor. Cycloheximide blocked SF formation when added as late as 6 h after initiation of TGF-β treatment without inhibition of p38Mapk activation (Figure 1, a and d), but it had no effect after 12 h (our unpublished results). Thus, de novo protein synthesis and p38Mapk activity are required for TGF-β–mediated actin SF formation in epithelial cells.

Table 1. Regulation of genes encoding actin-binding proteins by TGF-β1 in NMuMG cells

	Gene	Accession no. of cDNA clones	Fold Change ±SE	
			TGF-β1	TGF-β1+ SB202190
1	Actn1	BG077689	3.03 ± 0.66	2.20 ± 0.18
2	Actn1	BG065930	2.94 ± 0.48	2.37 ± 0.48
3	α-Tropomyosin	BG086016	1.81 ± 0.39	1.48 ± 0.09
4	α-Ttropomyosin	BG079039	2.15 ± 0.57	1.30 ± 0.04
5	β-Tropomyosin	BG076419	2.48 ± 0.09	1.52 ± 0.20
6	β-Tropomyosin	BG073088	2.37 ± 0.36	1.37 ± 0.36
7	β-Tropomyosin	BG087093	2.83 ± 0.43	1.83 ± 0.48
8	Tpm3	BG077822	1.28 ± 0.12	1.38 ± 0.19
9	Tpm3	BG078017	1.22 ± 0.08	1.40 ± 0.08
10	Tpm3	BG064681	1.28 ± 0.07	1.40 ± 0.08
11	Tpm3	BC029186	1.16 ± 0.15	0.91 ± 0.11
12	Tpm4	BG077934	0.96 ± 0.11	0.90 ± 0.18
13	Tpm4	AW537534	1.34 ± 0.12	1.46 ± 0.22
14	Cnn2 (H2)	BG079442	3.00 ± 0.25	3.11 ± 0.29

cDNA microarray analysis was performed using total RNA from NMuMG cells, which were untreated or treated with 2 ng/ml TGF-β1 for 24 h in the absence or presence of 10 μM SB202190. The data represent an average of three independent experiments.

TGF-β Up-regulates Expression of Genes Encoding Actin-binding Proteins

To identify TGF-β target genes that mediate actin remodeling, we compared gene expression profiles in NMuMG cells before and after treatment with TGF-β1 for 24 h using mouse cDNA microarrays. The results indicate that expression of 62 genes changed more than twofold after treatment with TGF-β1. Among these genes TGF-β stimulated expression of several genes encoding actin-binding proteins including tropomyosins (TM), α-actinin1, and calponin2 (Table 1). These proteins are known to be involved in the assembly of stable actin microfilament bundles (Ayscough, 1998; Danninger and Gimona, 2000; Tseng et al., 2002; Hossain et al., 2003). The α-tropomyosin and β-tropomyosin genes encoding high-molecular-weight tropomyosins were up-regulated 2–2.6-fold and were represented by two and three cDNA clones, respectively. Interestingly, Tpm3 and Tpm4 genes encoding low-molecular-weight tropomyosins were not regulated by TGF-β (Table 1).

Treatment with a p38Mapk inhibitor suppressed induction of tropomyosins by 30–45% without a significant effect on calponin2 (Table 1). Northern blot analysis with rat TM3 cDNA, a product of the α-TM gene, revealed a 1.6-fold increase in the TM mRNA levels at 4 h reaching a 3.6-fold induction at 24 h of TGF-β1 treatment (Figure 2a). Similar regulation was observed for α-actinin (Figure 2a). Cotreatment with a p38Mapk inhibitor reduced by 35% the induction of α-TM mRNA, without a significant effect on α-actinin1 (Figure 2a), suggesting that p38Mapk is involved in tropomyosin gene expression. Using RT-PCR we confirmed TGF-β–mediated regulation of calponin2 and that PAI-1, a known TGF-β-target gene, is regulated with kinetics similar to the newly identified TGF-β target genes (Figure 2b). The regulation of highly conserved α-TM and β-TM genes was further confirmed using RT-PCR with isoform specific primers (Figure 2c), because tropomyosin sequences are conserved. The specificity was also confirmed using cDNA clones for TM1, TM2, and
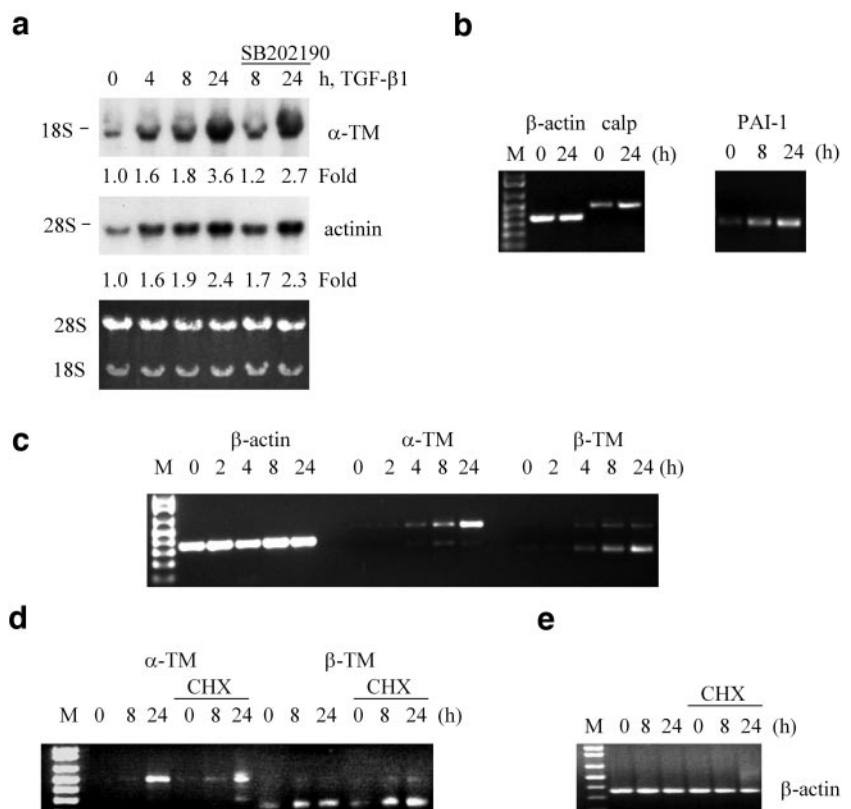

Figure 2. TGF-β regulates expression of genes encoding actin-binding proteins in NMuMG cells. (a) Northern blot analysis of TM2/3 and α-actinin1 mRNA levels in total RNA samples (15 μg/lane) from NMuMG cells treated with 2 ng/ml TGF-β1 in the absence or presence of 10 μM SB202190. Blots were quantified using PhosphorImager. Bottom panel shows ethidium bromide staining of total RNA. (b–e) Analysis of β-actin, PAI-1, calponin2, and α- and β-tropomyosin transcripts by PCR with reverse transcription in total RNA samples from NMuMG cells treated with 2 ng/ml TGF-β1. Where it is indicated, cells were treated with 10 μg/ml cycloheximide (CHX) 1 h before addition of TGF-β1.
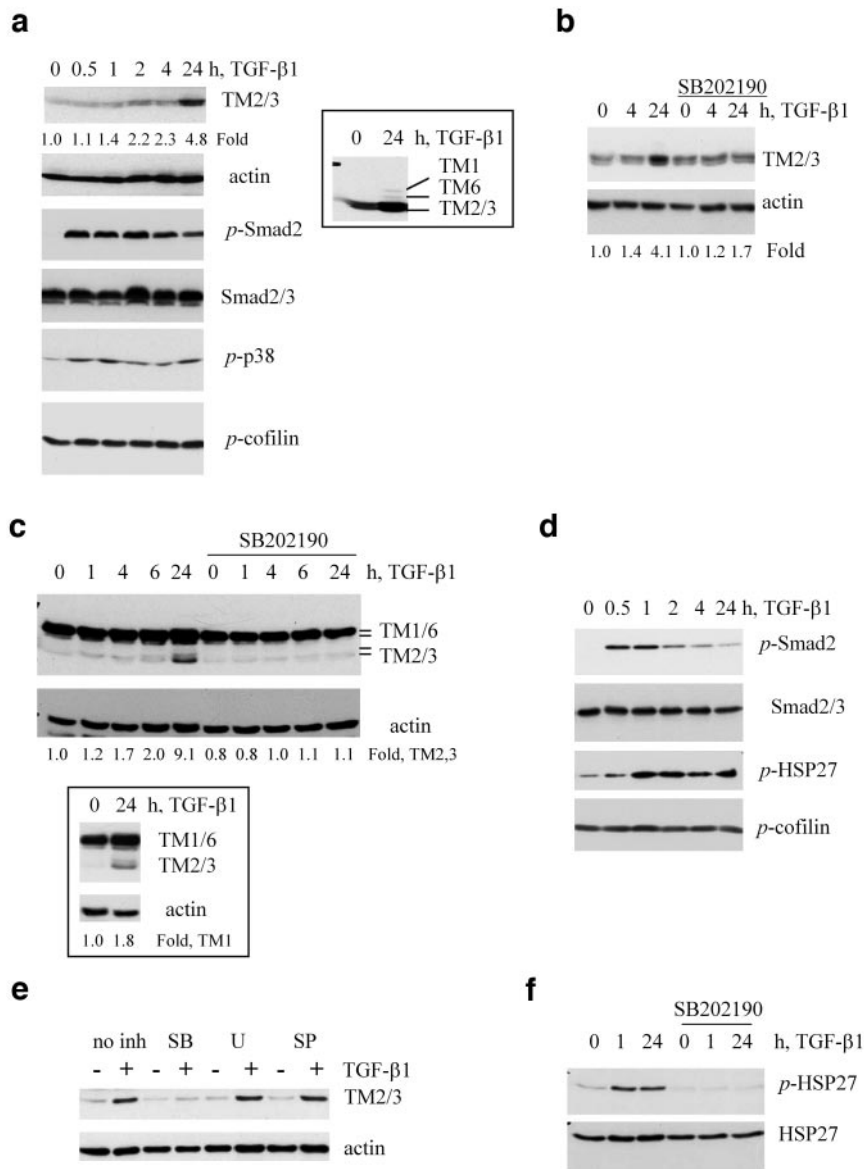
Figure 3. TGF-β regulates tropomyosins and HSP27 phosphorylation in epithelial cells. (a and b) Immunoblot analysis of actin and tropomyosins as well as phosphorylation of Smad2, HSP27, and cofilin using phospho-specific antibodies in NMuMG cells treated with 2 ng/ml TGF-β1. Where it is indicated 10 μM SB202190 was added 1 h before TGF-β treatment. Inset shows induction of TM1 and TM6 on a longer exposed film of the same immunoblot. (c–f) Immunoblot analysis of tropomyosin expression and phosphorylation of Smad2, p38Mapk, and cofilin in SiHa cells treated with 2 ng/ml TGF-β1. Where it is indicated, the cells were cotreated 1 h before addition of TGF-β with 10 μM SB202190 (SB), 5 μM U0126 (U), or 15 μM SP600125 (SP). Insert shows immunoblot with TM311 antibody using the same protein extracts as in c. Fold difference of tropomyosin levels relative to actin was estimated using NIH ImageJ software (http://rsb.info.nih.gov/nih-image/).

TM3 (our unpublished results). Examination of α- and β-TM mRNA levels in the cells cotreated with cycloheximide showed that TGF-β induction of these genes was not affected by cycloheximide, indicating that these genes are directly regulated by the TGF-β signaling pathway (Figure 2, d and e). Thus, we have identified tropomyosins α-actinin1 and calponin2 as novel TGF-β target genes that may account for TGF-β regulation of actin filament dynamics.

TGF-β Up-regulates Expression of Tropomyosins and Induces Phosphorylation of HSP27 in Epithelial Cells

In vertebrates, more than 10 different isoforms of high-molecular-weight tropomyosins are expressed from α- and β-TM genes and by alternative RNA splicing (Pittenger *et al.*, 1994). Tropomyosins form α-helical coil-coil dimers that bind along the length of the actin filaments interacting with 6–7 actin monomers are thought to be essential for the assembly and stabilization of actin filaments. (Ayscough, 1998). In this study we used the TM311 mAb recognizing tropomyosin 1 (TM1), a product of the β-TM gene, and

tropomyosin isoforms 2, 3, and 6 (TM2,3,6), products of the α-TM gene (Temm-Grove *et al.*, 1998). Immunoblot analysis with TM311 antibody followed by reblotting with anti-β-actin mAb showed that TGF-β induced a 4.8-fold increase in TM2 and TM3 in NMuMG cells (Figure 3a). Induction of TM1 and TM6 was also detected but required longer film exposures (Figure 3a, insert), suggesting that TM2 and TM3 are the main tropomyosin isoforms regulated by TGF-β at the protein level in NMuMG cells. The difference in the regulation of protein and mRNA levels of TM1 in response to TGF-β1 is not obvious and may be related to a tight regulation of α/β tropomyosin isoforms (Robbins, 1998). Analysis of Smad2 and p38Mapk phosphorylation in the same cells showed activation of Smad and p38 signaling at 30 min and a sustained level for at least 24 h (Figure 3a). Inhibition of p38Mapk significantly reduced the induction of tropomyosins without affecting basal level expression (Figure 3b), suggesting a more profound effect of p38Mapk on tropomyosin protein than on mRNA (see Figure 2a). Inhibition of p38Mapk did not block phosphorylation of Smad2
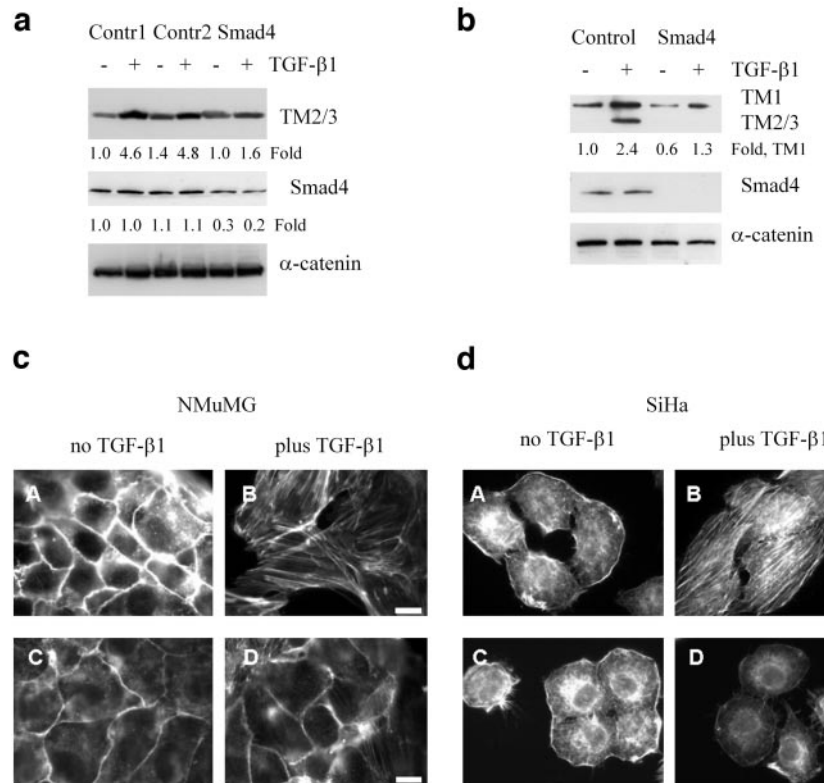
Figure 4. Smad signaling is required for TGF-β–induced expression of tropomyosins and stress fiber formation in epithelial cells. (a and b) Immunoblot analysis of tropomyosins and Smad4 in NMuMG cells (a) and SiHa cells (b) transfected with siRNAs against Smad4. (c and d) Actin filament staining with phalloidin-Alexa Green in NMuMG and SiHa cells transfected with control scramble siRNA (A and B) or siRNAs to Smad4 (C and D). The cells were treated with 2 ng/ml TGF-β1 for 24 h. Scale bar, 10 μm. Fold differences in tropomyosin and Smad4 levels relative to α-catenin were estimated using NIH ImageJ software.

and Smad-dependent transcription (Figure 1, b and c) and did not affect expression of calponin2 (Table 1).

TGF-β also mediated up-regulation of TMs and p38Mapk signaling in human cervical carcinoma SiHa cells (Figure 3, c–f), which respond to TGF-β with SFs (Bakin *et al.*, 2002). TGF-β stimulated a nearly twofold increase in TM1 and a ninefold increase in TM2/3 levels (Figure 3c). A comparable TGF-β–mediated induction of TMs and stress fiber formation were also observed in A549 lung epithelial cells (our unpublished results). SiHa cells express relatively low basal levels of TM2/3/6, but a high basal level of TM1 (Figure 3c). p38Mapk inhibitors blocked this up-regulation of TM2/3 (Figure 3, c and e), whereas inhibitors of MEK1/2 (U0126) and JNK, SP600125, did not (Figure 3e). Induction of the α-TM gene in SiHa cells at the mRNA level was confirmed by RT-PCR (see Figure 8a). We found that the activation of the Smad pathway and Smad3 levels were noticeably lower in SiHa cells (Figure 3d) than in NMuMG cells (Figure 3a). This may explain the moderate regulation of tropomyosins in SiHa cells compared with NMuMG cells and support the notion that Smads are involved in TGF-β–mediated regulation of tropomyosins.

The small heat shock protein HSP27 is a downstream target of p38Mapk signaling (Huot *et al.*, 1998). The HSP27 phosphorylation by p38Mapk-MAPKAP2/3 signaling at three serine residues increases a pool of HSP27 tetramers that facilitate actin polymerization (Huot *et al.*, 1998; Hedges *et al.*, 1999; Rogalla *et al.*, 1999). Using phospho-HSP27 antibodies we found that TGF-β stimulates a sustained phosphorylation of HSP27 in SiHa cells (Figure 3d). This is blocked by the p38Mapk inhibitor (Figure 3f). The actin filament dynamics is also controlled by the RhoA/ROCK/LIM-kinase pathway that regulates actin depolymerizing activity of ADF/cofilin by phosphorylation of a conserved serine3 in ADF/cofilin (Bamburg, 1999). Examination of cofilin phosphorylation in NMuMG (Figure 3a) and SiHa cells (Figure 3d) with phospho-Ser3–specific antibodies showed that levels of cofilin

phosphorylation did not change in response to TGF-β during stress fiber formation. These results indicate that TGF-β induction of stress fiber formation in epithelial cells is accompanied with an increase in expression of actin-binding proteins and p38Mapk-HSP27 signaling without a significant regulation of the ROCK/LIM-kinase/cofilin pathway.

The Smad Signaling Pathway Mediates Regulation of Tropomyosin Expression by TGF-β

To examine the involvement of Smads in TGF-β–induced expression of tropomyosins and SFs, we transfected NMuMG and SiHa cells with short interfering RNA duplexes (siRNA) against Smad4. Transfection of siRNAs significantly reduced Smad4 protein levels and TGF-β–induced expression of TM2/3 in NMuMG (Figure 4a). A more effective action of siRNAs was observed in SiHa cells where TM2/3 expression was prevented and TM1 level was reduced by 40–55% (Figure 4b). Staining of actin filaments with phalloidin-Alexa Green demonstrated a significant reduction in TGF-β–induced SFs in both cells lines transfected with siRNAs to Smad4 (Figure 4, c and d, panels C and D), compared with control siRNA (Figure 4, c and d, panels A and B). These results support a model that Smad signaling mediate induction of tropomyosin expression in response to TGFβ leading to formation of SFs in epithelial cells.

To test the contribution of specific Smads in the regulation of TMs and SFs, we used adenovirus-mediated expression of cDNAs encoding individual Smads in SiHa cells. These cells express low levels of Smad3 and Smad4 compared with NMuMG cells (Figure 3, a and d; Lee *et al.*, 2001). Flag-tagged Smad2 and Smad3 were expressed at comparable levels in SiHa cells infected with Smad-encoding adenoviruses (Figure 5, a and b). Smad3 significantly increased TGF-β–induced expression of tropomyosins compared with
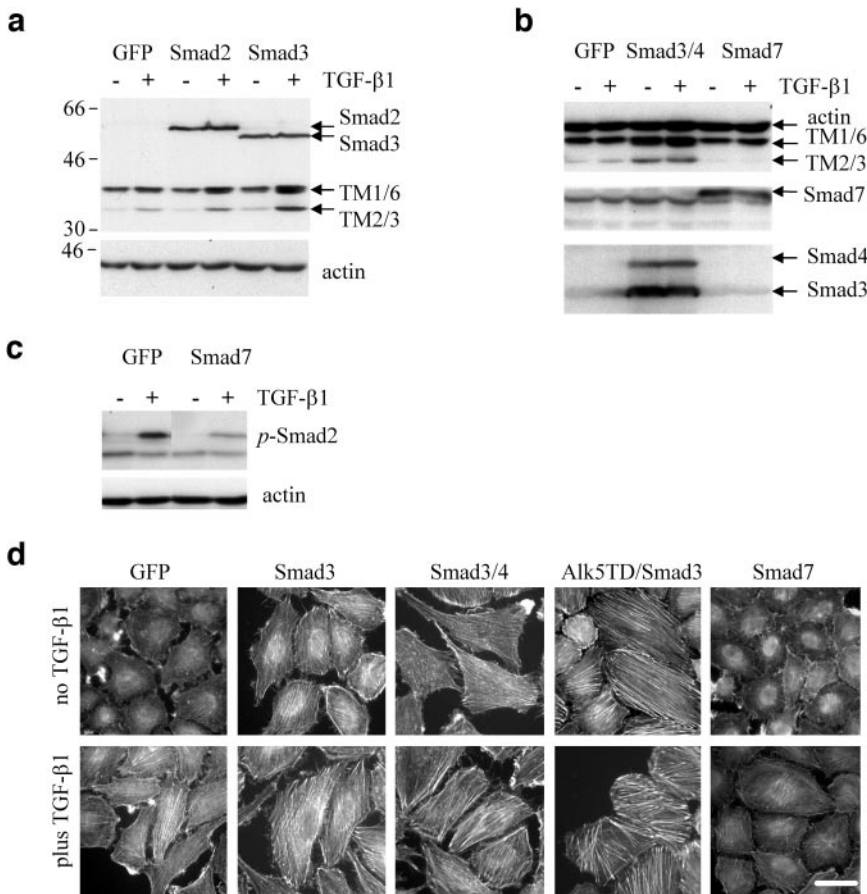
Figure 5. Smads mediate TGF-β–induced tropomyosin expression and stress fiber formation. (a and b) Tropomyosin expression in cells infected with adenoviruses encoding EGFP (GFP) and Flag-tagged Smad2, Smad3, Smad4, and Smad7. Cells were treated with 2 ng/ml TGF-β1 for 24 h. (c) Inhibition of TGF-β1–induced phosphorylation of Smad2 by adenoviral expression of Smad7 in SiHa cells. (d) Actin filaments staining in SiHa cells infected with adenoviruses: EGFP, Smad3, Smad4, Smad7, constitutively active Alk5T204D, or their combinations. The cells were treated with 2 ng/ml TGF-β1 for 24 h. Scale bars, 15 μm.

control EGFP-encoding adenovirus, whereas Smad2 exhibited only a moderate effect (Figure 5a). Coinfection with adenoviruses encoding Smad3 and Smad4 resulted in a marked increase of TMs even in the absence of added cytokine (Figure 5b), suggesting that Smad3 and Smad4 mediate TGF-β–regulated expression of tropomyosins. We next examined tropomyosin regulation by Smad7, an inhibitor of TGF-β signaling mediated by Smad2 and Smad3 (Massague, 1998). Expression of Smad7 inhibited TGF-β–induced expression of TM2/3 (Figure 5b) and phosphorylation of Smad2 (Figure 5c), whereas Smad6, an antagonist of bone morphogenic protein (BMP) signaling, had no effect (our unpublished results). In parallel, we examined actin filaments in SiHa cells infected with the adenoviral constructs (Figure 5d). As predicted, Smads that mediated enhancement of TM expression also increased SFs. Coexpression of Smad3 and Smad4 markedly increased SFs in the absence of exogenous TGF-β, which were further enhanced by the cytokine suggesting that other signaling events may also be involved in the assembly of stress fibers. Coexpression of constitutively active TGF-β type I receptor, Alk5T204D, and Smad3 resulted in SFs independent of exogenous TGF-β. Finally, expression of Smad7 significantly inhibited TGF-β–induced SF assembly (Figure 5e). These results demonstrate that Smad3 and Smad4 mediate TGF-β–induced expression of tropomyosins and SF formation.

Tropomyosins Are Required for SF Formation in Response to TGF-β

We confirmed that tropomyosins are localized with stable actin filaments resistant to Triton treatment. SiHa cells treated with TGF-β for 24 h were first incubated with Triton X-100 and then

fixed with 4% paraformaldehyde. Actin filaments were detected with phalloidin and tropomyosins with the TM311 antibody. Immunofluorescence microscopy showed that tropomyosins were localized along the actin microfilaments in a periodical pattern (Figure 6a).

To examine whether tropomyosins are required for TGF-β–mediated SF formation, SiHa cells were transfected with siRNA duplexes against tropomyosins (si-TMs) or a scrambled siRNA control. si-TMs effectively suppressed basal and TGF-β–induced expression of tropomyosins (Figure 6b). TGF-β induced SFs in cells transfected with a scrambled siRNA control (Figure 6c, panels A and B), whereas SFs were significantly reduced by si-TMs (Figure 6c, panels E and F). In control cells, TGF-β induced elongation of cells and localization of tropomyosins to actin filaments, whereas in the si-TM cells this response was significantly reduced (Figure 6c, panels C and D and G and H). A complementary experiment tested the gain-of-function by transfection of NMuMG and SiHa cells with expression vector for rat HA-tagged TM3. Expression of TM3 alone, without TGF-β treatment, was sufficient to induce SFs in both cell lines similar to cells treated with TGF-β1 (Figure 6d, red, panels C and D). Staining with fluorescein-labeled anti-HA antibody showed colocalization of HA-tagged TM3 with actin filaments (Figure 6d, panels A and B, and overlay). These results indicate that tropomyosins are both necessary and sufficient for TGF-β–induced stress fiber formation.

TGF-β Does Not Induce Stress Fibers but Stimulates Cell Migration in Metastatic Cells

Actin filaments are dynamic structures and stabilization of actin filaments limits cell movement. TGF-β induces stress fibers in NMuMG and SiHa cells and cells from both lines
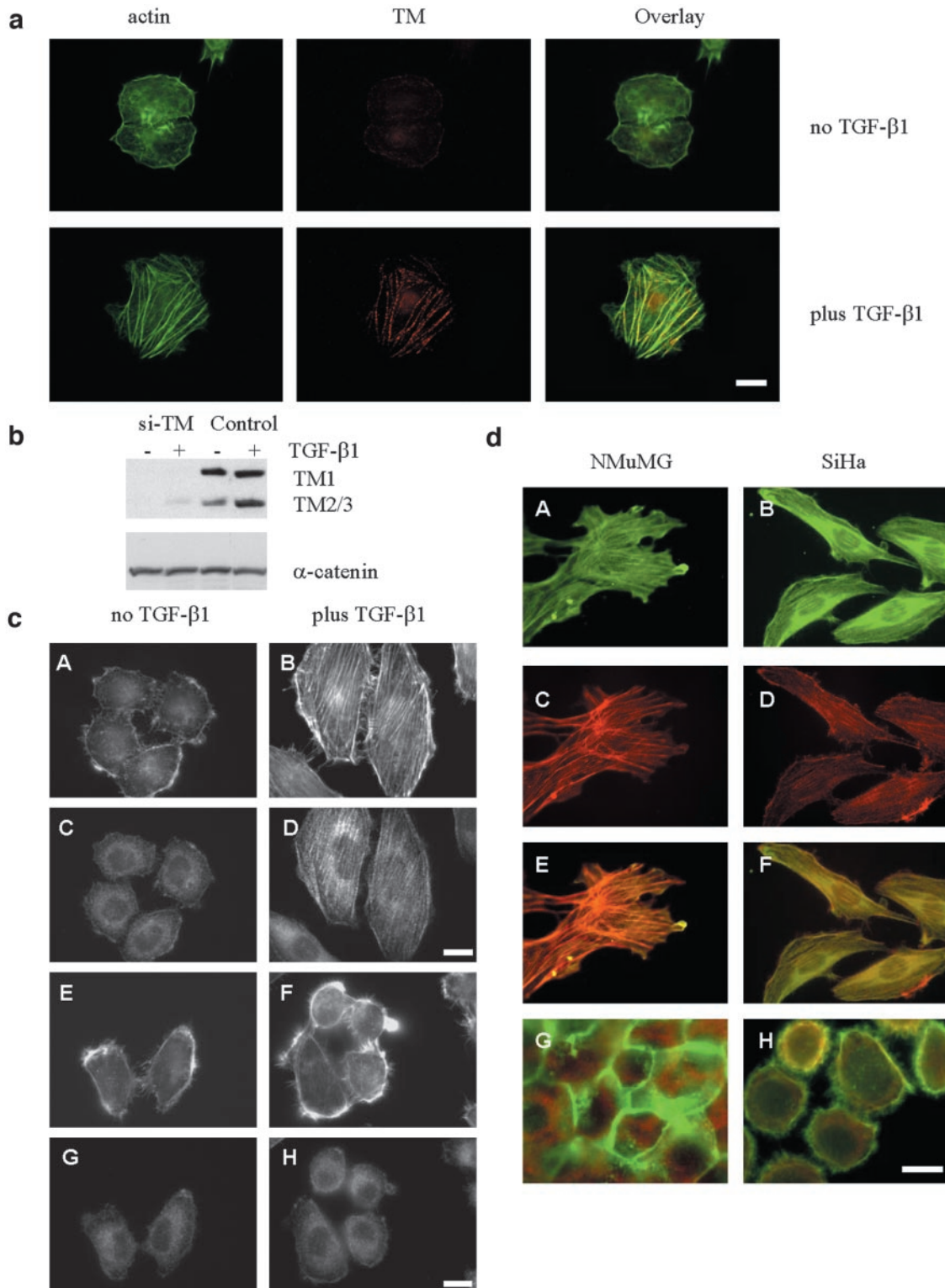
Figure 6. Tropomyosins are required for TGF-β–induced stress fiber formation. (a) Localization of tropomyosins (TM) to stable actin filaments (actin) resistant to 0.05% Triton X-100 treatment in SiHa cells untreated or treated with TGF-β1 for 24 h. Scale bar, 10 μM. (b) Suppression of tropomyosin expression in SiHa cells transfected with siRNA against TMs (si-TM) compared with a scrambled control. (c) Actin filaments (A, B, E, and F) and tropomyosin (C, D, G, and H) in SiHa cells, transfected with siRNA against tropomyosins (E–H) and a scrambled control siRNA (A–D). The cells were treated with 2 ng/ml TGF-β1 for 24 h. Scale bar, 10 μM. (d) Actin filaments in NMuMG and SiHa cells expressing HA-tagged TM3. Cells were stained with phalloidin-Texas Red and fluorescein-labeled anti-HA antibody (A–F). Overlay images are shown in panels E and F. Panels G and H show actin filaments and tropomyosins (TM311 antibody) in cells transfected with empty vector control. Scale bar, 15 μm.
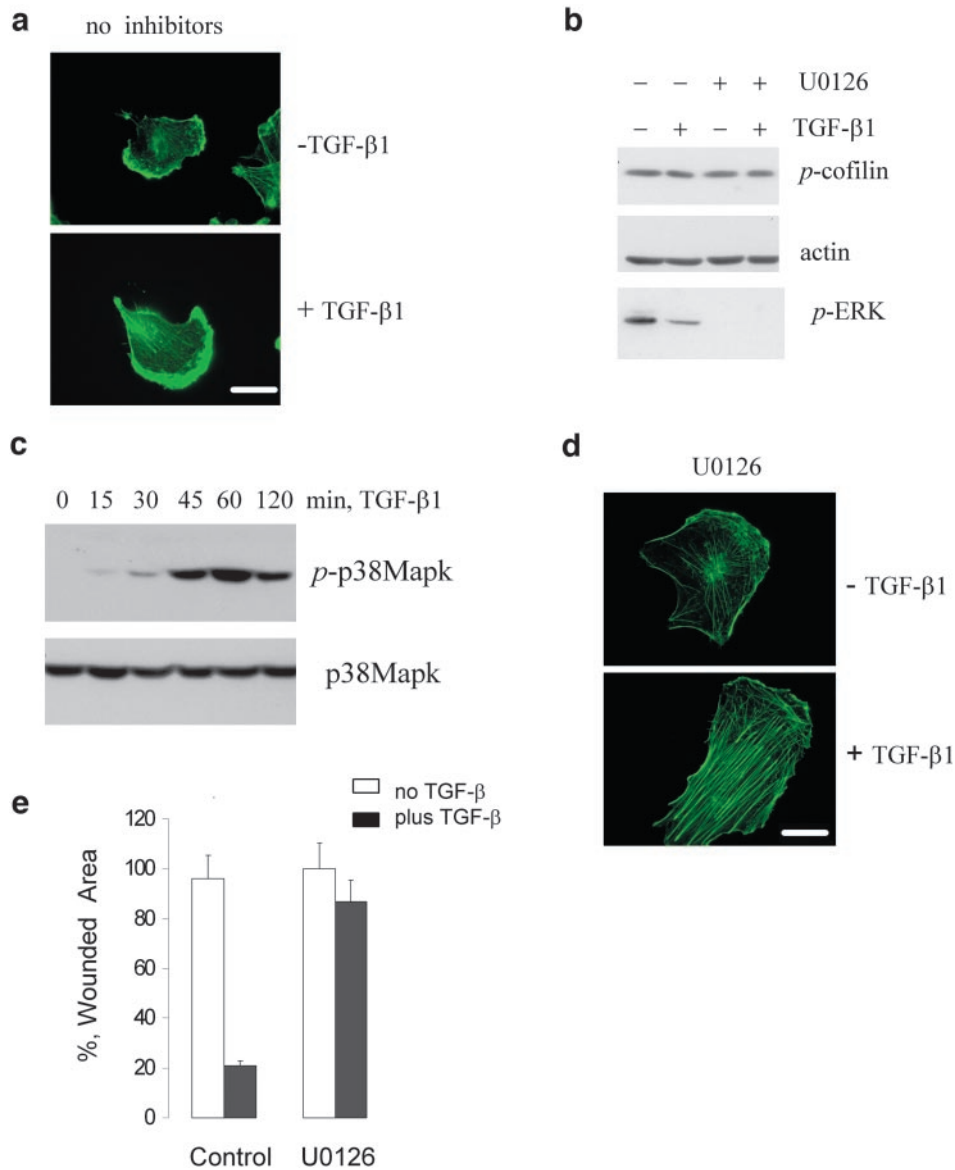
Figure 7. TGF-β and ERK signaling differentially regulate stress fiber formation. (a) Actin filaments staining in MDA-MB-231 cells treated with TGF-β1 for 24 h. (B) Phosphorylation of cofilin and ERK1/2 in MDA-MB-231 cells cotreated with TGF-β1 for 24 h and 5 μM U0126. (c) Immunoblot analysis of p38Mapk phosphorylation in MDA-MB-231 cells treated with 2 ng/ml TGF-β1. (d) Actin filaments staining in MDA-MB-231 cells cotreated with TGF-β1 and 5 μM U0126 for 24 h. (e) Wound closure in MDA-MB-231 cells treated with TGF-β1 in the absence or presence of 5 μM U0126. The experiment was done in triplicates and repeated at least two times. Scale bar, 20 μM.

fail to migrate in response to TGF-β in a wound closure assay (our unpublished results). TGF-β has been shown to stimulate migration of metastatic breast cancer MDA-MB-231 cells in wound closure assay (Bakin *et al.*, 2002). We hypothesized that TGF-β–mediated stress fiber response is altered in MDA-MB-231 cells. Accordingly, treatment of MDA-MB-231 cells with TGF-β did not result in the formation of stress fibers (Figure 7a). MDA-MB-231 cells express TGF-β receptors, Smad factors, and respond to TGF-β1 with activation of Smad, p38Mapk signaling, and regulation of gene expression (Bakin *et al.*, 2002; Dumont *et al.*, 2003 and Figure 7c). It has been reported that MDA-MB-231 cells have constitutively active Ras-ERK signaling (Kozma *et al.*, 1987; Ogata *et al.*, 2001), which may through the repression of the ROCK/LIM-kinase/cofilin pathway affect SF formation (Sa-

hai *et al.*, 2001; Pawlak and Helfman, 2002b). Thus, we examined phosphorylation of cofilin, a target of LIM kinase, in MDA-MB-231 cells. The immunoblot showed a relatively high basal level of the cofilin phosphorylation that was not modulated by TGF-β. Treatment of these cells with the MEK inhibitor did not affect the basal cofilin phosphorylation but blocked phosphorylation of ERK1/2 (Figure 7b). However, MEK inhibition significantly enhanced TGF-β–induced stress fiber formation (Figure 7d) and blocked TGF-β–mediated cell migration (Figure 7e). The TGF-β regulation of stress fibers was also restored by MEK inhibitor PD098059 and by inhibition of Raf kinase (our unpublished results). These results suggest that the ERK pathway suppresses TGF-β–mediated stress fiber formation in epithelial cells through a mechanism medi-
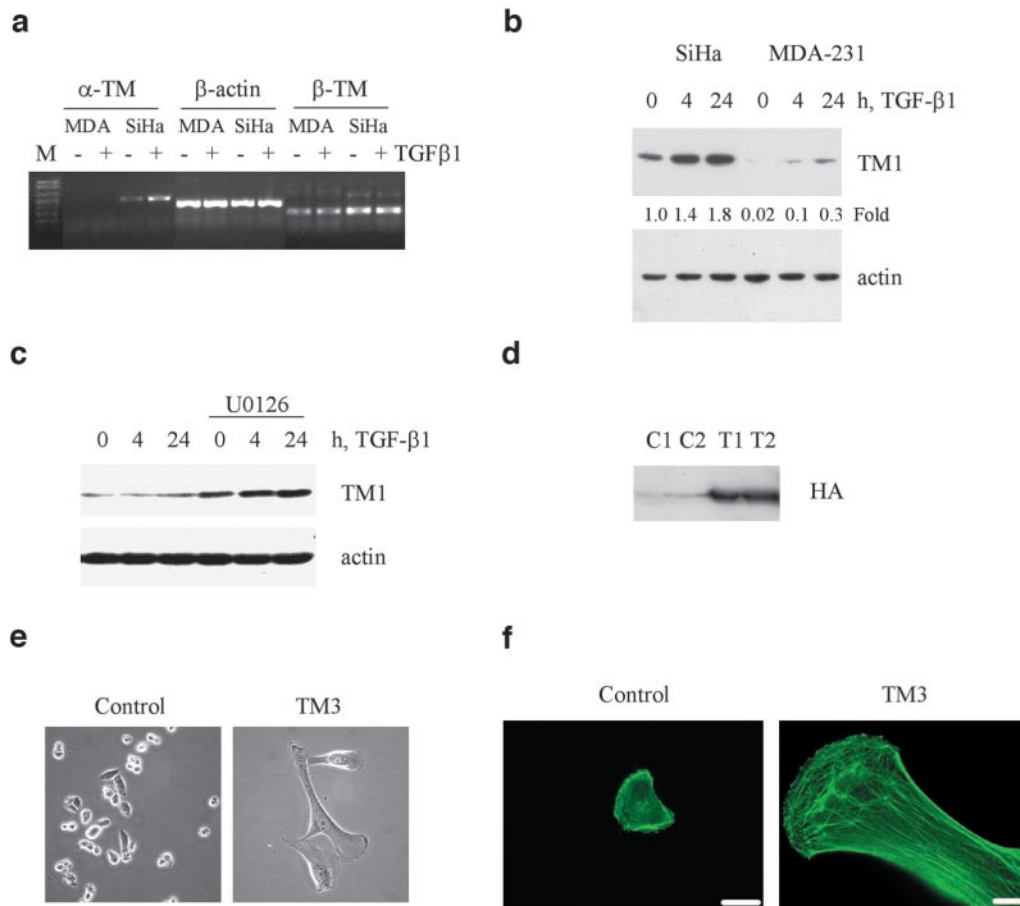
Figure 8. TGF-β and ERK signaling differentially regulates expression of tropomyosins. (a) Analysis of α-TM and β-TM transcripts by RT-PCR in total RNA samples from MDA-MB-231 (MDA) and SiHa cells treated with 2 ng/ml TGF-β1 for 24h. (b) Immunoblot analysis of tropomyosin expression in protein extracts (35 μg/lane) from SiHa and MDA-MB-231 cells treated with 2 ng/ml TGF-β1. (c) Tropomyosin protein expression in MDA-MB-231 cells cotreated with TGF-β1 and 5 μM U0126 for 24h. (d) Detection of HA-tagged rat TM3 with anti-HA antiserum in protein extracts from two independent transfections of MDA-MB-231 cells with expression vector encoding HA-tagged rat TM3 (T1 and T2) or a control empty vector (C1 and C2). (e) Phase-contrast images show flattening and size increase in TM3-transfected MDA-MB-231 cells compared with control cells. (f) Immunofluorescence images show a marked increase in actin stress fibers in TM3-transfected MDA-MB-231 cells. Scale bar, 20 μM. Fold differences in tropomyosin levels relative to actin were estimated using NIH ImageJ software.

ated by a pathway other than the ROCK/LIM-kinase/cofilin pathway.

Suppression of TGF-β–regulated Tropomyosin Expression by Ras-ERK Signaling in Metastatic MDA-MB-231 Cells

The Ras-ERK pathway has been implicated in suppression of tropomyosins and disruption of the actin cytoskeleton (Ljungdahl *et al.,* 1998; Shields *et al.,* 2002). We next examined whether the inability of TGF-β to induce stress fibers in MDA-MB-231 cells is associated with alteration of tropomyosin expression or function by Ras-ERK signaling. We compared expression of tropomyosins in MDA-MB-231 cells and SiHa cells, which show a low basal level of ERK phosphorylation. RT-PCR and immunoblot analysis showed that MDA-MB-231 cells express significantly less of TM1 mRNA and protein and undetectable levels of TM2/3 in comparison to SiHa cells (Figure 8, a and b). Treatment of MDA-MB-231 cells with the MEK inhibitor U0126 reduced ERK phosphorylation (Figure 7b), increased TGF-β–induced expression of TM1 (Figure 8c), and restored stress fibers (Figure 7d). Similar results were obtained with a Raf kinase inhibitor (our unpublished results). These data suggest that

Raf-ERK signaling down-regulates a basal and TGF-β–regulated expression of tropomyosin. Our findings also indicate that the α-tropomyosin gene is silenced in MDA-MB-231 cells.

We next examined whether ectopic expression of TM3, a product of the α-tropomyosin gene, will affect SFs and cell migration. MDA-MB-231 cells were transfected with expression vector encoding rat HA-tagged TM3 (Figure 8d) and analyzed for changes in cell morphology and actin filament assembly. Phase contrast images showed that TM3 expressing cells have a significant increase in cell size and a flatter more well-spread morphology compared with the refractile appearance of the parental cells or the control cells transfected with an empty vector (Figure 8e). Expression of TM3 markedly increased SFs in MDA-MB231 (Figure 8f) and inhibited cell motility assessed in the wound closure assay (our unpublished results). Interestingly, ectopic expression of either TM3 or TM2 inhibited proliferation of MDA-MB-231 cells increasing a number of multinucleated cells. We are currently developing inducible model to study effect of TMs on motility and growth of MDA-MB-231 cells. It has been also reported that overexpression of TM1 in MDA-MB-231 cells inhibits growth and motility of MDA-MB-231 cells (Raval *et al.,* 2003). Thus, overex-

pression of tropomyosins in metastatic MDA-MB-231 cells results in stress fibers and reduces cell motility. Collectively, the data presented above demonstrate that the Ras-ERK pathway inhibits TGF-β induction of stress fibers by suppressing expression of tropomyosins.

DISCUSSION

The molecular mechanism(s) underlying the prometastatic conversion of the TGF-β function is a major focus of current investigation by many research groups (reviewed in Derynck and Zhang, 2003; Roberts and Wakefield, 2003). In this study we found that the ability of TGF-β to induce stress fibers and, therefore, to control cell migration is significantly compromised in metastatic breast carcinoma cells. We provide evidence that tropomyosins are critical cellular components of Smad/p38Mapk-dependent actin stress fiber assembly in response to TGF-β in epithelial cells. We further show that the Ras-ERK pathway antagonizes TGF-β induction of tropomyosins and stress fibers. The restoration of tropomyosin expression results in stress fibers and reduces cell motility. These studies provide a direct causal link between TGF-β regulation of stress fibers and control of cell motility. These results suggest that the loss of the TGF-β stress fiber response in tumor cells is a critical step in prometastatic conversion of the TGF-β function.

We have investigated the mechanism of TGF-β regulation of actin filament dynamics and cell motility in normal and tumor epithelial cells. In untransformed epithelial cells TGF-β can rapidly induce membrane ruffling and actin polymerization at the cell edges, whereas a prolong incubation with TGF-β results in the formation of stable actin filament bundles (stress fibers; Bakin *et al.*, 2002; Edlund *et al.*, 2002). We found that inhibition of either de novo protein synthesis or p38Mapk blocked TGF-β induction of stress fibers, suggesting that novel transcription/translation and p38Mapk signaling are required for TGF-β–mediated stress fiber formation. Consistent with these findings expression of kinase-inactive p38Mapk inhibited TGF-β induction of actin stress fibers (Bakin *et al.*, 2002). Here we show that concomitantly with stress fibers TGF-β induced a sustained activation of p38Mapk signaling and phosphorylation of HSP27 (Figure 3), a downstream target of the p38Mapk-MAPKAP kinase 2 pathway (Stokoe *et al.*, 1992). Phosphorylated HSP27 and the triple aspartate mutant mimicking HSP27 phosphorylation at Ser15, Ser78, and Ser82 form small oligomers and tetramers that facilitate de novo actin polymerization (Huot *et al.*, 1998; Hedges *et al.*, 1999; Rogalla *et al.*, 1999). We found that although inhibition of de novo protein synthesis blocked stress fibers, it did not affect p38Mapk signaling (Figure 1d), suggesting that p38Mapk-HSP27 signaling is required but not sufficient for TGF-β induction of stress fibers. This notion is also supported by previous studies that have suggested involvement of Smad signaling in stress fiber formation (Piek *et al.*, 1999a).

We identified several TGF-β target genes including α- and β-tropomyosins, α-actinin1, and calponin2 encoding actin-binding proteins implicated in the assembly of stress fibers. Among these genes, tropomyosins (TMs) have been shown to play a critical role in the stress fiber assembly by stabilizing actin filaments and preventing access of actin-severing factors gelsolin and ADF/cofilin to filamentous actin (Pawlak and Helfman, 2001). We found that TGF-β specifically up-regulates expression of α- and β-TM genes encoding high-molecular-weight TMs and does not regulate Tpm3 and Tpm4 genes encoding low-molecular-weight TMs (Table 1). The expression of TMs correlated with the ability of

TGF-β to induce stress fibers in several epithelial cell lines including NMuMG, SiHa, and A549 cells. Moreover, suppression of TM expression with siRNAs completely blocked TGF-β induction of stress fibers in mouse and human cell lines, whereas ectopic expression of TM2 and TM3, products of the α-tropomyosin gene, was sufficient to induce stress fibers even in the absence of the cytokine (Figures 6 and 7). This is the first demonstration that TMs play an essential role in TGF-β–induced stress fiber formation in mouse and human epithelial cell lines.

The TGF-β induction of TM expression depends on p38Mapk and Smad signaling. Inhibition of p38Mapk blocked expression of TM proteins without a significant effect on TM mRNA levels. These results suggest that p38Mapk is involved in posttranscriptional control of TM expression, although a recent study has implicated p38Mapk in regulation of TM mRNA in intestinal epithelial cells (Shields *et al.*, 2002). Silencing of Smad4 with siRNAs suppressed tropomyosin expression and blocked stress fiber formation (Figure 4), whereas adenoviral expression of Smad factors showed that Smad3 and Smad4 are required for the induction of tropomyosins and formation of stress fibers in epithelial cells (Figure 5). Importantly, inhibitory Smad7, but not Smad6, blocks TGF-β induction of TM expression and stress fiber formation. These results demonstrate that Smad3/Smad4 and p38Mapk are required for TGF-β–induced TM expression and stress fiber formation in epithelial cells.

Tropomyosins have been implicated in regulation of actin filament dynamics and control of cell motility (Pawlak and Helfman, 2001). Early studies have found that cell transformation by oncogenic Ras and Src leads to down-regulation of tropomyosins and disruption of actin stress fiber filaments (Leonardi *et al.*, 1982; Hendricks and Weintraub, 1984). Subsequently, it has been shown that ectopic expression of tropomyosins in Ras-transformed fibroblasts restores stress fibers and significantly reduces cell motility and cell growth (Takenaga and Masuda, 1994; Braverman *et al.*, 1996; Gimona *et al.*, 1996; Janssen and Mier, 1997). The importance of tropomyosins in the control of tumor invasion and metastasis is highlighted by several studies indicating that high-grade tumors of breast, prostate, bladder, and brain express significantly lower levels of tropomyosins that that of normal tissues (Franzen *et al.*, 1996; Wang *et al.*, 1996; Hughes *et al.*, 2003; Raval *et al.*, 2003). Thus, tropomyosins and thereby stress fibers may play a critical role in the TGF-β control of tumor invasion and metastasis. In support of this idea, we found that TGF-β induction of tropomyosins and stress fibers is markedly reduced in metastatic breast cancer MDA-MB-231 cell line (Figure 7). MDA-MB-231 cells express constitutively active Ras-ERK signaling (Kozma *et al.*, 1987; Ogata *et al.*, 2001) that has been implicated in down-regulation of tropomyosins and disruption of actin stress fibers (Ljungdahl *et al.*, 1998; Shields *et al.*, 2002). We found that pharmacological inhibition of the Raf-ERK pathway significantly increased basal and TGF-β–induced levels of TM1, restored TGF-β induction of stress fibers, and inhibited cell motility without any effect on phosphorylation of cofilin (Figures 7 and 8). These results can be attributed at least in part to changes in Smad signaling. In fact, recent studies have shown that the Ras-ERK pathway attenuates Smad signaling by affecting the subcellular localization of Smad2 and Smad3 (Kretzschmar *et al.*, 1999) and by inducing a proteasome-mediated degradation of Smad4 (Saha *et al.*, 2001). We also found that the α-TM gene is not expressed in MDA-MB-231 cells. Our unpublished data indicate that the CpG island in the proximal promoter of the human α-TM
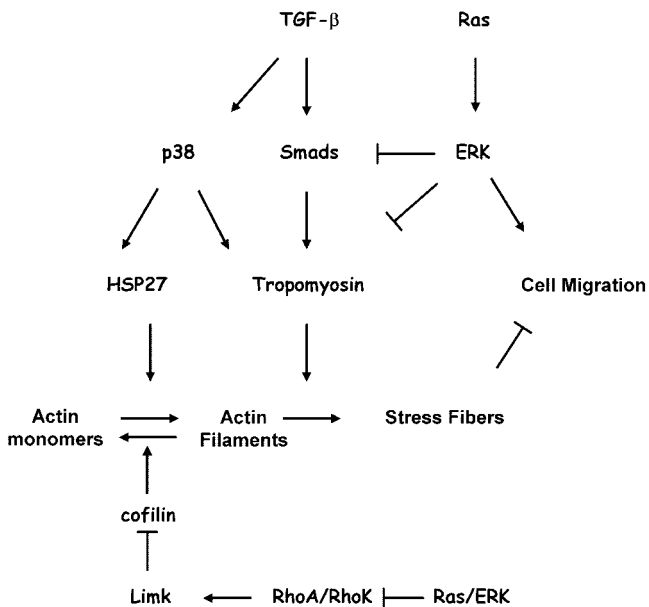
Figure 9. Opposing roles of the TGF-β and Ras-ERK signaling pathways in the regulation of actin filament dynamics and cell motility.

gene is methylated. The significance of this finding is currently under investigation. Importantly, ectopic expression of TM3 in MDA-MB-231 cells resulted in stress fibers (Figure 8) and severely affected cell motility. This finding is consistent with studies in rat NRK 1569 cells and mouse NIH-3T3 cells (Gimona *et al.*, 1996; Janssen and Mier, 1997). Our previous results suggest that Ras-ERK signaling does not affect TGF-β induction of membrane ruffling at the leading edge (Bakin *et al.*, 2002). Thus, Ras-ERK signaling suppresses TGF-β induction of tropomyosin expression and stress fibers leading to more motile and invasive phenotype.

The Rho-like GTPases, RhoA, Rac1, and CDC42, have been implicated in TGF-β mediated stress fiber formation (Moustakas and Stournaras, 1999; Bhowmick *et al.*, 2001; Bakin *et al.*, 2002; Edlund *et al.*, 2002). These GTPases through RhoA-ROCK/Rho-kinase and Rac/CDC42-Pak signaling can activate LIM kinases that negatively regulate ADF/cofilins by phosphorylating a conserved Serine3 in ADF/cofilins (Gungabissoon and Bamburg, 2003). ADF/cofilins regulate the turnover rates of actin filaments by promoting the dissociation of actin filaments into monomers (Bamburg, 1999). Thus, Rho-like GTPases through LIM kinases may contribute to stress fiber formation by inhibiting actin depolymerization. In this study we found that phosphorylation of cofilin was not modulated by TGF-β in three different cell lines, suggesting that the ROCK/LIM-kinase/cofilin pathway is not a target in TGF-β induction of stress fibers. Tropomyosins bound to filamentous actin prevent access of ADF/cofilins to actin filaments, thereby stabilizing actin filaments and reducing actin dynamics (Ono and Ono, 2002). In addition to tropomyosins, calponin2 and α-actinin1, two other TGF-β targets identified in this study, have been also implicated in stabilization of actin filaments (Panasenko and Gusev, 2001; Gimona *et al.*, 2003). It remains to be determined whether, in addition to tropomyosins, calponins and α-actinin play a role in formation of stress fibers in response to TGF-β by blocking ADF/cofilins and gelsolin from binding to actin filaments.

Our studies demonstrate an important role of tropomyosins in TGF-β regulation of stress fibers and cell migration (Figure 9). ERK signaling may inhibit TGF-β induction of stress fibers by suppressing Smad-dependent expression of tropomyosins. In addition, ERK signaling may affect stress fibers by disabling the RhoA/ROCK pathway (Pawlak and Helfman, 2002a, 2002b; Sahai *et al.*, 2001; Vial *et al.*, 2003). The suppression of tropomyosin expression by oncogenic Src (Hendricks and Weintraub, 1984) may also contribute to the cooperation of TGF-β and Src in tumorigenesis (Sieweke *et al.*, 1990). Thus, our study support an idea that the acquisition of metastatic phenotype by tumor cells results from the action of oncogenes and tumor suppressor genes regulating cell proliferation and survival (Bernards and Weinberg, 2002). Our results suggest that loss of TGF-β induction of stress fibers is an essential characteristic of a prometastatic conversion of TGF-β function and restoration of this response represents a potential target for the development of effective antimetastatic therapies.

ACKNOWLEDGMENTS

REFERENCES

Ayscough, K.R. (1998). In vivo functions of actin-binding proteins. Curr. Opin. Cell Biol. *10*, 102–111.

Bakin, A.V., and Curran, T. (1999). Role of DNA 5-methylcytosine transferase in cell transformation by fos. Science *283*, 387–390.

Bakin, A.V., Rinehart, C., Tomlinson, A.K., and Arteaga, C.L. (2002). p38 mitogen-activated protein kinase is required for TGF{beta}-mediated fibroblastic transdifferentiation and cell migration. J. Cell Sci. *115*, 3193–3206.

Bakin, A.V., Tomlinson, A.K., Bhowmick, N.A., Moses, H.L., and Arteaga, C.L. (2000). Phosphatidylinositol 3-kinase function is required for TGFbeta-mediated epithelial to mesenchymal transition and cell migration. J. Biol. Chem. *275*, 36803–36810.

Bamburg, J.R. (1999). Proteins of the ADF/cofilin family: essential regulators of actin dynamics. Annu. Rev. Cell Dev. Biol. *15*, 185–230.

Bernards, R., and Weinberg, R.A. (2002). A progression puzzle. Nature *418*, 823.

Bhowmick, N.A., Ghiassi, M., Bakin, A.V., Aakre, M., Lundquist, C.A., Engel, M., Arteaga, C.L., and Moses, H.L. (2001). TGFb mediates epithelial to mesenchymal transdifferentiation through a RhoA-dependent mechanism. Mol. Biol. Cell *12*, 27–36.

Braverman, R.H., Cooper, H.L., Lee, H.S., and Prasad, G.L. (1996). Antioncogenic effects of tropomyosin: isoform specificity and importance of protein coding sequences. Oncogene *13*, 537–545.

Cox, E.A., Sastry, S.K., and Huttenlocher, A. (2001). Integrin-mediated adhesion regulates cell polarity and membrane protrusion through the Rho family of GTPases. Mol. Biol. Cell *12*, 265–277.

Danninger, C., and Gimona, M. (2000). Live dynamics of GFP-calponin: isoform-specific modulation of the actin cytoskeleton and autoregulation by C-terminal sequences. J. Cell Sci. *113*, 3725–3736.

Derynck, R., Akhurst, R.J., and Balmain, A. (2001). TGF-beta signaling in tumor suppression and cancer progression. Nat. Genet. *29*, 117–129.

Derynck, R., and Zhang, Y.E. (2003). Smad-dependent and Smad-independent pathways in TGF-beta family signalling. Nature *425*, 577–584.

Dumont, N., Bakin, A.V., and Arteaga, C.L. (2003). Autocrine Transforming Growth Factor-beta Signaling Mediates Smad-independent Motility in Human Cancer Cells. J. Biol. Chem. *278*, 3275–3285.

Edlund, S., Landstrom, M., Heldin, C.H., and Aspenstrom, P. (2002). Transforming growth factor-beta-induced mobilization of actin cytoskeleton re-

quires signaling by small GTPases Cdc42 and RhoA. Mol. Biol. Cell *13*, 902–914.

Etienne-Manneville, S., and Hall, A. (2002). Rho GTPases in cell biology. Nature *420*, 629–635.

Franzen, B., Linder, S., Uryu, K., Alaiya, A.A., Hirano, T., Kato, H., and Auer, G. (1996). Expression of tropomyosin isoforms in benign and malignant human breast lesions. Br. J. Cancer *73*, 909–913.

Gimona, M., Kaverina, I., Resch, G.P., Vignal, E., and Burgstaller, G. (2003). Calponin repeats regulate actin filament stability and formation of podosomes in smooth muscle cells. Mol. Biol. Cell *14*, 2482–2491.

Gimona, M., Kazzaz, J.A., and Helfman, D.M. (1996). Forced expression of tropomyosin 2 or 3 in v-Ki-ras-transformed fibroblasts results in distinct phenotypic effects. Proc. Natl. Acad. Sci. USA *93*, 9618–9623.

Gimona, M., Watakabe, A., and Helfman, D. (1995). Specificity of dimer in tropomyosins: influence of alternatively spliced exons on homodimer and heterodimer assembly. Proc. Natl. Acad. Sci. USA *92*, 9776–9780.

Gungabissoon, R.A., and Bamburg, J.R. (2003). Regulation of growth cone actin dynamics by ADF/cofilin. J. Histochem. Cytochem. *51*, 411–420.

Hannigan, M., Zhan, L., Ai, Y., and Huang, C.K. (1998). The role of p38 MAP kinase in TGF-beta1-induced signal transduction in human neutrophils. Biochem. Biophys. Res. Commun. *246*, 55–58.

Hedges, J.C., Dechert, M.A., Yamboliev, I.A., Martin, J.L., Hickey, E., Weber, L.A., and Gerthoffer, W.T. (1999). A role for p38(MAPK)/HSP27 pathway in smooth muscle cell migration. J. Biol. Chem. *274*, 24211–24219.

Hendricks, M., and Weintraub, H. (1984). Multiple tropomyosin polypeptides in chicken embryo fibroblasts: differential repression of transcription by Rous sarcoma virus transformation. Mol. Cell. Biol. *4*, 1823–1833.

Hossain, M.M., Hwang, D.Y., Huang, Q.Q., Sasaki, Y., and Jin, J.P. (2003). Developmentally regulated expression of calponin isoforms and the effect of h2-calponin on cell proliferation. Am. J. Physiol. Cell Physiol. *284*, C156–C167.

Hughes, J.A., Cooke-Yarborough, C.M., Chadwick, N.C., Schevzov, G., Arbuckle, S.M., Gunning, P., and Weinberger, R.P. (2003). High-molecular-weight tropomyosins localize to the contractile rings of dividing CNS cells but are absent from malignant pediatric and adult CNS tumors. Glia *42*, 25–35.

Huot, J., Houle, F., Rousseau, S., Deschesnes, R.G., Shah, G.M., and Landry, J. (1998). SAPK2/p38-dependent F-actin reorganization regulates early membrane blebbing during stress-induced apoptosis. J. Cell Biol. *143*, 1361–1373.

Jaffe, A.B., and Hall, A. (2002). Rho GTPases in transformation and metastasis. Adv. Cancer Res. *84*, 57–80.

Janssen, R.A., and Mier, J.W. (1997). Tropomyosin-2 cDNA lacking the 3' untranslated region riboregulator induces growth inhibition of v-Ki-ras-transformed fibroblasts. Mol. Biol. Cell *8*, 897–908.

Kozma, S.C., Bogaard, M.E., Buser, K., Saurer, S.M., Bos, J.L., Groner, B., and Hynes, N.E. (1987). The human c-Kirsten ras gene is activated by a novel mutation in codon 13 in the breast carcinoma cell line MDA-MB231. Nucleic Acids Res. *15*, 5963–5971.

Kretzschmar, M., Doody, J., Timokhina, I., and Massague, J. (1999). A mechanism of repression of TGFbeta/ Smad signaling by oncogenic Ras. Genes Dev. *13*, 804–816.

Lee, S., Cho, Y.S., Shim, C., Kim, J., Choi, J., Oh, S., Zhang, W., and Lee, J. (2001). Aberrant expression of Smad4 results in resistance against the growth-inhibitory effect of transforming growth factor-beta in the SiHa human cervical carcinoma cell line. Int. J. Cancer *94*, 500–507.

Leonardi, C.L., Warren, R.H., and Rubin, R.W. (1982). Lack of tropomyosin correlates with the absence of stress fibers in transformed rat kidney cells. Biochim. Biophys. Acta *720*, 154–162.

Ljungdahl, S., Linder, S., Franzen, B., Binetruy, B., Auer, G., and Shoshan, M.C. (1998). Down-regulation of tropomyosin-2 expression in c-Jun-transformed rat fibroblasts involves induction of a MEK1-dependent autocrine loop. Cell Growth Differ. *9*, 565–573.

Massague, J. (1998). TGF-beta signal transduction. Annu. Rev. Biochem. *67*, 753–791.

Moustakas, A., and Stournaras, C. (1999). Regulation of actin organisation by TGF-beta in H-ras-transformed fibroblasts. J. Cell Sci. *112*, 1169–1179.

Ogata, H., Sato, H., Takatsuka, J., and De Luca, L.M. (2001). Human breast cancer MDA-MB-231 cells fail to express the neurofibromin protein, lack its type I mRNA isoform and show accumulation of P-MAPK and activated Ras. Cancer Lett. *172*, 159–164.

Ono, S., and Ono, K. (2002). Tropomyosin inhibits ADF/cofilin-dependent actin filament dynamics. J. Cell Biol. *156*, 1065–1076.

Panasenko, O.O., and Gusev, N.B. (2001). Mutual effects of alpha-actinin, calponin and filamin on actin binding. Biochim. Biophys. Acta *1544*, 393–405.

Pawlak, G., and Helfman, D.M. (2001). Cytoskeletal changes in cell transformation and tumorigenesis. Curr. Opin. Genet. Dev. *11*, 41–47.

Pawlak, G., and Helfman, D.M. (2002a). MEK mediates v-Src-induced disruption of the actin cytoskeleton via inactivation of the Rho-ROCK-LIM kinase pathway. J. Biol. Chem. *277*, 26927–26933. Epub 2002 May 14.

Pawlak, G., and Helfman, D.M. (2002b). Post-transcriptional down-regulation of ROCKI/Rho-kinase through an MEK-dependent pathway leads to cytoskeleton disruption in Ras-transformed fibroblasts. Mol. Biol. Cell *13*, 336–347.

Piek, E., Heldin, C.H., and Ten Dijke, P. (1999a). Specificity, diversity, and regulation in TGF-beta superfamily signaling. FASEB J. *13*, 2105–2124.

Piek, E., Moustakas, A., Kurisaki, A., Heldin, C.H., and ten Dijke, P. (1999b). TGF-(beta) type I receptor/ALK-5 and Smad proteins mediate epithelial to mesenchymal transdifferentiation in NMuMG breast epithelial cells. J. Cell Sci. *112*, 4557–4568.

Pittenger, M.F., Kazzaz, J.A., and Helfman, D.M. (1994). Functional properties of non-muscle tropomyosin isoforms. Curr. Opin. Cell Biol. *6*, 96–104.

Raval, G.N., Bharadwaj, S., Levine, E.A., Willingham, M.C., Geary, R.L., Kute, T., and Prasad, G.L. (2003). Loss of expression of tropomyosin-1, a novel class II tumor suppressor that induces anoikis, in primary breast tumors. Oncogene *22*, 6194–6203.

Robbins, J. (1998). Alpha-tropomyosin knockouts: a blow against transcriptional chauvinism. Circ. Res. *82*, 134–136.

Roberts, A.B., and Wakefield, L.M. (2003). The two faces of transforming growth factor {beta} in carcinogenesis. Proc. Natl. Acad. Sci. USA *100*, 8621–8623.

Rogalla, T. *et al.* (1999). Regulation of Hsp27 oligomerization, chaperone function, and protective activity against oxidative stress/tumor necrosis factor alpha by phosphorylation. J. Biol. Chem. *274*, 18947–18956.

Saha, D., Datta, P.K., and Beauchamp, R.D. (2001). Oncogenic Ras represses transforming growth factor-beta /Smad signaling by degrading tumor suppressor Smad4. J. Biol. Chem. *276*, 29531–29537.

Sahai, E., Olson, M.F., and Marshall, C.J. (2001). Cross-talk between Ras and Rho signalling pathways in transformation favours proliferation and increased motility. EMBO J. *20*, 755–766.

Saito, H., Tsujitani, S., Oka, S., Kondo, A., Ikeguchi, M., Maeta, M., and Kaibara, N. (2000). An elevated serum level of transforming growth factor-beta 1 (TGF-beta 1) significantly correlated with lymph node metastasis and poor prognosis in patients with gastric carcinoma. Anticancer Res. *20*, 4489–4493.

Shields, J.M., Mehta, H., Pruitt, K., and Der, C.J. (2002). Opposing roles of the extracellular signal-regulated kinase and p38 mitogen-activated protein kinase cascades in Ras-mediated downregulation of tropomyosin. Mol. Cell. Biol. *22*, 2304–2317.

Sieweke, M.H., Thompson, N.L., Sporn, M.B., and Bissell, M.J. (1990). Mediation of wound-related Rous sarcoma virus tumorigenesis by TGF-beta. Science *248*, 1656–1660.

Stokoe, D., Engel, K., Campbell, D.G., Cohen, P., and Gaestel, M. (1992). Identification of MAPKAP kinase 2 as a major enzyme responsible for the phosphorylation of the small mammalian heat shock proteins. FEBS Lett. *313*, 307–313.

Takenaga, K., and Masuda, A. (1994). Restoration of microfilament bundle organization in v-raf-transformed NRK cells after transduction with tropomyosin 2 cDNA. Cancer Lett. *87*, 47–53.

Temm-Grove, C.J., Jockusch, B.M., Weinberger, R.P., Schevzov, G., and Helfman, D.M. (1998). Distinct localizations of tropomyosin isoforms in LLC-PK1 epithelial cells suggests specialized function at cell-cell adhesions. Cell Motil. Cytoskeleton *40*, 393–407.

Tseng, Y., Schafer, B.W., Almo, S.C., and Wirtz, D. (2002). Functional synergy of actin filament cross-linking proteins. J. Biol. Chem. *277*, 25609–25616.

Vial, E., Sahai, E., and Marshall, C.J. (2003). ERK-MAPK signaling coordinately regulates activity of Rac1 and RhoA for tumor cell motility. Cancer Cell *4*, 67–79.

Wakefield, L.M., and Roberts, A.B. (2002). TGF-beta signaling: positive and negative effects on tumorigenesis. Curr Opin Genet Dev. *12*, 22–29.

Wang, F.L., Wang, Y., Wong, W.K., Liu, Y., Addivinola, F.J., Liang, P., Chen, L.B., Kantoff, P.W., and Pardee, A.B. (1996). Two differentially expressed genes in normal human prostate tissue and in carcinoma. Cancer Res. *56*, 3634–3637.

Autocrine Transforming Growth Factor-β Signaling Mediates Smad-independent Motility in Human Cancer Cells*

Nancy Dumont‡, Andrei V. Bakin§, and Carlos L. Arteaga‡§¶‖

From the Departments of ‡Cancer Biology and §Medicine and ¶Vanderbilt-Ingram Cancer Center, Vanderbilt University School of Medicine, Nashville, Tennessee 37232

Transforming growth factor-β (TGF-β) is a pleiotropic growth factor that plays a critical role in modulating cell growth, differentiation, and plasticity. There is increasing evidence that after cells lose their sensitivity to TGF-β-mediated growth inhibition, autocrine TGF-β signaling may potentially promote tumor cell motility and invasiveness. To understand the molecular mechanisms by which autocrine TGF-β may selectively contribute to tumor cell motility, we have generated MDA-MB-231 breast cancer cells stably expressing a kinase-inactive type II TGF-β receptor (TβRII-K277R). Our data indicate that TβRII-K277R is expressed, can associate with the type I TGF-β receptor, and block both Smad-dependent and -independent signaling pathways activated by TGF-β. In addition, wound closure and transwell migration assays indicated that the basal migratory potential of TβRII-K277R expressing cells was impaired. The impaired motility of TβRII-K277R cells could be restored by reconstituting TGF-β signaling with a constitutively active TGF-β type I receptor (ALK5^{TD}) but not by reconstituting Smad signaling with Smad2/4 or Smad3/4 expression. In addition, the levels of ALK5^{TD} expression sufficient to restore motility in the cells expressing TβRII-K277R were associated with an increase in phosphorylation of Akt and extracellular signal-regulated kinase 1/2 but not Smad2. These data indicate that different signaling pathways require different thresholds of TGF-β activation and suggest that TGF-β promotes motility through mechanisms independent of Smad signaling, possibly involving activation of the phosphatidylinositol 3-kinase/Akt and/or mitogen-activated protein kinase pathways.

Transforming growth factor-β (TGF-β)[1] is a pleiotropic polypeptide growth factor that is part of a superfamily of struc-

turally related ligands that includes the TGF-βs, activins, and bone morphogenetic proteins (BMPs) (1). TGF-β ligands play a critical role in modulating cell growth, differentiation, plasticity, and migration. They elicit their biological effects by binding to a heteromeric complex of transmembrane serine/threonine kinases, the type I and type II receptors. TGF-β ligands can also bind to a transmembrane proteoglycan referred to as the type III receptor, which is thought to present ligand to the signaling type I and type II receptors. Following ligand binding to the type II receptor, the type I receptor is recruited to the complex. This allows the type II receptor, which is a constitutively active kinase, to transphosphorylate and thereby activate the type I receptor (2). Multiple pathways have now been implicated in mediating TGF-β effects downstream of these receptors. These include the extracellular signal-regulated kinase (ERK) (3, 4), c-Jun NH₂-terminal kinase (JNK) (5–7), p38 mitogen-activated protein kinase (MAPK) (8, 9), and phosphatidylinositol 3-kinase (PI3K) pathways (10, 11). Several small GTPases can also be activated by TGF-β (12) and are involved in the activation of many of the above-mentioned signaling pathways. However, the Smad pathway was the first signaling pathway identified to mediate TGF-β effects and remains the best characterized (reviewed in Ref. 1).

Signal transduction through the Smad pathway involves phosphorylation of a set of intracellular signaling proteins termed receptor-regulated Smads (R-Smads) by the activated type I receptor. Once phosphorylated, R-Smads can associate with a common mediator Smad, Smad4, translocate to the nucleus, and regulate gene transcription. In addition to the R-Smads and the common mediator Smad, Smad4, there is a distinct, structurally related class of antagonistic Smads, Smad6 and Smad7, which inhibit TGF-β family signals. Smad6 preferentially inhibits BMP signaling by either competing with Smad4 for binding to R-Smads (13) or interfering with BMP receptor-mediated phosphorylation of Smads (14). Smad7 has been reported to inhibit both TGF-β and BMP signaling by binding to activated type I receptors and interfering with their ability to phosphorylate R-Smads (15, 16).

Although TGF-β1 was originally identified for its ability to cause reversible phenotypic transformation and anchorage-independent growth of fibroblasts (17, 18), TGF-β can act as both a tumor suppressor and a tumor promoter (19, 20). TGF-β elicits most of its tumor suppressor activity by potently inhibiting the proliferation of most epithelial cells. It is thought that escape from the growth inhibitory effects of TGF-β through

dysregulated expression or mutational inactivation of various components of the TGF-β signaling pathway can contribute to tumorigenesis (21–23). In addition, there is increasing evidence that after cells lose their sensitivity to TGF-β-mediated growth inhibition, autocrine TGF-β signaling may promote tumorigenesis. The importance of autocrine TGF-β signaling in tumor progression has been highlighted by several studies that have shown that expression of a dominant-negative type II TGF-β receptor (dnTβRII) in various tumor cells can prevent the conversion of cells from an epithelial to an invasive mesenchymal phenotype, delay tumor growth, and reduce metastases (24–27). These data suggest that TGF-β can act directly on tumor cells to promote tumor maintenance and progression. In addition to promoting epithelial to mesenchymal transformation of tumor cells, TGF-β can stimulate the motility of many cell types *in vitro*, suggesting that TGF-β production *in vivo* may enhance migration of tumor cells and thus contribute to tumor invasiveness and metastases. There is also evidence that TGF-β can increase cellular motility without affecting proliferation, suggesting that the effects on motility and proliferation may occur via different biochemical pathways (28).

To understand the molecular mechanisms by which autocrine TGF-β may selectively contribute to tumor cell motility, we have generated MDA-MB-231 breast cancer cells stably expressing dnTβRII. MDA-MB-231 cells express TGF-β receptors (29), secrete TGF-β (30), and, although they are resistant to the growth inhibitory effects of TGF-β (29), can respond to TGF-β with an increase in spreading (31) and invasiveness (32). In addition, there is evidence that blocking TGF-β signaling by administration of a neutralizing TGF-β antibody can inhibit MDA-MB-231 cell tumorigenicity and metastases in nude mice (33). In this paper we show that expression of dnTβRII in MDA-MB-231 cells impairs their basal migratory potential. This impairment in motility can be restored by expression of a constitutively active type I TGF-β receptor (ALK5^{TD}) but not by overexpression of Smad2/4 or Smad3/4. In addition, the levels of ALK5^{TD} expression sufficient to restore motility in the cells expressing dnTβRII are associated with an increase in phosphorylation of Akt and ERK1/2, but not Smad2, suggesting that Smad signaling is dispensable for autocrine TGF-β-mediated motility and that this response depends on alternative signaling pathways activated by TGF-β.

EXPERIMENTAL PROCEDURES

Cell Culture and Reagents—The MDA-MB-231 and MDA-MB-468 breast cancer cell lines were purchased from the American Type Culture Collection (Manassas, VA) and were maintained in Dulbecco's modified Eagle's medium supplemented with 10% fetal calf serum (FCS). The SW480.7 clone 15.13 (34) was a gift from Dr. Joan Massagué (Memorial Sloan-Kettering Cancer Center, New York, NY) and was maintained in Dulbecco's modified Eagle's medium supplemented with 10% FCS, 0.3 mg/ml Zeocin, and 0.7 mg/ml G418. TGF-β1 and BMP2 were obtained from R&D Systems (Minneapolis, MN). Peter ten Dijke (The Netherlands Cancer Institute, Amsterdam, The Netherlands) graciously provided the rabbit polyclonal sera directed against activin-like receptor kinases (ALKs) (35). Antibodies against the hemagglutinin (HA) epitope (catalog number sc-7392), the type II TGF-β receptor (catalog number sc-220), Smad4 (catalog number sc-7966), and p38 MAPK (catalog number sc-7972) were from Santa Cruz Biotechnology (Santa Cruz, CA). Antibodies to fibronectin (catalog number F14420) and Smad2/3 (catalog number S66220) were from Transduction Laboratories (San Diego, CA). The C-terminal phospho-Smad2 antibody (catalog number 06-829) was obtained from Upstate Biotechnology, Inc. (Lake Placid, NY). The C-terminal phospho-Smad1 antibody (catalog number 9511) and the phospho-p38 MAPK antibody (catalog number 9211S) were from Cell Signaling Technology (Beverly, MA). Monoclonal antibodies to actin (catalog number A-4700) and the FLAG epitope (catalog number F3165), as well as the polyclonal antibody to α-catenin (catalog number C2081), were obtained from Sigma. Phalloidin-Texas Red and Hoechst 3342 were from Molecular Probes (Eugene, OR). LY294002, SB202190, and JNKiII were purchased from Calbiochem. The MEK inhibitor, UO126, was purchased from Promega (Madison, WI).

Generation of Stable Cell Lines—To generate MDA-MB-231 cells stably expressing dnTβRII, we obtained a construct encoding a kinase-inactive TβRII mutant in which the lysine at position 277 has been mutated to arginine (pGABE-TβRII-K277R) (25) from Martin Oft (UCSF, San Francisco, CA). Lysine 277 corresponds to an invariant lysine found in the ATP-binding site of subdomain II in all protein kinases, and even its substitution with arginine results in loss of kinase activity (36). The pGABE vector is a modified version of the commonly used retroviral vector pBABE in which the puromycin cassette has been replaced by enhanced green fluorescent protein (GFP). In this construct, TβRII-K277R is HA-tagged, and its expression is driven by the viral long terminal repeat, whereas expression of GFP is driven by the SV40 promoter. MDA-MB-231 cells were transfected with the control pGABE vector or the pGABE-TβRII-K277R vector utilizing LipofectAMINE reagent (Invitrogen) according to the manufacturer's instructions. Following transfection, cells expressing GFP were sorted by flow cytometry. Clones were then isolated by sorting individual cells from the >95% positive GFP pool.

Affinity Labeling of Cells with ^{125}I-TGF-β1 and Immunoprecipitation of HA-tagged TβRII-K277R—^{125}I-TGF-β1 was obtained from PerkinElmer Life Sciences. Near confluent MDA-MB-231 cells, as well as clones and pools stably expressing GFP alone (GABE) or GFP and TβRII-K277R (dnTβRII) in 12-well plates, were washed three times over 30 min with 500 μl of ice-cold 0.1% bovine serum albumin dissolved in Dulbecco's phosphate-buffered saline (D-PBS) containing Ca^{2+} and Mg^{2+}. The cells were then affinity labeled with 100 pM ^{125}I-TGF-β1 as described previously (37), with slight modifications. Briefly, after a 3-h incubation with 100 pM ^{125}I-TGF-β1 at 4 °C, the cells were washed with 500 μl of ice-cold D-PBS, and the ligand-receptor complexes were cross-linked with 400 μl of 1 mM bis(sulfosuccinimidyl)suberate (BS^3; Pierce) for 10 min on ice. The cross-linking reaction was stopped with the addition of 100 μl of 500 mM glycine. Cells were washed twice with 500 μl of D-PBS and solubilized with 125 μl of 20 mM Tris buffer, pH 7.4, containing 1% Triton X-100, 10% glycerol, 1 mM EDTA, 1 mM phenylmethylsulfonyl fluoride, 2 μg/ml aprotinin, 2 μg/ml leupeptin, 2 μg/ml pepstatin, and 2 μg/ml soybean trypsin inhibitor. Solubilized material was centrifuged for 10 min at 4 °C to pellet cell debris. The supernatants were transferred to one-fifth volume of 5× electrophoresis sample buffer, boiled, and vortexed. All samples were analyzed using 3–12% SDS-PAGE and visualized by autoradiography. For immunoprecipitation experiments, the radiolabeled cell lysate from a T75 flask was centrifuged at 5000 × *g*, and the supernatant was split into eight equal aliquots and incubated with antibodies directed against ALKs 1, 2, and 5, the type II TGF-β receptor, or HA overnight at 4 °C. Aliquots of radiolabeled cell lysates incubated with normal rabbit serum or no antibody were used as controls.

Immunoblot Analysis—Cells were washed twice with ice-cold D-PBS and lysed with 50 mM Tris, 150 mM NaCl buffer containing 1% Nonidet P-40, 0.25% deoxycholate, 1 mM EDTA, 20 mM sodium fluoride, 1 mM sodium orthovanadate, 1 mM phenylmethylsulfonyl fluoride, 2 μg/ml aprotinin, 2 μg/ml leupeptin, 2 μg/ml pepstatin, and 2 μg/ml soybean trypsin inhibitor. Protein content was quantitated utilizing the BCA protein assay reagent (Pierce). Protein extracts were separated by 7.5% or 10% SDS-PAGE and transferred to nitrocellulose membranes at 100 volts for 2 h. Membranes were blocked with 5% nonfat dry milk in TBS-T (20 mM Tris-HCl, pH 7.6, 150 mM NaCl, 0.1% Tween 20 (v/v)) for 1 h at room temperature and incubated with primary antibodies diluted in TBS-T plus 2.5% nonfat dry milk over night at 4 °C. The membranes were then washed four times for 10 min with TBS-T, incubated with horseradish peroxidase-conjugated secondary antibodies for 1 h at room temperature, and rewashed four times for 10 min with TBS-T. Immunoreactive bands were visualized by chemiluminescence (Pierce).

Immunofluorescence—Cells grown on glass coverslips (22 × 22 mm) in 35-mm wells were washed twice with D-PBS, fixed with 4% paraformaldehyde in D-PBS for 15 min, permeabilized with 0.1% Triton X-100 for 10 min, and blocked with 3% nonfat dry milk in D-PBS for 60 min, all at room temperature. Cells were then incubated with primary mouse monoclonal antibodies diluted in 1% nonfat dry milk/D-PBS for 1 h at room temperature and washed three times with D-PBS, followed by incubation with a CY3-conjugated anti-mouse antibody in 1% nonfat dry milk/PBS for an additional hour at room temperature. In some experiments, cell nuclei were stained with 1 μg/ml Hoechst for 10 min at room temperature. After three 10-min washes with D-PBS, coverslips were mounted onto 25 × 75-mm microslides using AquaPolyMount (Polysciences Inc., Warrington, PA). Fluorescent images were captured using a Princeton Instruments cooled CCD digital camera from a Zeiss Axiophot upright microscope.

FIG. 1. **TβRII-K277R is expressed in MDA-MB-231 cells.** MDA-MB-231 parental cells, as well as clones and pools stably expressing GFP alone (*G15–5*, *G15–6*, and *G15 Pool*) or GFP and TβRII-K277R (*dn15–2*, *dn15–3*, *dn15–5*, and *dn15–11* clones and *dn15 Pool*), were affinity labeled with 100 pM ^{125}I-TGF-β1 and cross-linked with BS^3. Labeled ligand-receptor complexes were resolved by SDS-PAGE using a 3–12% gradient gel and visualized by autoradiography (*A*) or lysed and incubated with a mouse monoclonal anti-HA antibody for immunoprecipitation of HA-tagged TβRII-K277R (*B*). Immunoprecipitates were resolved by SDS-PAGE using a 7.5% polyacrylamide gel and visualized by autoradiography. Affinity labeled but non-immunoprecipitated (*NIP*) G15–5 cells were loaded as a reference (*lane 1*).
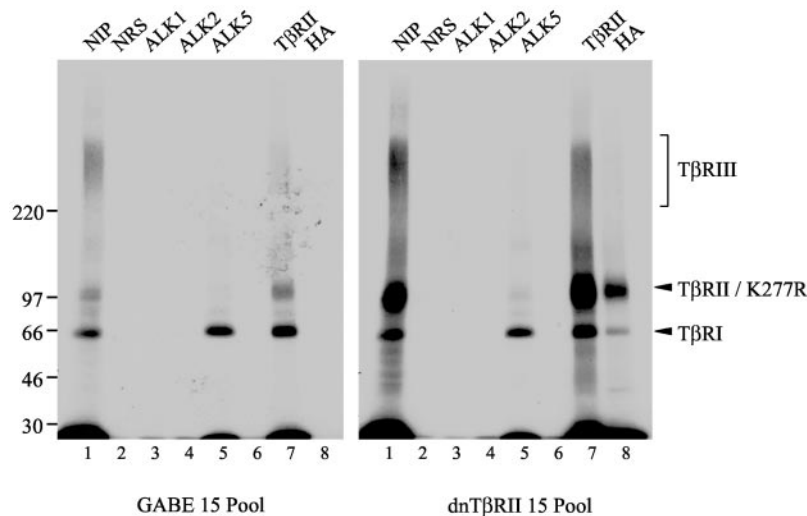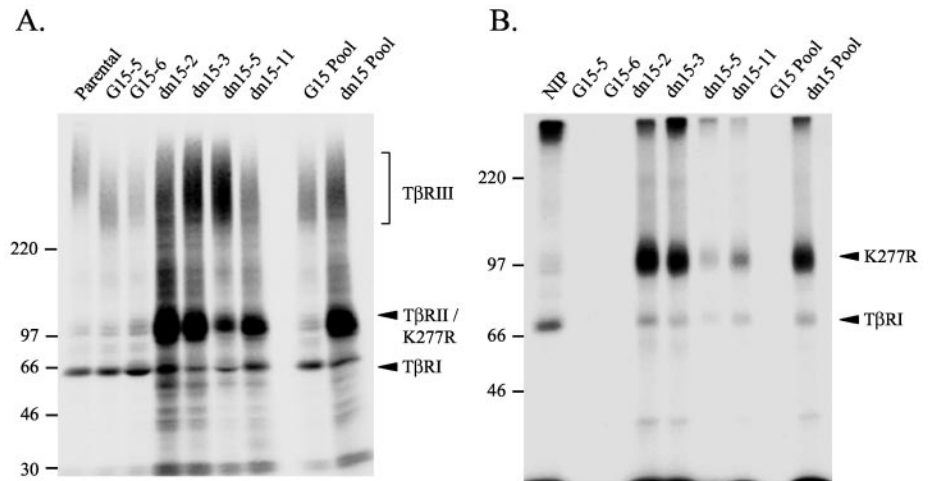
FIG. 2. **TβRII-K277R can associate with TβRI.** MDA-MB-231 pools expressing GFP alone (*GABE 15 Pool*; *left panel*) or GFP and TβRII-K277R (*dnTβRII 15 Pool*; *right panel*) were affinity labeled with 100 pM ^{125}I-TGF-β1, cross-linked with BS^3, lysed, and incubated with normal rabbit serum (*NRS*), polyclonal rabbit antisera directed against various type I TGF-β superfamily receptors (*ALK1*, *ALK2*, and *ALK5*), the type II TGF-β receptor (*TβRII*), or HA as indicated. Immunoprecipitates were resolved by SDS-PAGE using a 3–12% polyacrylamide gel and visualized by autoradiography. Affinity labeled but non-immunoprecipitated (*NIP*) cells were loaded as a reference (*lane 1*).

*Transcription Reporter Assays*—Cells were transiently transfected with 1 μg per 35-mm dish of the Smad-dependent heterologous promoter reporter construct p(CAGA)$_{12}$-Luciferase (38) provided by Dr. Jean-Michel Gauthier (Laboratoire Glaxo Wellcome, Les Ulis Cedex, France) along with 0.01 μg per 35-mm dish of pCMV-Renilla using FuGENE 6 reagent (Roche Molecular Biochemicals) according to the manufacturer's protocol. The following day, cells were split into 24-well plates, and ~45 h post-transfection, cells were either left unstimulated or were stimulated with 40 pM TGF-β1 for 16–20 h. All cells were then washed with D-PBS and lysed. Firefly and *Renilla reniformis* luciferase activities were measured using Promega's dual luciferase reporter assay system according to the manufacturer's protocol. Luciferase activity was normalized utilizing the ratio of Firefly to *R. reniformis* luciferase activity and presented as -fold induction. All assays were done in triplicate wells, and each experiment was repeated at least twice.

Wound Closure and Transwell Motility Assays—For wound closure assays, confluent cell monolayers were wounded by manually scraping the cells with a pipette tip. Following wounding, wound size was verified with an ocular ruler to ensure that all wounds were the same width. The cell culture medium was then replaced with fresh medium, and wound closure was monitored by microscopy at various times.

Transwell motility assays were performed utilizing 5-μm pore, 6.5-mm polycarbonate transwell filters (Corning Costar Corp., Cambridge, MA). For these assays, single cell suspensions were seeded in serum-free medium containing 0.1% bovine serum albumin onto the upper surface of the filters and allowed to migrate toward various concentrations of FCS. After a 16–20-h incubation period, cells on the upper surface of the filter were wiped off with a cotton swab, and the cells that had migrated to the underside of the filter were fixed, stained with 0.5% crystal violet, and counted by brightfield microscopy at ×200 in five random fields.

Adenoviral Expression of ALKs and Smads—The adenoviral con-

struct encoding FLAG-tagged Smad4 (39) was obtained from Dr. Harold Moses (Vanderbilt University, Nashville, TN). All other adenoviral constructs encoding FLAG-tagged Smads or HA-tagged constitutively active mutants of the TGF-β (ALK5^{T204D}), activin (ALK2^{Q207D}), and BMP (ALK3^{Q233D}) type I receptors (40) were generously provided by Dr. Kohei Miyazono (Japanese Foundation for Cancer Research, Tokyo, Japan). Stocks of recombinant viruses for each of these constructs were generated in 293 cells and titered utilizing the Takara assay (Takara Biomedicals, Tokyo, Japan). Cells were then infected with these or a control β-galactosidase adenovirus at a multiplicity of infection (m.o.i.) that resulted in >90% cell infection (~15 plaque-forming units/cell or less). The efficiency of infection was evaluated by *in situ* staining of cells for β-galactosidase activity 48 h following infection.

RESULTS

TβRII-K277R Is Expressed in MDA-MB-231 Cells—To abrogate TGF-β signaling in MDA-MB-231 cells, an expression vector encoding GFP and kinase-inactive TβRII was transfected into cells. Expression of the kinase-inactive TβRII-K277R mutant was verified by affinity labeling cell surface receptors with ^{125}I-TGF-β1 (Fig. 1A). Because TβRII-K277R has an intact extracellular domain, it can still bind TGF-β and should therefore co-migrate with endogenous TβRII. Cell surface labeling of parental cells resulted in the labeling of three proteins corresponding to the endogenous type I, II, and III TGF-β receptors. There was little or no change in the amount of receptor labeling observed in the control cells expressing GFP alone (GABE 15 Pool) compared with parental cells. However, in the pool expressing TβRII-K277R (dnTβRII 15 Pool),

FIG. 3. **Expression of TβRII-K277R impairs TGF-β signaling.** *A*, near confluent clones expressing GFP alone (G15–5 and G15–6) or GFP and TβRII-K277R (dn15–2, dn15–3, and dn15–11) were incubated overnight under serum-free conditions, stimulated with 80 pM TGF-β1 for the times indicated, washed, and lysed. Protein extracts (50 μg/lane) were separated by 10% SDS-PAGE followed by immunoblot analysis for phospho-Smad2 (*p-Smad2*) and total Smad2/3. *B*, cells were grown on glass coverslips for 48 h and serum-starved for 16 h followed by treatment with 40 pM TGF-β1 for 1 h. Cells were then prepared for indirect immunofluorescence staining of Smad2. Nuclear localization of Smad2 was confirmed by staining the same cells with Hoechst. *C*, cells were transiently transfected with p(CAGA)$_{12}$-Luciferase along with pCMV-Renilla. The following day, cells were split to six wells of a 24-well plate, treated with 40 pM TGF-β1 for 16 h, washed, and lysed. Firefly and *Renilla* luciferase activities were measured using Promega's dual luciferase reporter assay system. Fold induction of luciferase activity (*y axis*) is based on the ratio of Firefly to *Renilla* luciferase activities. Each *data point* represents the mean ± S.D. of three wells. *D*, near confluent pools expressing GFP alone (*G15*) or GFP and TβRII-K277R (*dn15*) were incubated overnight under serum-free conditions, stimulated with 80 pM TGF-β1 for the times indicated, and prepared for immunoblot analysis as in *A*. The fibronectin blot (*Fn*) was probed with an antibody directed against actin as a loading control, whereas the phospho-Smad2 (*p-Smad2*) and phospho-p38 MAPK (*p-p38 MAPK*) blots were probed with antibodies directed against the unphosphorylated forms of the respective proteins to verify equal loading.
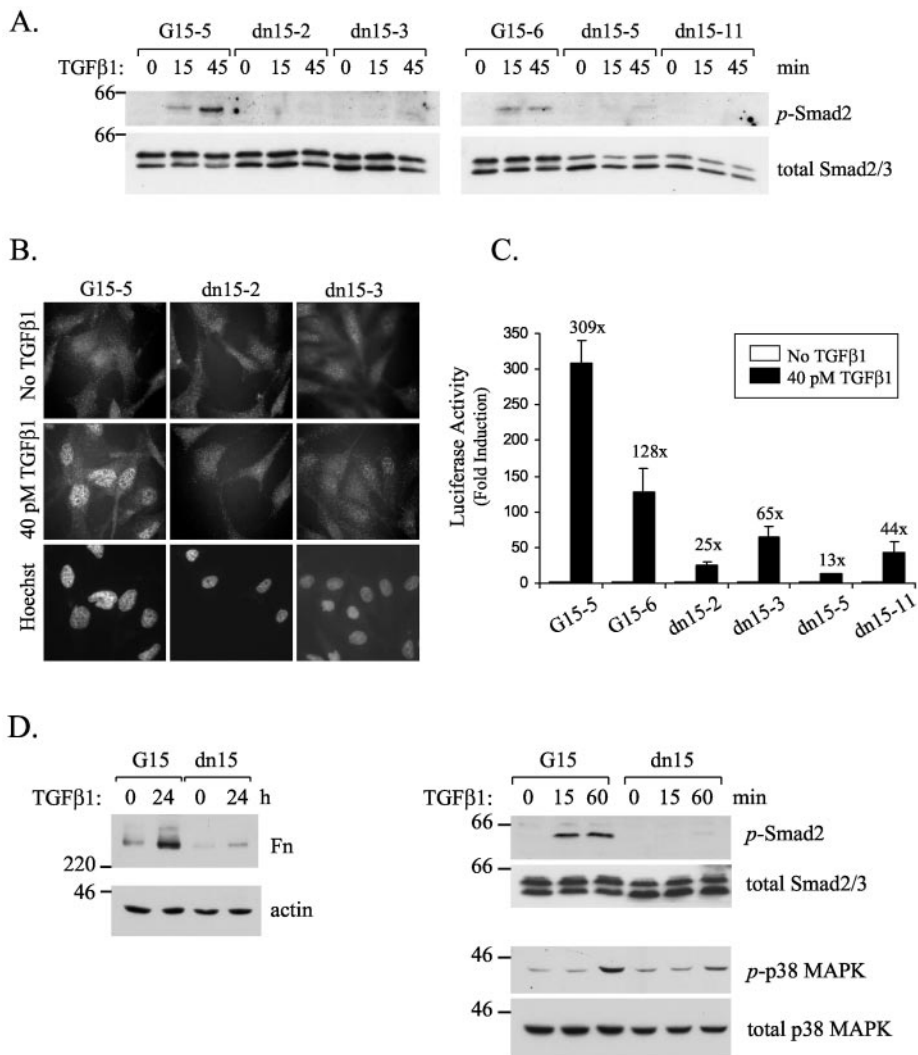
there was a significant increase in the amount of labeled type II receptor, suggesting that the exogenous receptor was expressed. Individual clones obtained from each of these pools expressing either GFP alone (G15–5, -6) or GFP and TβRII-K277R (dn15–2, -3, -5, -11) displayed a similar pattern of labeling.

To confirm that this increase in the labeling of TβRII was indeed because of expression of the HA-tagged TβRII-K277R, extracts from affinity labeled cells were immunoprecipitated with an HA antibody. As shown in Fig. 1*B*, the HA antibody immunoprecipitated a labeled type II receptor in the pool and clones expressing TβRII-K277R but not in the control pool or clones expressing GFP alone, confirming transgene expression. The type I TGF-β receptor appeared to co-immunoprecipitate with TβRII-K277R in these experiments. This was confirmed in subsequent co-immunoprecipitation experiments (see Fig. 2).

TβRII-K277R Is Functional in MDA-MB-231 Cells—Having ascertained that TβRII-K277R was expressed, we then examined whether it was functional. Immunoprecipitation experiments revealed that when affinity labeled cells expressing TβRII-K277R were precipitated with an HA antibody, a labeled protein the size of a type I receptor co-precipitated with TβRII-K277R (see Fig. 1*B* and Fig. 2, *right panel*, *lane 8*). We confirmed that this was TβRI by precipitating similarly labeled cells with various TGF-β superfamily type I receptor antibodies, including ALK1, -2, and -5. Only the ALK5 (TβRI), but not the ALK1 or ALK2 antibodies, precipitated the cross-linked

type I receptor (Fig. 2). Although the TβRII antibody co-precipitated ALK5 efficiently, the ALK5 antibody co-precipitated TβRII only weakly (see Fig. 2, *lane 5*, *both panels*). In the control GABE 15 Pool, the HA antibody failed to precipitate any proteins, as expected. Immunoprecipitations with a TβRII antibody were carried out in both pools as a positive control, and both resulted in the co-precipitation of TβRI (Fig. 2, *lane 7*, *both panels*). These data indicate that TβRII-K277R associates with TβRI.

To determine whether TβRII-K277R prevented TGF-β signaling, we examined its effect on the ability of TβRI to phosphorylate Smad2. Immunoblot analysis of TGF-β1-treated cell lysates using a phospho-specific Smad2 antibody revealed that although TGF-β1 could induce phosphorylation of Smad2 in both GABE clones (G15–5 and G15–6), its ability to do so in the TβRII-K277R clones (dn15–2, -3, -5, -11) was impaired (Fig. 3*A*). This impairment was not because of a decrease in total Smad2 protein, as reprobing with an antibody directed against total Smad2/3 did not reveal any significant change in protein levels. We next examined the effect of TβRII-K277R expression on TGF-β-induced Smad translocation to the nucleus by immunofluorescence (Fig. 3*B*). In the GABE clone Smad2 staining was relatively diffuse, but upon TGF-β1 treatment for 60 min, Smad2 staining became concentrated in the nucleus. In contrast, in the TβRII-K277R clones, there was little or no change in Smad2 staining following TGF-β1 treatment, suggesting impaired TGF-β-mediated translocation of Smad2 to the nu-

FIG. 4. **Expression of TβRII-K277R impairs motility.** *A*, confluent cell monolayers of clones expressing GFP alone (*G15–5* and *G15–6*) or GFP and TβRII-K277R (*dn15–2*, *dn15–3*, and *dn15–11*) were wounded with a pipette tip. Following wounding, cell culture medium was replaced with fresh medium, and wound closure was monitored by microscopy at the times indicated. *B*, single cell suspensions of pools expressing GFP alone (*G15 Pool*) or GFP and TβRII-K277R (*dn15 Pool*) in serum-free medium containing 0.1% bovine serum albumin were seeded onto 5 μM polycarbonate transwell filters and allowed to migrate toward increasing concentrations of FCS, as indicated. After 20 h, cells on the underside of the filters were fixed, stained, and counted. The results are represented quantitatively in the *bar graph below* the representative *filter micrographs*. Each *data point* represents the mean ± S.D. of two wells.
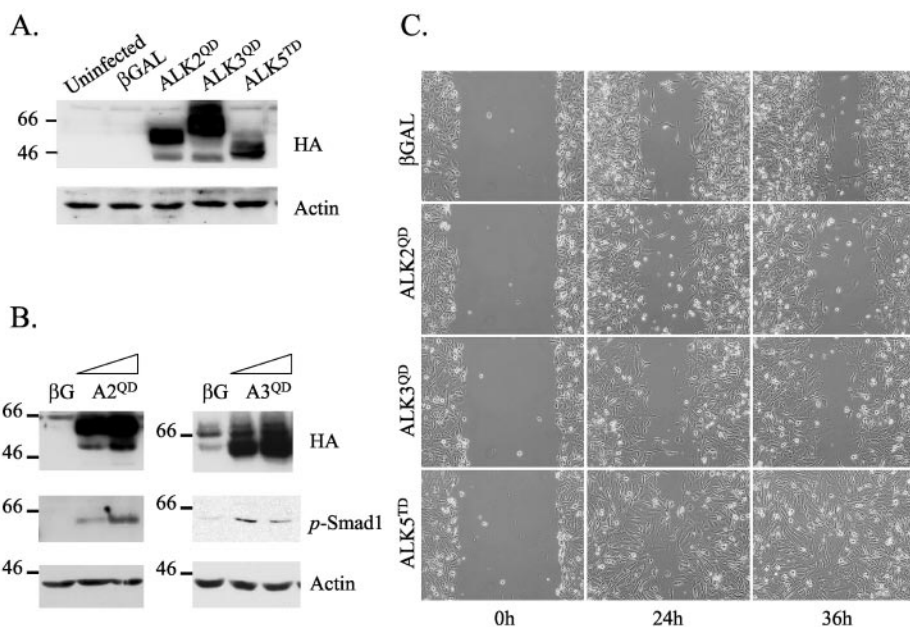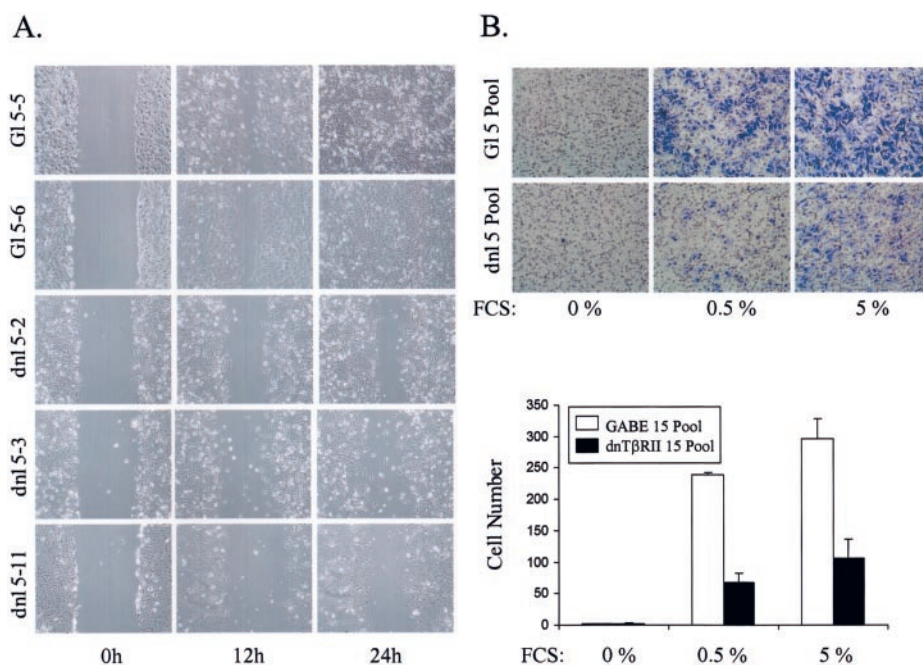

FIG. 5. **Expression of ALK5^{TD}/TβRI restores motility in TβRII-K277R cells.** Clone dn15–2 was infected with adenoviruses encoding HA-tagged constitutively active mutants of the activin (*ALK2^{QD}*), BMP (*ALK3^{QD}*) or TGF-β (*ALK5^{TD}*) type I receptors at an m.o.i. of 15. Uninfected cells and cells infected with a β-galactosidase (*βGAL*) adenovirus at a similar m.o.i. were used as controls. Approximately 48 h following infection, ALK expression (*A*) and function (*B*) were verified by immunoblot analysis utilizing an anti-HA or a phospho-specific Smad1 antibody, as indicated. The blots were also probed with an actin antibody to verify equal loading. The effect of ALK expression on wound closure was monitored by microscopy at the times indicated (*C*).

cleus. We then examined the effect of TβRII-K277R on TGF-β1-induced transcription. A reporter construct containing twelve Smad binding elements repeated in tandem, p(CAGA)$_{12}$-Luciferase, was transiently transfected into the GABE and TβRII-K277R clones, along with pCMV-Renilla. Normalized luciferase activity indicated that TGF-β1 could induce transcription of both reporter constructs in the GABE clones, but its ability to do so in the TβRII-K277R clones was impaired (Fig. 3*C*).

To determine whether signaling pathways other than the Smad pathway were also affected by expression of TβRII-K277R, we examined fibronectin expression, which has been reported to be induced by TGF-β in a JNK-dependent but Smad4-independent manner (6). We chose to perform these experiments in our pools as the results obtained in these cells are representative of those obtained in the clones (compare phospho-Smad2 blots in Fig. 3, *A* and *D*). Following TGF-β stimulation for 24 h, we observed an increase in fibronectin expression in the GABE pool, but this induction was decreased

significantly in the pool expressing TβRII-K277R, as was the basal level of fibronectin expression (Fig. 3*D*). We were unable to detect any induction of phosphorylation of JNK in response to TGF-β in our GABE pools (data not shown). However, we did observe an increase in phosphorylation of p38 MAPK following TGF-β stimulation for 60 min, and this induction of phosphorylation was slightly attenuated in the pool expressing TβRII-K277R (Fig. 3*D*).

TβRII-K277R Impairs the Motility of MDA-MB-231 Cells— Next we examined the effect of TβRII-K277R expression on the motility of MDA-MB-231 cells in a wound closure assay. In the GABE clones, cells migrated into the wounded area and closed the wound within 24 h, whereas in the TβRII-K277R clones the wound remained open at 24 h (Fig. 4*A*). This difference in motility did not appear to be because of an effect on proliferation, because when the experiment was performed in the presence of mitomycin C, a compound that inhibits cell division, the same results were obtained (data not shown). Thus, expression

FIG. 6. **Expression of Smad2/4 or Smad3/4 does not restore motility in TβRII-K277R cells.** Cells were infected with both FLAG-tagged Smad2 and Smad4 (*S2/4*) or FLAG-tagged Smad3 and Smad4 (*S3/4*) encoding adenoviruses at an m.o.i. of 3 for Smad2/3 and an m.o.i. of 15 for Smad4. Uninfected cells (*Uninf.*) and cells infected with a β-galactosidase (*βGAL*) adenovirus were used as controls. Approximately 48 h following infection, Smad expression was verified by immunoblot analysis utilizing an anti-FLAG antibody (*A*). The ability of Smads to restore TGF-β signaling in dn15–2 was evaluated in transcription reporter assays utilizing the TGF-β responsive transcription reporter p(CAGA)$_{12}$-Luciferase (*B*). The effect of Smad expression on wound closure in the control G15 Pool (*top panel*) and dn15–2 clone (*bottom panel*) was monitored by microscopy at the times indicated (*C*).
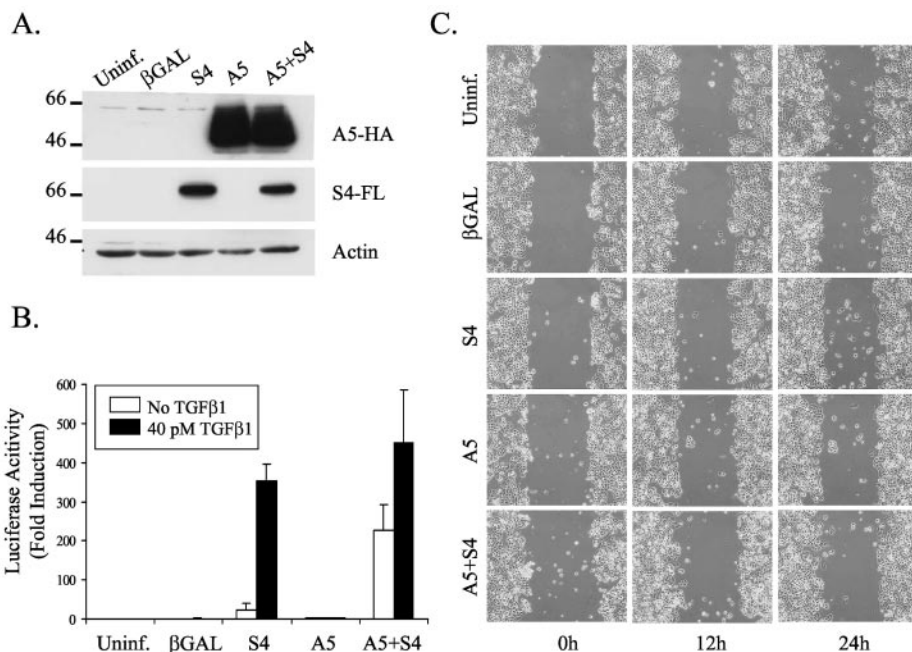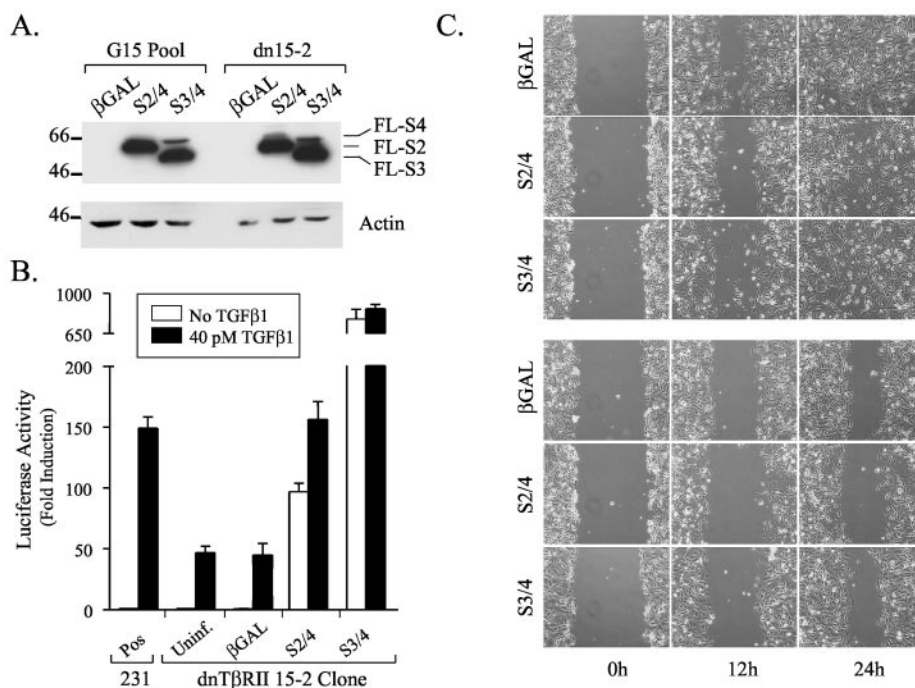

FIG. 7. **Effect of ALK5^{TD} on the motility of MDA-MB-468 cells −/+ Smad4.** Cells were infected with adenoviruses encoding FLAG-tagged Smad4 (*S4*), HA-tagged ALK5^{TD} (*A5*), or both (*A5+S4*) at an m.o.i. of 15. Uninfected cells (*Uninf.*) and cells infected with a β-galactosidase (*βGAL*) adenovirus were used as controls. Approximately 48 h following infection, exogenous Smad4 and ALK5^{TD} expression was verified by immunoblot analysis utilizing anti-FLAG and anti-HA antibodies, respectively. The blots were also probed with an actin antibody to verify equal loading (*A*). The ability of Smad4 and ALK5^{TD} to activate Smad-dependent signaling was evaluated in transcriptional reporter assays utilizing the Smad-dependent p(CAGA)$_{12}$-Luciferase reporter construct (*B*), and their effect on motility was examined in wound closure assays (*C*).

of TβRII-K277R in MDA-MB-231 cells appears to impair their motility, independent of changes in proliferation. As an alternative measure of cell motility, we also examined the effect of TβRII-K277R on the ability of cells to migrate in a transwell assay system. We observed a 3- to 4-fold reduction in the ability of cells expressing TβRII-K277R to migrate toward FCS, as compared with control cells expressing GFP alone (Fig. 4*B*).

The Impaired Motility of TβRII-K277R Cells Is TGF-β Type I Receptor-specific—Because the impaired motility of TβRII-K277R cells was observed in the absence of exogenous TGF-β stimulation, we wished to determine whether this impairment was TGF-β-specific. To do so, we chose to restore TGF-β signaling in TβRII-K277R cells by expressing a constitutively active mutant of TβRI. Mutation of threonine 204 in ALK5 (TβRI) to aspartic acid leads to constitutive activation of the type I receptor kinase, allowing it to induce signals in the

absence of ligands or type II receptors (41). Likewise, mutation of corresponding threonine and glutamine residues in the activin (42) and BMP (43) type I receptors to aspartic acid also leads to constitutive activation of these kinases. To test for TGF-β specificity, cells expressing TβRII-K277R were infected with adenoviruses encoding HA-tagged constitutively active mutants of the TGF-β (ALK5^{TD}), activin (ALK2^{QD}), and BMP (ALK3^{QD}) type I receptors (40). Uninfected cells or cells infected with a β-galactosidase adenovirus at the same m.o.i. were used as controls. The efficiency of infection was >90% as evaluated by *in situ* staining of cells for β-galactosidase activity 48 h following infection (data not shown). At this time, expression of the mutant type I receptors was confirmed by immunoblot analysis utilizing an HA antibody (Fig. 5*A*), and their effect on motility was assessed in wound closure assays. Motility was only restored in cells expressing ALK5^{TD} (Fig. 5*C*). Although

A.

B.

FIG. 8. **Effect of exogenous TGF-β1 stimulation on the motility of SW480.7 cells −/+ Smad4.** Cells in 6-well plates were either left untreated (*left panel*) or treated with 3 μM ponasterone (*right panel*) for 40 h to induce Smad4 expression. Cells were then wounded, washed, and incubated with serum-free medium in the presence of 0, 4, 20, or 100 pM TGF-β1 for 24 h. Wound closure was monitored by microscopy at the times indicated (*B*). At the conclusion of the wound closure experiment, cells were lysed, and Smad4 expression was examined by immunoblot analysis utilizing a monoclonal antibody directed against Smad4 (*A*). The blots were also probed with an actin antibody to verify equal loading. Ponasterone was maintained in the culture medium of selected wells throughout the experiment.
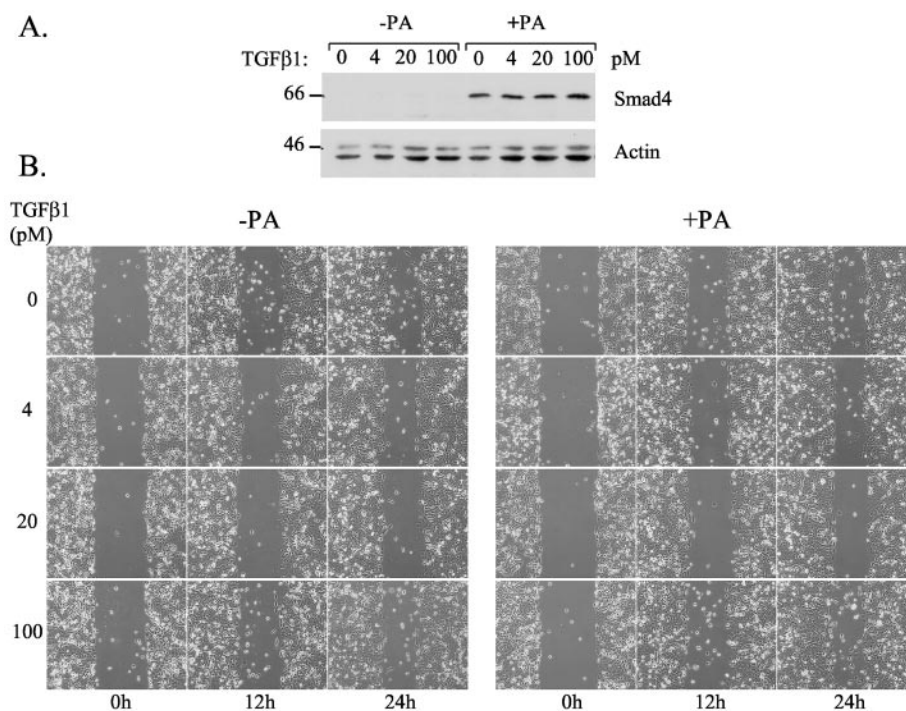
ALK2^{QD} and ALK3^{QD} were expressed and functional, as evidenced by their ability to induce Smad1 phosphorylation (Fig. 5B), they failed to restore motility in cells expressing TβRII-K277R (Fig. 5C). These results suggest that the impaired motility of TβRII-K277R cells is TβRI (ALK5)-specific.

Restoration of Smad Signaling Does Not Rescue the Impaired Motility of TβRII-K277R Cells—Although there is evidence that Smad signaling is critical for the anti-proliferative effects mediated by TGF-β (44, 45), it is unclear whether TGF-β-mediated motility requires Smad signaling. We reasoned that if Smads are required for TGF-β-mediated motility, blockade of Smad signaling with dominant-negative Smad mutants or with the inhibitory Smad, Smad7, should impair motility. However, expression of either dominant-negative Smad4 or Smad7 in the MDA-MB-231 parental cells resulted in cell death (data not shown). Therefore, it was not possible to address whether TGF-β-mediated motility requires Smad signaling utilizing this approach. Instead, we chose to overexpress the TGF-β R-Smads, Smad2 or Smad3, along with Smad4, in cells expressing TβRII-K277R to determine whether reconstitution of Smad signaling could restore motility. Cells were infected with adenoviruses encoding FLAG-tagged Smad2 and Smad4 or FLAG-tagged Smad3 and Smad4, and exogenous Smad expression was confirmed by immunoblot analysis utilizing an anti-FLAG antibody (Fig. 6A). The ability of Smad2/4 and Smad3/4 to activate Smad-dependent signaling was examined utilizing the Smad-dependent transcription reporter construct, p(CAGA)$_{12}$-Luciferase. Expression of Smad3/4 resulted in a marked increase in basal transcription (Fig. 6B). Stimulation with TGF-β1 did not cause any further increase in transcription, suggesting that Smad signaling was activated maximally. Despite this, Smad3/4 failed to restore motility in the cells expressing TβRII-K277R (Fig. 6C, *bottom panel*) and had no effect on the motility of control cells expressing GFP alone (Fig. 6C, *top panel*). Activation of basal transcription was not as marked with Smad2/4, as expected, because Smad2 itself cannot bind DNA (46). However, despite nearly 100-fold induction of transcription following infection at the maximally tolerated m.o.i., this combination also failed to restore motility in the cells expressing TβRII-K277R (Fig. 6C, *bottom panel*) and had no effect on

the motility of control cells expressing GFP alone (Fig. 6C, *top panel*). These results indicate that reconstitution of Smad signaling alone is not sufficient to restore autocrine TGF-β-mediated motility in cells expressing TβRII-K277R, nor is it sufficient to enhance the motility of control MDA-MB-231 cells.

Re-expression of Smad4 in Smad4-defective Cancer Cells Does Not Enhance Motility—To determine whether Smads are required for cancer cell migration, we examined whether activation of TGF-β signaling could promote motility in the absence of Smad signaling utilizing Smad4 null MDA-MB-468 breast cancer cells (47). Smad4 and ALK5^{TD} were expressed, either alone or in combination, by adenoviral transduction, and their effects on the motility of MDA-MB-468 cells were examined in wound closure assays. Expression of HA-tagged ALK5^{TD} and FLAG-tagged Smad4 was confirmed by immunoblot analysis (Fig. 7A), and their ability to activate Smad-dependent signaling was examined in transcription reporter assays utilizing the Smad-dependent p(CAGA)$_{12}$-Luciferase reporter construct (Fig. 7B). As expected, in the absence of Smad4 (uninfected, β-galactosidase, ALK5^{TD} alone), TGF-β1 was unable to stimulate transcription in these cells. However, upon re-expression of Smad4 a marked increase in both TGF-β1-mediated and ALK5^{TD}-mediated transcription was observed, indicating that both Smad4 and ALK5^{TD} were indeed functional in these cells. Despite this, neither Smad4 nor ALK5^{TD} had any effect on cell motility, whether they were expressed alone or in combination (Fig. 7C). The fact that ALK5^{TD} could not promote motility, even when Smad4 was co-expressed with it, suggests that MDA-MB-468 cells are not responsive to the pro-migratory effects of TGF-β.

To determine whether TGF-β could induce migration in the absence of Smad signaling in other cells, the Smad4 defective SW480.7 colorectal cells, conditionally expressing Smad4 via an ecdysone-inducible system (34), were utilized. Cells were stimulated with increasing concentrations of TGF-β1 in the absence or presence of 3 μM ponasterone to induce Smad4 expression. Smad4 expression in ponasterone-treated cells was confirmed by immunoblot analysis (Fig. 8A), and its effect on TGF-β-mediated motility was examined in wound closure assays. Again, as in the MDA-MB-468 cells, these cells failed to

A.

B.

C.

FIG. 9. **Different signaling pathways require different thresholds of TGF-β activation.** Clone dn15–2 was infected with an adenovirus encoding an HA-tagged constitutively active mutant of the TGF-β type I receptor ($ALK5^{TD}$) at m.o.i. values of 0, 5, 10, or 15, as indicated. Approximately 48 h following infection, cells were wounded, and the effect of $ALK5^{TD}$ expression on wound closure was monitored by microscopy at the times indicated (*B*). At the conclusion of the migration assay, cells were lysed, $ALK5^{TD}$ expression was confirmed by HA immunoblot, and the activation status of candidate signaling pathways was examined utilizing phospho-specific antibodies, as indicated (*A*). Actin was examined as a loading control. In *C*, clone dn15–2 was re-infected with $ALK5^{TD}$ at m.o.i. values of 0, 5, 15, 30, or 60, as indicated, and the activation status of candidate signaling pathways was re-examined utilizing phospho-specific antibodies as in *A*.
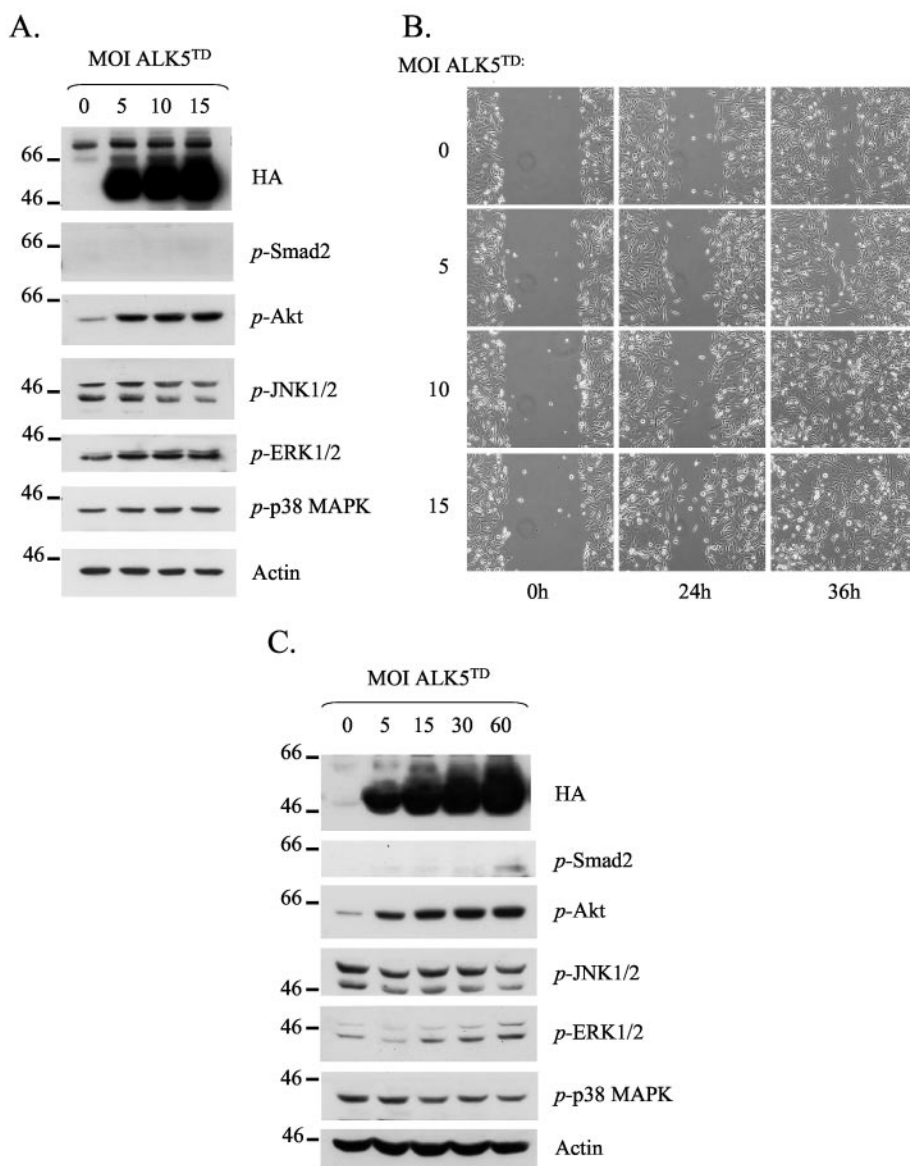
respond to TGF-β both in the absence and presence of Smad4 (Fig. 8*B*). Taken together, these data indicate that reconstitution of Smad signaling alone is not sufficient to promote migration of cancer cells.

Different Signaling Pathways Require Different Thresholds of TGF-β Activation—To determine whether Smad signaling is actually required in addition to other pathways activated by TGF-β to promote migration, we examined what signaling pathways were activated under conditions where motility was restored following $ALK5^{TD}$ expression in cells expressing TβRII-K277R (see Fig. 5*C* and Fig. 9*B*). For these experiments, expression of $ALK5^{TD}$ was confirmed by HA immunoblot (Fig. 9*A*), and the activation status of candidate signaling pathways was examined utilizing phospho-specific antibodies. Under these conditions, we observed an increase in the phosphorylation of Akt and ERK1/2, with little or no change in the phosphorylation of JNK or p38 MAPK (Fig. 9*A*). Interestingly, the levels of $ALK5^{TD}$ expression that were sufficient to restore motility were not sufficient to induce phosphorylation of Smad2. Additional experiments indicated that ~4-fold greater $ALK5^{TD}$ expression was required for induction of Smad2 phosphorylation (Fig. 9*C*). At that m.o.i., the viral load *per se* interfered with the ability of the cells to migrate. These data indi-

cate that different signaling pathways require different thresholds of TGF-β activation, as do different biological effects mediated by TGF-β (27), and suggest that TGF-β may promote motility through mechanisms independent of Smad signaling, possibly involving activation of the PI3K-Akt and/or MAPK pathways. Consistent with this, the ability of TGF-β to promote migration was impaired in the presence of the PI3K inhibitor, LY294002 (Fig. 10*A*), as well as in the presence of JNK, MEK, and p38 MAPK pathway inhibitors (Fig. 10*B*).

DISCUSSION

In this study, abrogation of autocrine TGF-β signaling in MDA-MB-231 breast cancer cells resulted in an impairment in basal cell migration, which could not be restored by reconstituting Smad signaling, suggesting that Smad signaling alone is not sufficient for autocrine TGF-β-mediated motility. Consistent with this, reconstitution of Smad signaling in the Smad4-defective MDA-MB-468 and SW480.7 cells did not promote migration. In addition, restoration of migration following restoration of TGF-β signaling in cells expressing TβRII-K277R was associated with an increase in phosphorylation of Akt and ERK1/2 but not Smad2. These results indicate that Smad signaling is dispensable for TGF-β-mediated motility and that
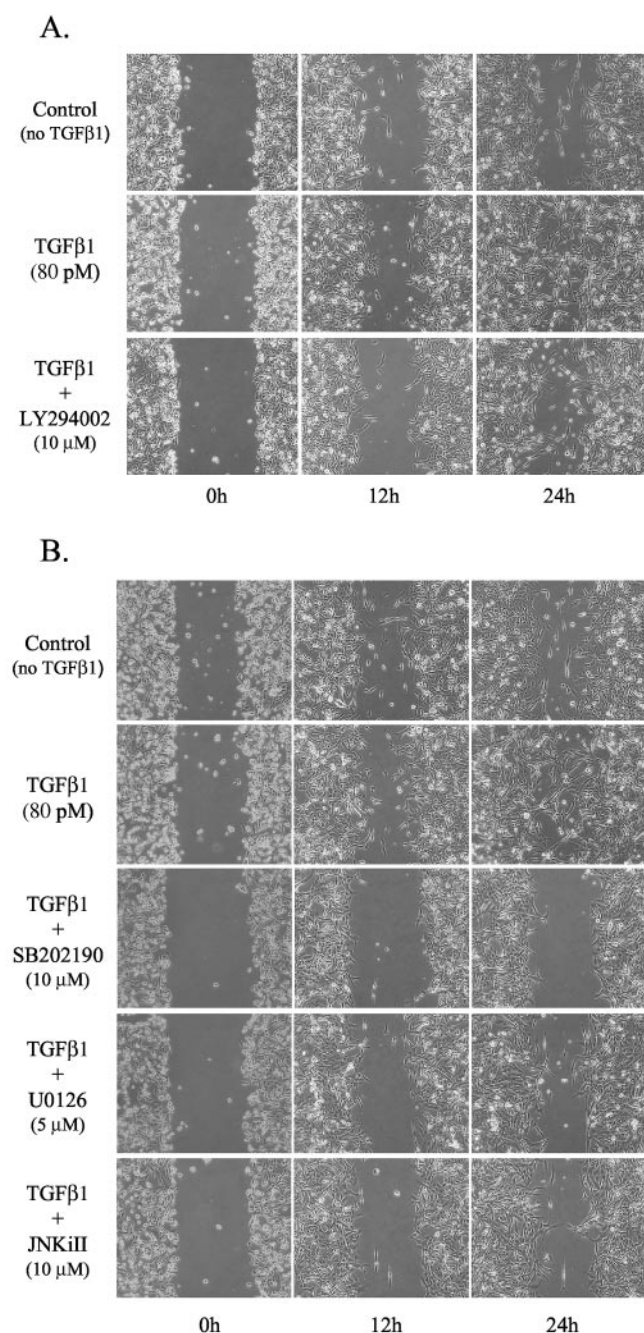
FIG. 10. **TGF-β-induced motility requires activation of multiple signaling pathways.** Confluent MDA-MB-231 cell monolayers were wounded with a pipette tip. Following wounding, cells were washed, the cell culture medium was replaced with serum-free medium, and the cells were stimulated with 80 pM TGF-β1 in the absence or presence of the PI3K inhibitor, LY294002 (*A*) or the p38 MAPK (*SB202190*), MEK (*UO126*), and JNK (*JNKiII*) inhibitors, as indicated (*B*). Wound closure was monitored by microscopy at the times indicated.

this response is instead mediated through alternative pathways activated by TGF-β. In support of this, the ability of TGF-β to promote migration was blocked in the presence of pharmacological inhibitors of the PI3K, p38 MAPK, MEK, and JNK pathways.

Although Smads have been implicated as critical mediators of many TGF-β responses (48–52), the role of Smads in cancer cell migration has, to the best of our knowledge, not been reported. Previous studies in non-transformed cells have generated conflicting data on the requirement of Smad signaling for cell migration (50, 53–55). In one study, expression of dom-

inant-negative Smad3 in non-transformed murine mammary cells had no effect on TGF-β-mediated motility even though it blocked the anti-mitogenic effect of TGF-β (53). This suggests that Smad3 is not required for this response or that residual Smad3 signaling, not blocked by expression of dominant-negative Smad3, is sufficient to mediate motility. This would be consistent with the idea that different biological responses require different thresholds of TGF-β signaling (27). Thus, complete abrogation of Smad3 signaling might be required to observe an impairment in TGF-β-mediated motility whereas partial blockade of Smad function might be sufficient to block the anti-proliferative effects of TGF-β.

Interestingly, expression of either dnSmad4 or antagonistic Smad7 in MDA-MB-231 cells resulted in cell death. Although overexpression of Smad7 has been reported to sensitize various cell types to cell death (56), expression of dnSmad4 has not been associated with such a response. There is, however, increasing evidence that TGF-β can promote the survival of both transformed (7, 57, 58) and non-transformed (59–61) cells. Whether Smad signaling is required for these pro-survival effects of TGF-β is not known. In addition, re-expression of Smad4 in Smad4-defective SW480 has been reported to induce a more adhesive and flat phenotype (62). These results suggest that blockade of Smad signaling could potentially lead to loss of adhesion and result in anoikis. This could explain our inability to express dnSmad4 and Smad7 in MDA-MB-231 cells.

Because we were unable to assess the requirement for Smads in autocrine TGF-β-mediated motility by abrogating Smad signaling, we chose to address this question by activating Smad signaling in cells expressing TβRII-K277R. Having ascertained that the impaired motility of TβRII-K277R cells was indeed TβRI-specific, we overexpressed the TGF-β R-Smads, Smad2 or Smad3, each with Smad4, to determine whether autocrine TGF-β-mediated motility was Smad-dependent. Despite their ability to activate Smad-dependent transcription, neither Smad combination restored the impaired motility of the TβRII-K277R cells. We (data not shown) and others (62) have observed an increase in cell spreading following Smad overexpression. It is tempting to speculate that this increased cell spreading may be associated with increased adhesion, which interferes with cell migration. This could potentially explain why restoration of Smad signaling in TβRII-K277R cells failed to restore migration. These data suggest that in breast cancer cells, autocrine TGF-β signaling mediates motility in a Smad-independent manner or that alternative pathways, in addition to the Smad signaling pathway, are required for these effects.

To address this question, we examined what signaling pathways were activated under conditions where motility was restored in TβRII-K277R cells following expression of a constitutively active type I TGF-β receptor. In these experiments, we observed an increase in the phosphorylation of Akt and ERK1/2 but not Smad2. These data further imply that Smad signaling is not required for TGF-β-mediated motility. Although expression of ALK5^{TD} may induce a low level of Smad phosphorylation, which cannot be detected by immunoblot analysis, it is unlikely that Smads are required for autocrine TGF-β-mediated motility as reconstitution of Smad signaling in both MDA-MB-468 and SW480.7 cancer cell lines failed to promote motility, and expression of both low and high levels of either Smad2/4 or Smad3/4 failed to rescue the impaired motility of MDA-MB-231 cells expressing dnTβRII. Thus, alternative signaling pathways activated by TGF-β are more likely to be important for migration. Indeed, blockade of the PI3K, p38 MAPK, MEK, and JNK pathways with pharmacological inhibitors impaired TGF-β-stimulated migration. The fact that inhibitors of p38 MAPK and JNK interfered with TGF-β-induced

migration even though ALK5[TD] failed to alter their phosphorylation status suggests that these signaling pathways, though not activated further by TGF-β in our experimental system, are required for basal cell migration. In agreement with this, we have indeed observed an impairment in the basal migratory potential of these cells in the presence of these inhibitors (data not shown).

The observation that different levels of ALK5[TD] expression resulted in differential activation of downstream targets (Fig. 9*C*) indicates that different signaling pathways require different thresholds of TGF-β activation. In agreement with this, others have reported that expression of dnTβRII in NMuMG mammary cells impairs TGF-β-mediated Smad-dependent inhibition of proliferation but not TGF-β-mediated activation of p38 MAPK (9). In addition, there is evidence that different biological responses mediated by TGF-β also require different thresholds of TGF-β signaling. For example, expression of dnTβRII in squamous carcinoma cells has been reported to block the growth inhibitory effects of TGF-β but not its ability to induce EMT (26). Likewise, expression of dnTβRII in 4T1 murine mammary cancer cells impairs TGF-β-mediated transcription but fails to block motility (27). Because TGF-β signaling was not completely abrogated in the squamous and mammary cancer cells (26, 27), the molecular mechanisms by which autocrine TGF-β may selectively contribute to tumor progression could not be fully addressed in those studies. Because we have expressed TβRII-K277R at levels high enough to block both Smad and non-Smad pathways in MDA-MB-231 cells, the model we have generated should prove useful in dissecting the signaling pathways required for the diverse effects elicited by TGF-β in cancer.

Our data indicate that autocrine TGF-β-mediated motility of cancer cells is Smad-independent. This implies that non-transformed cells and transformed cells utilize different mechanisms to promote motility as others have reported that Smad3 null monocytes and keratinocytes exhibit significantly reduced migration to TGF-β1 in transwell motility assays (54). Moreover, Smad3 appears to be required for TGF-β-mediated monocyte chemotaxis *in vivo*, as mice lacking the Smad3 gene display a blunted monocyte chemotactic response following cutaneous wounding (54). Studies in *Drosophila* also suggest that Smads may be required for cell migration as mutations in Mad, the *Drosophila* receptor-activated Smad, impair migration of the epidermis during dorsal closure (55). Finally, recent studies in endothelial cells have indicated that TGF-β acting through ALK1 stimulates migration in a Smad-dependent manner, whereas TGF-β acting through ALK5 inhibits cell migration in a Smad-dependent manner (50). Taken together, these studies highlight the importance of Smads in TGF-β-regulated migration of non-transformed cells.

Despite compelling evidence for the role of Smads in non-transformed cell migration, a lack of requirement for Smad signaling in TGF-β-mediated cancer cell migration is consistent with previous studies that have shown that TGF-β can increase cellular motility of prostate cancer cells without affecting proliferation, suggesting that the effects on motility and proliferation may occur via different biochemical pathways (28). Likewise, expression of Smad7 in pancreatic cancer cells has been shown to abrogate the anti-proliferative effects of TGF-β but enhance matrix-associated transcriptional responses, highlighting a dissociation between the matrix and anti-proliferative effects induced by TGF-β (63). If the biological effects of TGF-β that can contribute to tumor progression were Smad-independent, it might be possible to selectively disrupt those pathways, while ensuring that the tumor suppressive, Smad-dependent pathways are maintained. The signaling pathways currently implicated in mediating the various pro- and anti-tumorigenic effects of TGF-β indicate that this may in fact be possible. For example, recent studies aimed at identifying the mechanisms by which TGF-β1 elicits EMT in mammary cells have indicated that the PI3K, RhoA, and p38 MAPK pathways are involved in this process (8, 9, 11, 53). However, whether Smad signaling, which has been implicated in both the anti-proliferative (44, 45) and pro-apoptotic (64, 65) effects of TGF-β, is also required for TGF-β-mediated EMT is unclear. In one study, adenoviral expression of low levels of constitutively active ALK5 induced EMT only if Smad2/4 or Smad3/4 were co-expressed (66). In contrast, other investigators have reported that inhibition of Smad signaling either by overexpression of Smad7 or dominant-negative Smad3 did not affect the transdifferentiation, arguing against the involvement of Smads in EMT (53). Because epithelial transdifferentiation to a mesenchymal phenotype is often associated with acquisition of motile properties, the mechanisms through which TGF-β mediates EMT may be similar to those required for TGF-β-mediated motility. Indeed, the PI3K, RhoA, and p38 MAPK signaling pathways, which are required for TGF-β-mediated EMT, have also been implicated in TGF-β-mediated motility (8, 11, 53). Likewise, we have observed that blockade of these and other pathways interfere with TGF-β-induced motility (Fig. 10), suggesting that multiple pathways cooperate to elicit this effect. It will be of interest to determine whether Smad signaling is required for other effects mediated by TGF-β, as a dissociation between the pathways required for the tumor suppressive *versus* the tumor promoting effects of TGF-β could lead to opportunities to selectively inhibit the non-desirable effects of TGF-β without compromising its tumor suppressive function.

REFERENCES

1. Massagué, J. (1998) *Annu. Rev. Biochem.* **67,** 753–791
2. Wrana, J. L., Attisano, L., Wieser, R., Ventura, F., and Massagué, J. (1994) *Nature* **370,** 341–347
3. Frey, R. S., and Mulder, K. M. (1997) *Cancer Res.* **57,** 628–633
4. Mulder, K. M. (2000) *Cytokine Growth Factor Rev.* **11,** 23–35
5. Atfi, A., Djelloul, S., Chastre, E., Davis, R., and Gespach, C. (1997) *J. Biol. Chem.* **272,** 1429–1432
6. Hocevar, B. A., Brown, T. L., and Howe, P. H. (1999) *EMBO J.* **18,** 1345–1356
7. Huang, Y., Hutter, D., Liu, Y., Wang, X., Sheikh, M. S., Chan, A. M., and Holbrook, N. J. (2000) *J. Biol. Chem.* **275,** 18234–18242
8. Bakin, A. V., Rinehart, C., Tomlinson, A. K., and Arteaga, C. L. (2002) *J. Cell Sci.* **115,** 3193–3206
9. Bhowmick, N. A., Zent, R., Ghiassi, M., McDonnell, M., and Moses, H. L. (2001) *J. Biol. Chem.* **276,** 46707–46713
10. Higaki, M., and Shimokado, K. (1999) *Arterioscler. Thromb. Vasc. Biol.* **19,** 2127–2132
11. Bakin, A. V., Tomlinson, A. K., Bhowmick, N. A., Moses, H. L., and Arteaga, C. L. (2000) *J. Biol. Chem.* **275,** 36803–36810
12. Edlund, S., Landstrom, M., Heldin, C. H., and Aspenstrom, P. (2002) *Mol. Biol. Cell* **13,** 902–914
13. Hata, A., Lagna, G., Massagué, J., and Hemmati-Brivanlou, A. (1998) *Genes Dev.* **12,** 186–197
14. Ishisaki, A., Yamato, K., Hashimoto, S., Nakao, A., Tamaki, K., Nonaka, K., ten Dijke, P., Sugino, H., and Nishihara, T. (1999) *J. Biol. Chem.* **274,** 13637–13642
15. Hayashi, H., Abdollah, S., Qiu, Y., Cai, J., Xu, Y. Y., Grinnell, B. W., Richardson, M. A., Topper, J. N., Gimbrone, M. A., Jr., Wrana, J. L., and Falb, D. (1997) *Cell* **89,** 1165–1173
16. Souchelnytskyi, S., Nakayama, T., Nakao, A., Moren, A., Heldin, C. H., Christian, J. L., and ten Dijke, P. (1998) *J. Biol. Chem.* **273,** 25364–25370
17. Moses, H. L., Branum, E. L., Proper, J. A., and Robinson, R. A. (1981) *Cancer Res.* **41,** 2842–2848
18. Roberts, A. B., Anzano, M. A., Lamb, L. C., Smith, J. M., and Sporn, M. B. (1981) *Proc. Natl. Acad. Sci. U. S. A.* **78,** 5339–5343
19. de Caestecker, M. P., Piek, E., and Roberts, A. B. (2000) *J. Natl. Cancer Inst.* **92,** 1388–1402
20. Wakefield, L. M., and Roberts, A. B. (2002) *Curr. Opin. Genet. Dev.* **12,** 22–29

21. Hata, A., Shi, Y., and Massagué, J. (1998) *Mol. Med. Today* **4,** 257–262
22. Kim, S. J., Im, Y. H., Markowitz, S. D., and Bang, Y. J. (2000) *Cytokine Growth Factor Rev.* **11,** 159–168
23. Massagué, J., Blain, S. W., and Lo, R. S. (2000) *Cell* **103,** 295–309
24. Yin, J. J., Selander, K., Chirgwin, J. M., Dallas, M., Grubbs, B. G., Wieser, R., Massagué, J., Mundy, G. R., and Guise, T. A. (1999) *J. Clin. Invest.* **103,** 197–206
25. Oft, M., Heider, K. H., and Beug, H. (1998) *Curr. Biol.* **8,** 1243–1252
26. Portella, G., Cumming, S. A., Liddell, J., Cui, W., Ireland, H., Akhurst, R. J., and Balmain, A. (1998) *Cell Growth Differ.* **9,** 393–404
27. McEearchern, J. A., Kobie, J. J., Mack, V., Wu, R. S., Meade-Tollin, L., Arteaga, C. L., Dumont, N., Besselsen, D., Seftor, E., Hendrix, M. J., Katsanis, E., and Akporiaye, E. T. (2001) *Int. J. Cancer.* **91,** 76–82
28. Morton, D. M., and Barrack, E. R. (1995) *Cancer Res.* **55,** 2596–2602
29. Kalkhoven, E., Roelen, B. A., de Winter, J. P., Mummery, C. L., van den Eijnden-van Raaij, A. J., van der Saag, P. T., and van der Burg, B. (1995) *Cell Growth Differ.* **6,** 1151–1161
30. Martinez-Carpio, P. A., Mur, C., Fernandez-Montoli, M. E., Ramon, J. M., Rosel, P., and Navarro, M. A. (1999) *Cancer Lett.* **147,** 25–29
31. Arnoletti, J. P., Albo, D., Granick, M. S., Solomon, M. P., Castiglioni, A., Rothman, V. L., and Tuszynski, G. P. (1995) *Cancer* **76,** 998–1005
32. Farina, A. R., Coppa, A., Tiberio, A., Tacconelli, A., Turco, A., Colletta, G., Gulino, A., and Mackay, A. R. (1998) *Int. J. Cancer* **75,** 721–730
33. Arteaga, C. L., Hurd, S. D., Winnier, A. R., Johnson, M. D., Fendly, B. M., and Forbes, J. T. (1993) *J. Clin. Invest.* **92,** 2569–2576
34. Calonge, M. J., and Massagué, J. (1999) *J. Biol. Chem.* **274,** 33637–33643
35. ten Dijke, P., Yamashita, H., Ichijo, H., Franzen, P., Laiho, M., Miyazono, K., and Heldin, C. H. (1994) *Science* **264,** 101–104
36. Wrana, J. L., Attisano, L., Carcamo, J., Zentella, A., Doody, J., Laiho, M., Wang, X. F., and Massagué, J. (1992) *Cell* **71,** 1003–1014
37. Dumont, N., O'Connor-McCourt, M. D., and Philip, A. (1995) *Mol. Cell. Endocrinol.* **111,** 57–66
38. Dennler, S., Itoh, S., Vivien, D., ten Dijke, P., Huet, S., and Gauthier, J. M. (1998) *EMBO J.* **17,** 3091–3100
39. McDonnell, M. A., Law, B. K., Serra, R., and Moses, H. L. (2001) *Exp. Cell Res.* **263,** 265–273
40. Fujii, M., Takeda, K., Imamura, T., Aoki, H., Sampath, T. K., Enomoto, S., Kawabata, M., Kato, M., Ichijo, H., and Miyazono, K. (1999) *Mol. Biol. Cell* **10,** 3801–3813
41. Wieser, R., Wrana, J. L., and Massagué, J. (1995) *EMBO J.* **14,** 2199–2208
42. Jones, C. M., Armes, N., and Smith, J. C. (1996) *Curr. Biol.* **6,** 1468–1475
43. Akiyama, S., Katagiri, T., Namiki, M., Yamaji, N., Yamamoto, N., Miyama, K., Shibuya, H., Ueno, N., Wozney, J. M., and Suda, T. (1997) *Exp. Cell Res.* **235,** 362–369
44. Liu, X., Sun, Y., Constantinescu, S. N., Karam, E., Weinberg, R. A., and Lodish, H. F. (1997) *Proc. Natl. Acad. Sci. U. S. A.* **94,** 10669–10674
45. Datto, M. B., Frederick, J. P., Pan, L., Borton, A. J., Zhuang, Y., and Wang, X. F. (1999) *Mol. Cell. Biol.* **19,** 2495–2504
46. Dennler, S., Huet, S., and Gauthier, J. M. (1999) *Oncogene* **18,** 1643–1648
47. Schutte, M., Hruban, R. H., Hedrick, L., Cho, K. R., Nadasdy, G. M., Weinstein, C. L., Bova, G. S., Isaacs, W. B., Cairns, P., Nawroz, H., Sidransky, D., Casero, R. A., Jr., Meltzer, P. S., Hahn, S. A., and Kern, S. E. (1996) *Cancer Res.* **56,** 2527–2530
48. Piek, E., Ju, W. J., Heyer, J., Escalante-Alcalde, D., Stewart, C. L., Weinstein, M., Deng, C., Kucherlapati, R., Bottinger, E. P., and Roberts, A. B. (2001) *J. Biol. Chem.* **276,** 19945–19953
49. Jang, C. W., Chen, C. H., Chen, C. C., Chen, J. Y., Su, Y. H., and Chen, R. H. (2002) *Nat. Cell. Biol.* **4,** 51–58
50. Goumans, M. J., Valdimarsdottir, G., Itoh, S., Rosendahl, A., Sideras, P., and ten Dijke, P. (2002) *EMBO J.* **21,** 1743–1753
51. Kakonen, S. M., Selander, K. S., Chirgwin, J. M., Yin, J. J., Burns, S., Rankin, W. A., Grubbs, B. G., Dallas, M., Cui, Y., and Guise, T. A. (2002) *J. Biol. Chem.* **277,** 24571–24578
52. Chen, C. R., Kang, Y., Siegel, P. M., and Massague, J. (2002) *Cell* **110,** 19–32
53. Bhowmick, N. A., Ghiassi, M., Bakin, A., Aakre, M., Lundquist, C. A., Engel, M. E., Arteaga, C. L., and Moses, H. L. (2001) *Mol. Biol. Cell* **12,** 27–36
54. Ashcroft, G. S., Yang, X., Glick, A. B., Weinstein, M., Letterio, J. L., Mizel, D. E., Anzano, M., Greenwell-Wild, T., Wahl, S. M., Deng, C., and Roberts, A. B. (1999) *Nat. Cell. Biol.* **1,** 260–266
55. Hudson, J. B., Podos, S. D., Keith, K., Simpson, S. L., and Ferguson, E. L. (1998) *Development* **125,** 1407–1420
56. Lallemand, F., Mazars, A., Prunier, C., Bertrand, F., Kornprost, M., Gallea, S., Roman-Roman, S., Cherqui, G., and Atfi, A. (2001) *Oncogene* **20,** 879–884
57. Berking, C., Takemoto, R., Schaider, H., Showe, L., Satyamoorthy, K., Robbins, P., and Herlyn, M. (2001) *Cancer Res.* **61,** 8306–8316
58. Muraoka, R. S., Dumont, N., Ritter, C. A., Dugger, T. C., Brantley, D. M., Chen, J., Easterly, E., Roebuck, L. R., Ryan, S., Gotwals, P. J., Koteliansky, V., and Arteaga, C. L. (2002) *J. Clin. Invest.* **109,** 1551–1559
59. Poulsen, K. T., Armanini, M. P., Klein, R. D., Hynes, M. A., Phillips, H. S., and Rosenthal, A. (1994) *Neuron* **13,** 1245–1252
60. Chin, B. Y., Petrache, I., Choi, A. M., and Choi, M. E. (1999) *J. Biol. Chem.* **274,** 11362–11368
61. Shin, I., Bakin, A. V., Rodeck, U., Brunet, A., and Arteaga, C. L. (2001) *Mol. Biol. Cell* **12,** 3328–3339
62. Schwarte-Waldhoff, I., Klein, S., Blass-Kampmann, S., Hintelmann, A., Eilert, C., Dreschers, S., Kalthoff, H., Hahn, S. A., and Schmiegel, W. (1999) *Oncogene* **18,** 3152–3158
63. Kleeff, J., Ishiwata, T., Maruyama, H., Friess, H., Truong, P., Buchler, M. W., Falb, D., and Korc, M. (1999) *Oncogene* **18,** 5363–5372
64. Schuster, N., and Krieglstein, K. (2002) *Cell Tissue Res.* **307,** 1–14
65. Yang, Y. A., Tang, B., Robinson, G., Hennighausen, L., Brodie, S. G., Deng, C. X., and Wakefield, L. M. (2002) *Cell Growth Differ.* **13,** 123–130
66. Piek, E., Moustakas, A., Kurisaki, A., Heldin, C. H., and ten Dijke, P. (1999) *J. Cell Sci.* **112,** 4557–4568

Truncating mutations in the ACVR2 gene attenuates activin signaling in prostate cancer cells

Michael R. Rossi, Yurij Ionov, Andrei V. Bakin, John K. Cowell*

Department of Cancer Genetics, Roswell Park Cancer Institute, Elm and Carlton Streets, Buffalo, NY 14263

Received 4 March 2005; accepted 9 May 2005

Abstract

Activins are classified as members of the TGFβ superfamily of signaling molecules and both activin and TGFβ ligands signal through structurally and functionally related serine/threonine kinase receptors. Defects in these signaling pathways have been associated with the initiation and progression of the cancer phenotype. Inactivating mutations in the TGFβ type II receptor gene, *TGFβR2*, have been identified in a variety of tumors and cell lines, particularly those with microsatellite instability (MSI). More recently, mutations in the activin type II receptor gene, *ACVR2*, were identified in colon and pancreatic cell lines and tumors with MSI. Because prostate tumors appear to have a high incidence of MSI, we analyzed prostate cancer cell lines, with and without MSI, for *ACVR2* and *TGFβR2* mutations. Our analysis of 6 prostate cell lines revealed mutations in the *ACVR2* gene in 22Rv-1, LAPC-4, DU145, and LNCaP cells and mutations in the *TGFβR2* gene in 22Rv-1 and LAPC-4. PC3 and H660 cells were wild-type for *ACVR2* and *TFGβR2*. All of the *ACVR2* mutations were truncating mutations, and using an activin response assay, we demonstrate that truncating mutations of the ACVR2 gene result in a significant reduction in activin mediated cell signaling. Inactivation of *ACVR2* is a common event in prostate cancer cells suggesting it may play an important role in the development of prostate cancer. © 2005 Elsevier Inc. All rights reserved.

1. Introduction

The transforming growth factor β (TGFβ) superfamily of cytokines control various biological and physiological processes [1]. Most of the TGFβ families of ligands signal through receptor serine/threonine kinases that are divided into type I and type II receptors [2,3]. TGFβ and activin proteins specifically bind to their respective type II receptors, which in turn lead to recruitment and activation of type I receptors [4,5]. Activin and TGFβ receptors differ functionally in the fact that the activin type II receptors can bind other ligands, such as myostatin, BMP2, BMP7, and nodal, in addition to activin, whereas TGFβ signals only through its own type II receptors [6].

The parallel signaling pathways of activin and TGFβ are well characterized in a number of cell types [1], and aberrant TGFβ and activin signaling has been identified in numerous cancers [7]. Activins and TGFβ form an active complex with their type I and type II receptors, and the type I receptors phosphorylate Smad proteins (SMADs) which

regulate gene transcription. In response to activin, SMADs activate transcription through a ternary complex consisting of SMAD2, SMAD4, and FAST-1, which bind to an activin-response element (ARE) in gene promoter regions [3]. SMADs also activate transcription in response to TGFβ, but this response is mediated by SMAD2/3/4 [8]. Because the activin type II receptor (ACVR2) and the TGFβ type II receptor (TGFβR2) are at the interface of ligand initiated signaling, loss or mutation of either or both of these genes can have far-reaching effects in terms of gene expression [9,10].

ACVR2 shares 37% homology with *TGFβR2* at the amino acid level [11] and has two polyadenine regions within its open reading frame, whereas *TGFβR2* has only one polyadenine tract within its coding region. These microsatellite regions consist of 10 adenines [$(A)_{10}$] in exon 3 of *TGFβR2* and eight adenines [$(A)_8$] in exons 3 and 10 of *ACVR2*. Mononucleotide stretches can be hotspots for frameshift mutations, particularly in cells with diminished or deficient mismatch repair [12,13]. A single frameshift mutation in either the $(A)_{10}$ region of *TGFβR2* or the $(A)_8$ region in exon 3 of *ACVR2* would lead to functional gene inactivation through nonsense mediated decay of the

---

* Corresponding author. Tel.: (716) 845-5714; fax: (716) 845-1698.
 E-mail address: John.Cowell@RoswellPark.org (J.K. Cowell).

mutant mRNA. Frameshift mutations in the $(A)_8$ tract in exon 10 of *ACVR2*, however, effectively results in a truncated version of the *ACVR2* protein [14–16].

TGFβR2 mutations were first identified in pancreatic tumors and have since been identified in a variety of other tumor types [17]. *ACVR2* mutations, however, are not as well characterized in cancer. Mutations in *ACVR2* were first reported in pituitary tumors, exclusively as frameshift mutations in the $(A)_8$ tract of exon 10 [18]. More recently, colon and pancreatic cell lines were demonstrated to have predominantly similar frameshift mutations in exon 10 of the ACVR2 gene [14]. This data was supported by additional studies in microsatellite unstable colon tumors which showed loss of *ACVR2* expression as determined by immunohistochemistry using an antibody that targeted an epitope that was present in the wild-type but not the truncated ACVR2 protein [16]. In breast cancer, ACVR2 expression was diminished or absent in high grade tumors, but this study did not entail mutation analysis [19].

Because *TGFβR2* mutations often coincide with *ACVR2* mutations in colon cells [14], we analyzed the *ACVR2* and *TGFβR2* genes in prostate cancer cell lines. In this report, we identify mutations in both the *TGFβR2* and *ACVR2* genes in prostate cancer cells, and demonstrate that truncating *ACVR2* mutations result in their diminished transcriptional response to activin.

2. Materials and methods

2.1. DNA extraction and sequencing

Prostate cancer cell lines were grown at 37°C with 10% CO_2 in DMEM supplemented with 5% FBS and antibiotics, with the exception of LAPC-4 cells, which were grown in RPMI 1640 supplemented with 15% FBS and antibiotics. DNA was extracted from prostate cancer cell lines using a standard phenol-chloroform extraction protocol [20]. PCR was performed according to the Phusion™ high-fidelity DNA polymerase protocol (Finnzymes OY, Espoo, Finland). using 100 ng of genomic DNA and exon specific primers for ACVR2 (Ex3F 5′-AAAAACACTTGTTGTAGG-GTCAG-3′, Ex3R 5′-TGTTTCCAATCTACAGTT-GAGCA-3′; Ex10F 5′-CCAGTTTGAAAGTCAGGAGGA-3′, Ex10R 5′-TGGAAT-TTCAAATGAAAAGCTAAC-3′; Ex11F 5′-CTGCTGTGGCGTTTGAGTAT-3′, Ex11R 5′-TCCCAGAGCAACATTTTTCA-3′), and TGFβR2 (Ex3F 5′-CCTCGCTTCCAATGA-ATCTC-3′, Ex3R 5′-TCCCACACCCT-TAAGAGAAGAA-3′). The PCR products were gel purified and sequenced using the Applied Biosystems' PRISM 3100 Genetic Analyzer (Foster City, CA).

2.2. Gene expression analysis of prostate cancer cell lines

Total RNA was isolated from prostate cancer cell lines using TRIzol® reagent (Invitrogen, Carlsbad, CA). Reverse transcription of 2 μg of total RNA was performed using the SuperScript II® protocol (Invitrogen). PCR primers included ACVR2 (For 5′-GCGTTTGCCGTCTTTCTTAT-3′; Rev 5′-CAGCCAACAACCTTGTTTCA-3′), TGFβR2 (For 5′-CACCGCACGTTCAGA-AGTC-3′; Rev 5′-GAGGCT GATGCCTGTCACTT-3′), Androgen Receptor (For 5′-GTGGATGGGCTGAAAAATC-3′; Rev 5′-ACTTGCA CAGAGATGATCT-3′) and β-actin (For: 5′-CCTCGCCT TTGCC-GATCC-3′; Rev: 5′-GGATCTTCATGAGGTAG TC-3′).

2.3. Plasmids

Wild-type and truncated ACVR2 sequences were generated by RT-PCR using RNA isolated from PC3 and 22Rv-1 cells, respectively. PCR products were cloned into the pCDNA3.1 vector (Invitrogen) at the HindIII-XbaI site, and verified by sequence analysis. pGL2-pARE3-Lux was provided by J. Massague and pCS2-Fast1-Myc was a gift from M. Whitman.

2.4. Luciferase assay

A protocol similar to that described by Kumar et al., was used to assay for activin response in 22Rv1 cells [21]. Cells were plated in 24 well plates at approximately 60% confluency 16 hours prior to transfection. Plasmid cocktails consisting of 150 ng each of pGL2-pARE3-Lux, CS2-Fast1-Myc, and TR-ACVR2 or FL-ACVR2 combined with 50 ng of pEGFP-C3 (BD Biosciences, Franklin Lakes, NJ), 2 μL of Lipofectamine™ (Invitrogen), and 25 μL of DMEM in a total volume of 35 μL. This mixture was kept at room temperature for 30 minutes, before adding 1.5 μL of Lipofectamine™ and 25 μL of DMEM. This final mixture was incubated an additional 15 minutes at room temperature while the cells were washed twice with 1× PBS before adding 150 μL of DMEM without antibiotics or FBS to each well. Transfection mixtures were added directly to the wells containing DMEM alone, and the cells were incubated at standard conditions for 4 hours. One hundred microliters of DMEM with 10% FBS was added to each well, and the cells were incubated for approximately 14 hours. Cells were monitored for transfection efficiency by counting fluorescent cells expressing green florescent protein (GFP) before the contents of each well was removed and replaced with 250 μL of DMEM with 10% FBS. Cells were incubated for 36 hours, and contents of the wells were supplemented with 100 μL of DMEM with 0.1% bovine serum albumin and 25 ng/mL activin A (R&D systems, Minneapolis, MN). Cells were incubated an additional 18 hours before 100 μL of Steady-Glo® (Promega, Madison, WI) was added to each well. Contents of the wells were transferred to a 96-well plate after a 10-minute room temperature incubation, and the plate was scanned using a luminometer with Steady-Glo® analysis software (Promega). All

transfections were done in triplicate, and the results were validated in 2 independent experiments.

3. Results

3.1. Mutation analysis of ACVR2

Mutation analysis was performed using genomic DNA from six prostate cancer cell lines. Based on a previous study of mutations in the *ACVR2* gene in colon and pancreatic cancer cells [14], we analyzed exons 3, 10, and 11. LAPC-4 and 22Rv1 cells contained homozygous deletions of a single adenine in the $(A)_8$ tract of exon 10, and heterozygous deletions of a single adenine were observed in the same region of exon 10 in DU145 and LNCaP cells (Fig. 1). PC3 and H660 cells did not have mutations in exon 10. No mutations were found in either exon 3 or exon 11 in any of cell lines tested (data not shown). Exon 11 was included in our analysis based on the report of a frameshift deletion in this exon in PX280 pancreatic cancer cells [14].

3.2. Mutation analysis of TGFβR2

Mutations in the $(A)_{10}$ tract of exon 3 of the *TGFβR2* gene has been demonstrated in 12% of prostate tumors with microsatellite instability (MSI) [22]. As shown in Fig. 2, 22Rv1 carries a homozygous deletion of an adenine in exon 3, and LAPC-4 cells show a heterozygous loss of one adenine in the $(A)_{10}$ tract. PC3, DU145, H660, and LNCaP were not mutated in this microsatellite region.

3.3. ACVR2 gene and protein organization

The GenAtlas database (http://www.dsi.univ-paris5.fr/genatlas/) was used to identify the intron/exon boundaries for *ACVR2* (Fig. 3A). The *ACVR2* gene is comprised of 11 exons, with 2 coding microsatellite regions in exons 3 and 10. The Pfam (http://www.sanger.ac.uk/Software/Pfam/) domain composition of the ACVR2 protein consists of a signal peptide followed by an activin receptor domain, a transmembrane domain, and a protein (serine/threonine) kinase domain. Deletion of a single "A" in the $(A)_8$ tract of exon 10 results in a frameshift with subsequent premature termination of the reading frame at amino acid 440 (Fig. 3C). Although frameshift mutations that occur prior to the last exon of a gene often result in the degradation of gene products through the process of nonsense-mediated decay [23,24], the frameshift mutations in exon 10 of the *ACVR2* gene somehow escape degradation [14]. It was our hypothesis that this truncation of the ACVR2 protein leads to diminished activin signaling due to partial loss of the protein kinase domain (see below).

3.4. Gene expression analysis

RT-PCR analysis was performed using gene specific primers for *ACVR2*, *TGFβR2*, androgen receptor (AR), and β-actin (Fig. 4). The *ACVR2* gene was expressed in all of the prostate cells that we tested, and this is consistent with reports in colon and pancreas samples with *ACVR2* mutations [14,16]. In contrast to ACVR2, however,
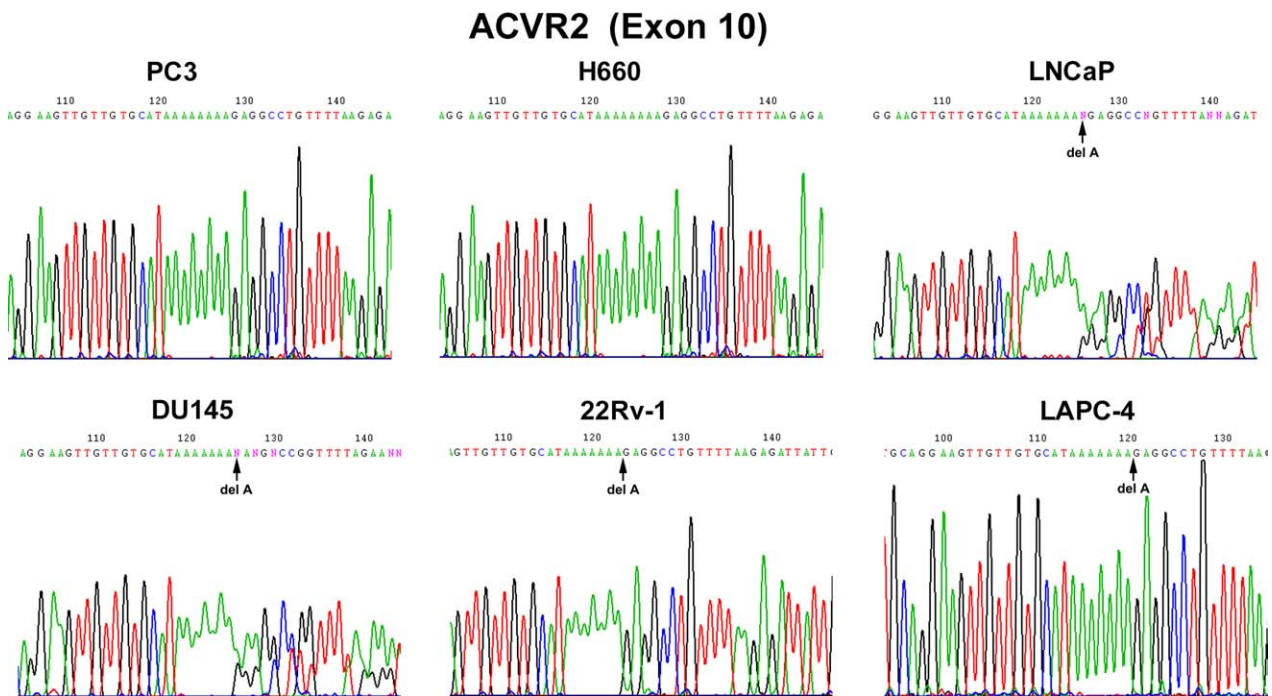

Fig. 1. *ACVR2* mutation analysis. Mutation analysis of exon 10 $(A)_8$ of *ACVR2* from genomic DNA of 6 prostate cancer cell lines revealed homozygous frameshift mutations resulting from the deletion of a single "A" in the $(A)_8$ tract of exon 10 in LAPC-4 and 22Rv-1 cells. Heterozygous deletion of one "A" was also seen in DU145 and LNCaP cells. PC3 and H660 cells were not mutated.
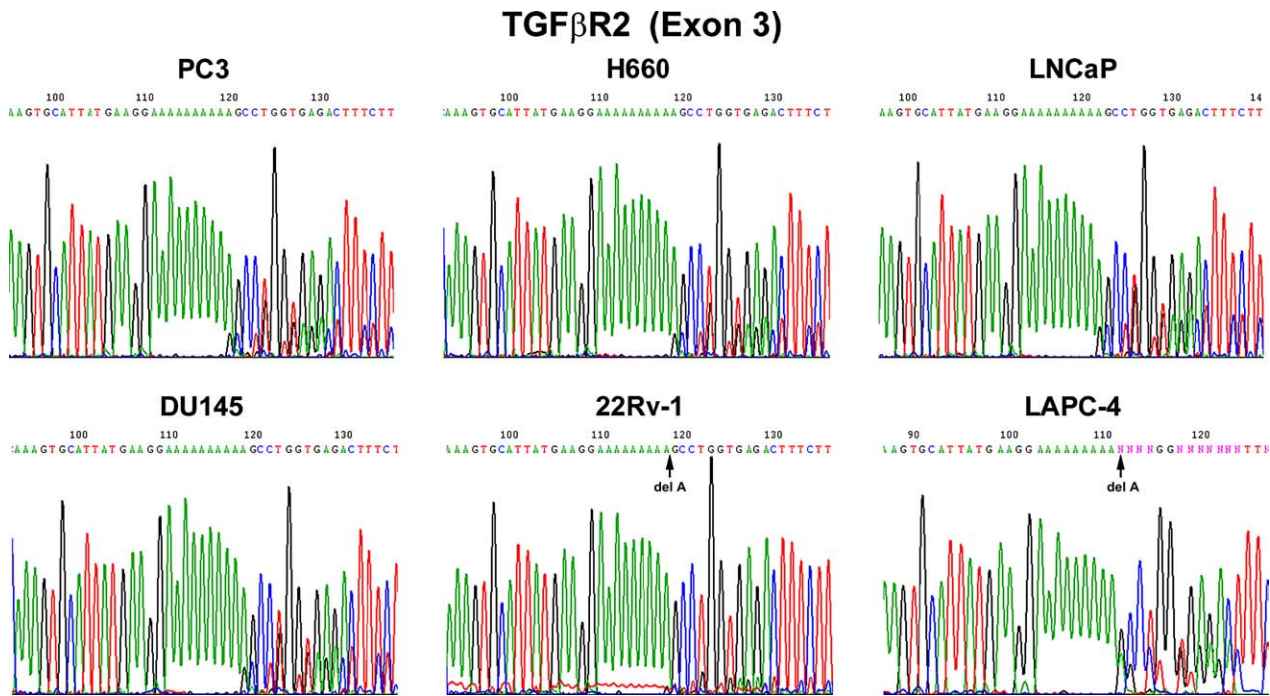
TGFβR2 (Exon 3)

Fig. 2. *TGFβR2* mutation analysis. Genomic DNA from six prostate cancer cell lines were analyzed for mutations in exon 3 (A)$_{10}$ of the *TGFβR2* gene. Homozygous deletion of a single "A" was detected in 22Rv-1 cells, and a hemizygous frameshift mutation was identified in LAPC-4 cells. PC3, H660, DU145, and LNCaP cells did not have mutations in exon 3 of the *TGFβR2* gene.

TGFβR2 and the AR were differentially expressed in the cell lines we tested. TGFβR2 was strongly expressed in PC3 and DU145 cells, moderately expressed in H660 cells, and weakly expressed in LAPC4 cells. In PC3 and DU145 cells, 2 bands were present in the PCR product. The lower band is a 443 bp product expected from the *TGFβR2* gene whereas the upper band represents the 518 bp expected from the *TGFβR2B* gene. NCI-H660 cells showed only a single lower band, and the shadowy upper band suggests that TGFβR2B expression is reduced relative to TGFβR2 in theses cells. A faint band was seen in LAPC-4 cells, which we assumed is a consequence of the heterozygous mutation of *TGFβR2*. TGFβR2 was not expressed in either 22Rv1 or LNCaP cells which is consistent with previous reports [25,26]. Although the mechanism of inactivation in LNCaP cells has yet to be determined, to the best of our knowledge, this is the first report of the *TGFβR2* mutation in 22Rv1 cells.

Finally, we included the *AR* gene in our study because over-expression of the *AR* gene has been correlated with
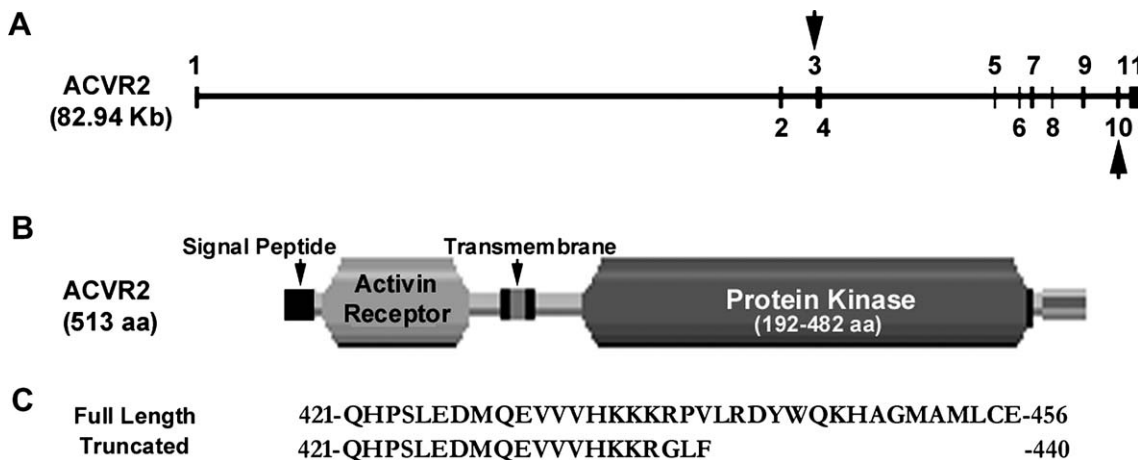

Fig. 3. *ACVR2* and the functional consequence of *ACVR2* frameshift mutations. *(A)* The GenAtlas depiction of the *ACVR2* intron/exon organization. The *ACVR2* gene consists of 11 coding exons, 2 of which contain coding microsatellites (arrows). Exons 3 and 10, each contain (A)$_8$ tracts that encode part of the activin receptor and protein kinase domains, respectively. *(B)* The Pfam representation of the functional domains of the 513 amino acid ACVR2 protein. *(C)* The deletion of a single "A" in exon 10 (A)$_8$ alters the reading frame to produce a truncated 440 amino acid protein.
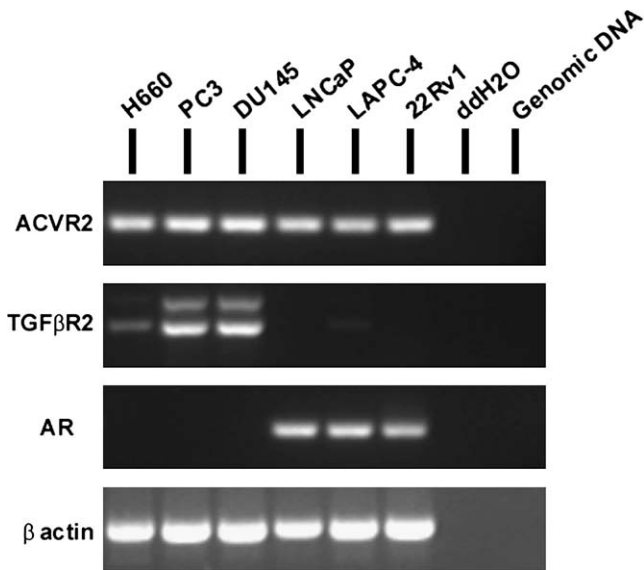
Fig. 4. Gene expression analysis of prostate cancer cell lines. RT-PCR analysis demonstrates the expression of *ACVR2*, *TGFβR2*, and the *AR* genes relative to β-actin in prostate cancer cells. *AVCR2* gene expression was identified in all the cell lines tested, but *TGFβR2* and *AR* were differentially expressed (see text).

androgen ablation resistant prostate cancers and generally poor prognosis [27]. The AR status of these 6 prostate cell lines is in keeping with previous reports [28], and our data suggests that there is a reciprocal expression pattern of the *TGFβR2* and the *AR* genes.

3.5. *Truncated* ACVR2 *has attenuated activin mediated signaling*

To investigate the functional significance of the truncated (TR) variant of the ACVR2 in prostate cancer, we used a luciferase reporter assay to measure the response to activin in cells where ACVR2 was re-introduced. Liu et al. [29] had previously demonstrated that activin-initiated cell signaling in the R-1B/L17 lung epithelial cell line occurred only in the presence of both the activin-response element (ARE) and the activin signal transducer, FAST1. Consequently, 22Rv1 cells were co-transfected with an ARE construct (pGL2-ARE3-Lux) and either truncated or wild-type ACVR2 expression vectors in pCDNA3.1. As shown in Fig. 5, in the presence of activin and FAST1, 22Rv1 cells expressing an exogenous wild-type ACVR2 had a 2.8 fold increase in the level of ARE expression compared to those expressing the truncated form, TR-ACVR2. This was a significant increase according to a two-tailed Student t-test ($P < 0.022$).

4. Discussion

In this study, we have demonstrated that *ACVR2* mutations were present in 4 of the 6 prostate cancer cell lines

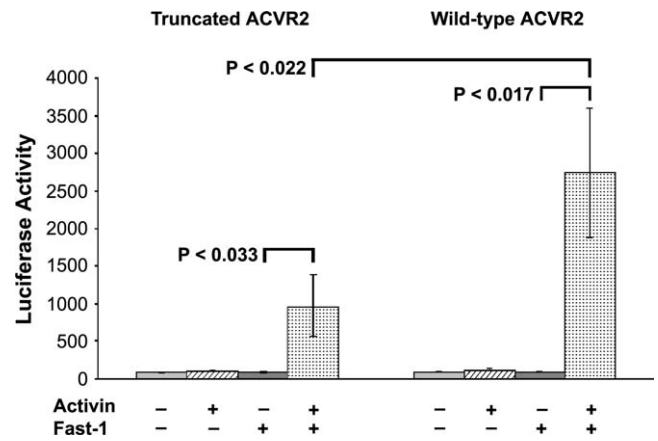
Fig. 5. Effect of truncated ACVR2 on activin mediated cell signaling. 22Rv-1 cells were transiently transfected with truncated or wild-type ACVR2 and an activin receptor luciferase construct (ARE3-Lux) with or without FAST1. As shown, 22Rv-1 cells responded to activin only in the presence of FAST1. A 9-fold increase ($P < 0.033$) in luciferase activity was seen in cells that expressed both FAST1 and truncated *ACVR2* in the presence of exogenous activin compared with untreated cells. For cells that expressed both the wild type ACVR2 and FAST1, there was a 26 fold ($P < 0.017$) increase in transcriptional response to activin in cells treated with activin as compared to the baseline. There was a 2.8 fold ($P < 0.022$) difference in the response to activin in 22Rv-1 cells transfected with full-length as compared to truncated ACVR2.

that we examined. Moreover, we have shown that truncating mutations in the *ACVR2* gene in prostate cancer cell lines significantly reduces the cellular response to activin. Previous reports of truncating *ACVR2* mutations in cancer cells did not address the biological consequence of these mutations in terms of activin response [14,16,18], and our findings suggest that activin response may also be diminished in those colon and pancreatic cells with similar truncating mutations in the *ACVR2* gene. These findings also raise important questions about the selective advantage for cells that have diminished but not complete loss of *ACVR2* function.

Complete inactivation of *ACVR2* is not developmentally lethal, but knockout mice have been reported to be sterile [30], as well as having pancreatic anomalies [31]. Although not reported, adult *ACVR2* null mice have a higher incidence of tumors of the ovaries, kidneys, skin, and occasionally the liver compared to *ACVR2* wild-type mice (personal communication from Itaru Kojima).

In other models, truncations of *ACVR2* involving loss of the protein kinase domain are believed to have a dominant negative effect on activin signaling [32], and the biological consequences can include inhibited cellular differentiation and reduced cell proliferation [33]. In terms of human cancers, however, the ramifications of *ACVR2* mutations must be viewed in the context of the synergistic effects of aberrant gene expression and altered signaling pathways.

Human prostate carcinoma cell lines can be classified by several pertinent characteristics relevant to prostatic tumors. These parameters include *AR* and *TP53* status,

MSI, and PSA expression [28]. There is no immediately apparent correlation between any of these factors in the cell lines that we tested, but the expression data presented here suggests that prostate cancer cells that expressed TGFβR2 do not express the AR. Also, 3 of the 4 cell lines that showed mutations in *ACVR2* did not express the *TGFβR2* gene, but did express the AR. These findings suggest that the diminished ACVR2 signaling capacity, in the context of TGFβR2 and AR expression status, may contribute to enhance the proliferative capacity of prostate cells.

Activin is a growth modulator [34,35], and at least in the case of gastrointestinal cancers, it appears that truncating mutations in *ACVR2* are often accompanied by inactivating mutations in *TGFβR2*. In fact, *TGFβR2* mutations appear to be more frequent than *ACVR2* mutations in gastrointestinal cancers [14]. In prostate, dominant negative *TGFβR2* mutants have been associated with both abnormal prostatic morphology and tumor metastasis [36,37], and our data suggests that *ACVR2* mutations may occur twice as frequently as *TGFβR2* mutations in prostate cancer cells. Clearly, loss of function in either one or both of these type II receptors may have a deleterious effect on growth regulatory mechanisms.

As mentioned previously, AR expression has been correlated with prostate tumors with poor clinical outcomes. Treatment of LNCaP cells with activin has been shown to enhance the expression of the AR [38], and most androgen-independent or hormone refractory prostate cancers express the AR [39]. Overexpression of the AR can be mediated via its interaction with SMAD3, a downstream target of TGFβ signaling [40,41]. Moreover, the interaction between SMAD3 and the AR can be disrupted by SMAD4 [42] and, although a role for SMAD4 has yet to be elucidated in prostate cancer, it is frequently lost in colon cancer [43]. Our data demonstrates that FAST1, which is involved in a ternary complex with SMAD2 and SMAD4 [29], is necessary for activin signaling in 22Rv1 cells, implying that additional members of the *ACVR2* pathway are likely mutated or lost in prostate cancer.

TGFβR2 mutations have been reported in prostate tumors [22], and one of the caveats of this work is that mutations in *TGFβR2* and *ACVR2*, which have coding microsatellites, are a consequence of MSI. It has been proposed, however, that *ACVR2* mutations in colon cancer cell lines may not be a consequence of the MSI phenotype because *ACVR2* and *TGFβR2* mutations are also present in non-MSI carcinomas [14]. MSI, however, occurs in approximately 50% of all prostatic tumors [22,28] which, together with our data, strongly suggests a role for compromised *ACVR2* function in the development of prostate cancer.

Acknowledgments

References

[1] Shi Y, Massague J. Mechanisms of TGF-beta signaling from cell membrane to the nucleus. Cell 2003;113:685–700.

[2] Mathews LS, Vale WW. Expression cloning of an activin receptor, a predicted transmembrane serine kinase. Cell 1991;65:973–82.

[3] Massague J. TGF-beta signal transduction. Ann Rev Biochem 1998;67: 753–91.

[4] Attisano L, Wrana JL, Montalvo E, Massague J. Activation of signaling by the activin receptor complex. Mol Cell Bio 1996;16:1066–73.

[5] Lebrun JJ, Vale WW. Activin and inhibin have antagonistic effects on ligand-dependent heteromerization of the type I and type II activin receptors and human erythroid differentiation. Mol Cell Biol 1997;17: 1682–91.

[6] Harrison CA, Gray PC, Fischer WH, Donaldson C, Choe S, Vale W. An activin mutant with disrupted ALK4 binding blocks signaling via type II receptors. J Biol Chem 2004;279:28036–44.

[7] Massague J, Blain SW, Lo RS. TGFbeta signaling in growth control, cancer, and heritable disorders. Cell 2000;103:295–309.

[8] Lagna G, Hata A, Hemmati-Brivanlou A, Massague J. Partnership between DPC4 and SMAD proteins in TGF-beta signaling pathways. Nature 1996;383:832–6.

[9] Derynck R, Zhang Y, Feng XH. Smads: transcriptional activators of TGF-beta responses. Cell 1998;95:737–40.

[10] Massague J, Wotton D. Transcriptional control by the TGF-beta/-Smad signaling system. EMBO J 2000;19:1745–54.

[11] Tatusova TA, Madden TL. BLAST 2 Sequences, a new tool for comparing protein and nucleotide sequences. FEMS Microbiol Lett 1999;174:247–50.

[12] Ionov Y, Peinado MA, Malkhosyan S, Shibata D, Perucho M. Ubiquitous somatic mutations in simple repeated sequences reveal a new mechanism for colonic carcinogenesis. Nature 1993;363:558–61.

[13] Markowitz S, Wang J, Myeroff L, Parsons R, Sun L, Lutterbaugh J, Fan RS, Zborowska E, Kinzler KW, Vogelstein B. Inactivation of the type II TGF-beta receptor in colon cancer cells with microsatellite instability. Science 1995;268:1336–8.

[14] Hempen PM, Zhang L, Bansal RK, Iacobuzio-Donahue CA, Murphy KM, Maitra A, Vogelstein B, Whitehead RH, Markowitz SD, Willson JK, Yeo CJ, Hruban RH, Kern SE. Evidence of selection for clones having genetic inactivation of the activin A type II receptor (ACVR2) gene in gastrointestinal cancers. Cancer Res 2003;63:994–9.

[15] Olaru A, Mori Y, Yin J, Wang S, Kimos MC, Perry K, Xu Y, Sato F, Selaru FM, Deacu E, Sterian A, Shibata D, Abraham JM, Meltzer SJ. Loss of heterozygosity and mutational analyses of the ACTRII gene locus in human colorectal tumors. Lab Invest 2003;83:1867–71.

[16] Jung B, Doctolero RT, Tajima A, Nguyen AK, Keku T, Sandler RS, Carethers JM. Loss of activin receptor type 2 protein expression in microsatellite unstable colon cancers. Gastroenterology 2004;126: 654–9.

[17] Venkatasubbarao K, Ahmed MM, Swiderski C, Harp C, Lee EY, McGrath P, Mohiuddin M, Strodel W, Freeman JW. Novel mutations in the polyadenine tract of the transforming growth factor beta type II receptor gene are found in a subpopulation of human pancreatic adenocarcinomas. Genes Chromosomes Cancer 1998;22:138–44.

[18] D'Abronzo FH, Swearingen B, Klibanski A, Alexander JM. Mutational analysis of activin/transforming growth factor-beta type I and type II receptor kinases in human pituitary tumors. J. Clin. Endocrinol Metab 1999;84:1716–21.

[19] Jeruss JS, Sturgis CD, Rademaker AW, Woodruff TK. Down-regulation of activin, activin receptors, and smads in high-grade breast cancer. Cancer Res 2003;63:3783–90.

[20] Sambrook J, Fritsch EF, Maniatis T. Molecular Cloning: A Laboratory Manual. 2nd ed. New York, NY: Cold Spring Harbor Laboratory Press, 1989.

[21] Kumar A, Novoselov V, Celeste AJ, Wolfman NM, ten Dijke P, Kuehn MR. Nodal signaling uses activin and transforming growth factor-beta receptor-regulated Smads. J Biol Chem 2001;276:656–61.

[22] Bhattacharyya N, Tao J, Klein EA, Banerjee S. Alterations of transforming growth factor beta receptor II, insulin growth factor receptor II genes in microsatellite unstable prostate carcinomas. Oncol Rep 2004;11:231–6.

[23] Maquat LE. Nonsense-mediated mRNA decay: splicing, translation and mRNP dynamics. Nat. Rev. Mol. Cell Biol 2004;5:89–99.

[24] Ionov Y, Matsui S, Cowell JK. A role for p300/CREB binding protein genes in promoting cancer progression in colon cancer cell lines with microsatellite instability. Proc Natl Acad Sci USA 2004;101:1273–8.

[25] Sramkoski RM, Pretlow TG 2nd, Giaconia JM, Pretlow TP, Schwartz S, Sy MS, Marengo SR, Rhim JS, Zhang D, Jacobberger JW. A new human prostate carcinoma cell line, 22Rv1. In Vitro Cell Dev Biol Anim 1999;35:403–9.

[26] Guo Y, Kyprianou N. Overexpression of transforming growth factor (TGF) beta1 type II receptor restores TGF-beta1 sensitivity and signaling in human prostate cancer cells. Cell Growth Differ 1998;9: 185–93.

[27] Gerald WL. Genome-wide gene expression analysis of prostate carcinoma. Semin Oncol 2003;30:635–48.

[28] van Bokhoven A, Varella-Garcia M, Korch C, Johannes WU, Smith EE, Miller HL, Nordeen SK, Miller GJ, Lucia MS. Molecular characterization of human prostate carcinoma cell lines. Prostate 2003;57:205–25.

[29] Liu F, Pouponnot C, Massague J. Dual role of the Smad4/DPC4 tumor suppressor in TGFbeta-inducible transcriptional complexes. Genes Dev 1997;11:3157–67.

[30] Matzuk MM, Kumar TR, Bradley A. Different phenotypes for mice deficient in either activins or activin receptor type II. Nature 1995;374:356–60.

[31] Shiozaki S, Tajima T, Zhang YQ, Furukawa M, Nakazato Y, Kojima I. Impaired differentiation of endocrine and exocrine cells of the pancreas in transgenic mouse expressing the truncated type II activin receptor. Biochim Biophys Acta 1999;1450:1–11.

[32] Liu F, Shao LE, Yu J. Truncated activin type II receptor inhibits erythroid differentiation in K562 cells. J Cell Biochem 2000;78:24–33.

[33] Maeshima A, Shiozaki S, Tajima T, Nakazato Y, Naruse T, Kojima I. Number of glomeruli is increased in the kidney of transgenic mice expressing the truncated type II activin receptor. Biochem Biophys Res Commun 2000;268:445–9.

[34] Sehy DW, Shao LE, Yu AL, Tsai WM, Yu J. Activin A-induced differentiation in K562 cells is associated with a transient hypophosphorylation of RB protein and the concomitant block of cell cycle at G1 phase. J Cell Biochem 1992;50:255–65.

[35] Spencer SJ, Rabinovici J, Jaffe RB. Human recombinant activin-A inhibits proliferation of human fetal adrenal cells in vitro. J Clin Endocrinol Metab 1990;71:1678–80.

[36] Kundu SD, Kim IY, Yang T, Doglio L, Lang S, Zhang X, Buttyan R, Kim SJ, Chang J, Cai X, Wang Z, Lee C. Absence of proximal duct apoptosis in the ventral prostate of transgenic mice carrying the C3(1)-TGF-beta type II dominant negative receptor. Prostate 2000;43: 118–124.

[37] Tu WH, Thomas TZ, Masumori N, Bhowmick NA, Gorska AE, Shyr Y, Kasper S, Case T, Roberts RL, Shappell SB, Moses HL, Matusik RJ. The loss of TGF-beta signaling promotes prostate cancer metastasis. Neoplasia 2003;5:267–77.

[38] Zhang Z, Zhao Y, Batres Y, Lin MF, Ying SY. Regulation of growth and prostatic marker expression by activin A in an androgen-sensitive prostate cancer cell line LNCAP. Biochem. Biophys. Res Commun 1997;234:362–65.

[39] Heinlein CA, Chang C. Androgen receptor in prostate cancer. Endocr Rev 2004;25:276–308.

[40] Hayes SA, Zarnegar M, Sharma M, Yang F, Peehl DM, ten Dijke P, Sun Z. Smad 3 represses androgen receptor-mediated transcription. Cancer Res 2001;61:2112–8.

[41] Kang HY, Lin HK, Hu YC, Yeh S, Huang KE, Chang C. From transforming growth factor ß signaling to androgen action: identification of Smad 3 as an androgen receptor coregulator in prostate cancer cells. Proc Natl Acad Sci USA 2001;98:3018–23.

[42] Kang HY, Huang KE, Chang SY, Ma WL, Lin WJ, Chang C. Differential modulation of androgen receptor-mediated transactivation by Smad3 and tumor suppressor Smad4. J Biol Chem 2002;277:43749–56.

[43] Salovaara R, Roth S, Loukola A, Launonen V, Sistonen P, Avizienyte E, Kristo P, Jarvinen H, Souchelnytskyi S, Sarlomo-Rikala M, Aaltonen LA. Frequent loss of SMAD4/DPC4 protein in colorectal cancers. Gut 2002;51:56–9.

Truncating mutations in the ACVR2 gene attenuates activin signaling in prostate cancer cells

Michael R. Rossi, Yurij Ionov, Andrei V. Bakin, John K. Cowell*

Department of Cancer Genetics, Roswell Park Cancer Institute, Elm and Carlton Streets, Buffalo, NY 14263

Received 4 March 2005; accepted 9 May 2005

Abstract
Activins are classified as members of the TGFβ superfamily of signaling molecules and both activin and TGFβ ligands signal through structurally and functionally related serine/threonine kinase receptors. Defects in these signaling pathways have been associated with the initiation and progression of the cancer phenotype. Inactivating mutations in the TGFβ type II receptor gene, *TGFβR2*, have been identified in a variety of tumors and cell lines, particularly those with microsatellite instability (MSI). More recently, mutations in the activin type II receptor gene, *ACVR2*, were identified in colon and pancreatic cell lines and tumors with MSI. Because prostate tumors appear to have a high incidence of MSI, we analyzed prostate cancer cell lines, with and without MSI, for *ACVR2* and *TGFβR2* mutations. Our analysis of 6 prostate cell lines revealed mutations in the *ACVR2* gene in 22Rv-1, LAPC-4, DU145, and LNCaP cells and mutations in the *TGFβR2* gene in 22Rv-1 and LAPC-4. PC3 and H660 cells were wild-type for *ACVR2* and *TFGβR2*. All of the *ACVR2* mutations were truncating mutations, and using an activin response assay, we demonstrate that truncating mutations of the ACVR2 gene result in a significant reduction in activin mediated cell signaling. Inactivation of *ACVR2* is a common event in prostate cancer cells suggesting it may play an important role in the development of prostate cancer. © 2005 Elsevier Inc. All rights reserved.

1. Introduction

The transforming growth factor β (TGFβ) superfamily of cytokines control various biological and physiological processes [1]. Most of the TGFβ families of ligands signal through receptor serine/threonine kinases that are divided into type I and type II receptors [2,3]. TGFβ and activin proteins specifically bind to their respective type II receptors, which in turn lead to recruitment and activation of type I receptors [4,5]. Activin and TGFβ receptors differ functionally in the fact that the activin type II receptors can bind other ligands, such as myostatin, BMP2, BMP7, and nodal, in addition to activin, whereas TGFβ signals only through its own type II receptors [6].

The parallel signaling pathways of activin and TGFβ are well characterized in a number of cell types [1], and aberrant TGFβ and activin signaling has been identified in numerous cancers [7]. Activins and TGFβ form an active complex with their type I and type II receptors, and the type I receptors phosphorylate Smad proteins (SMADs) which

regulate gene transcription. In response to activin, SMADs activate transcription through a ternary complex consisting of SMAD2, SMAD4, and FAST-1, which bind to an activin-response element (ARE) in gene promoter regions [3]. SMADs also activate transcription in response to TGFβ, but this response is mediated by SMAD2/3/4 [8]. Because the activin type II receptor (ACVR2) and the TGFβ type II receptor (TGFβR2) are at the interface of ligand initiated signaling, loss or mutation of either or both of these genes can have far-reaching effects in terms of gene expression [9,10].

ACVR2 shares 37% homology with *TGFβR2* at the amino acid level [11] and has two polyadenine regions within its open reading frame, whereas *TGFβR2* has only one polyadenine tract within its coding region. These microsatellite regions consist of 10 adenines $[(A)_{10}]$ in exon 3 of *TGFβR2* and eight adenines $[(A)_8]$ in exons 3 and 10 of *ACVR2*. Mononucleotide stretches can be hotspots for frameshift mutations, particularly in cells with diminished or deficient mismatch repair [12,13]. A single frameshift mutation in either the $(A)_{10}$ region of *TGFβR2* or the $(A)_8$ region in exon 3 of *ACVR2* would lead to functional gene inactivation through nonsense mediated decay of the

---

* Corresponding author. Tel.: (716) 845-5714; fax: (716) 845-1698.
E-mail address: John.Cowell@RoswellPark.org (J.K. Cowell).

mutant mRNA. Frameshift mutations in the $(A)_8$ tract in exon 10 of *ACVR2*, however, effectively results in a truncated version of the *ACVR2* protein [14–16].

TGFβR2 mutations were first identified in pancreatic tumors and have since been identified in a variety of other tumor types [17]. *ACVR2* mutations, however, are not as well characterized in cancer. Mutations in *ACVR2* were first reported in pituitary tumors, exclusively as frameshift mutations in the $(A)_8$ tract of exon 10 [18]. More recently, colon and pancreatic cell lines were demonstrated to have predominantly similar frameshift mutations in exon 10 of the ACVR2 gene [14]. This data was supported by additional studies in microsatellite unstable colon tumors which showed loss of *ACVR2* expression as determined by immunohistochemistry using an antibody that targeted an epitope that was present in the wild-type but not the truncated ACVR2 protein [16]. In breast cancer, ACVR2 expression was diminished or absent in high grade tumors, but this study did not entail mutation analysis [19].

Because *TGFβR2* mutations often coincide with *ACVR2* mutations in colon cells [14], we analyzed the *ACVR2* and *TGFβR2* genes in prostate cancer cell lines. In this report, we identify mutations in both the *TGFβR2* and *ACVR2* genes in prostate cancer cells, and demonstrate that truncating *ACVR2* mutations result in their diminished transcriptional response to activin.

2. Materials and methods

2.1. DNA extraction and sequencing

Prostate cancer cell lines were grown at 37°C with 10% CO_2 in DMEM supplemented with 5% FBS and antibiotics, with the exception of LAPC-4 cells, which were grown in RPMI 1640 supplemented with 15% FBS and antibiotics. DNA was extracted from prostate cancer cell lines using a standard phenol-chloroform extraction protocol [20]. PCR was performed according to the Phusion™ high-fidelity DNA polymerase protocol (Finnzymes OY, Espoo, Finland). using 100 ng of genomic DNA and exon specific primers for ACVR2 (Ex3F 5′-AAAAACACTTGTTGTA GG-GTCAG-3′, Ex3R 5′-TGTTTCCAATCTACAGTT-G AGCA-3′; Ex10F 5′-CCAGTTTGAAAGTCAGGAGGA-3′, Ex10R 5′-TGGAAT-TTCAAATGAAAAGCTAAC-3′; Ex11F 5′-CTGCTGTGGCGTTTGAGTAT-3′, Ex11R 5′-TCCCAGAGCAACATTTTTCA-3′), and TGFβR2 (Ex3F 5′-CCTCGCTTCCAATGA-ATCTC-3′, Ex3R 5′-TCCCACACCCT-TAAGAGAAGAA-3′). The PCR products were gel purified and sequenced using the Applied Biosystems' PRISM 3100 Genetic Analyzer (Foster City, CA).

2.2. Gene expression analysis of prostate cancer cell lines

Total RNA was isolated from prostate cancer cell lines using TRIzol® reagent (Invitrogen, Carlsbad, CA). Reverse transcription of 2 μg of total RNA was performed using the SuperScript II® protocol (Invitrogen). PCR primers included ACVR2 (For 5′-GCGTTTGCCGTCTTTCTTAT-3′; Rev 5′-CAGCCAACAACCTTGTTTCA-3′), TGFβR2 (For 5′-CACCGCACGTTCAGA-AGTC-3′; Rev 5′- GAGGCT GATGCCTGTCACTT-3′), Androgen Receptor (For 5′- GTGGATGGGCTGAAAAATC-3′; Rev 5′- ACTTGCA CAGAGATGATCT-3′) and β-actin (For: 5′-CCTCGCCT TTGCC-GATCC-3′; Rev: 5′-GGATCTTCATGAGGTAG TC-3′).

2.3. Plasmids

Wild-type and truncated ACVR2 sequences were generated by RT-PCR using RNA isolated from PC3 and 22Rv-1 cells, respectively. PCR products were cloned into the pCDNA3.1 vector (Invitrogen) at the HindIII-XbaI site, and verified by sequence analysis. pGL2-pARE3-Lux was provided by J. Massague and pCS2-Fast1-Myc was a gift from M. Whitman.

2.4. Luciferase assay

A protocol similar to that described by Kumar et al., was used to assay for activin response in 22Rv1 cells [21]. Cells were plated in 24 well plates at approximately 60% confluency 16 hours prior to transfection. Plasmid cocktails consisting of 150 ng each of pGL2-pARE3-Lux, CS2-Fast1-Myc, and TR-ACVR2 or FL-ACVR2 combined with 50 ng of pEGFP-C3 (BD Biosciences, Franklin Lakes, NJ), 2 μL of Lipofectamine™ (Invitrogen), and 25 μL of DMEM in a total volume of 35 μL. This mixture was kept at room temperature for 30 minutes, before adding 1.5 μL of Lipofectamine™ and 25 μL of DMEM. This final mixture was incubated an additional 15 minutes at room temperature while the cells were washed twice with 1× PBS before adding 150 μL of DMEM without antibiotics or FBS to each well. Transfection mixtures were added directly to the wells containing DMEM alone, and the cells were incubated at standard conditions for 4 hours. One hundred microliters of DMEM with 10% FBS was added to each well, and the cells were incubated for approximately 14 hours. Cells were monitored for transfection efficiency by counting fluorescent cells expressing green florescent protein (GFP) before the contents of each well was removed and replaced with 250 μL of DMEM with 10% FBS. Cells were incubated for 36 hours, and contents of the wells were supplemented with 100 μL of DMEM with 0.1% bovine serum albumin and 25 ng/mL activin A (R&D systems, Minneapolis, MN). Cells were incubated an additional 18 hours before 100 μL of Steady-Glo® (Promega, Madison, WI) was added to each well. Contents of the wells were transferred to a 96-well plate after a 10-minute room temperature incubation, and the plate was scanned using a luminometer with Steady-Glo® analysis software (Promega). All

transfections were done in triplicate, and the results were validated in 2 independent experiments.

3. Results

3.1. Mutation analysis of ACVR2

Mutation analysis was performed using genomic DNA from six prostate cancer cell lines. Based on a previous study of mutations in the *ACVR2* gene in colon and pancreatic cancer cells [14], we analyzed exons 3, 10, and 11. LAPC-4 and 22Rv1 cells contained homozygous deletions of a single adenine in the $(A)_8$ tract of exon 10, and heterozygous deletions of a single adenine were observed in the same region of exon 10 in DU145 and LNCaP cells (Fig. 1). PC3 and H660 cells did not have mutations in exon 10. No mutations were found in either exon 3 or exon 11 in any of cell lines tested (data not shown). Exon 11 was included in our analysis based on the report of a frameshift deletion in this exon in PX280 pancreatic cancer cells [14].

3.2. Mutation analysis of TGFβR2

Mutations in the $(A)_{10}$ tract of exon 3 of the *TGFβR2* gene has been demonstrated in 12% of prostate tumors with microsatellite instability (MSI) [22]. As shown in Fig. 2, 22Rv1 carries a homozygous deletion of an adenine in exon 3, and LAPC-4 cells show a heterozygous loss of one adenine in the $(A)_{10}$ tract. PC3, DU145, H660, and LNCaP were not mutated in this microsatellite region.

3.3. ACVR2 gene and protein organization

The GenAtlas database (http://www.dsi.univ-paris5.fr/genatlas/) was used to identify the intron/exon boundaries for *ACVR2* (Fig. 3A). The *ACVR2* gene is comprised of 11 exons, with 2 coding microsatellite regions in exons 3 and 10. The Pfam (http://www.sanger.ac.uk/Software/Pfam/) domain composition of the ACVR2 protein consists of a signal peptide followed by an activin receptor domain, a transmembrane domain, and a protein (serine/threonine) kinase domain. Deletion of a single "A" in the $(A)_8$ tract of exon 10 results in a frameshift with subsequent premature termination of the reading frame at amino acid 440 (Fig. 3C). Although frameshift mutations that occur prior to the last exon of a gene often result in the degradation of gene products through the process of nonsense-mediated decay [23,24], the frameshift mutations in exon 10 of the *ACVR2* gene somehow escape degradation [14]. It was our hypothesis that this truncation of the ACVR2 protein leads to diminished activin signaling due to partial loss of the protein kinase domain (see below).

3.4. Gene expression analysis

RT-PCR analysis was performed using gene specific primers for *ACVR2*, *TGFβR2*, androgen receptor (AR), and β-actin (Fig. 4). The *ACVR2* gene was expressed in all of the prostate cells that we tested, and this is consistent with reports in colon and pancreas samples with *ACVR2* mutations [14,16]. In contrast to ACVR2, however,
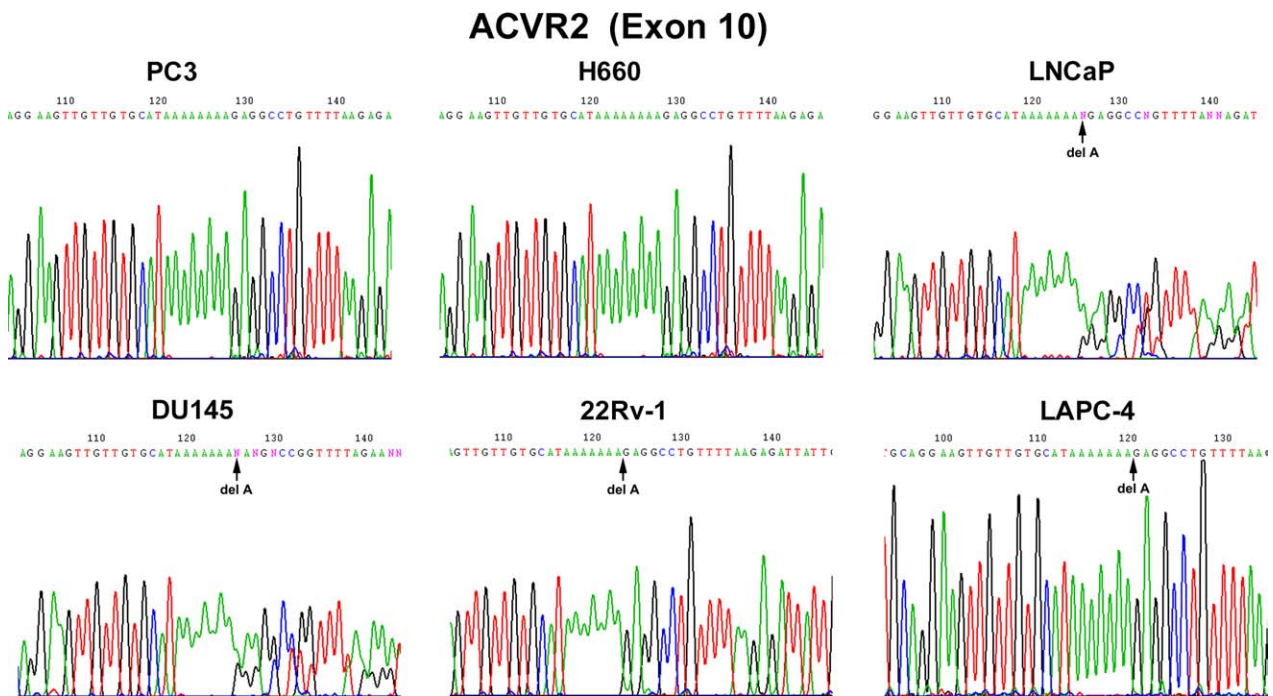

Fig. 1. *ACVR2* mutation analysis. Mutation analysis of exon 10 $(A)_8$ of *ACVR2* from genomic DNA of 6 prostate cancer cell lines revealed homozygous frameshift mutations resulting from the deletion of a single "A" in the $(A)_8$ tract of exon 10 in LAPC-4 and 22Rv-1 cells. Heterozygous deletion of one "A" was also seen in DU145 and LNCaP cells. PC3 and H660 cells were not mutated.
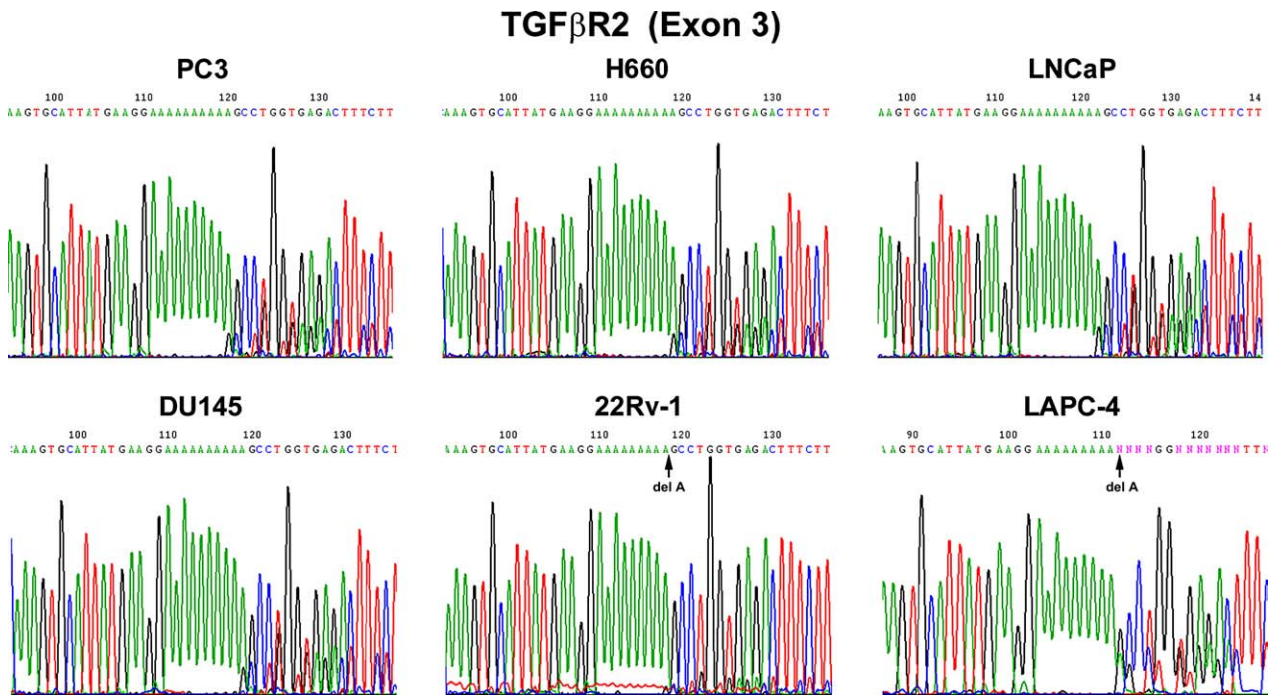
TGFβR2 (Exon 3)

Fig. 2. *TGFβR2* mutation analysis. Genomic DNA from six prostate cancer cell lines were analyzed for mutations in exon 3 (A)$_{10}$ of the *TGFβR2* gene. Homozygous deletion of a single "A" was detected in 22Rv-1 cells, and a hemizygous frameshift mutation was identified in LAPC-4 cells. PC3, H660, DU145, and LNCaP cells did not have mutations in exon 3 of the *TGFβR2* gene.

TGFβR2 and the AR were differentially expressed in the cell lines we tested. TGFβR2 was strongly expressed in PC3 and DU145 cells, moderately expressed in H660 cells, and weakly expressed in LAPC4 cells. In PC3 and DU145 cells, 2 bands were present in the PCR product. The lower band is a 443 bp product expected from the *TGFβR2* gene whereas the upper band represents the 518 bp expected from the *TGFβR2B* gene. NCI-H660 cells showed only a single lower band, and the shadowy upper band suggests that TGFβR2B expression is reduced

relative to TGFβR2 in theses cells. A faint band was seen in LAPC-4 cells, which we assumed is a consequence of the heterozygous mutation of *TGFβR2*. TGFβR2 was not expressed in either 22Rv1 or LNCaP cells which is consistent with previous reports [25,26]. Although the mechanism of inactivation in LNCaP cells has yet to be determined, to the best of our knowledge, this is the first report of the *TGFβR2* mutation in 22Rv1 cells.

Finally, we included the *AR* gene in our study because over-expression of the *AR* gene has been correlated with
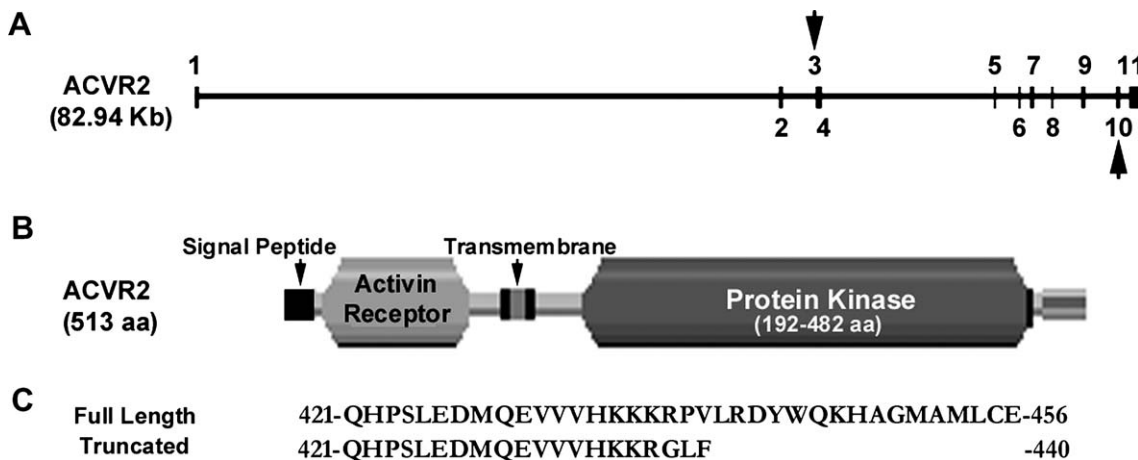

Fig. 3. *ACVR2* and the functional consequence of *ACVR2* frameshift mutations. *(A)* The GenAtlas depiction of the *ACVR2* intron/exon organization. The *ACVR2* gene consists of 11 coding exons, 2 of which contain coding microsatellites (arrows). Exons 3 and 10, each contain (A)$_8$ tracts that encode part of the activin receptor and protein kinase domains, respectively. *(B)* The Pfam representation of the functional domains of the 513 amino acid ACVR2 protein. *(C)* The deletion of a single "A" in exon 10 (A)$_8$ alters the reading frame to produce a truncated 440 amino acid protein.
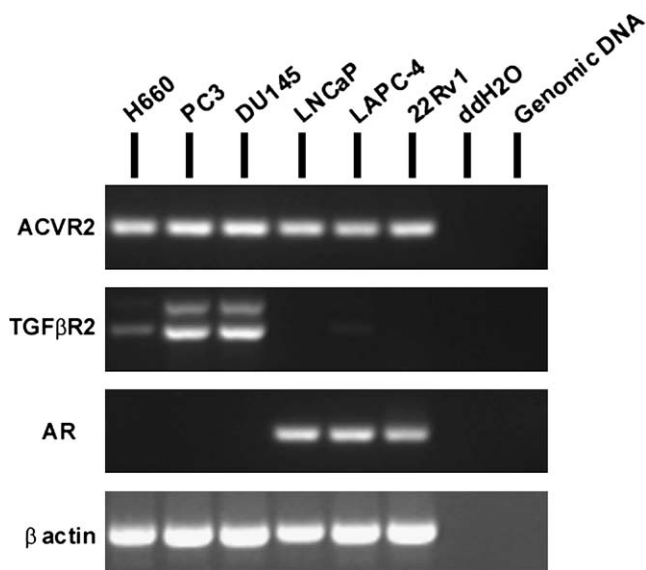
Fig. 4. Gene expression analysis of prostate cancer cell lines. RT-PCR analysis demonstrates the expression of *ACVR2*, *TGFβR2*, and the *AR* genes relative to β-actin in prostate cancer cells. *AVCR2* gene expression was identified in all the cell lines tested, but *TGFβR2* and *AR* were differentially expressed (see text).

androgen ablation resistant prostate cancers and generally poor prognosis [27]. The AR status of these 6 prostate cell lines is in keeping with previous reports [28], and our data suggests that there is a reciprocal expression pattern of the *TGFβR2* and the *AR* genes.

3.5. Truncated ACVR2 has attenuated activin mediated signaling

To investigate the functional significance of the truncated (TR) variant of the ACVR2 in prostate cancer, we used a luciferase reporter assay to measure the response to activin in cells where ACVR2 was re-introduced. Liu et al. [29] had previously demonstrated that activin-initiated cell signaling in the R-1B/L17 lung epithelial cell line occurred only in the presence of both the activin-response element (ARE) and the activin signal transducer, FAST1. Consequently, 22Rv1 cells were co-transfected with an ARE construct (pGL2-ARE3-Lux) and either truncated or wild-type ACVR2 expression vectors in pCDNA3.1. As shown in Fig. 5, in the presence of activin and FAST1, 22Rv1 cells expressing an exogenous wild-type ACVR2 had a 2.8 fold increase in the level of ARE expression compared to those expressing the truncated form, TR-ACVR2. This was a significant increase according to a two-tailed Student t-test ($P < 0.022$).

4. Discussion

In this study, we have demonstrated that *ACVR2* mutations were present in 4 of the 6 prostate cancer cell lines
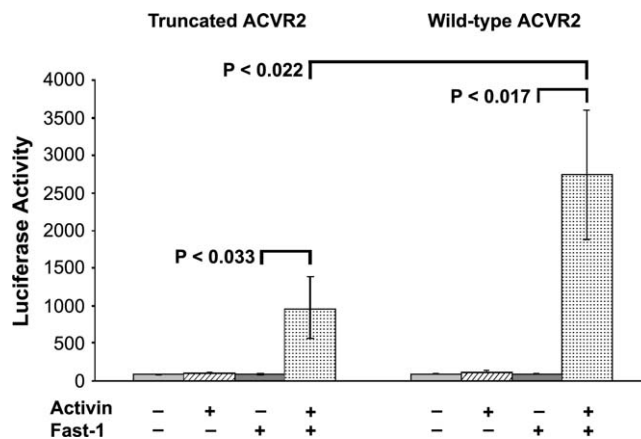

Fig. 5. Effect of truncated ACVR2 on activin mediated cell signaling. 22Rv-1 cells were transiently transfected with truncated or wild-type ACVR2 and an activin receptor luciferase construct (ARE3-Lux) with or without FAST1. As shown, 22Rv-1 cells responded to activin only in the presence of FAST1. A 9-fold increase ($P < 0.033$) in luciferase activity was seen in cells that expressed both FAST1 and truncated *ACVR2* in the presence of exogenous activin compared with untreated cells. For cells that expressed both the wild type ACVR2 and FAST1, there was a 26 fold ($P < 0.017$) increase in transcriptional response to activin in cells treated with activin as compared to the baseline. There was a 2.8 fold ($P < 0.022$) difference in the response to activin in 22Rv-1 cells transfected with full-length as compared to truncated ACVR2.

that we examined. Moreover, we have shown that truncating mutations in the *ACVR2* gene in prostate cancer cell lines significantly reduces the cellular response to activin. Previous reports of truncating *ACVR2* mutations in cancer cells did not address the biological consequence of these mutations in terms of activin response [14,16,18], and our findings suggest that activin response may also be diminished in those colon and pancreatic cells with similar truncating mutations in the *ACVR2* gene. These findings also raise important questions about the selective advantage for cells that have diminished but not complete loss of *ACVR2* function.

Complete inactivation of *ACVR2* is not developmentally lethal, but knockout mice have been reported to be sterile [30], as well as having pancreatic anomalies [31]. Although not reported, adult *ACVR2* null mice have a higher incidence of tumors of the ovaries, kidneys, skin, and occasionally the liver compared to *ACVR2* wild-type mice (personal communication from Itaru Kojima).

In other models, truncations of *ACVR2* involving loss of the protein kinase domain are believed to have a dominant negative effect on activin signaling [32], and the biological consequences can include inhibited cellular differentiation and reduced cell proliferation [33]. In terms of human cancers, however, the ramifications of *ACVR2* mutations must be viewed in the context of the synergistic effects of aberrant gene expression and altered signaling pathways.

Human prostate carcinoma cell lines can be classified by several pertinent characteristics relevant to prostatic tumors. These parameters include *AR* and *TP53* status,

MSI, and PSA expression [28]. There is no immediately apparent correlation between any of these factors in the cell lines that we tested, but the expression data presented here suggests that prostate cancer cells that expressed TGFβR2 do not express the AR. Also, 3 of the 4 cell lines that showed mutations in *ACVR2* did not express the *TGFβR2* gene, but did express the AR. These findings suggest that the diminished ACVR2 signaling capacity, in the context of TGFβR2 and AR expression status, may contribute to enhance the proliferative capacity of prostate cells.

Activin is a growth modulator [34,35], and at least in the case of gastrointestinal cancers, it appears that truncating mutations in *ACVR2* are often accompanied by inactivating mutations in *TGFβR2*. In fact, *TGFβR2* mutations appear to be more frequent than *ACVR2* mutations in gastrointestinal cancers [14]. In prostate, dominant negative *TGFβR2* mutants have been associated with both abnormal prostatic morphology and tumor metastasis [36,37], and our data suggests that *ACVR2* mutations may occur twice as frequently as *TGFβR2* mutations in prostate cancer cells. Clearly, loss of function in either one or both of these type II receptors may have a deleterious effect on growth regulatory mechanisms.

As mentioned previously, AR expression has been correlated with prostate tumors with poor clinical outcomes. Treatment of LNCaP cells with activin has been shown to enhance the expression of the AR [38], and most androgen-independent or hormone refractory prostate cancers express the AR [39]. Overexpression of the AR can be mediated via its interaction with SMAD3, a downstream target of TGFβ signaling [40,41]. Moreover, the interaction between SMAD3 and the AR can be disrupted by SMAD4 [42] and, although a role for SMAD4 has yet to be elucidated in prostate cancer, it is frequently lost in colon cancer [43]. Our data demonstrates that FAST1, which is involved in a ternary complex with SMAD2 and SMAD4 [29], is necessary for activin signaling in 22Rv1 cells, implying that additional members of the *ACVR2* pathway are likely mutated or lost in prostate cancer.

TGFβR2 mutations have been reported in prostate tumors [22], and one of the caveats of this work is that mutations in *TGFβR2* and *ACVR2*, which have coding microsatellites, are a consequence of MSI. It has been proposed, however, that *ACVR2* mutations in colon cancer cell lines may not be a consequence of the MSI phenotype because *ACVR2* and *TGFβR2* mutations are also present in non-MSI carcinomas [14]. MSI, however, occurs in approximately 50% of all prostatic tumors [22,28] which, together with our data, strongly suggests a role for compromised *ACVR2* function in the development of prostate cancer.

Acknowledgments

References

[1] Shi Y, Massague J. Mechanisms of TGF-beta signaling from cell membrane to the nucleus. Cell 2003;113:685–700.

[2] Mathews LS, Vale WW. Expression cloning of an activin receptor, a predicted transmembrane serine kinase. Cell 1991;65:973–82.

[3] Massague J. TGF-beta signal transduction. Ann Rev Biochem 1998;67:753–91.

[4] Attisano L, Wrana JL, Montalvo E, Massague J. Activation of signaling by the activin receptor complex. Mol Cell Bio 1996;16:1066–73.

[5] Lebrun JJ, Vale WW. Activin and inhibin have antagonistic effects on ligand-dependent heteromerization of the type I and type II activin receptors and human erythroid differentiation. Mol Cell Biol 1997;17:1682–91.

[6] Harrison CA, Gray PC, Fischer WH, Donaldson C, Choe S, Vale W. An activin mutant with disrupted ALK4 binding blocks signaling via type II receptors. J Biol Chem 2004;279:28036–44.

[7] Massague J, Blain SW, Lo RS. TGFbeta signaling in growth control, cancer, and heritable disorders. Cell 2000;103:295–309.

[8] Lagna G, Hata A, Hemmati-Brivanlou A, Massague J. Partnership between DPC4 and SMAD proteins in TGF-beta signaling pathways. Nature 1996;383:832–6.

[9] Derynck R, Zhang Y, Feng XH. Smads: transcriptional activators of TGF-beta responses. Cell 1998;95:737–40.

[10] Massague J, Wotton D. Transcriptional control by the TGF-beta/Smad signaling system. EMBO J 2000;19:1745–54.

[11] Tatusova TA, Madden TL. BLAST 2 Sequences, a new tool for comparing protein and nucleotide sequences. FEMS Microbiol Lett 1999;174:247–50.

[12] Ionov Y, Peinado MA, Malkhosyan S, Shibata D, Perucho M. Ubiquitous somatic mutations in simple repeated sequences reveal a new mechanism for colonic carcinogenesis. Nature 1993;363:558–61.

[13] Markowitz S, Wang J, Myeroff L, Parsons R, Sun L, Lutterbaugh J, Fan RS, Zborowska E, Kinzler KW, Vogelstein B. Inactivation of the type II TGF-beta receptor in colon cancer cells with microsatellite instability. Science 1995;268:1336–8.

[14] Hempen PM, Zhang L, Bansal RK, Iacobuzio-Donahue CA, Murphy KM, Maitra A, Vogelstein B, Whitehead RH, Markowitz SD, Willson JK, Yeo CJ, Hruban RH, Kern SE. Evidence of selection for clones having genetic inactivation of the activin A type II receptor (ACVR2) gene in gastrointestinal cancers. Cancer Res 2003;63:994–9.

[15] Olaru A, Mori Y, Yin J, Wang S, Kimos MC, Perry K, Xu Y, Sato F, Selaru FM, Deacu E, Sterian A, Shibata D, Abraham JM, Meltzer SJ. Loss of heterozygosity and mutational analyses of the ACTRII gene locus in human colorectal tumors. Lab Invest 2003;83:1867–71.

[16] Jung B, Doctolero RT, Tajima A, Nguyen AK, Keku T, Sandler RS, Carethers JM. Loss of activin receptor type 2 protein expression in microsatellite unstable colon cancers. Gastroenterology 2004;126:654–9.

[17] Venkatasubbarao K, Ahmed MM, Swiderski C, Harp C, Lee EY, McGrath P, Mohiuddin M, Strodel W, Freeman JW. Novel mutations in the polyadenine tract of the transforming growth factor beta type II receptor gene are found in a subpopulation of human pancreatic adenocarcinomas. Genes Chromosomes Cancer 1998;22:138–44.

[18] D'Abronzo FH, Swearingen B, Klibanski A, Alexander JM. Mutational analysis of activin/transforming growth factor-beta type I and type II receptor kinases in human pituitary tumors. J. Clin. Endocrinol Metab 1999;84:1716–21.

[19] Jeruss JS, Sturgis CD, Rademaker AW, Woodruff TK. Down-regulation of activin, activin receptors, and smads in high-grade breast cancer. Cancer Res 2003;63:3783–90.

[20] Sambrook J, Fritsch EF, Maniatis T. Molecular Cloning: A Laboratory Manual. 2nd ed. New York, NY: Cold Spring Harbor Laboratory Press, 1989.

[21] Kumar A, Novoselov V, Celeste AJ, Wolfman NM, ten Dijke P, Kuehn MR. Nodal signaling uses activin and transforming growth factor-beta receptor-regulated Smads. J Biol Chem 2001;276:656–61.

[22] Bhattacharyya N, Tao J, Klein EA, Banerjee S. Alterations of transforming growth factor beta receptor II, insulin growth factor receptor II genes in microsatellite unstable prostate carcinomas. Oncol Rep 2004;11:231–6.

[23] Maquat LE. Nonsense-mediated mRNA decay: splicing, translation and mRNP dynamics. Nat. Rev. Mol. Cell Biol 2004;5:89–99.

[24] Ionov Y, Matsui S, Cowell JK. A role for p300/CREB binding protein genes in promoting cancer progression in colon cancer cell lines with microsatellite instability. Proc Natl Acad Sci USA 2004;101:1273–8.

[25] Sramkoski RM, Pretlow TG 2nd, Giaconia JM, Pretlow TP, Schwartz S, Sy MS, Marengo SR, Rhim JS, Zhang D, Jacobberger JW. A new human prostate carcinoma cell line, 22Rv1. In Vitro Cell Dev Biol Anim 1999;35:403–9.

[26] Guo Y, Kyprianou N. Overexpression of transforming growth factor (TGF) beta1 type II receptor restores TGF-beta1 sensitivity and signaling in human prostate cancer cells. Cell Growth Differ 1998;9: 185–93.

[27] Gerald WL. Genome-wide gene expression analysis of prostate carcinoma. Semin Oncol 2003;30:635–48.

[28] van Bokhoven A, Varella-Garcia M, Korch C, Johannes WU, Smith EE, Miller HL, Nordeen SK, Miller GJ, Lucia MS. Molecular characterization of human prostate carcinoma cell lines. Prostate 2003;57:205–25.

[29] Liu F, Pouponnot C, Massague J. Dual role of the Smad4/DPC4 tumor suppressor in TGFbeta-inducible transcriptional complexes. Genes Dev 1997;11:3157–67.

[30] Matzuk MM, Kumar TR, Bradley A. Different phenotypes for mice deficient in either activins or activin receptor type II. Nature 1995;374:356–60.

[31] Shiozaki S, Tajima T, Zhang YQ, Furukawa M, Nakazato Y, Kojima I. Impaired differentiation of endocrine and exocrine cells of the pancreas in transgenic mouse expressing the truncated type II activin receptor. Biochim Biophys Acta 1999;1450:1–11.

[32] Liu F, Shao LE, Yu J. Truncated activin type II receptor inhibits erythroid differentiation in K562 cells. J Cell Biochem 2000;78:24–33.

[33] Maeshima A, Shiozaki S, Tajima T, Nakazato Y, Naruse T, Kojima I. Number of glomeruli is increased in the kidney of transgenic mice expressing the truncated type II activin receptor. Biochem Biophys Res Commun 2000;268:445–9.

[34] Sehy DW, Shao LE, Yu AL, Tsai WM, Yu J. Activin A-induced differentiation in K562 cells is associated with a transient hypophosphorylation of RB protein and the concomitant block of cell cycle at G1 phase. J Cell Biochem 1992;50:255–65.

[35] Spencer SJ, Rabinovici J, Jaffe RB. Human recombinant activin-A inhibits proliferation of human fetal adrenal cells in vitro. J Clin Endocrinol Metab 1990;71:1678–80.

[36] Kundu SD, Kim IY, Yang T, Doglio L, Lang S, Zhang X, Buttyan R, Kim SJ, Chang J, Cai X, Wang Z, Lee C. Absence of proximal duct apoptosis in the ventral prostate of transgenic mice carrying the C3(1)-TGF-beta type II dominant negative receptor. Prostate 2000;43: 118–124.

[37] Tu WH, Thomas TZ, Masumori N, Bhowmick NA, Gorska AE, Shyr Y, Kasper S, Case T, Roberts RL, Shappell SB, Moses HL, Matusik RJ. The loss of TGF-beta signaling promotes prostate cancer metastasis. Neoplasia 2003;5:267–77.

[38] Zhang Z, Zhao Y, Batres Y, Lin MF, Ying SY. Regulation of growth and prostatic marker expression by activin A in an androgen-sensitive prostate cancer cell line LNCAP. Biochem. Biophys. Res Commun 1997;234:362–65.

[39] Heinlein CA, Chang C. Androgen receptor in prostate cancer. Endocr Rev 2004;25:276–308.

[40] Hayes SA, Zarnegar M, Sharma M, Yang F, Peehl DM, ten Dijke P, Sun Z. Smad 3 represses androgen receptor-mediated transcription. Cancer Res 2001;61:2112–8.

[41] Kang HY, Lin HK, Hu YC, Yeh S, Huang KE, Chang C. From transforming growth factor ß signaling to androgen action: identification of Smad 3 as an androgen receptor coregulator in prostate cancer cells. Proc Natl Acad Sci USA 2001;98:3018–23.

[42] Kang HY, Huang KE, Chang SY, Ma WL, Lin WJ, Chang C. Differential modulation of androgen receptor-mediated transactivation by Smad3 and tumor suppressor Smad4. J Biol Chem 2002;277:43749–56.

[43] Salovaara R, Roth S, Loukola A, Launonen V, Sistonen P, Avizienyte E, Kristo P, Jarvinen H, Souchelnytskyi S, Sarlomo-Rikala M, Aaltonen LA. Frequent loss of SMAD4/DPC4 protein in colorectal cancers. Gut 2002;51:56–9.

WAVE3 promotes cell motility and invasion through the regulation of MMP-1, MMP-3, and MMP-9 expression

Khalid Sossey-Alaoui[*,1], Tamara A. Ranalli[1,2], Xiurong Li, Andrei V. Bakin, John K. Cowell

Department of Cancer Genetics, Roswell Park Cancer Institute, Elm and Carlton Streets, Buffalo, NY 14263, USA

Abstract

WAVE3 is a member of the WASP/WAVE family of proteins, which play a critical role in the regulation of actin polymerization, cytoskeleton organization, and cell motility. We show here that knockdown of the WAVE3 protein, using RNA interference in MDA-MB-231 cells, decreases phospho-p38 MAPK levels, but not those of phospho-AKT, phospho-ERK, or phospho-JNK. Knockdown of WAVE3 expression also inhibited the expression levels of MMP-1, MMP-3, and MMP-9, but not MMP-2. MMP production could be restored by PMA treatment, without affecting siRNA-mediated WAVE3 knockdown. The WAVE3-mediated downregulation of p38 activity and MMP production is independent of the presence of both WAVE1 and WAVE2, whose expression levels were not affected by loss of WAVE3. We also show that the downstream effect of the WAVE3 knockdown is the inhibition of cell motility and invasion, coupled with increased actin stress fiber formation, as well as reorganization of focal adhesion complexes. These findings suggest that WAVE3 regulates actin cytoskeleton, cell motility, and invasion through the p38 MAPK pathway and MMP production.
© 2005 Elsevier Inc. All rights reserved.

Keywords: WAVE3; Cell motility; MMP

Introduction

The WASP (Wiskott–Aldrich Syndrome Protein) and WAVE (WASP Verprolin-homologous) family of structurally related proteins plays a critical role in actin polymerization and cytoskeletal organization, which are required for a wide variety of cellular processes, such as cell shape changes, cytokinesis, cell motility, and membrane traffic [1,2]. This family of proteins is comprised of 5 distinct members that form two distinct subfamilies based on structural homology [3,4]. The WASP subfamily includes the WASP protein, mutations of which lead to the development of the Wiskott–Aldrich syndrome [5,6], and its more widely expressed homologue N-WASP [7]. The WAVE subfamily of proteins contains three members, WAVE1, WAVE2, and WAVE3 [8,9], wherein WAVE3 was found to be associated with low-grade neuroblastoma [10]. The WASP/WAVE proteins function as downstream effectors of the Rho GTPases that are involved in the regulation of the actin cytoskeleton [4]. Members of the WASP subfamily are activated through Cdc42 to induce filopodia, while the WAVE proteins function downstream of Rac to induce the formation of lamellipodia. All members of the WASP/ WAVE family of proteins share a tripartite VCA (Verprolin homology, Cofilin homology, and Acidic) domain. Activation of the WASP/WAVE proteins leads to the exposure of the VCA domain, which can then bind to the Arp2/3 complex and initiate rapid polymerization of actin filaments [11,12]. Activation of actin polymerization ultimately leads to cytoskeletal remodeling, which is necessary for cellular proliferation and migration [1].

WASP/WAVE proteins differ in both the signaling inputs that they receive and in their mechanisms of regulation [11–14]. In the absence of extracellular signals, WASP and

---

* Corresponding author. Fax: +1 716 845 1698.
  E-mail address: Khalid.Sossey-Alaoui@RoswellPark.org
(K. Sossey-Alaoui).
  [1] These authors contributed equally to this work.
  [2] Present address: BioHelix, 32 Tozer Road, Beverly, MA 01915, USA.

N-WASP are autoinhibited through intramolecular interactions between the CRIB (Cdc42- and Rac-Interactive Binding) domain and the VCA domain [15]. On the other hand, WAVE1 and WAVE2 proteins were shown to be sequestered in an inactive state through the formation of a complex with four other proteins, PIR121, Nap125, HSPC300, and Abi1 [13,14,16]. WAVE3 has recently been shown to be included in similar protein complex, as WAVE1 and WAVE2 [17]. However, whether or not WAVE3 activity is regulated in a similar manner is not yet known.

The expression profiles of the WAVE genes clearly show an overlap in the expression of all three WAVE transcripts in several embryonic and adult tissues [3], and previous studies have also shown co-localization of the three WAVE proteins in multimeric proteins complexes [12,18], which suggests the involvement of the WAVE proteins in similar cellular pathways. Although WAVE1 and WAVE2 are both expressed in mouse embryonic fibroblasts, they were found to have distinct roles in cell migration [19]. WAVE1 was found to be required for the formation of dorsal ruffles, while WAVE2 is required for the formation of peripheral ruffles, two membrane-based actin structures that are necessary for the initiation of cell migration [19]. These data suggest independent roles for the WAVE proteins. Other evidence for the non-redundant roles of the WAVE proteins in the regulation of actin cytoskeleton comes from the knockout of WAVE1 and WAVE2 genes in mice, which resulted in severe organ malformation and embryonic lethality, in addition to defects in cell motility in the embryonic fibroblasts derived from these mice [20–22]. The observed phenotypes are believed to be specific for the targeted WAVE protein, as the expression levels of the non-targeted WAVE proteins remained unchanged. Together, these observations clearly support independent roles for each WAVE protein.

A recent study has found that WAVE1 activity is required for matrix metalloproteinase 2 (MMP-2)-dependent migration, as well as the formation of dorsal ruffles [19]. Degradation of the extracellular matrix (ECM) via MMP activity is also essential for many normal physiological processes, e.g., during development, cell migration, growth, and wound healing [23]. On the other hand, increased expression and activity of MMPs are also associated with tumor invasion, metastasis, and angiogenesis [24,25]. Expression of most MMPs is normally low in tissues, and only induced when remodeling of the extracellular matrix is required. MMP expression is primarily regulated at the transcriptional level, although stabilization of MMP transcripts in response to growth factors, as well as the influence of cytokines, also plays a role in the regulation of MMP activity [26].

A number of independent studies have primarily focused on elucidating the roles of WAVE1 and WAVE2 in remodeling the actin cytoskeleton and in cell motility, whereas comparatively little is known about the exact functional role

of WAVE3 in these processes. Interestingly, we previously reported that loss of WAVE3 function might be associated with the development of low-grade neuroblastoma, suggesting that WAVE3 plays a role in the development of this type of malignancy [10]. In the present study, we focused on the analysis of the functional consequences of downregulating WAVE3 using RNA interference (RNAi). RNAi is a powerful technique that utilizes short double-stranded RNA that specifically targets mRNA to induce gene silencing by degradation [27,28]. We have examined the effect of WAVE3 knockdown on distinct MAPK signaling and on the regulation of the expression of different MMPs. We show that knockdown of WAVE3 expression affects the activity of the p38 pathway, but not that of AKT, ERK1/2, or JNK. WAVE3-mediated downregulation of p38 activity is independent of both WAVE1 and WAVE2 expression, as WAVE3 knockdown does not alter the transcription levels of either WAVE1 or WAVE2. We also show that WAVE3 down-regulation clearly decreases the expression of MMP-1, -3, and -9. Finally, we show a link between the knockdown of WAVE3 expression and the inhibition of cell migration and invasion using both the in vitro wound closure and Matrigel assays. The results presented here provide evidence for a novel role of WAVE3 in the regulation of MMP activity via the p38 pathway, supporting its crucial role in cell migration and invasion.

Materials and methods

Materials

The siRNA oligonucleotides were purchased from Dharmacon (Littleton, CO) and annealed according to manufacturer's instructions. The siRNA sequences used are listed in Table 1. All siRNAs were 21 nucleotides long and contained symmetric 3′-overhangs of two deoxythymidines. SuperScript II Reverse Transcriptase Kits and Taq polymerase were obtained from Invitrogen (Carlsbad, CA). PCR primers were synthesized by Integrated DNA Technologies (Coralville, IA). The primer sequences used for GAPDH were 5′-GAAGGGAAGGTCGGAGT-3′ for the forward primer and 5′-GAAGATGGTGATGGGATTT-3′ for the reverse primers; for MMP-2, 5′-ATGACAGCTG-CACCACTGAG-3′ for the forward primer and 5′-CTCCT-

Table 1

Sequence information on the three siRNA designed against WAVE3 mRNA according to the sequence obtained from National Center for Biotechnology Information database (accession no. NM_006646)

siRNA duplex	Targeted region	Sequence—sense
siWAVE3-a	93–111	5′-UAGUACUCUUGCCGCUAUC-3′
siWAVE3-b	265–283	5′-GAGGUCUCACUACAGGAUA-3′
siWAVE3-c	4398–4416	5′-UGUAUCAGCCAGAGUAGCA-3′

The nucleotide numbers of the targeted region are from the start codon.

GAATGCCCTTGATGT-3′ for the reverse primer; and for MMP-9, 5′-AGTTCCCGGAGTGAGTTGAA-3′ for the forward primer and 5′-CTCCACTCCTCCCTTTCCTC-3′ for the reverse primers. Primers for WAVE1, 2, and 3, and MMP-1 and MMP-3 were as previously reported [10,29]. The antibodies used in this study were: human WAVE3/Scar and GST obtained from Upstate Biotechnology (Charlottesville, VA); phosphorylated Thr180/Tyr182 of p38 human MAP Kinase, total human p38 MAP Kinase, phosphorylated Ser473 of human AKT, total human AKT, phosphorylated Thr185/Tyr187 of human ERK 1/2, total human ERK 1/2, phosphorylated Thr183/Tyr185 of JNK MAP Kinase, and total human JNK were obtained from Cell Signaling Technology (Beverly, MA); and human PI3-Kinase p85 obtained from BD Biosciences (San Diego, CA). The secondary antibodies used were donkey anti-rabbit and goat anti-mouse from Jackson ImmunoResearch (West Grove, PA). The p38 MAPK inhibitor 4-(4-fluorophenyl)-2(4-methylsulfinylphenyl)-5-(pyridyl)1H-imidazol (SB203580) was obtained from Calbiochem (San Diego, CA). The MMP activator phorbol myristate acetate (PMA) and the Platelet Derived Growth Factor (PDGF) were obtained from Sigma (St. Louis, MO). Gel electrophoresis reagents were from Bio-Rad (Hercules, CA).

Methods

Cell culture and transfections

The human neuroblastoma IMR5 cells, human neuroblastoma SK-N-AS cells, and human adenocarcinoma MDA-MB-231 cells were obtained from ATCC. Cells were cultured at 37°C with 10% CO_2 in Dulbecco's modified Eagle's medium (DMEM) supplemented with 4.5 g/l glucose, 10% fetal bovine serum (FBS, Invitrogen), 2 mM glutamine, and antibiotics. For transient transfections, approximately 2.5×10^5 cells were plated in either 60-mm dishes or 6-well plates in DMEM without antibiotics 24 h prior to transfection. Transfections were performed using oligofectamine (Invitrogen) in OPTI-MEM (Invitrogen) media as directed by the manufacturer. Approximately 4–12 h after transfection, media were supplemented with DMEM containing 10% FBS without antibiotics.

Reverse transcriptase-PCR

Cells were lysed in Trizol reagent (Invitrogen) and total RNA was extracted according to the manufacturer's instructions. RNA was quantified using a Spectrophotometer (Beckman-Coulter Fullerton, CA), and 1 μg of RNA was used to generate cDNA with the SuperScript II RT-PCR kit (Invitrogen). Reverse transcription was performed according to the manufacturer's instructions, and the cDNA generated was used as a template for 30 cycles of PCR amplification for analysis of gene expression using a PTC-100 Thermal Cycler from MJ Research (Waltham, MA).

Wound closure assay

MDA-MB-231 cells of 80–90% confluent were treated for 48–72 h with various siRNAs, where after the cell monolayer was 'wounded' by dragging a sterile pipette tip across the plate to create a cell free area and photographed using an inverted Leica DM IRB microscope fitted with a CCD camera (Leica Microsystems, Germany). 24 h after wounding, cells were photographed again to document migration across the wound line.

Drug treatment

72 h after siRNA treatment, either SB203580 (20 nM) or PMA (100 nM) was added to the culture, and cells were incubated for an additional 30 min prior to harvesting the cells. No drugs were added to the control cells. RNA and/or protein were purified from both treated and untreated cells.

Western analysis

Cellular lysates containing equivalent amounts of total protein (50 μg) were resolved on a 10% SDS–polyacrylamide gel, followed by transfer to nitrocellulose (Bio-Rad, Hercules, Ca) or Immobilon-P (Millipore, Billerica, MA) membrane using the Bio-Rad gel and transfer apparatus (Hercules, CA). Membranes were incubated in 5% whole milk (or bovine serum albumin, BSA) for 1 h at room temperature, washed with PBS, followed by incubation with the primary antibody (as specified) overnight at 4°C. Membranes were then washed and incubated in the appropriate secondary antibody at room temperature for 1 h, and the immunocomplexes were visualized using the Western Lights Chemiluminescence Detection kit from Perkin-Elmer (Boston, MA).

Immunofluorescence

Cells were grown on glass coverslips and fixed in 4% paraformaldehyde for 20 min in phosphate-buffered saline (PBS) at room temperature and then washed with PBS. The cells were then permeabilized in 0.2% Triton X-100 in PBS for 15 min, washed again with PBS, and incubated in the blocking solution containing 5% BSA in PBS for 2 h at room temperature. Primary and secondary antibodies were diluted to the recommended concentration in 5% BSA in PBS. Cells were first incubated with the primary antibody for 1 h and then washed before the addition of the secondary antibody again for 1 h. Actin filaments (F-actin) were stained with Alexa green-conjugated phalloidin obtained from Molecular Probes (Eugene, OR). The coverslips were mounted on object slides using Vectashield mounting medium containing DAPI from Vector Laboratories (Burlingame, CA). Fluorescent images were captured using a NikonTE2000-E inverted microscope.

Biocoat Matrigel assay

The invasive potential of MDA-MB-231 cells transfected with either oligofectamine reagent, WAVE3 siRNA, or the control siRNA was assessed using the Matrigel invasion

assay from BD Biosciences (San Diego, CA). 72 h after siRNA treatment, cells were harvested by trypsinization, counted, and 5×10^4 cells were added to the Matrigel chambers. One chamber consists of a cell insert and a well. The bottom of the cell insert is covered with a filter containing multiple 8-μm pores and is coated with a basement membrane matrix (Matrigel). Cells, in 500 μl of serum-free DMEM media, were seeded in the cell insert and placed in the well, which was filled with 750 μl of DMEM and supplemented with 10% FBS. After 24-h incubation at 37°C and 5% CO_2, the noninvasive cells present on the upper surface of the filter were wiped out with a sterile cotton swab. The cells that were able to migrate through the Matrigel onto the lower surface of the filter were fixed and stained with Diff-Quick (American Scientific Products, McGaw Park, IL), and counted using light microscopy. The lower surface of the filter was photographed using an inverted Leica DM IRB microscope fitted with a CCD camera (Leica Microsystems, Germany).

Cell proliferation assay

Cells were transfected as described above and at indicated time points, then harvested with trypsin-EDTA, washed one time with PBS, and counted with a hemacytometer. Cell viability was assessed using trypan blue staining, where the total number of viable cells in the various treatment groups was established to determine growth rate. Assays were performed in duplicate, and the values plotted were the average of two independent experiments.

Results

siRNA targeting of WAVE3

To study the function of WAVE3, we designed three different siRNAs, siW3-a, siW3-b, and siW3-c (Table 1), which targeted different regions of the human WAVE3 transcript (accession no. NM_006646). Both siW3-a and siW3-b targeted the coding region, whereas siW3-c targeted the 3′ untranslated region of WAVE3. Initially, we used the IMR5 and SK-N-AS neuroblastoma cell lines, where WAVE3 is abundantly expressed, to establish the efficiency of WAVE3 mRNA knockdown using these siRNAs. Cells were treated in parallel with either an anti-WAVE3 siRNA or the transfection reagent alone, and compared with untreated cells. After 72 h, the mRNA levels of both WAVE3 and GAPDH were analyzed by RT-PCR (Figs. 1A and B). GAPDH mRNA levels in both the IMR5 (Fig. 1A) and SK-N-SH cell lines (Fig. 1B) were not affected by either the siRNA or oligofectamine treatment. For both cell lines, the siW3-a siRNA was the most efficient in reducing WAVE3 mRNA levels. siW3-a reduced WAVE3 mRNA levels by approximately 90% at a concentration of 240 pmol (Figs. 1A and B). Treatment of MDA-MB-231 cells with the same concentrations of siW3-a was even more efficient and
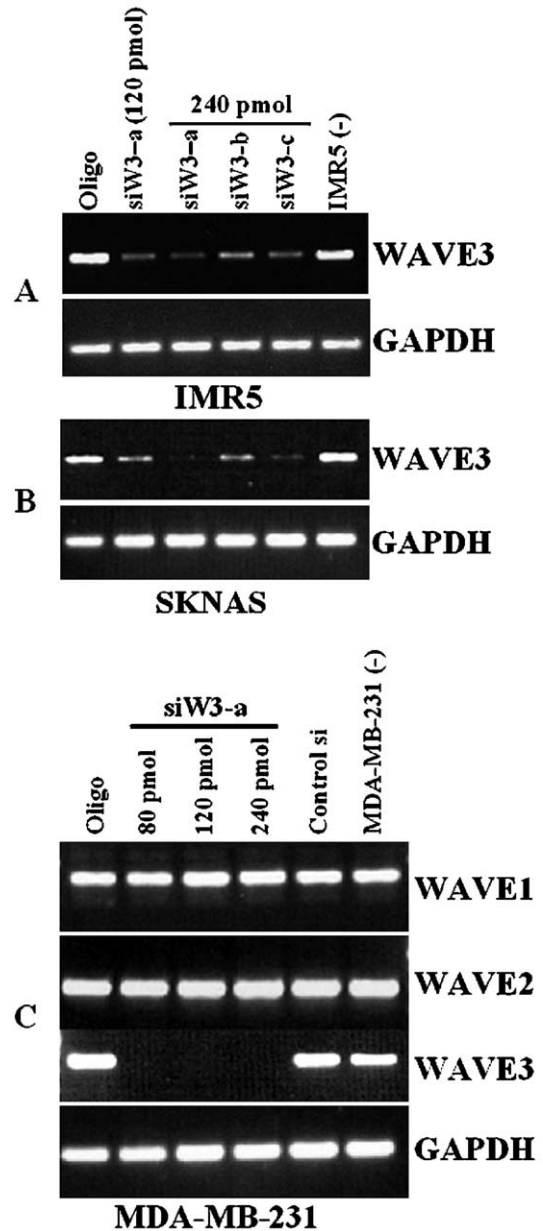

Fig. 1. Knockdown of WAVE3 expression using small interfering RNA (siRNA). (A) RT-PCR analysis shows reduced mRNA levels of WAVE3 in IMR5 and SK-N-AS cells treated with the indicated amounts of siWAVE3-a, -b, or -c siRNAs (siW3-a, siW3-b, siW3-c, respectively), but not in cells treated with oligofectamine (Oligo), the control siRNA (Control si), or the untreated cells (−). RNA was harvested 72 h post-transfection and subjected to RT-PCR as described in Materials and methods. GAPDH levels show that equivalent amounts of RNA were used. (B) RT-PCR analysis shows reduced mRNA levels of WAVE3, but not WAVE1 and WAVE2, in MDA-MB-231 cells treated with increasing amounts of siW3-a siRNA. mRNA levels of WAVE1, 2, and 3 in cells treated with oligofectamine (Oligo), the control siRNA (Control si), or the untreated cells (−) remained unchanged.

resulted in knockdown of the WAVE3 mRNA below detectable levels (Fig. 1C). Thus, siW3-a siRNA was used in all the subsequent experiments. To determine whether siW3-a affects the mRNA expression levels of the highly homologous WAVE1 and WAVE2 genes, we compared

mRNA levels for all three WAVE genes in MDA-MB-231 cells following treatment with three different concentrations (80 pmol, 120 pmol, and 240 pmol) of siW3-a (Fig. 1C). While the WAVE3 mRNA was reduced below detectable levels by all three concentrations of siW3-a, mRNA levels of either WAVE1 or WAVE2 were not affected (Fig. 1C). Thus, within this family of genes, siW3-a appears to be highly specific for WAVE3, and so was used for all subsequent experiments.

Time-dependent gene silencing of WAVE3 in MDA-MB-231 cells

To determine the duration of the WAVE3 mRNA knockdown effect using siW3-a, we used RT-PCR to measure mRNA levels in MDA-MB-231 cells 24, 48, 72, and 120 h after a single siRNA treatment (240 pmol). Reduction in WAVE3 transcript levels could be seen as early as 24 h post-treatment (Fig. 2A). Maximal silencing occurred between 48 and 72 h (Fig. 2A). Low levels of WAVE3 mRNA were again detectable after 120 h post-treatment (Fig. 2A), demonstrating the transient effect of the siRNA treatment.
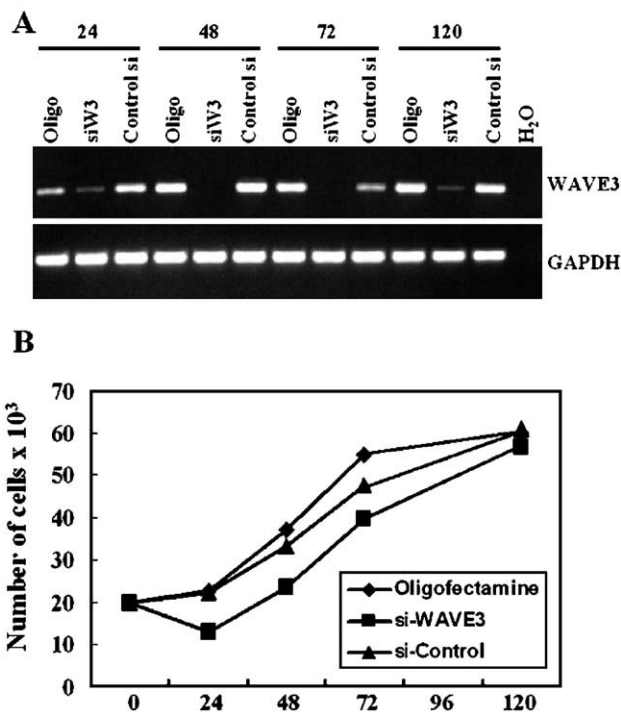

Fig. 2. Time-dependent gene silencing of WAVE3 using siRNA in MDA-MB-231 cells. (A) RT-PCR analysis of WAVE3 mRNA from MDA-MB-231 cells treated with oligofectamine (Oligo), transfected with 240 pmol of si-WAVE3-a siRNA (siW3), or with the control siRNA (Control si). GAPDH was used as a loading control for mRNA levels. Cells were harvested at the indicated time points (in hours) after transfection. (B) Graphical representation of the growth rate, as determined by total number of viable cells in the culture, as a function of time after transfection. The average of two independent experiments is plotted on the graph. The *x*-axis corresponds to the time in hours after siRNA transfection and the *y*-axis corresponds to number of cells.

We next investigated the effect of WAVE3 knockdown on cellular proliferation. MDA-MB-231 cells were transfected with siW3-a (240 pmol) and cell numbers were determined 24, 48, 72, and 120 h post-treatment (Fig. 2A). After 24 h, only the siW3-a-treated cells showed an approximate 40% reduction in cell numbers, but recovered soon after. The initial cell death was probably caused by a mild toxic effect of the WAVE3 siRNA since, by comparison, cells in control treatments were unaffected. After 48 h and 72 h, where WAVE3 mRNA knockdown reached its maximum (Fig. 2B), the number of siW3-treated cells was only 20–30% lower than the control cells (Fig. 2A). By 120 h post-treatment, the WAVE3 siRNA-treated cells attained the same number of cells as either the oligofectamine-treated or control siRNA-treated cells (Fig. 2B). These results demonstrate that knockdown of WAVE3 expression does not seem to have a direct effect on cell proliferation, since there is no direct correlation between WAVE3 expression levels and cell number during siRNA treatment.

Downregulation of WAVE3 impairs motility and invasiveness of MDA-MB-231 cells

The WASP/WAVE proteins are known to be involved in the processes that govern cellular motility [4,16,30,31]. To determine whether knockdown of WAVE3 expression affects motility and/or invasion, we used MDA-MB-231 cells in Matrigel assays. Cells treated with oligofectamine alone were able to migrate freely through the Matrigel (Fig. 3A), whereas this ability was lost in cells treated with 240 pmol of siW3-a (Fig. 3B). This observation suggests that WAVE3 has a role in cell motility/invasiveness.

The wound closure assay [32,33] determines the ability of cells to eliminate a "gap" created by physically disrupting a linear portion of confluent cells and is used as another measure of cell motility. When MDA-MB-231 cells were treated with either oligofectamine or 240 pmol of siW3-a for 72 h and then assayed for their wound closing ability (Fig. 3B), cells treated with oligofectamine readily closed the gap over 24 h whereas cells treated with siW3-a did not (Fig. 3C). Thus, it appears that loss of WAVE3 function inhibits cell motility in this assay.

Downregulation of WAVE3 mRNA results in a decrease in MMP expression

An important process associated with migration during tumor invasion is degradation of the extracellular matrix [26,34], usually through the action of matrix metalloproteinases (MMP). To determine whether reduced WAVE3 protein levels affect MMP expression, we treated MDA-MB-231 cells with either 240 pmol of siW3-a or oligofectamine for 72 h, and used RT-PCR to monitor the expression levels of several MMPs (Fig. 4A). Treatment of MDA-MB-231 cells with siW3-a resulted in a clear decrease in the
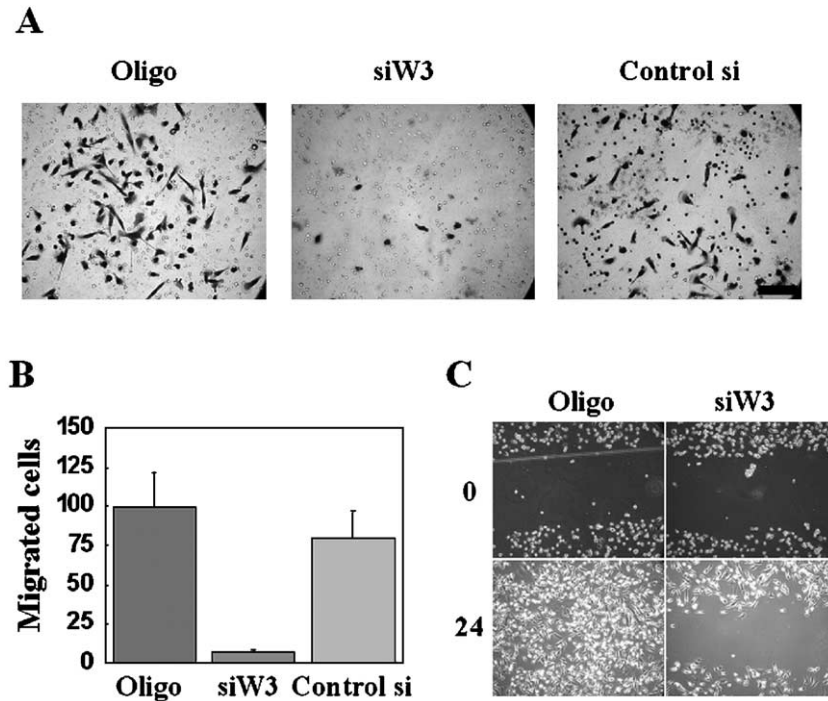
Fig. 3. Knockdown of WAVE3 expression impairs migration of MDA-MB-231 cells. (A) MDA-MB-231 cells were treated with oligofectamine (Oligo), transfected with 240 pmol of siW3-a (siW3) or with the control siRNA (Control si) for 72 h, and transferred to a Matrigel chamber. After 24 h post-transfer, the migrated cells were stained and photographed. (B) Graphical depiction of the number of cells that migrated through the Matrigel matrix. The x-axis corresponds to the treatment and the y-axis corresponds to the number of migrated cells. (C) Wound closure assay using MDA-MB-231 cells that were treated with oligofectamine alone (Oligo) or transfected with 240 pmol of siW3-a for 72 h prior to wounding as described in Materials and methods. Cells were photographed immediately after wounding and again 24 h later.

mRNA levels of both MMP-1 and MMP-9 compared with control treatments, but MMP-2 was not affected (Fig. 4A). MMP-3 expression was not detected in either the control cells or the siW3-a-treated cells (not shown). These results suggest that WAVE3 is likely involved in the regulation of MMP-1 and MMP-9 expression.
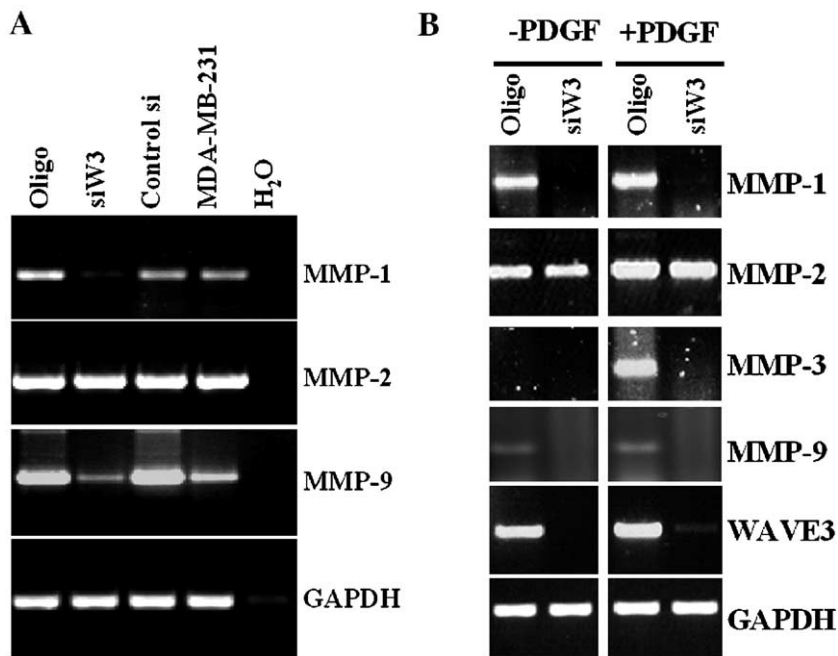

Fig. 4. WAVE3 downregulation inhibits MMPs expression. (A) RT-PCR analysis of MDA-MB-231 cells that were transfected with si-W3-a (240 pmol) and harvested 72 h post-transfection. Cells were treated with oligofectamine (Oligo), siW3-a, the control siRNA (Control-si), or remained untreated (MDA-MB-231). mRNA expression levels of MMP-1, -2, -9, and GAPDH are shown.

The platelet-derived growth factor (PDGF) is a potent activator of cell motility [35,36]. Therefore, we analyzed the effect of WAVE3 downregulation in MDA-MB-231 cells treated with PDGF. Parallel cultures of MDA-MB-231 cells were treated with either siW3-a (240 pmol) or oligofectamine for 72 h. Prior to harvesting, some of the cultures of MDA-MB-231 cells were treated with PDGF (50 ng/ml) for 30 min, and RT-PCR was then used to determine mRNA levels for MMP-1, MMP-2, MMP-3, MMP-9, WAVE3, and GAPDH (Fig. 4B). Treatment with si-W3-a resulted in an almost complete knockdown of WAVE3 expression, whether the cells were treated with PDGF or not (Fig. 4B). While expression of MMP-2 was not affected by siW3-a treatment in both the control cells and the PDGF-treated cells, expression of MMP-1 and MMP-9, however, was clearly suppressed by siW3-a, and treatment with PDGF was not able to restore their expression (Fig. 4B). Expression of MMP-3 could be seen only in the PDGF-treated cells, and prior treatment of these cells with siW3-a inhibited the PDGF-mediated stimulation of MMP-3 expression (Fig. 4B). These results clearly show that expressions of MMP-1 and MMP-9 are dependent on the expression of WAVE3 and independent of the presence of PDGF. Furthermore, the expression of MMP-3, which is modulated by PDGF, may also be regulated by WAVE3.

Treatment of MDA-MB-231 cells with signal transduction inhibitors alters MMP-1 and MMP-9 mRNA levels

Activation of several signal transduction pathways, e.g., involving JNK, p38 MAPK, and ERK, has been shown to increase the mRNA levels and activity of most MMPs, including MMP-1, MMP-3, and MMP-9. This is achieved either by activating their transcription or increasing the stability of their mRNAs [26,34,37,38]. Because of the relatively low endogenous levels of MMP-3 mRNA in MDA-MB-231 cells, we focused our analysis on the effect of WAVE3 downregulation on the levels of MMP-1 and MMP-9, which are abundantly expressed in this cell line.

Cells that were treated with the p38 MAP kinase inhibitor SB203580 showed reduced MMP-1 and MMP-9 mRNAs levels compared to untreated cells (Fig. 5). On the other hand, cells treated with PMA, a potent activator of MMPs through stimulation of the PKC pathway [39], resulted in an increase in MMP-1 and MMP-9 mRNA levels which are comparable to those seen in controls, even in the presence of siW3-a-mediated downregulation of WAVE3 (Fig. 5). Treatment of MDA-MB-231 cells with either SB203580 or PMA, however, had no effect on endogenous WAVE3 mRNA levels, nor did it affect the siW3-a-mediated knockdown of WAVE3. These results suggest that the WAVE3-mediated regulation of MMP-1 and MMP-9 expression is independent PDGF or takes place downstream of PKC.
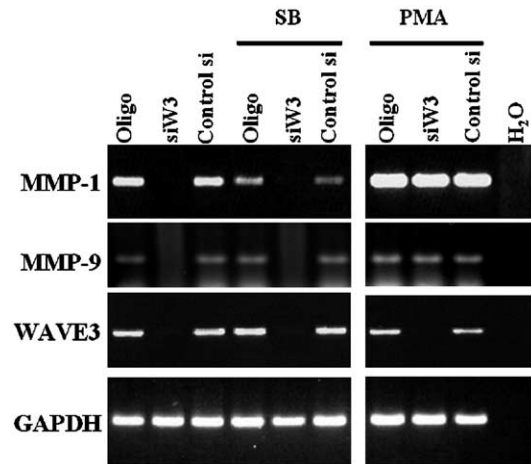

Fig. 5. Signal transduction inhibitors affect MMP-1 and MMP-9 expression in cells treated with WAVE3 siRNA. RT-PCR analysis of cells transfected with oligofectamine (Oligo), siW3-a (240 pmol), or a control siRNA (Control-si) for 72 h, after which cells remained untreated or treated with either SB203580 (SB) or PMA (PMA) for 30 min prior to being harvested. mRNA levels for MMP-1, MMP-9, WAVE3, and GAPDH were determined by semi-quantitative PCR.

Downregulation of WAVE3 by siRNA decreases p38 MAP kinase phosphorylation

Cell motility and invasion can be influenced by phospho-activation of a variety of key regulators of signal transduction pathways. We therefore analyzed the p38, ERK1/2, and JNK MAP kinase phosphorylation status in MDA-MB-231 cells treated with 240 pmol of siW3-a. Western blot analysis (Fig. 6) of cells treated with siW3-a shows the loss of the WAVE3 protein (pWAVE3). The same cells showed reduced levels of phospho-p38, but not total p38 protein levels, compared with controls (Fig. 6). In contrast, phospho-ERK1/2 levels were not altered in any treatment group (Fig. 6), and phospho-AKT levels were not affected by the WAVE3 siRNA treatment, nor were the total protein levels of ERK 1/2, AKT, and p85 (Fig. 6). No changes in the phosphorylation levels of JNK were detected (not shown). Phosphorylation of p38 MAP kinase was shown to up-regulate the MAP kinase pathway, which leads to an increase in mRNA stability of both MMP-1 and MMP-3 [26,40]. These results suggest that the p38-mediated stabilization of MMP mRNAs might be directly regulated by WAVE3 activity.

Downregulation of WAVE3 by siRNA increases stress-fiber formation in vivo and alters the distribution and organization of focal adhesions

Actin cytoskeleton remodeling plays a central role in cell motility [41]. The Rac family of GTP-binding proteins is thought to mediate formation of focal adhesions during the process of lamellipodia formation [42,43]. Since knockdown of WAVE3 was shown to clearly reduce the migration ability of MDA-MB-231 cells (Figs. 3A/B), we investigated whether this phenotypic effect was related to actin
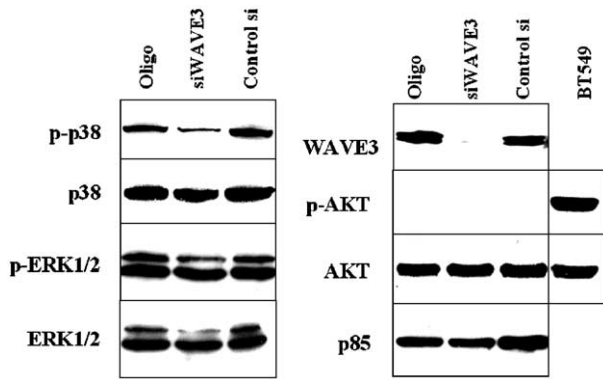
Fig. 6. Knockdown of WAVE3 expression inhibits p38 MAP kinase activity. MDA-MB-231 cells were transfected with either oligofectamine (Oligo), siW3-a (240 pmol), or a control siRNA (Control-si) for 72 h. Protein from total cellular lysate (50 μg) was subjected to SDS–PAGE followed by Western analysis using antibodies against phosphorylated p38, ERK 1/2, and AKT, and total p38, RK 1/2, p38, p85, and WAVE3. The BT549 adenocarcinoma cell line, which has a constitutively active AKT, was used as a control for phospho-AKT activity.

Discussion

The ability of a cell to migrate is critical for many normal physiological processes, as well as for tumor progression and metastasis. Members of the WAVE family of proteins are key components of the actin polymerization machinery downstream of Rac, leading to cell migration [4]. The specific role of each member of this family in cell migration is, however, not known. RNA interference (RNAi), a process by which double-stranded RNA induces the silencing of homologous endogenous genes, has been used to alter gene expression in a wide variety of organisms with a wide range of success [27,28]. In almost all cases, treatment of in vitro-cultured cells with siRNA results in phenotypic and/or morphological changes, therefore making the RNAi technology a useful tool to analyze gene function. We used RNAi to specifically knockdown the expression of WAVE3 in MDA-MB-231 cells and analyze its role in cell migration and invasion.

We were able to show that knockdown of WAVE3 expression was evident from 24 h until approximately 5 days after transfection, allowing us to analyze several phenotypic and physiological changes that resulted from WAVE3 downregulation. Inhibition of WAVE3 expression in MDA-MB-231 cells did not affect cell proliferation, since the growth rate was only transiently inhibited during the first 24 h post-transfection, but recovered to normal levels by 48 h. Interestingly, the most striking phenotype apparent from the WAVE3 knockdown was an inhibition in cellular motility as measured by the wound closure assay, as well as the inhibition of invasion shown in the Matrigel assay. Consistent with the data that have previously been generated for WAVE1 and 2 [19], we found that knockdown of WAVE3 expression did not alter the expression levels of the closely related WAVE1 and WAVE2 genes. This demonstrates that the observed phenotypes are specific to WAVE3

cytoskeleton reorganization involving the formation of either stress fibers or focal adhesion complexes. MDA-MB-231 cells that had been treated with 240 pmol of siW3-a were stained with Alexa green-conjugated phalloidin to detect actin filaments and with anti-vinculin antibody to detect focal adhesion complexes (Fig. 7). WAVE3 down-regulation resulted in a dramatic increase of stable actin filaments (stress fibers), as well as in the reorganization of focal adhesions at the edge of cells (Fig. 7). The focal adhesions, which were distributed in a random fashion in cells treated with oligofectamine alone, showed a more organized radial distribution along the edge of cells treated with siW3-a. The increase of stress fibers and the organization of the focal adhesions are strongly associated with the WAVE3-mediated inhibition of cell motility and the WAVE3-mediated decrease in MMP activity.
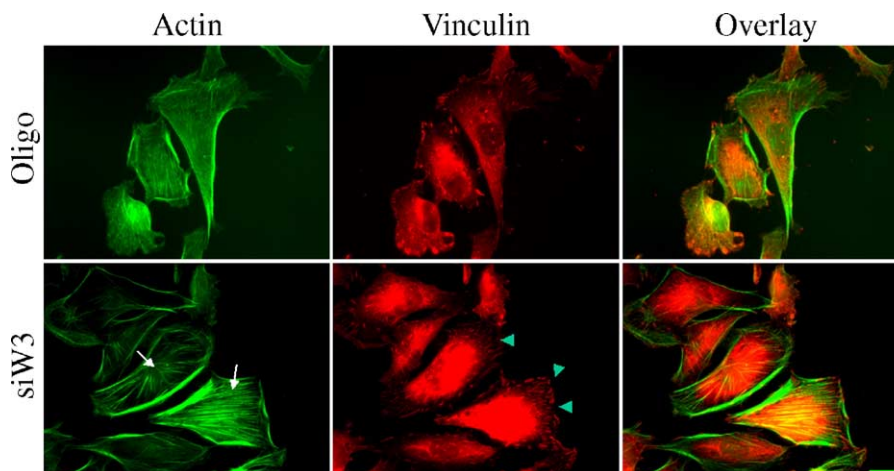

Fig. 7. Knockdown of WAVE3 expression affects actin cytoskeleton organization. MDA-MB-231 cells were treated with oligofectamine alone (upper panel) or transfected with 240 pmol of siW3-a for 72 h. Cells were then stained with Alex green-conjugated-phalloidin (green) to detect actin filaments or with anti-vinculin antibody (red) to detect focal adhesion complexes. The change in the organization of the focal adhesion complexes is indicative of lack of motility in the siW3-a-treated cells. Scale bar, 20 μm.

and provides further evidence for a non-redundant function for each WAVE protein.

The MAPK pathway plays an important role in regulating many fundamental processes such as cell growth, migration, and differentiation [44–46]. MAPK exerts its role by funneling the signal that it receives from Ras to the nucleus, where regulation of gene transcription affects the fate of cells. MAPK has been shown not only to be involved in transmitting transduction signal to the nucleus, but also to regulate cytoplasmic activities such as cell migration [47]. Activation of MAPK pathways also results in alterations in the expression levels and activity of MMPs, which in turn, are responsible for the degradation of extracellular matrix, and as such, are required for cell migration [38]. Because downregulation of WAVE1, but not WAVE2, was shown to affect MMP-2 activity [19], we investigated the effect of knockdown of WAVE3 expression on the expression levels of other MMPs, including MMP-2. Although MMP-2 expression levels were not affected by WAVE3 down-regulation, we found that the expression levels of MMP-1, -3, and -9 were severely inhibited as a result WAVE3 downregulation. Thus, these results provide the first link between WAVE3 expression and the regulation of expression of these MMPs. We also found that the WAVE3-mediated regulation of the expression of MMP-1, -3, and -9, but not MMP-2, was dependant on the levels of phosphorylation of p38 MAPK, but not of that of ERK and JNK MAP Kinases or AKT.

A possible mechanism underlying WAVE3 regulation of MMP levels may be a result of one of the modalities of action of PMA. PMA is potent activator of the protein kinase C (PKC), which results in the activation of the MEK/ERK MAPK pathway. On the other hand, the expressions of several MMPs, including MMP-2 and MMP-3, were shown to be regulated downstream of PKC, through the MEK/ERK MAPK pathway, but not the p38 MAPK pathway [29]. We have, however, shown that treatment of MDA-MB-231 cells with PMA resulted not only in an increase in the expression levels of MMP-1 and MMP-3, but also in bypassing the negative effect of WAVE3 downregulation on the expression of these MMPs. PMA treatment also resulted in an increase in the phosphorylation levels of p38 MAPK (not shown), suggesting a role for PKC in the regulation of p38 MAPK. Indeed, a recent study by Yin and colleagues has clearly demonstrated that p38 MAPK activation is also dependent on the PKC δ isozyme, but not on that of PKC α or PKC ε isozymes [48]. Thus, we suggest that WAVE3 might act downstream of PKC δ to regulate the expression of MMP-1, -3, and -9.

While the expression of MMP-1 and MMP-9 was clearly suppressed by siW3 siRNA, expression of MMP-3 was induced only after treatment with PDGF. The expression of MMP-3, however, was inhibited in the presence of siW3-a, suggesting that the expression of MMP-3 is also regulated by WAVE3 and that the WAVE3-mediated regulation of MMP-3 expression is modulated by PDGF.

Cell migration is tightly linked to dynamic changes in the actin cytoskeleton, such as membrane ruffles [41,49]. A study by Miki and colleagues has shown that suppression of MAPK activation resulted in a significant reduction of membrane ruffling [50]. Although the results of this study did not determine which suppression MAPK activity was responsible for the inhibition of membrane ruffle formation, a clear link between the MAPK pathway and the regulation of actin cytoskeleton organization was established.

Knockdown of WAVE3 expression in MDA-MB-231 cells was associated with a decrease of phosphorylation of p38 MAPK, which resulted in inhibition of the migration and invasion abilities of MDA-MB-231 cells. The inhibition of cell migration and invasion also correlated with an increase in the thickness and number of actin stress fibers as well as a remodeling of focal adhesions around the entire cell periphery, consistent with previously reported observations [51]. It is not clear how downregulation of WAVE3 expression inhibits p38 activation. It has been shown, however, that WAVE3 is activated downstream of Rac [50] and that Rac is also capable of activating the MAPK pathway in various cell lines [52,53]. The intermediate effectors between WAVE3 and p38 activation still remain to be identified. While a direct link between the WAVE proteins and MMPs has yet to be demonstrated, the effects of WAVE1 knockdown and WAVE3 knockdown targeted functionally diverse MMPs, therefore providing additional evidence for unique, non-overlapping roles of the WAVE proteins in the cell.

Acknowledgments

References

[1] T.H. Millard, S.J. Sharp, L.M. Machesky, Signalling to actin assembly via the WASP (Wiskott–Aldrich syndrome protein)-family proteins and the Arp2/3 complex, Biochem. J. 380 (2004) 1–17.

[2] S. Suetsugu, T. Takenawa, Regulation of cortical actin networks in cell migration, Int. Rev. Cytol. 229 (2003) 245–286.

[3] K. Sossey-Alaoui, K. Head, N. Nowak, J.K. Cowell, Genomic organization and expression profile of the human and mouse WAVE gene family, Mamm. Genome 14 (2003) 314–322.

[4] T. Takenawa, H. Miki, WASP and WAVE family proteins: key molecules for rapid rearrangement of cortical actin filaments and cell movement, J. Cell Sci. 114 (2001) 1801–1809.

[5] J.M. Derry, H.D. Ochs, U. Francke, Isolation of a novel gene mutated in Wiskott–Aldrich syndrome, Cell 78 (1994) 635–644.

[6] K. Devriendt, A.S. Kim, G. Mathijs, S.G. Frints, M. Schwartz, J.J. Van Den Oord, G.E. Verhoef, M.A. Boogaerts, J.P. Fryns, D. You, M.K. Rosen, P. Vandenberghe, Constitutively activating mutation in WASP causes X-linked severe congenital neutropenia, Nat. Genet. 27 (2001) 313–317.

[7] M. Fukuoka, S. Suetsugu, H. Miki, K. Fukami, T. Endo, T. Takenawa, A novel neural Wiskott–Aldrich syndrome protein (N-WASP) binding protein, WISH, induces Arp2/3 complex activation independent of Cdc42, J. Cell Biol. 152 (2001) 471–482.

[8] H. Miki, S. Suetsugu, T. Takenawa, WAVE, a novel WASP-family protein involved in actin reorganization induced by Rac, EMBO J. 17 (1998) 6932–6941.

[9] S. Suetsugu, H. Miki, T. Takenawa, Identification of two human WAVE/SCAR homologues as general actin regulatory molecules which associate with the Arp2/3 complex, Biochem. Biophys. Res. Commun. 260 (1999) 296–302.

[10] K. Sossey-Alaoui, G. Su, E. Malaj, B. Roe, J.K. Cowell, WAVE3, an actin-polymerization gene, is truncated and inactivated as a result of a constitutional t(1;13)(q21;q12) chromosome translocation in a patient with ganglioneuroblastoma, Oncogene 21 (2002) 5967–5974.

[11] S. Burns, G.O. Cory, W. Vainchenker, A.J. Thrasher, Mechanisms of WASP-mediated haematological and immunological disease, Blood 104 (2004) 3454–3462.

[12] A. Oda, H. Miki, I. Wada, H. Yamaguchi, D. Yamazaki, S. Suetsugu, M. Nakajima, A. Nakayama, K. Okawa, H. Miyazaki, K. Matsuno, H.D. Ochs, L.M. Machesky, H. Fujita, T. Takenawa, WAVE/scars in platelets, Blood 105 (2004) 2148–3141.

[13] A. Gautreau, H.Y. Ho, J. Li, H. Steen, S.P. Gygi, M.W. Kirschner, Purification and architecture of the ubiquitous WAVE complex, Proc. Natl. Acad. Sci. U. S. A. 101 (2004) 4379–4383.

[14] M. Innocenti, A. Zucconi, A. Disanza, E. Frittoli, L.B. Areces, A. Steffen, T.E. Stradal, P.P. Di Fiore, M.F. Carlier, G. Scita, Abi1 is essential for the formation and activation of a WAVE2 signalling complex, Nat. Cell Biol. 6 (2004) 319–327.

[15] A.S. Kim, L.T. Kakalis, N. Abdul-Manan, G.A. Liu, M.K. Rosen, Autoinhibition and activation mechanisms of the Wiskott–Aldrich syndrome protein, Nature 404 (2000) 151–158.

[16] S. Eden, R. Rohatgi, A.V. Podtelejnikov, M. Mann, M.W. Kirschner, Mechanism of regulation of WAVE1-induced actin nucleation by Rac1 and Nck, Nature 418 (2002) 790–793.

[17] C.F. Stovold, T.H. Millard, L.M. Machesky, Inclusion of Scar/WAVE3 in a similar complex to Scar/WAVE1 and 2, BMC Cell Biol. 6 (2005) 11.

[18] R.S. Westphal, S.H. Soderling, N.M. Alto, L.K. Langeberg, J.D. Scott, Scar/WAVE-1, a Wiskott–Aldrich syndrome protein, assembles an actin-associated multi-kinase scaffold, EMBO J. 19 (2000) 4589–4600.

[19] S. Suetsugu, D. Yamazaki, S. Kurisu, T. Takenawa, Differential roles of WAVE1 and WAVE2 in dorsal and peripheral ruffle formation for fibroblast cell migration, Dev. Cell 5 (2003) 595–609.

[20] J.P. Dahl, J. Wang-Dunlop, C. Gonzales, M.E. Goad, R.J. Mark, S.P. Kwak, Characterization of the WAVE1 knock-out mouse: implications for CNS development, J. Neurosci. 23 (2003) 3343–3352.

[21] D. Yamazaki, S. Suetsugu, H. Miki, Y. Kataoka, S. Nishikawa, T. Fujiwara, N. Yoshida, T. Takenawa, WAVE2 is required for directed cell migration and cardiovascular development, Nature 424 (2003) 452–456.

[22] C. Yan, N. Martinez-Quiles, S. Eden, T. Shibata, F. Takeshima, R. Shinkura, Y. Fujiwara, R. Bronson, S.B. Snapper, M.W. Kirschner, R. Geha, F.S. Rosen, F.W. Alt, WAVE2 deficiency reveals distinct roles in embryogenesis and Rac-mediated actin-based motility, EMBO J. 22 (2003) 3602–3612.

[23] S.D. Shapiro, Matrix metalloproteinase degradation of extracellular matrix: biological consequences, Curr. Opin. Cell Biol. 10 (1998) 602–608.

[24] P. Basset, A. Okada, M.P. Chenard, R. Kannan, I. Stoll, P. Anglard, J.P. Bellocq, M.C. Rio, Matrix metalloproteinases as stromal effectors

[25] P. Vihinen, V.M. Kahari, Matrix metalloproteinases in cancer: prognostic markers and therapeutic targets, Int. J. Cancer 99 (2002) 157–166.

[26] N. Reunanen, S.P. Li, M. Ahonen, M. Foschi, J. Han, V.M. Kahari, Activation of p38 alpha MAPK enhances collagenase-1 (matrix metalloproteinase (MMP)-1) and stromelysin-1 (MMP-3) expression by mRNA stabilization, J. Biol. Chem. 277 (2002) 32360–32368.

[27] S.M. Hammond, S. Boettcher, A.A. Caudy, R. Kobayashi, G.J. Hannon, Argonaute2, a link between genetic and biochemical analyses of RNAi, Science 293 (2001) 1146–1150.

[28] S.M. Hammond, A.A. Caudy, G.J. Hannon, Post-transcriptional gene silencing by double-stranded RNA, Nat. Rev., Genet. 2 (2001) 110–119.

[29] P. Kunapuli, C.S. Kasyapa, L. Hawthorn, J.K. Cowell, LGI1, a putative tumor metastasis suppressor gene, controls in vitro invasiveness and expression of matrix metalloproteinases in glioma cells through the ERK1/2 pathway, J. Biol. Chem. 279 (2004) 23151–23157.

[30] G.O. Cory, A.J. Ridley, Cell motility: braking WAVEs, Nature 418 (2002) 732–733.

[31] T.D. Pollard, L. Blanchoin, R.D. Mullins, Molecular mechanisms controlling actin filament dynamics in nonmuscle cells, Annu. Rev. Biophys. Biomol. Struct. 29 (2000) 545–576.

[32] N. Dumont, A.V. Bakin, C.L. Arteaga, Autocrine transforming growth factor-beta signaling mediates Smad-independent motility in human cancer cells, J. Biol. Chem. 278 (2003) 3275–3285.

[33] Y. Ueda, S. Wang, N. Dumont, J.Y. Yi, Y. Koh, C.L. Arteaga, Overexpression of HER2 (erbB2) in human breast epithelial cells unmasks transforming growth factor beta-induced cell motility, J. Biol. Chem. 279 (2004) 24505–24513.

[34] J. Westermarck, V.M. Kahari, Regulation of matrix metalloproteinase expression in tumor invasion, FASEB J. 13 (1999) 781–792.

[35] C. Betsholtz, Biology of platelet-derived growth factors in development, Birth Defects Res. Part C. Embryo. Today 69 (2003) 272–285.

[36] K.E. Bornfeldt, E.W. Raines, L.M. Graves, M.P. Skinner, E.G. Krebs, R. Ross, Platelet-derived growth factor. Distinct signal transduction pathways associated with migration versus proliferation, Ann. N. Y. Acad. Sci. 766 (1995) 416–430.

[37] T.P. Garrington, G.L. Johnson, Organization and regulation of mitogen-activated protein kinase signaling pathways, Curr. Opin. Cell Biol. 11 (1999) 211–218.

[38] J. Westermarck, S.P. Li, T. Kallunki, J. Han, V.M. Kahari, p38 mitogen-activated protein kinase-dependent activation of protein phosphatases 1 and 2A inhibits MEK1 and MEK2 activity and collagenase 1 (MMP-1) gene expression, Mol. Cell. Biol. 21 (2001) 2373–2383.

[39] B.D. Sudbeck, P. Baumann, G.J. Ryan, K. Breitkopf, R. Nischt, T. Krieg, C. Mauch, Selective loss of PMA-stimulated expression of matrix metalloproteinase 1 in HaCaT keratinocytes is correlated with the inability to induce mitogen-activated protein family kinases, Biochem. J. 339 (1999) 167–175.

[40] K.R. Mahtani, M. Brook, J.L. Dean, G. Sully, J. Saklatvala, A.R. Clark, Mitogen-activated protein kinase p38 controls the expression and posttranslational modification of tristetraprolin, a regulator of tumor necrosis factor alpha mRNA stability, Mol. Cell. Biol. 21 (2001) 6461–6469.

[41] T.J. Mitchison, L.P. Cramer, Actin-based cell motility and cell locomotion, Cell 84 (1996) 371–379.

[42] A.L. Bishop, A. Hall, Rho GTPases and their effector proteins, Biochem. J. 348 (Pt. 2) (2000) 241–255.

[43] N. Tapon, A. Hall, Rho, Rac and Cdc42 GTPases regulate the organization of the actin cytoskeleton, Curr. Opin. Cell Biol. 9 (1997) 86–92.

[44] T.S. Lewis, P.S. Shapiro, N.G. Ahn, Signal transduction through MAP kinase cascades, Adv. Cancer Res. 74 (1998) 49–139.

[45] A. Minden, A. Lin, F.X. Claret, A. Abo, M. Karin, Selective activation

of the JNK signaling cascade and c-Jun transcriptional activity by the small GTPases Rac and Cdc42Hs, Cell 81 (1995) 1147–1157.

[46] M.J. Robinson, M.H. Cobb, Mitogen-activated protein kinase pathways, Curr. Opin. Cell Biol. 9 (1997) 180–186.

[47] R.L. Klemke, S. Cai, A.L. Giannini, P.J. Gallagher, P. de Lanerolle, D.A. Cheresh, Regulation of cell motility by mitogen-activated protein kinase, J. Cell Biol. 137 (1997) 481–492.

[48] L. Yin, N. Bennani-Baiti, C.T. Powell, Phorbol ester-induced apoptosis of C4-2 cells requires both a unique and a redundant protein kinase C signaling pathway, J. Biol. Chem. 280 (2004) 5533–5541.

[49] K. Kawamura, K. Takano, S. Suetsugu, S. Kurisu, D. Yamazaki, H. Miki, T. Takenawa, T. Endo, N-WASP and WAVE2 acting downstream of phosphatidylinositol 3-kinase are required for myogenic cell migration induced by hepatocyte growth factor, J. Biol. Chem. 279 (2004) 54862–54871.

[50] H. Miki, M. Fukuda, E. Nishida, T. Takenawa, Phosphorylation of WAVE downstream of mitogen-activated protein kinase signaling, J. Biol. Chem. 274 (1999) 27605–27609.

[51] L.M. McHardy, R. Sinotte, A. Troussard, C. Sheldon, J. Church, D.E. Williams, R.J. Andersen, S. Dedhar, M. Roberge, C.D. Roskelley, The tumor invasion inhibitor dihydromotuporamine C activates RHO, remodels stress fibers and focal adhesions, and stimulates sodium-proton exchange, Cancer Res. 64 (2004) 1468–1474.

[52] O.A. Coso, M. Chiariello, J.C. Yu, H. Teramoto, P. Crespo, N. Xu, T. Miki, J.S. Gutkind, The small GTP-binding proteins Rac1 and Cdc42 regulate the activity of the JNK/SAPK signaling pathway, Cell 81 (1995) 1137–1146.

[53] A. Minden, M. Karin, Regulation and function of the JNK subgroup of MAP kinases, Biochim. Biophys. Acta 1333 (1997) F85–F104.

npg

Silencing of the Tropomyosin-1 gene by DNA methylation alters tumor suppressor function of TGF-*β*

Andrea E Varga[1], Nina V Stourman[1], Qiao Zheng[1], Alfiya F Safina[1], Lei Quan[1], Xiurong Li[1], Khalid Sossey-Alaoui[1] and Andrei V Bakin*,[1]

[1]*Department of Cancer Genetics, Roswell Park Cancer Institute, Buffalo, NY 14263, USA*

Loss of actin stress fibers has been associated with cell transformation and metastasis. TGF-*β* induction of stress fibers in epithelial cells requires high molecular weight tropomyosins encoded by TPM1 and TPM2 genes. Here, we investigated the mechanism underlying the failure of TGF-*β* to induce stress fibers and inhibit cell migration in metastatic cells. RT–PCR analysis in carcinoma cell lines revealed a significant reduction in TPM1 transcripts in metastatic MDA-MB-231, MDA-MB-435 and SW620 cell lines. Treatment of these cells with demethylating agent 5-aza-2′-deoxycytidine (5-aza-dC) increased mRNA levels of TPM1 with no effect on TPM2. Importantly, 5-aza-dC treatment of MDA-MB-231 cells restored TGF-*β* induction of TPM1 and formation of stress fibers. Forced expression of TPM1 by using Tet-Off system increased stress fibers in MDA-MB-231 cells and reduced cell migration. A potential CpG island spanning the TPM1 proximal promoter, exon 1, and the beginning of intron 1 was identified. Bisulfite sequencing showed significant cytosine methylation in metastatic cell lines that correlated with a reduced expression of TPM1. Together these results suggest that epigenetic suppression of TPM1 may alter TGF-*β* tumor suppressor function and contribute to metastatic properties of tumor cells.
Oncogene (2005) **24**, 5043–5052. doi:10.1038/sj.onc.1208688; published online 9 May 2005

Introduction

The transforming growth factor beta (TGF-*β*) signaling pathway is a major cellular growth inhibitory and proapoptotic pathway in epithelial, endothelial, hematopoietic and other cell types (Roberts and Wakefield, 2003). Clinical and experimental studies indicate that TGF-*β* can enhance the metastatic behavior of the tumor cells (Saito *et al.*, 2000; Derynck *et al.*, 2001). This apparent paradox has been associated with a progressive decline in TGF-*β* antitumorigenic function

and a gain of protumorigenic activities including induction of epithelial to mesenchymal transition (EMT), cell migration and invasion during tumor progression (Derynck *et al.*, 2001; Roberts and Wakefield, 2003). Oncogenic Ras, Src and ErbB2 as well as alterations in TGF-*β* signaling mediated by Smads, mitogen-activated protein (MAP) kinases, Rho kinases and Akt/PKB are thought to contribute to the metastatic phenotype (Derynck *et al.*, 2001; Roberts and Wakefield, 2003).

The actin cytoskeleton plays a central role in the regulation of cellular processes linked to metastasis including cell proliferation, apoptosis, anchorage-independent cell growth, cell migration, and invasion (Jaffe and Hall, 2002). Oncogenic transformation alters regulation and organization of the actin cytoskeleton by suppressing actin-binding proteins involved in stabilization of actin microfilaments (Pawlak and Helfman, 2001) or by disabling the RhoA/ROCK pathway (Sahai *et al.*, 2001; Pawlak and Helfman, 2002a, b; Vial *et al.*, 2003). In normal and tumor epithelial cells, TGF-*β* regulates dynamics of the actin cytoskeleton (Bakin *et al.*, 2002; Edlund *et al.*, 2002) through mechanisms involving Smads (Piek *et al.*, 1999), Rho kinase (Bhowmick *et al.*, 2001) and p38 MAP kinase (Hannigan *et al.*, 1998; Bakin *et al.*, 2002; Edlund *et al.*, 2002). A recent study has shown that high molecular weight (HMW) tropomyosins are critical components of Smad/p38MAPK-dependent actin stress fiber formation in response to TGF-*β* in epithelial cells (Bakin *et al.*, 2004). In normal and tumor nonmetastatic epithelial cells TGF-*β* upregulates HMW tropomyosins through p38MAPK- and Smad-dependent mechanisms leading to the formation of stable actin filaments (stress fibers) and reduction of cell motility (Bakin *et al.*, 2004). Tropomyosins have been implicated in the assembly and stabilization of actin filaments and control of cell motility (Pawlak and Helfman, 2001). Tropomyosins form *α*-helical coil-coil dimers that bind along the length of the actin filaments interacting with 6–7 actin monomers and stabilize actin filaments (Ayscough, 1998). In vertebrates, more than 10 different isoforms of HMW tropomyosins are expressed from TPM1 (*α*-TM) and TPM2 (*β*-TM) genes, and by alternative RNA splicing (Pittenger *et al.*, 1994). Early studies have shown that cell transformation by oncogenic Ras and Src leads to downregulation of HMW tropomyosins and

disruption of actin stress fiber filaments (Leonardi et al., 1982; Hendricks and Weintraub, 1984). Subsequently, it has been found that ectopic expression of HMW tropomyosins in Ras-transformed fibroblasts restores stress fibers and significantly reduces cell motility and cell growth (Braverman et al., 1996; Gimona et al., 1996; Janssen and Mier, 1997). Several studies have reported that high-grade tumors of breast, prostate, bladder and brain express significantly lower levels of HMW tropomyosins compared to normal tissues (Franzen et al., 1996; Wang et al., 1996; Hughes et al., 2003; Raval et al., 2003; Pawlak et al., 2004). Thus, HMW tropomyosins and thereby stress fibers may play a critical role in control of tumor invasion and metastasis.

Previously, we have reported that TPM1 was not regulated by TGF-β1 in metastatic breast cancer MDA-MB-231 cells (Bakin et al., 2004), although these cells express TGF-β receptors and Smad signaling components (Dumont et al., 2003). Here we investigated the mechanism underlying suppression of TPM1 gene expression in metastatic cells. Our data show that suppression of TPM1 gene expression is associated with hypermethylation of CpG sites within the TPM1 promoter in metastatic breast and colon cell lines. Demethylation of MDA-MB-231 cells restored TGF-β induction of TPM1 expression and stress fiber formation. Expression of tropomyosin in MDA-MB-231 cells using Tet-Off system inhibited cell migration. Thus, epigenetic inactivation of TPM1 may alter TGF-β tumor suppressor function and contribute to acquisition of malignant phenotype.

Results

Stress fiber formation in response to TGF-β in epithelial cells

We investigated TGF-β induction of tropomyosins and actin stress fibers in human lung epithelial A549 cells, cervical carcinoma SiHa cells and breast carcinoma MDA-MB-231 cells (Figure 1a). Treatment of cells with TGF-β resulted in the formation of stress fibers in SiHa and A549 cells, but not in MDA-MB-231 cells (Figure 1a). Tropomyosin expression was analysed with the TM311 monoclonal antibody recognizing the N-terminal epitope in tropomyosin 1 (TM1), a TPM2 gene product, and tropomyosin isoforms 2, 3 and 6 (TM2,3,6), products of the TPM1 gene (Temm-Grove et al., 1998). Immunoblotting showed that TGF-β stimulated expression of TM1-3, and 6 in A549 and SiHa cells. TPM1 gene products were not expressed in MDA-MB-231 cells, while TM1, a TPM2 product, was expressed at significantly lower levels compared to SiHa cells (Figure 1b). RT–PCR with gene-specific primers showed TPM2 mRNA expression in both cell lines, whereas TPM1 mRNA was induced by TGF-β in SiHa and A549 cells but not in MDA-MB-231 cells (Figure 1c). MDA-MB-231 cells express TGF-β receptors, Smad factors, and respond to TGF-β with activation of Smad and p38 MAPK signaling, as well
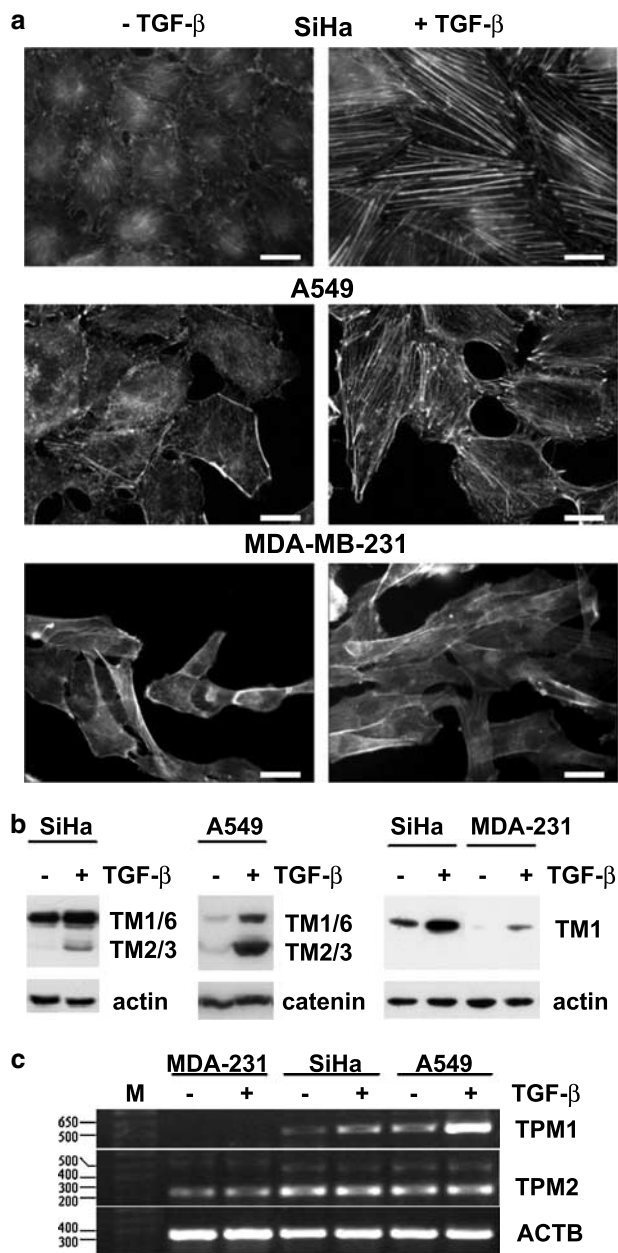

Figure 1 Actin stress fibers and tropomyosin expression are upregulated by TGF-β1 in epithelial cells. (a) Staining of actin filaments with phalloidin Alexa Green. Induction of stress fibers after 24 h incubation with TGF-β1. Scale bar, 20 μm. (b) Increased accumulation of tropomyosins in SiHa, A549, and MDA-MB-231 cells after TGF-β1 treatment for 24 h, as shown by immunoblotting with the TM311 antibody. (c) RT–PCR analysis of mRNA levels for TPM1, TPM2 and β-actin in MDA-MB-231, SiHa and A549 cell lines treated with TGF-β1 for 24 h

as regulation of gene expression (Bakin et al., 2002; Dumont et al., 2003). Hence, the absence of TPM1 expression in MDA-MB-231 cells could arise from genetic or epigenetic abnormalities in the TPM1 gene or because tissue-specific differences in cell lines used.

Together, these results indicate that the ability of TGF-β to induce stress fibers in epithelial cells correlates

with expression of HMW tropomyosins, and that the absence of TGF-β-induced stress fibers in MDA-MB-231 cells may be associated with loss of TPM1 expression and low expression of TPM2.

Suppression of TPM1 expression in metastatic breast cancer cell lines by DNA methylation

To rule out the involvement of tissue-specific differences, mRNA levels of TPM1 and TPM2 were compared in several commonly used human mammary and colon epithelial cell lines by RT–PCR. TPM1 transcripts were expressed in normal MCF10A and several breast carcinoma cell lines, but were absent or found at lower levels in metastatic MDA-MB-231 and MDA-MB-435 cell lines (Figure 2a). TPM2 transcripts were present at comparable levels in all examined breast cell lines (Figure 2a). Of note, although TPM2 was expressed in MCF7 cells no TM1 protein was detected by immunoblotting (A Bakin, unpublished; Bharadwaj and Prasad, 2002), suggesting a post-transcriptional regulation of the TPM2 gene expression in these cells. To further test a correlation between TPM1 expression and a metastatic behavior of tumor cells, tropomyosin transcripts were examined in two colon cancer cell lines established from primary tumor (SW480) and a metastatic lesion (SW620) of the same patient (Gagos et al., 1995). TPM2 was expressed in both cell lines, whereas TPM1 transcripts were below a detection level in metastatic SW620 cells (Figure 2d). These results indicate that TPM1 is expressed in normal mammary epithelial cells, but significantly reduced or absent in metastatic cell lines.

To determine whether DNA methylation contributes to suppression of the TPM1 gene in breast cancer MDA-MB-231 and MDA-MB-435 cell lines, tumor cells were treated with demethylating agent 5-aza-dC. RT–PCR analysis showed that 5-aza-dC treatment restored TPM1 expression in MDA-MB-435 cells to the levels comparable with MCF10A and MCF7 cell lines (Figure 2b). Treatment with 5-aza-dC of MDA-MB-231 cells increased TPM1 mRNA levels that were further upregulated by TGF-β1 (Figure 2c). TPM2 transcripts were reduced by approximately 40% in 5-aza-dC-treated cells (Figure 2d), although, TPM2 protein level (TM1 isoform) was induced (Figure 3b), suggesting indirect effect of 5-aza-dC on TPM2 expression. These results indicate that DNA methylation may be involved in suppression of the TPM1 gene expression in metastatic carcinoma cell lines, and that low expression of HMW tropomyosins correlates with metastatic phenotype of tumor cells.

Re-expression of TPM1 in MDA-MB-231 cells results in stress fiber formation

To verify RT–PCR data and to test effects of TPM1 expression on stress fiber formation, we examined tropomyosin proteins and actin filaments in 5-aza-dC-treated MDA-MB-231 cells. Smad2/3 phosphorylation in response to TGF-β1 was not affected in MDA-MB-
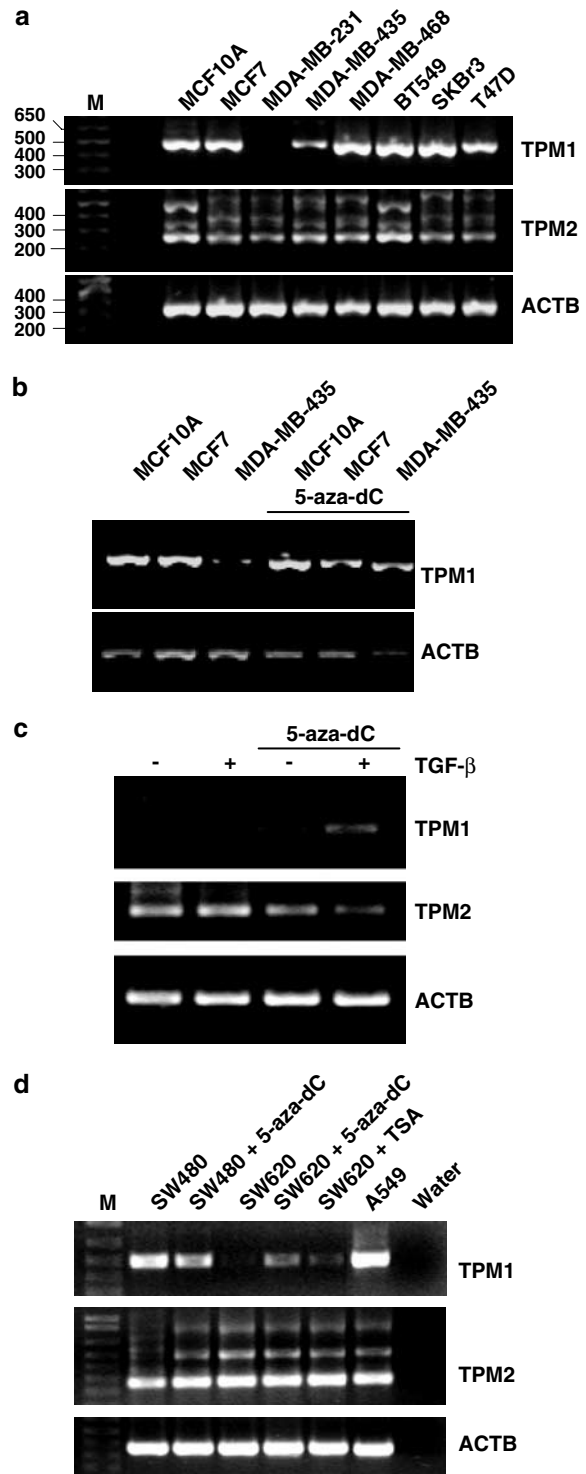
Figure 2 RT–PCR analysis of TPM1 and TPM2 expression. (a) TPM1 and TPM2 mRNA levels in human mammary epithelial cell lines. In (a–d), β-actin (ACTB) was used as a control. (b) Effect of 5-aza-dC treatment on TPM1 mRNA levels in human mammary epithelial cell lines. (c) TPM1 and TPM2 expression in MDA-MB-231 cells treated with 5-aza-dC and TGF-β1. (d) TPM1 and TPM2 mRNA in human colon carcinoma SW480 and SW620 cells, and lung carcinoma A549 cells

a

5-aza-dC

0 1 0 1 h, TGF-β

p-Smad2/3

Smad2/3

b

5-aza-dC

0 6 24 0 6 24 h, TGF-β

TM1
TM3

actin

c

5-aza-dC

0 1 24 0 1 24 h, TGF-β

p-ERK1/2

ERK1/2

catenin

d

- TGF-β   Control   + TGF-β
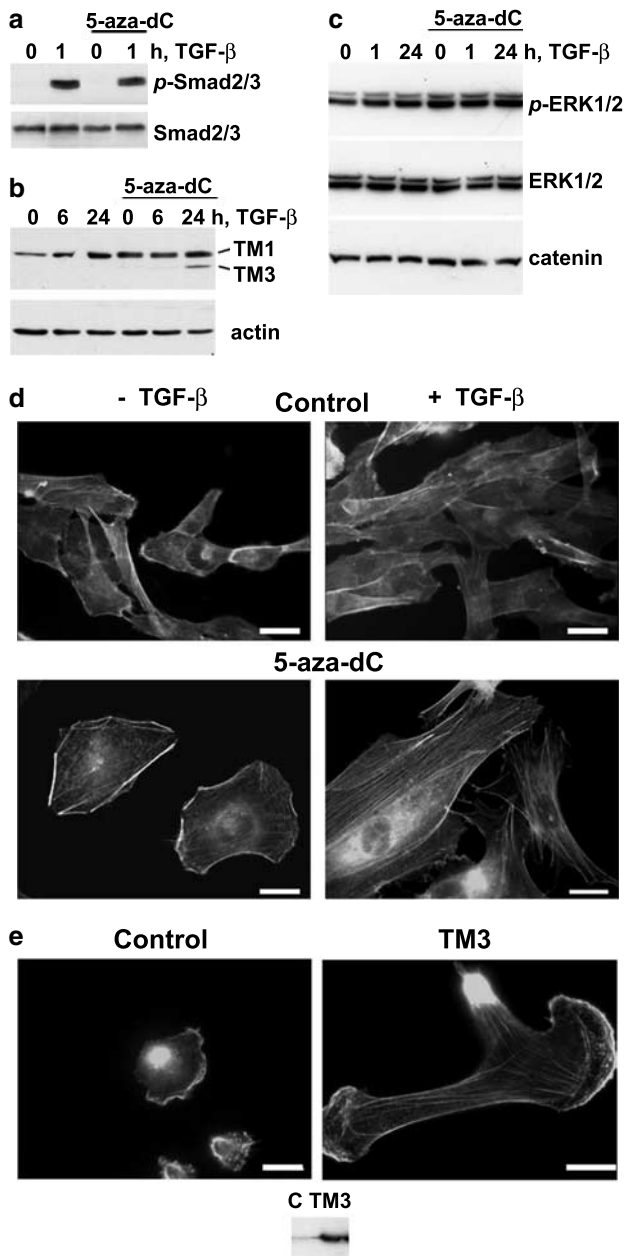
5-aza-dC

e

Control   TM3

C TM3

Figure 3 Restoration of TGF-β-mediated induction of tropomyosins and stress fibers in MDA-MB-231 cells treated with 5-aza-dC. (**a**) Phosphorylation of Smad2/3 in cells treated with 5-aza-dC and TGF-β1. (**b**) Immunoblot detection of TM proteins using TM311 antibody in cells treated with TGF-β1. (**c**) Immunoblot with antibodies to phospho-ERK1/2 ERK1/2, and α-catenin in cells treated with 2 ng/ml TGF-β1. (**d**) Phalloidin staining of actin microfilaments in control and 5-aza-dC-treated MDA-MB-231 cells incubated −/+ 2 ng/ml TGF-β1 for 24 h. (**e**) Actin microfilaments in MDA-MB-231 cells transfected with plasmid encoding HA-tagged-TM3 and empty vector control. Inset shows immunoblot with anti-HA antibody. Scale bar, 20 μm.

231 cells by 5-aza-dC treatment (Figure 3a). Immunoblot analysis revealed induction of TM2/3 isoforms by TGF-β1 in 5-aza-dC-treated MDA-MB-231 cells and enhancement of basal TM1 expression (Figure 3b). Since MEK–ERK signaling may affect tropomyosin

Control   5-aza-dC
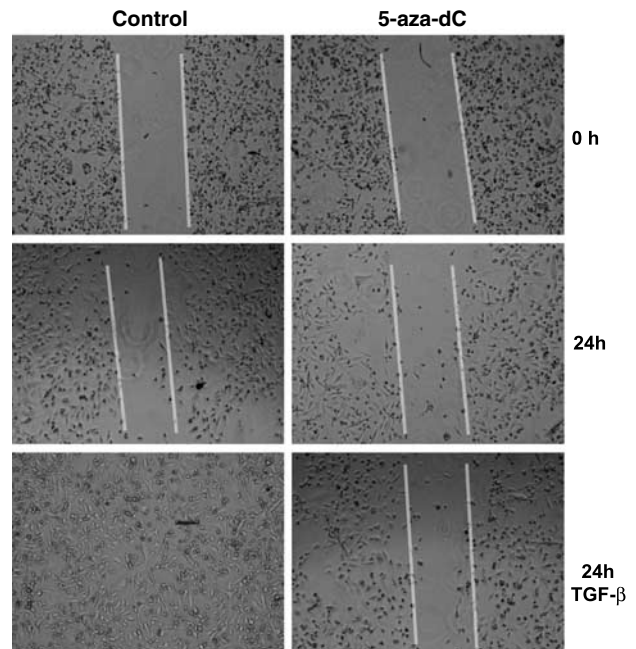
0 h

24h

24h
TGF-β

Figure 4 Inhibition of cell migration by 5-aza-dC treatment. Wound closure in monolayers of control and 5-aza-dC-treated MDA-MB-231 cells in the presence or absence of 1 ng/ml TGF-β1. Microphotographs were taken at ×100 magnification. Lines show wound edges. The wound is closed in control cells incubated with TGF-β1 but not in 5-aza-dC-treated cells

expression (Bakin *et al.*, 2004), we examined phosphorylation and total levels of ERK1/2 in control and 5-aza-dC-treated MDA-MB-231 cells. Immunoblots showed that 5-aza-dC-treatment did not decrease levels of phospho-ERK1/2 and total ERK1/2 (Figure 3c). This result indicates that induction of TPM1 in 5-aza-dC-treated MDA-MB-231 cells cannot be explained by inhibition of ERK1/2.

Phalloidin staining showed higher levels of microfilaments in 5-aza-dC-treated MDA-MB-231 cells compared to control cells that were further enhanced by treatment with TGF-β1 (Figure 3d). Importantly, 5-aza-dC treatment inhibited wound closure in MDA-MB-231 cell monolayers in response to TGF-β1, indicating that de-methylation reduces cell migration (Figure 4).

We then asked whether ectopic expression of TM3 encoded by the TPM1 gene, in MDA-MB-231 cells is sufficient for stress fiber formation. Rat TM3 cDNA (Gimona *et al.*, 1996) was transiently transfected in MDA-MB-231 cells and expression of HA-tagged TM3 was confirmed by immunoblotting (Figure 3e, inset). Actin microfilament fibers were significantly increased in TM3-expressing cells even in the absence of TGF-β1 compared to control cells (Figure 3e). Selection of stable TM3 clones failed as TM3-expressing cells did not grow and eventually died due to block in cytokinesis and accumulation of multiple nuclei. To overcome this problem we generated MDA-MB-231 Tet-Off cells with inducible expression of rat TM3. Expression of tropomyosin was induced by incubating the Tet-Off cells in the absence of doxycycline (Figure 5a). The achieved

level of tropomyosin was nearly 50% of MCF7 cells. TM3-expressing cells showed an increase in actin microfilament fibers and reduction in actin ruffles at the cell edges compared to cells grown in the presence of doxycycline when TM3 is not expressed (Figure 5b). Migration of TM3-expressing cells in transwell assay was reduced approximately 1.7-fold (Figure 5c, d).

These results suggest that DNA methylation is involved in silencing of the TPM1 gene in MDA-MB-

Figure 5 Expression of TM3 using Tet-Off system in MDA-MB-231 cells increases actin fibers and reduces cell migration. (**a**) Immunoblot of tropomyosin and α-catenin, a loading control, in MDA-MB-231-Tet-Off cell line incubated alone or with 1 μg/ml doxycycline for 24 h. (**b**) Removal of doxycycline increases actin microfilament fibers in MDA-MB-231-Tet-Off cells. Scale bar, 20 μm. (**c**) Transwell migration assay of the Tet-Off cells incubated alone or with 2 μg/ml doxycycline for 16 h. The cells that had migrated through pores to the lower surface were stained with Diff-quick stain. (**d**) Average amount of cells per field. Cells were counted from five random fields at ×200 magnification. Assays were carried out in duplicates

231 cells, and that re-expression of TPM1 leads to stress fibers and reduces cell migration.

Identification of a CpG island in the TPM1 promoter

The TPM1 gene is expressed in most tissues and its disruption in mice results in early embryonic lethality, suggesting that it is critically involved in development (Robbins, 1998). We hypothesized that TPM1 may contain a CpG island in the promoter. As no studies have reported on the DNA structure of human TPM1 gene, database-mining was performed to define the exon–intron structure, promoter and CpG island of human TPM1 gene. Comparison of the 5′ cDNA sequences of mammalian TPM1 with mouse and human genomic DNA (gDNA) sequences obtained from BLAT (http://genome.ucsc.edu/cgi-bin/hgBlat) using ClustalW (http://www.ebi.ac.uk/clustalw) revealed that the 5′-end of the mouse cDNA is located within 21 bp from a TATATA sequence, which is identical in both human and mouse gDNA sequences (Figure 6a). The potential TATA box is located in the highly conserved gDNA region containing several Sp1-like binding sequences.

The analysis of gDNA sequences using BLAT revealed two large CpG islands in both human *TPM1* and mouse *Tpm1*, with one near exon 1 and the other in a region further downstream, in a sequence aligning with rat exon 1b (GenBank accession M34137). The CpG islands of both human and mouse TPM1 conformed to the CpG island definition (Antequera and Bird, 1993; Cross and Bird, 1995). The two human TPM1 CpG islands are of length 1.829 kb with 163 CpG sites, a G/C content of 67% and a CpG : GpC ratio of 0.8; and 1.208 kb with 110 CpG sites, a G/C content of 70% and a CpG : GpC ratio of 0.71, covering putative exons 1 and 1b, respectively. The human 1.8 kb TPM1 CpG island encompasses the transcription start, exon 1 and a portion of intron 1 (Figure 6a). This region contains several potential Sp1-binding sites overlapping with CpG dinucleotides. To test whether Sp1 is involved in TPM1 expression, mouse mammary epithelial NMuMG cells were treated with TGF-β1 in the presence of MTA, which inhibits Sp1 binding to DNA and TGF-β1-induced gene expression (Chung et al., 1996; Albo et al., 1997; Greenwel et al., 1997; Park et al., 2000). Treatment with 200 nM MTA significantly reduced basal and TGF-β1-induced levels of TPM1 transcripts, suggesting involvement of Sp1-like factors in TGF-β1-mediated induction of the TPM1 expression (Figure 6b).

Thus, both human and mouse TPM1 genes contain CpG islands, and the proximal promoter CpG island includes a putative transcription start site, the TATA box and Sp1-like sites.

Methylation of the TPM1 CpG island in metastatic cell lines

We investigated DNA methylation of the human 1.8 kb TPM1 CpG island by the bisulfite-sequencing method (Frommer et al., 1992). PCR primers were designed to
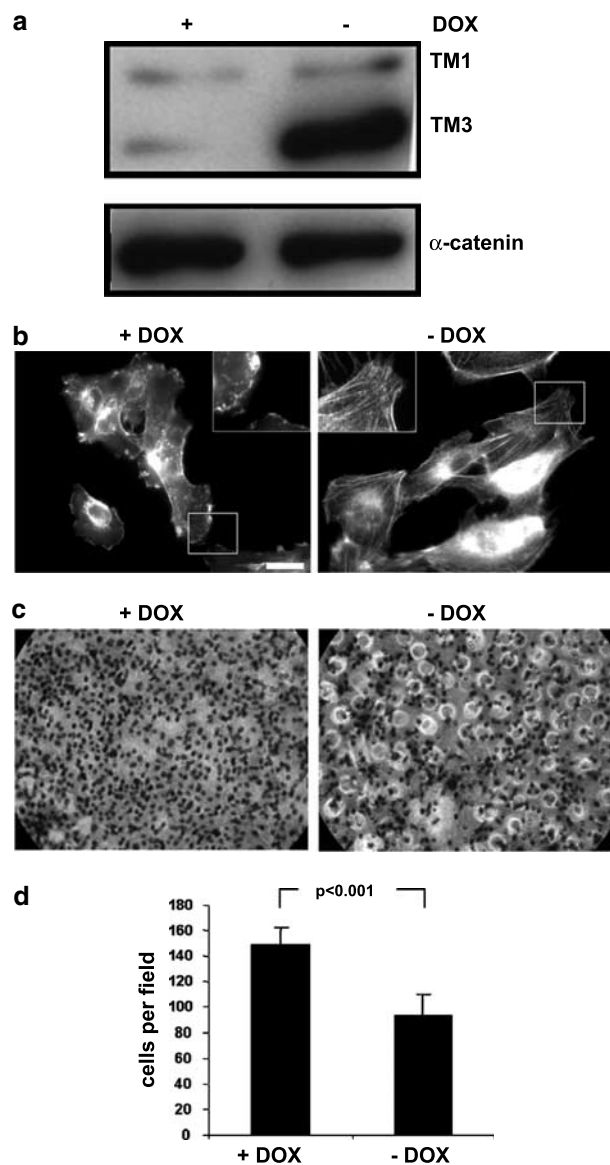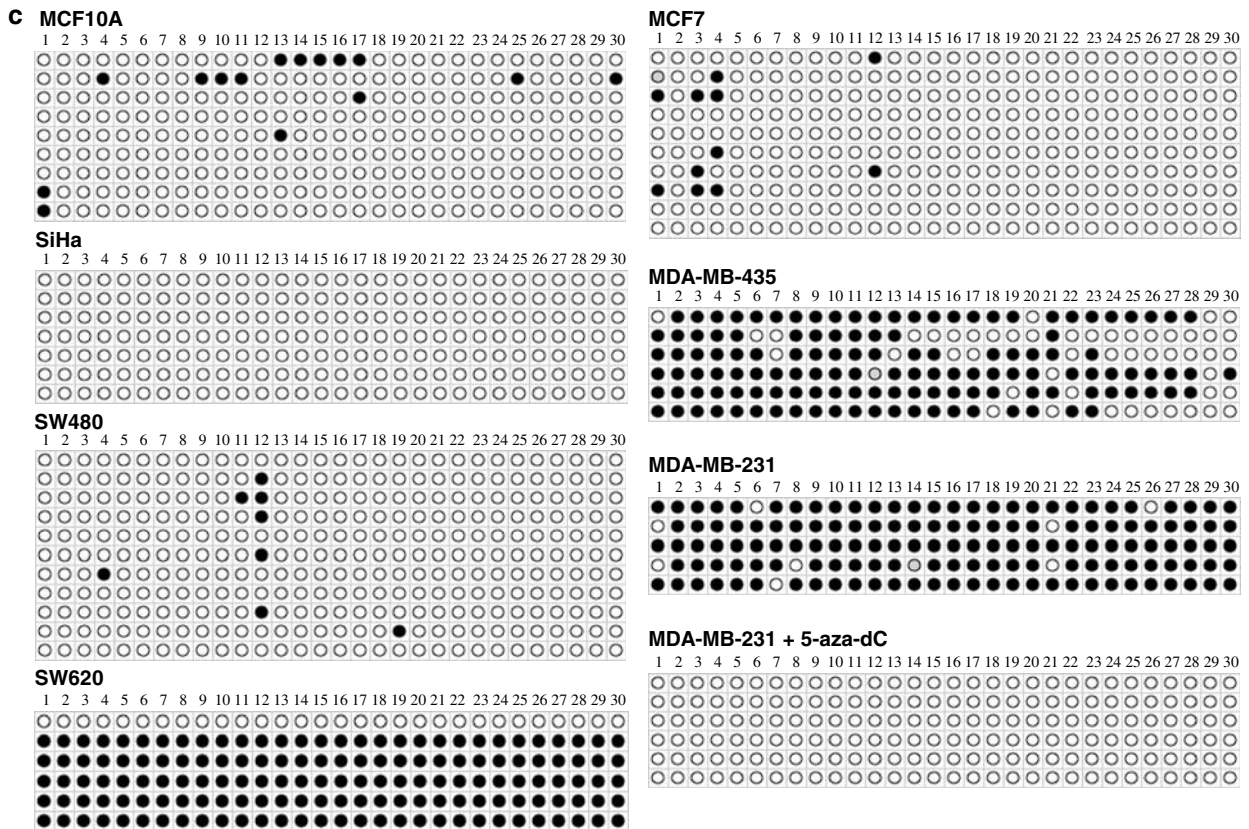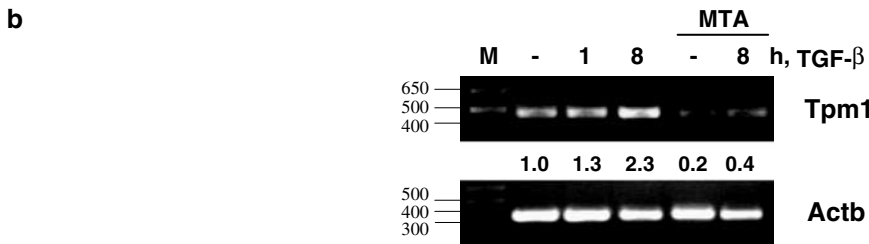
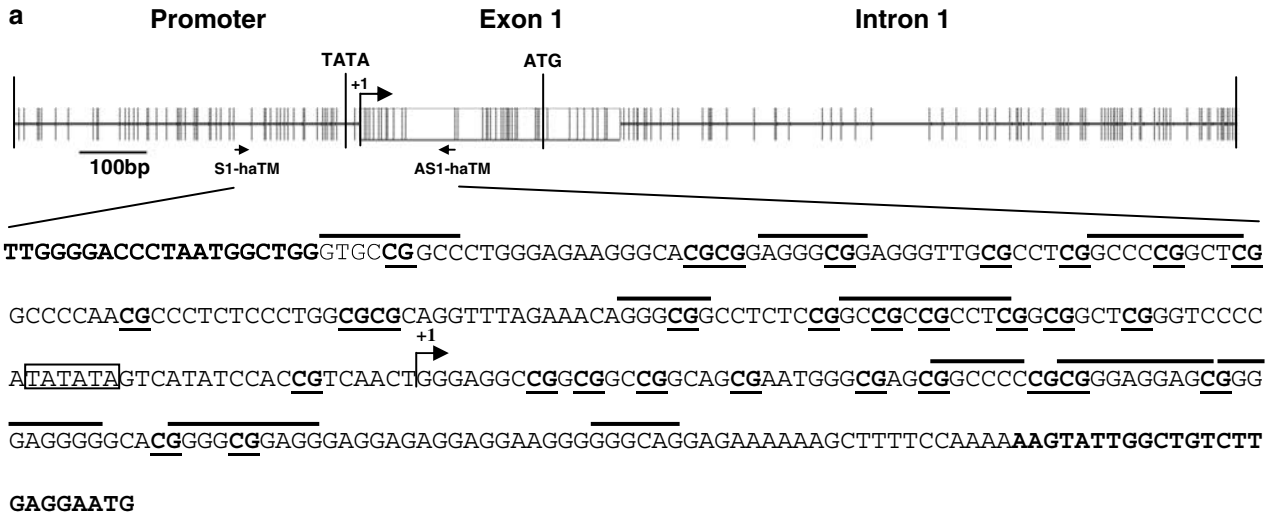amplify a 328 bp fragment of TPM1 containing 30 CpG dinucleotides and several potential Sp1-binding sites (Figure 6a). gDNA samples from several cell lines were extracted and treated with bisulfite. DNA fragments were amplified using bisulfite-treated DNA samples, subcloned, and both DNA strands were sequenced. The

a

Promoter   Exon 1   Intron 1

TATA   ATG

+1

100bp   S1-haTM   AS1-haTM

TTGGGGACCCTAATGGCTGGGTGC**CG**GCCCTGGGAGAAGGGCA**CGCG**GAGGG**CG**GAGGGTTG**CG**CCT**CG**GCCCC**CG**GCT**CG**

GCCCCAA**CG**CCCTCTCCCTGG**CGCG**CAGGTTTAGAAACAGGG**CG**GCCTCTC**CG**GC**CG**C**CG**CCT**CG**GC**CG**GCT**CG**GGTCCCC

+1

A TATATA GTCATATCCAC**CG**TCAACTGGGAGGC**CG**GC**CG**GC**CG**GCAG**CG**AATGGG**CG**AG**CG**GCCCC**CGCG**GGAGGAGC**CG**GG

GAGGGGGCA**CG**GGG**CG**GAGGGAGGAGAGGAGGAAGGGGGGCAGGAGAAAAAAGCTTTTCCAAAA**AAGTATTGGCTGTCTT**

GAGGAATG

b

MTA

M   -   1   8   -   8   h, TGF-β

650
500
400   **Tpm1**

1.0   1.3   2.3   0.2   0.4

500
400
300   **Actb**

c   MCF10A

SiHa

SW480

SW620

MCF7

MDA-MB-435

MDA-MB-231

MDA-MB-231 + 5-aza-dC

bisulfite modification was complete in all reactions, as all cytosine residues not associated with CpG dinucleotides were converted to thymine residues (data not shown). The methylation status of 30 CpG dinucleotides sites in cell lines is shown in Figure 6c. DNA-bisulfite-sequencing showed a nearly complete methylation of CpG sites in MDA-MB-231 cells and a high degree of methylation in MDA-MB-435 cells (Figure 6c). The level of DNA methylation inversely correlated with expression level of TPM1 mRNA in these cells (Figure 6c and 2a). 5-aza-dC-treatment of MDA-MB-231 resulted in demethylation of cytosine residues (Figure 6c) and increased TPM1 expression (Figure 2c, 3b). Colon cancer SW480 cell line showed a low level of DNA methylation and also expressed TPM1 mRNA (compare Figure 6c and 2d). Metastatic SW620 cell line showed a high level of DNA methylation (Figure 6c) and very low levels of TPM1, which was upregulated by 5-aza-dC treatment (Figure 2d).

Thus, high level of methylation of TPM1 promoter region correlates with low TPM1 expression and demethylation of DNA upregulates TPM1 expression in metastatic cell lines.

Discussion

The molecular mechanism(s) underlying the prometastatic conversion of the TGF-β function at the late stages of tumorigenesis is not well understood (Derynck *et al.*, 2001; Roberts and Wakefield, 2003). TGF-β function in development of highly invasive and metastatic tumors has been associated with induction of EMT, cell migration and activity of matrix proteinases (Derynck *et al.*, 2001; Wakefield and Roberts, 2002). Recent studies have shown that stimulation of cell migration by TGF-β inversely correlates with expression of HMW tropomyosins encoded by TPM1 and TPM2 genes involved in formation of stable actin filaments (stress fibers) (Bakin *et al.*, 2004). Here, we report that TPM1 promoter hypermethylation correlates with a reduced expression of tropomyosins and inability of TGF-β to induce stress fibers in metastatic carcinoma cells.

Tropomyosins are actin-binding proteins involved in stabilization of actin filaments and control of cell motility (Pawlak and Helfman, 2001). Although the role of tropomyosins in muscle contraction is well established, their role in non-muscle cells is less clear. Several lines of evidence suggest that HMW tropomyosins encoded by TPM1 (α-TM) and TPM2 (β-TM) genes may contribute in tumor suppressor activity of TGF-β: (i) HMW tropomyosins are required for TGF-β-mediated formation of stress fibers and inhibition of cell migration (Bakin *et al.*, 2004); (ii) oncogenic Ras and Src downregulate HMW tropomyosins leading to disruption of actin stress fiber filaments (Hendricks and Weintraub, 1981; Leonardi *et al.*, 1982) and ectopic expression of HMW tropomyosins in Ras- or Src-tranformed cells restores stress fibers and reduces cell motility and cell growth (Braverman *et al.*, 1996; Gimona *et al.*, 1996; Janssen and Mier, 1997); and (iii) high-grade tumors of breast, prostate, bladder, and brain express significantly lower levels of HMW tropomyosins compared to normal tissues (Franzen *et al.*, 1996; Wang *et al.*, 1996; Hughes *et al.*, 2003; Raval *et al.*, 2003; Pawlak *et al.*, 2004).

In this study, a marked reduction in HMW tropomyosin was found in metastatic breast and colon cancer cell lines (Figure 2). Low tropomyosin levels in metastatic breast cancer MDA-MB-231 cells correlated with a reduced stress fiber formation in response to TGF-β (Figure 1). Recently, we have reported that Ras-MEK signaling decreases TPM2 expression and stress fiber formation in MDA-MB-231 cells (Bakin *et al.*, 2004). The current study showed the absence of basal and TGF-β1-regulated expression of the TPM1 gene in MDA-MB-231 cells, although these cells express TGF-β receptors and Smad signaling components (Dumont *et al.*, 2003). TPM1 mRNA expression is also reduced in metastatic breast cancer MDA-MB-435 cell line and in metastatic colon cancer SW620 cell line (Figure 2). Interestingly, colon cancer SW480 cell line established from the primary lesion of the same patient expressed higher level of TPM1 compared to metastatic SW620. These findings show that low level of TPM1 expression correlates with metastatic phenotype of tumor cells.

Treatment of metastatic breast and colon cancer cell lines with demethylating agent 5-aza-dC increased TPM1 expression (Figure 2). Previously, one study has reported that 5-aza-dC treatment upregulates expression of TPM2, but not TPM1, in MCF7 and MDA-MB-231 cell lines (Bharadwaj and Prasad, 2002), while another group showed that both TPM1 and TPM2 are up-regulated in fibrosarcoma HT1080 cells (Shields *et al.*, 2002). Both of the studies used Northern blot probes that do not distinguish TPM1 and TPM2 genes. In the

Figure 6 The human TPM1 promoter and methylation of a CpG island. (**a**) Depiction of the 1829 bp CpG island within the human TPM1 promoter. The transcription initiation site is shown as $+1$. The TATA-like sequence is boxed. Sp1-like sites are depicted above the sequence. The CpG dinucleotides are in bold font and underlined. The positions of the bisulfite-specific primers relative to the promoter and exon 1 are shown. (**b**) Effect of mithramycin A on Tpm1 expression in response to TGF-β1 in NMuMG cells examined by RT–PCR. β-actin (Actb) is a control. (**c**) Methylation analysis of 30 CpG pairs from a 328 bp region of the human TPM1 CpG island in human cell lines and tissue samples. The presence of methylated cytosine at CpG sites in DNA from cancer-derived cell lines and 5-aza-dC-treated MDA-MB-231. PCR fragments of bisulfite treated DNA were cloned into pGEM-Teasy and sequenced in both directions. The sequencing results for the individual CpG sites are depicted. Each horizontal line depicts a single clone and black circles represent methylated cytosines; open circles: unmethylated cytosines; and gray circles: equivocal data. CpG sites are positioned with respect to the $+1$ (Figure 4): $-162, -143, -141, -134, -124, -119, -113, -108, -99, -85, -83, -64, -55, -51, -48, -43, -40, -35, -8, +8, +11, +15, +21, +29, +33, +40, +42, +51, +64, +69$

current study, RT–PCR with TPM1 and TPM2 gene-specific primers was used to show that TPM2 transcripts are expressed at comparable levels in all tested breast cancer and normal cell lines, whereas TPM1 is down-regulated in metastatic MDA-MB-231, MDA-MB-435 and SW620 cell lines (Figure 2). 5-aza-dC treatment significantly enhanced TPM1 mRNA levels but not TPM2 in all three metastatic cell lines (Figure 2). These data suggest that methylation may not regulate TPM2 expression directly. Demethylation of MDA-MB-231 cells restored the ability of TGF-β to induce TPM1 expression, stress fibers and reduced cell migration (Figures 3 and 4), suggesting that silencing of TPM1 by DNA methylation reduces stress fibers and enhances cell motility.

Importantly, expression of TPM1 gene product in MDA-MB-231 cells using Tet-Off system increased stress fibers and reduced cell migration (Figure 5). However, TGF-β can induce stress fibers even in the absence of TPM1 expression (Bakin et al., 2004). A forced expression of either TPM1 or TPM2 can reduce anchorage-independent cell growth (Boyd et al., 1995; Braverman et al., 1996; Masuda et al., 1996) and TPM2 can induce anoikis (Raval et al., 2003). These facts suggest that a critical threshold level of HMW tropomyosins encoded by TPM1 and TPM2 genes is required for stress fiber formation in response to TGF-β in epithelial cells.

Database-mining revealed in both human and mouse TPM1 genes a CpG island within a proximal promoter region, which includes the TATA box, a putative transcription start site, and several Sp1-like sites (Figure 5). Bisulfite sequencing showed a high degree of cytosine methylation within the $-186 +142$ region of the TPM1 promoter in metastatic cell lines, but not in cell lines established from non-neoplastic (MCF10A) or primary tumors (MCF7, SiHa and SW480) (Figure 5c). Treatment with demethylating agent of metastatic breast cancer MDA-MB-231 cells removed methylation and upregulated TPM1 expression, suggesting an inverse correlation between TPM1 expression and hypermethylation of the TPM1 promoter.

Basal expression of TPM1 appears to not require Smad4 since TPM1 is expressed in Smad4-null MDA-MB-468 cells (Figure 2). However, Smad4 is required for TGF-β induction of TPM1 (Bakin et al., 2004). Experiments with MTA suggest that Sp1 or Sp1-like factors may contribute to basal and TGF-β-mediated expression of TPM1 (Figure 5b). Thus, TPM1 may represent a group of TGF-β target genes that are regulated by both Sp1 and Smads including p21CIP1 (Moustakas and Kardassis, 1998), alpha2 collagen (Chung et al., 1996; Greenwel et al., 1997) and p15Ink4B (Feng et al., 2000). Interestingly, Sp1-mediated expression of p21Cip1 is sensitive to DNA methylation (Zhu et al., 2003). Thus, cytosine methylation in Sp1-like sites of the TPM1 promoter may contribute in suppression of basal and TGF-β-induced expression of TPM1.

In summary, our studies revealed that hypermethylation of the TPM1 promoter associates with a reduced TPM1 expression in metastatic cell lines. Suppression of

TPM1 may underlie failure of TGF-β to induce stress fibers and to inhibit migration in metastatic cells. Thus, epigenetic suppression of tropomyosin-mediated stress fibers may represent an essential characteristic of pro-metastatic changes in TGF-β function and restoration of the stress fiber response is a potential strategy for antimetastatic therapy.

Materials and methods

Cell lines

Human cell lines of breast carcinoma MCF7, MDA-MB-231, MDA-MB-435, MDA-MB-453, MDA-MB-468, BT549, SKBr3 and T-47D, normal breast MCF10A, cervical carcinoma SiHa, colon carcinoma SW480 and SW620, lung carcinoma A549 and mouse mammary epithelial cell line NMuMG were purchased from American Tissue Culture Collection (ATCC). Cell lines were cultured as recommended by ATCC.

Generation of Tet-Off MDA-MB-231 cells

Human breast carcinoma MDA-MB-231 cells (ATCC) were cotransfected with pBabe-Puro and ptTA-IRES-Neo plasmid (tTA, tet activator, IRES, internal ribosome entry site) (Yu et al., 1999). Puromycin-resistant clones exhibiting TGF-β responses equal to parental cells were selected in the presence of 1 μg/ml of puromycin. Two clones with a tight regulation of the tet-responsive reporter plasmid pBI-MCS-EGFP (Yu et al., 1999) were chosen to generate inducible cell lines. cDNA for rat tropomyosin 3 isoform (Gimona et al., 1996) was subcloned in pBluescript II KS(+) (Stratagene) at BamHI/XbaI sites and then shuttled into pTRE2hyg (BD Biosciences Clontech, Palo Alto, CA, USA) at NotI/SalI sites to generate pTRE2hygTM3. The MDA-MB-231 Tet-Off cell lines were transfected with pTRE2hyg-TM3 encoding un-tagged rat TM3 and cells retaining TGF-β responses were selected in the presence of 200 μg/ml hygromycin and 2 μg/ml doxycycline. Induction of TM3 expression by removal of doxycycline was confirmed by immunoblotting with TM311 antibody.

Antibodies, plasmids and other reagents

TGF-β1 was obtained from R&D Systems. The following antibodies were used: mouse monoclonal to Smad2/3 (BD Transduction Laboratories, BD Biosciences); rabbit polyclonal to hemaglutinin (HA) epitope (Santa Cruz Biotechnology, Inc.); mouse monoclonal TM311 to tropomyosin (Sigma); to phospho-Smad2/3, phosphor-ERK1/2 and total ERK1/2 (Cell Signaling). Phalloidin-Alexa Green and phalloidin-Texas Red were from Molecular Probes.

Isolation of DNA and RNA

DNA was isolated using the high salt extraction method (Miller et al., 1988). RNA was isolated as described in Bakin and Curran (1999).

5-aza-2′-deoxycytidine and TGF-β1 treatment of cell lines

MDA-MB-231 cells (1 × 10⁶) were seeded into 25 cm² flasks and were treated with 2 μM 5-aza-2′-deoxycytidine (5-aza-dC) for 48 h. Cells were washed with PBS, and were incubated in fresh media for a further 48 h. Cells were seeded into 25 cm² flasks and 2 μM 5-aza-dC treatment was repeated, followed by

the addition of media containing 5% serum. The next day, to cells requiring TGF-β1 treatment, 2 ng/ml TGF-β1 was added for 24 h. DNA, RNA and protein were extracted from samples. MCF10A, MCF7 and MDA-MB-435 were treated with 5-aza-dC as previously described (Li *et al.*, 2004).

Mithramycin A (MTA) treatment of cells

NMuMG cells (6×10^5) were seeded in media containing 5% serum. Cells were subsequently left untreated or treated with both 200 μM MTA and 2 ng/ml TGF-β1 for 1 or 8 h. Total RNA was analysed by RT–PCR for expression of TPM1 and β-actin.

RT–PCR

Amplification of transcripts was performed using 50 ng of total RNA and the one-step RT-PCR system from Invitrogen according to the manufacturer's protocol, using primers designed with the assistance of Primer3 (http://frodo.wi.mit.edu/cgi-bin/primer3/primer3_www.cgi). PCR in the one-step system were performed at an annealing temperature of 55°C within a linear range of amplification. Primer sequences: human TPM1, GenBank Acc# NM_000366, forward: 5′-GCTGGTGTCACTGCAAAAGA-3′, reverse: 5′-CTGCAGCCATTAATGCTTTC-3′; human TPM2, GenBank Acc# NM_003289, forward: 5′-AAGGAGGCCCAGGAGAAACT-3′, reverse: 5′-CTTCCTTCAGCTGCATCTCC-3′; human β-actin, GenBank Acc# NM_001101, forward: 5′-GCTCGTCGTCGACAACGGCTC-3′, reverse: 5′-CAAACATGATCTGGGTCATCTTCTC-3′; mouse Tpm1, GenBank Acc# NM_024427, forward: 5′-GCTGGTGTCACTGCAAAAGA-3′, reverse: 5′-CCTGAGCCTCCAGTGACTTC-3′; and mouse β-actin, GenBank Acc# NM_007393, forward: 5′-GCTGGTCGTCGACAACGGCTC-3′, reverse: 5′-CAAACATGATCTGGGTCATCTTTTC-3′. Forward and reverse primers for human TPM1 and TPM2 genes cover amino acids 43–48 and 205–209 of TPM1, and 65–71 and 145–150 amino acids of TPM2, respectively. The associated product sizes for human TPM1, TPM2, β-actin and mouse Tpm1 and β-actin were 506, 258, 353, 506 and 352 bp respectively.

Transient transfection

Plasmids encoding rat HA-tagged TM2 and TM3 isoforms (Gimona *et al.*, 1995) were obtained from David Helfman (CSHL, Cold Spring Harbor, NY, USA). In total, 10 μg plasmid was transfected with FuGENE 6 (Roche) into MDA-MB-231 cells, according to the manufacturer's instructions.

Identification of CpG island within the TPM1 promoter and bisulfite sequencing

The promoter region of human and mouse TPM1 genes were initially predicted using BLAST against rat exonic sequences, and then analysed in BLAT at http://genome.ucsc.edu/cgi-bin/hgBlat (Genome Bioinformatics Group, University of California, USA). Both human and mouse CpG islands were identified in BLAT. Primers S1-hαTM (5′-TTGGGGATTT-TAATGGTTGG-3′) and AS1-hαTM (5′-CATTCCTCAAAA-CAACCAATACTT-3′) amplifying bisulfite-treated DNA were designed with Primer3. Bisulfite treatment was performed as previously described (Varga *et al.*, 2004). PCR reactions were carried out under the following conditions: 3 min at 94°C, followed by 40 cycles of 30 s at 94°C, 30 s at 50°C, and 55 s at 72°C, followed by a final elongation for 7 min at 72°C before holding at 4°C. PCR products were resolved on a 1% agarose gel, purified with a PCR purification kit (Marligen Biosciences,

USA) and cloned into pGEM-Teasy (Promega, USA). Clones were isolated and sequenced in both directions and CpG sites were analysed for methylation.

Immunoblot analysis

Cells were incubated in medium containing 5% serum for 24 h prior to treatment with 2 ng/ml TGF-β1. Cells were lysed in buffer containing 20 mM Tris, pH 7.4, 137 mM NaCl, 1% NP-40, 10% glycerol, 20 mM NaF, 1 mM Na orthovanadate, 1 mM PMSF, 2 μg/ml aprotinin and 2 μg/ml leupeptin. Immunoblot analyses of whole-cell extracts were performed as described (Bakin *et al.*, 2002).

Immunofluorescence microscopy

Cells (10^5 cells/well) were grown in DMEM containing 5% FBS on glass coverslips (22×22 mm) for 24 h before treatment with 2 ng/ml TGF-β1. Cells were fixed with 4% paraformaldehyde and stained as described (Bakin *et al.*, 2002). Actin filaments were stained with phalloidin-Alexa Green or phalloidin-Texas Red and tropomyosins were visualized using TM311 antibody. Fluorescent images were captured using a Nikon TE2000-E inverted microscope.

Transwell migration

The MDA-MB-231-Tet-Off-TM3 cells were incubated in the presence or absence of 2 μg/ml doxycycline for 24 h prior to the migration assay. Cells (1×10^5/well) were placed in DMEM/1%FBS in the upper chamber of 5-μm pore (24-well) transwells (Costar, High Wycombe Bucks, UK) and incubated alone or with 2 μg/ml doxycycline for 16 h. The cells were fixed in 100% methanol and cells remaining at the top of the polycarbonate membrane were removed with cotton swabs. The cells that had migrated through pores to the lower surface were stained with Diff-quick stain (VWR Scientific). Membranes were mounted on 25×75-mm² microslides. Cells were counted from five random fields at $\times 200$ magnification. Experiments were performed in duplicates.

Wound closure assay

MDA-MB-231 cells ($1–2 \times 10^5$/well) were seeded in 12-well plates. Cells were incubated in serum-free medium for 24 h prior to wounding. The wounds were made by scraping with plastic tip across the cell monolayer. The wounded cells were treated or untreated with 2 ng/ml TGF-β1. Phase contrast images were recorded at the time of wounding (0 h) and 20 h thereafter. Experiments were repeated with two independent 5-aza-dC treatments.

References

Albo D, Berger DH, Wang TN, Hu X, Rothman V and Tuszynski GP. (1997). *Surgery*, **122,** 493–499; discussion 499–500.

Antequera F and Bird A. (1993). *PNAS*, **90,** 11995–11999.

Ayscough KR. (1998). *Curr. Opin. Cell. Biol.*, **10,** 102–111.

Bakin AV and Curran T. (1999). *Science*, **283,** 387–390.

Bakin AV, Rinehart C, Tomlinson AK and Arteaga CL. (2002). *J. Cell. Sci.*, **115,** 3193–3206.

Bakin AV, Safina A, Rinehart C, Daroqui C, Darbary H and Helfman DM. (2004). *Mol. Biol. Cell.*, **15,** 4682–4694.

Bharadwaj S and Prasad GL. (2002). *Cancer Lett.*, **183,** 205–213.

Bhowmick NA, Ghiassi M, Bakin AV, Aakre M, Lundquist CA, Engel M, Arteaga CL and Moses HL. (2001). *Mol. Biol. Cell*, **12,** 27–36.

Boyd J, Risinger JI, Wiseman RW, Merrick BA, Selkirk JK and Barrett JC. (1995). *Proc. Natl. Acad. Sci. USA*, **92,** 11534–11538.

Braverman RH, Cooper HL, Lee HS and Prasad GL. (1996). *Oncogene*, **13,** 537–545.

Chung KY, Agarwal A, Uitto J and Mauviel A. (1996). *J. Biol. Chem.*, **271,** 3272–3278.

Cross SH and Bird AP. (1995). *Curr. Opin. Genet. Dev.*, **5,** 309–314.

Derynck R, Akhurst RJ and Balmain A. (2001). *Nat. Genet.*, **29,** 117–129.

Dumont N, Bakin AV and Arteaga CL. (2003). *J. Biol. Chem.*, **278,** 3275–3285.

Edlund S, Landstrom M, Heldin CH and Aspenstrom P. (2002). *Mol. Biol. Cell.*, **13,** 902–914.

Feng XH, Lin X and Derynck R. (2000). *EMBO J.*, **19,** 5178–5193.

Franzen B, Linder S, Uryu K, Alaiya AA, Hirano T, Kato H and Auer G. (1996). *Br. J. Cancer*, **73,** 909–913.

Frommer M, McDonald L, Millar D, Collis C, Watt F, Grigg G, Molloy P and Paul C. (1992). *PNAS*, **89,** 1827–1831.

Gagos S, Hopwood VL, Iliopoulos D, Kostakis A, Karayannakos P, Yatzides H, Skalkeas GD and Pathak S. (1995). *Anticancer Res.*, **15,** 369–378.

Gimona M, Kazzaz JA and Helfman DM. (1996). *Proc. Natl. Acad. Sci. USA*, **93,** 9618–9623.

Gimona M, Watakabe A and Helfman D. (1995). *PNAS*, **92,** 9776–9780.

Greenwel P, Inagaki Y, Hu W, Walsh M and Ramirez F. (1997). *J. Biol. Chem.*, **272,** 19738–19745.

Hannigan M, Zhan L, Ai Y and Huang CK. (1998). *Biochem. Biophys. Res. Commun.*, **246,** 55–58.

Hendricks M and Weintraub H. (1981). *Proc. Natl. Acad. Sci. USA*, **78,** 5633–5637.

Hendricks M and Weintraub H. (1984). *Mol. Cell. Biol.*, **4,** 1823–1833.

Hughes JA, Cooke-Yarborough CM, Chadwick NC, Schevzov G, Arbuckle SM, Gunning P and Weinberger RP. (2003). *Glia*, **42,** 25–35.

Jaffe AB and Hall A. (2002). *Adv. Cancer Res.*, **84,** 57–80.

Janssen RA and Mier JW. (1997). *Mol. Biol. Cell*, **8,** 897–908.

Leonardi CL, Warren RH and Rubin RW. (1982). *Biochim. Biophys. Acta*, **720,** 154–162.

Li X, Cowell JK and Sossey-Alaoui K. (2004). *Oncogene*, **23,** 1474–1480.

Masuda A, Takenaga K, Kondoh F, Fukami H, Utsumi K and Okayama H. (1996). *Oncogene*, **12,** 2081–2088.

Miller SA, Dykes DD and Polesky HF. (1988). *Nucleic Acids Res.*, **16,** 1215.

Moustakas A and Kardassis D. (1998). *Proc. Natl. Acad. Sci. USA*, **95,** 6733–6738.

Park IK, Lyu MA, Yeo SJ, Han TH and Kook YH. (2000). *Biochim. Biophys. Acta*, **1490,** 302–310.

Pawlak G and Helfman DM. (2001). *Curr. Opin. Genet. Dev.*, **11,** 41–47.

Pawlak G and Helfman DM. (2002a). *J. Biol. Chem.*, **277,** 26927–26933, Epub 2002. May 14.

Pawlak G and Helfman DM. (2002b). *Mol. Biol. Cell*, **13,** 336–347.

Pawlak G, McGarvey TW, Nguyen TB, Tomaszewski JE, Puthiyaveettil R, Malkowicz SB and Helfman DM. (2004). *Int. J. Cancer*, **110,** 368–373.

Piek E, Moustakas A, Kurisaki A, Heldin CH and ten Dijke P. (1999). *J. Cell. Sci.*, **112,** 4557–4568.

Pittenger MF, Kazzaz JA and Helfman DM. (1994). *Curr. Opin. Cell. Biol.*, **6,** 96–104.

Raval GN, Bharadwaj S, Levine EA, Willingham MC, Geary RL, Kute T and Prasad GL. (2003). *Oncogene*, **22,** 6194–6203.

Robbins J. (1998). *Circ. Res.*, **82,** 134–136.

Roberts AB and Wakefield LM. (2003). *PNAS*, **100,** 8621–8623.

Sahai E, Olson MF and Marshall CJ. (2001). *EMBO J.*, **20,** 755–766.

Saito H, Tsujitani S, Oka S, Kondo A, Ikeguchi M, Maeta M and Kaibara N. (2000). *Anticancer Res.*, **20,** 4489–4493.

Shields JM, Mehta H, Pruitt K and Der CJ. (2002). *Mol. Cell. Biol.*, **22,** 2304–2317.

Temm-Grove CJ, Jockusch BM, Weinberger RP, Schevzov G and Helfman DM. (1998). *Cell Motil. Cytoskeleton*, **40,** 393–407.

Varga AE, Leonardos L, Jackson P, Marreiros A and Cowled PA. (2004). *Neoplasia*, **6,** 128–135.

Vial E, Sahai E and Marshall CJ. (2003). *Cancer Cell.*, **4,** 67–79.

Wakefield LM and Roberts AB. (2002). *Curr. Opin. Genet. Dev.*, **12,** 22–29.

Wang FL, Wang Y, Wong WK, Liu Y, Addivinola FJ, Liang P, Chen LB, Kantoff PW and Pardee AB. (1996). *Cancer Res.*, **56,** 3634–3637.

Yu J, Zhang L, Hwang PM, Rago C, Kinzler KW and Vogelstein B. (1999). *Proc. Natl. Acad. Sci. USA*, **96,** 14517–14522.

Zhu WG, Srinivasan K, Dai Z, Duan W, Druhan LJ, Ding H, Yee L, Villalona-Calero MA, Plass C and Otterson GA. (2003). *Mol. Cell. Biol.*, **23,** 4056–4065.